STUDY OF MACROMOLECULES IN PHLOEM EXUDATE OF *Lupinus albus*

By

CAREN RODRIGUEZ MEDINA

School of Plant Biology
The University of Western Australia

This thesis is presented for the degree of Doctor of Philosophy of
The University of Western Australia
2009

ABSTRACT

The phloem long distance translocation system is not only involved in the transport of nutrients and photo-assimilates to different organs of the plant, but it also appears to be important for the transport of information molecules including growth-regulators, proteins and RNA. Translocation of signals appears to be involved in the coordination of developmental processes and also in the response of the plant to environmental cues. Much of the information about macromolecules in phloem comes from analyses of exudates collected from the stylets of sap sucking insects or from incisions made to the vasculature.

Among the legumes, members of the genus *Lupinus* exude phloem 'freely' from incisions made to the vasculature at most organs of the plant. This feature was exploited in this study to document some of the macromolecules present in exudate of *L. albus* and which might represent potential mobile signals. Phloem exudate was collected mainly from the sutures of developing pods and from inflorescence racemes. Two-dimensional polyacrylamide gel electrophoresis and tandem mass spectrometry were used to identify 83 proteins in exudate. Analysis of a cDNA library constructed from exudate identified 609 unique transcripts. Both proteins and mRNA were classified into functional groups. The largest group was related to general and energy metabolism, suggesting some metabolic activity probably to support the sieve element (SE). Other significant functional groups were represented by proteins and transcripts involved in protein synthesis, turnover and sorting, and in redox homeostasis. Proteins in these categories could play a role in maintaining the functions and stability of proteins in SE. Macromolecules involved in signalling such as transcripts encoding proteins mediating calcium levels and the Flowering locus T (FT) protein were also identified in phloem exudate of *L. albus*. FT protein has been recently identified as a mobile signal that induces flowering. Protein sequence data obtained in this study provides valuable information for future studies on the flowering signal in legumes. Both proteins and transcripts associated with photosynthesis were identified in exudate confirming some contamination by the contents of damaged chloroplast-containing cells at the wound site. However, the study concluded that the majority of macromolecules in exudate were

derived from phloem companion cells (CC) and that contamination at the wound site was probably negligible.

Using both northern blot and real time RT-PCR analyses high levels of miR399, miR395 and miR168 (previously identified in phloem exudate) confirmed these miRNA as components of the SE. Exudates collected from fruit vasculature, the apices of primary and tertiary branch inflorescences as well as from the base of the stem below the lowest set of leaves indicated distinct miRNA composition at each site, suggesting specificity in their phloem loading and possibly functional significance. An increase of miR399 in lupin phloem exudate and leaf tissue in response to phosphate (Pi) deficiency was observed, providing evidence that miRNA in legumes respond to Pi deficiency, as has been demonstrated for other plant species from which phloem exudates have been analysed. Translocation of naturally occurring miRNA from *Arabidopsis* wild-type to *hen1-6* mutant was investigated using grafting approaches. The *hen1* mutant accumulates low, sometimes even undetectable levels of miRNA due to the lack of methylation. No translocation of the five miRNA assayed under nutrient replete (non stress) conditions was observed. Translocation of miR395 in response to sulphur (S) deficiency was also investigated, and while conclusive evidence of translocation was not obtained, the data suggested some movement from roots to shoots (possibly in xylem) of a signal in response to S-deficiency. Future work is required to provide greater insight into the translocation path and identity of this S-deficiency signal. This study suggests that not all miRNA identified in phloem exudates are mobile, which raises the question about their biological relevance in SE and how they reached this location (e.g. through the action of a non-selective transport mechanism). However, there is also the possibility that miRNA are translocated only in response to specific internal or external cues not tested in this study.

This is the first study that provides information on macromolecules present in the phloem exudate of a member of the Fabaceae. The information obtained from this work, provides a basis for future studies in the identification of potential mobile signals that may play a role in a communication network that traffics information around the plant, regulating its various developmental processes and responding to environmental cues.

DECLARATION

The work described in this thesis is entirely my own except where stated specifically and has not previously been accepted for a degree at this or any other institution

Caren Rodriguez
January 2009

TABLE OF CONTENTS

ABBREVIATIONS

A amperes
ACC aminocyclopropane-carboxylate
ACN acetonitrile
ADF actin depolymerizing factors
AGO argonaute
BSA bovine serum albumin
BYMV bean yellow mosaic virus
CC companion cell
CHAPS (3-[(3-cholamidopropyl)dimethyl-ammonio]-1-propanesulfonate)
cDNA complementary DNA
d days
DCL1 RNase III DICER-Like1
DEPC diethylpyrocarbonate
DNA deoxyribonucleic acid
DTT dithiothreitol
EDTA ethylenediamine tetraacetic acid
ER endoplasmic reticulum
EST expressed sequence tag
g gram
g acceleration due to gravity
GSH glutathione
GST glutathione S-transferase
h hour
H_2O_2 hydrogen peroxide
HEN1 hua enhancer1
HYL1 hyponastic leaves1
HPLC high-performance liquid chromatography
IAA iodoacetamide
IEF isoelectric focusing
IPG immobilised pH gradient
kDa kilodalton
kVh kilovolt hour

LB Luria-Bertani

M molar

MALDI-TOF-MS matrix-assisted laser desorption/ionization time-of-flight mass spectrometry

m milli- or metres

mg milligram

min minutes

ml millilitre

mm millimetre

MWCO molecular weight cut off

n nano-

NCBI National Center for Biotechnology Information

nm nanometres

NO nitric oxide

PAGE polyacrylamide gel electrophoresis

Pi inorganic phosphate

PPU plasmodesmata pore unit

PRP pathogenesis-related-protein

PTGS post-transcriptional gene silencing

RNA ribonucleic acid

ROS reactive oxygen species

S sulphur

SAM S-adenosylmethionine

SDS sodium dodecylsulphate

SE sieve element

sec seconds

SEL size exclusion limit

SPITC sulphophenyl isothiocyanate

SuSy sucrose synthase

TBE Tris-borate-EDTA

TBS Tris buffered saline

TCA trichloroacetic acid

TEMED tetramethylethylenediamine

TFA trifluoroacetic acid

Tris tris(hydroxymethyl)amino methane

UBC ubiquitin-conjugating

UDP-Glc UDP glucose

UGPase UDP-Glc pyrophosphorylase

V volts

vol volumes

W watts

µ micro-

µE microeinstein

ACKNOWLEDGEMENTS

I am indebted to Dr. Penny Smith and Prof. Craig Atkins who have not only been fantastic supervisors but also good friends always willing to support me in the academic field, and who also helped me to overcome hard moments in my personal life. I am extremely grateful with the University of Western Australia for the financial assistance awarding me a Scholarship for International Research fees, SIRF as well as a University Postgraduate Award that made my dream possible; truth is that not many students from Colombia enjoy this kind of opportunities and I feel very fortunate for that.

I would like to thank my good friends Kylie, Danica, Simone, Grey, Hi, Mathias, Julia and Anthea for their constant support and encouragement. When one is so far from home friends become family and I feel very fortunate to have found such a beautiful Australian family of friends. Special thanks to Danica, my always smiley proof-reader for her patience, fruitful discussions, laughs and friendly guidance through the magic world of the proteins (her favourite world). Thanks also to Angela Ho for her valuable assistance with real-time RT-PCR, endless patience and always answering my questions in such a good attitude including after work hours.

I would like to thank the staff at the Centre for Microscopy, Characterisation and Analysis for the excellent scientific and technical assistance specially to Dr. Kathy Heel, Dr. Peta Clode, John Murphy, Lyn Kirilak and of course Prof. John Khuo for his encouragement, sage advice, great patience and for honouring me with his friendship.

Thanks heaps to my phloem exudate collection team Penny, Anthea, Megan and Craig for pretending it was a lot of fun and help me to get enough volumes of the ‘precious’ exudate that made possible my study.

Thanks to Dr. Rhonda Foley for her assistance with the phloem exudate cDNA library construction. Thanks to Steven Mole and Leon Hodgson for growing and maintenance of field-grown lupin plants and always showing genuine interest in my studies.

I would like to thank my beautiful mother for her endless support, for teaching me perseverance and the value of hard and honest work, for her bravery and her love of life. Thanks also to my family for their enormous support and encouragement.

Finally, I would like to thank my friend Aleks who always believed in my abilities and got as excited as I was when I was awarded an International Postgraduate Scholarship at UWA. I thank him for his generosity, mountains of ice cream and hot chocolate, beautiful sunsets and for showing me that there are still people in the world that care about the others. I wish you all the best in your search of your own meaning of happiness my friend…

CHAPTER 1

GENERAL INTRODUCTION

During the course of evolution, the increasing size and complexity of the land plants meant that their nutrition could no longer rely on cell to cell transfer of solutes, but required long-distance transport systems (van Bel *et al*., 2002). For the translocation of minerals and water from the soil solution, arrays of cells differentiated to form capillaries of dead vessels (xylem) through which water and solutes are transported as a consequence of the negative tensional gradient generated by transpiration. However, for long-distance transfer of photoassimilates and other solutes, a system of live cells (phloem) connected by perforated cell walls (sieve tubes) evolved that enabled water-driven directional mass flow of their contents from source organs, principally leaves, to sink organs and tissues (roots and reproductive structures) where the assimilates are used for growth or storage (van Bel *et al*., 2002). The xylem and phloem arrays are grouped closely together in vascular bundles to form a network that connects all plant parts and serves as a distribution network within all organs.

In addition to a pivotal role in the delivery of nutrients to distantly located organs, the plant vascular system also appears to be important for transport and delivery of signals and information molecules like plant growth regulators, bioactive peptides, proteins, and ribonucleoprotein complexes (Ruiz-Medrano *et al*., 2001; van Bel, 2003).

Phloem vascular tissue

Functional phloem in angiosperms is comprised of arrays of sieve element (SE)/companion cell (CC) complexes which originate from the same cambial precursor cell (van Bel and van Rijen, 1994). Immature SE contain all cellular components characteristic of young plant cells and initially are indistinguishable from other young cells of the phloem. As the SE differentiates it undergoes drastic changes including breakdown of the nucleus and of the tonoplast. The autophagy is selective and results in loss of the ribosomes, microtubules and

microfilaments so that at maturity, the SE is greatly reduced in complexity, retaining stacked endoplasmic reticulum (ER), a small number of plastids and a few dilated mitochondria, all of which occupy a parietal position within the cell, closely appressed to the plasmalemma (Evert, 1990; van Bel, 2003). A diagram of the ultrastructural features of the SE and CC complex based on observations in *Vicia faba* (van Bel 2003) is shown in Figure 1.1. As nuclear control of metabolic processing in the SE was lost in the course of evolution, the assistance of neighbouring CC was invoked to help in the maintenance and functioning of the SE (van Bel and Knoblauch, 2000). SE and CC are intimately connected to one another at maturity through specialized, branched plasmodesmata across their adjoining cell walls (Haywood *et al.*, 2002). The CC functions in maintenance of the associated SE, its nucleus acting as the control centre for both cells by regulating exchange of macromolecules through the SE-CC plasmodesmata (Lucas *et al*., 2001). Consequently, any macromolecule identified in the mature SE was either retained after being synthesized when the cell was immature or was delivered through its connection from an associated CC (van Bel, 2003; Walz *et al*., 2004). This direct cell-cell communication is believed to selectively mediate trafficking of macromolecules to the translocation stream. Files of SE connected by their end walls via enlarged plasmodesmata form a low resistance pathway for the mass flow of their contents over large distances in the plant (Sjölund, 1997). Thus the phloem links distantly located tissues and organs as well as providing a means to distribute assimilates and other nutrients, consequently it may have important regulatory and developmental functions (Ding *et al.*, 2003; Ruiz-Medrano *et al*, 1999; Xoconostle-Cázares *et al*., 1999).

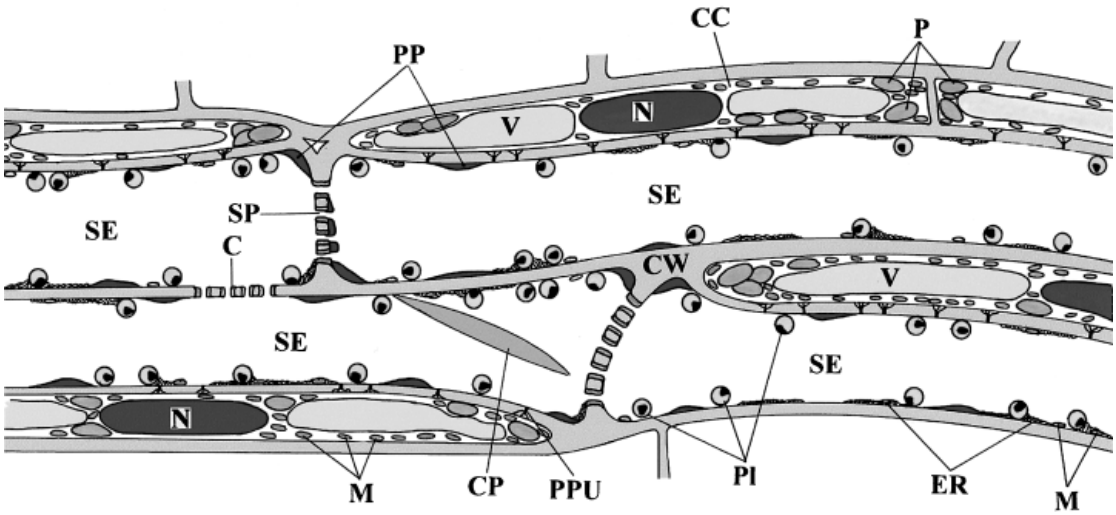

Figure 1.1. Ultrastructural features of the sieve element (SE) and companion cell (CC) complex in *Vicia faba*. After selective autophagy, SE plastids (PI), stacked endoplasmic reticulum (ER) and a few mitochondria (M) remain in a mature SE. These organelles occupy a parietal position and are evenly distributed along the SE plasma membrane. Parietal proteins (PP) are locally aggregated. Sieve elements are connected through sieve plates (SP) which are surrounded by callose collars (C). SE and their associated CC are connected through specialised, branched plasmodesmata units (PPU). A large crystalline protein cluster (CP), typical of the Fabaceae, rests close to the sieve plate. Abr: CW, cell wall; N, nucleus; P, plastids; V, vacuole (van Bel, 2003).

Solutes are 'loaded' into the phloem in 'source' organs, principally leaves. Here, massive photosynthate accumulation as sugar (mostly sucrose) generates a high turgor. The pressure gradient along sieve tubes causes a volume displacement away from the sources (Balachandran *et al*., 1997). The sieve tube sap 'moves' toward sites of lower turgor at the 'sink' organs and tissues where the solutes are 'unloaded' (van Bel, 2003). While some aspects of the mass flow concept of phloem translocation remain to be elucidated, it is well supported by experimental observation, and provides a sound basis for the development of models for 'source-sink' relations as they apply to both nutrition and signalling functions (Atkins and Smith, 2007).

A prerequisite for a successful interaction between the SE and its adjacent CC is an intimate symplasmic contact through specialized plasmodesmata. The cytoplasmic contacts on the side walls of the SE have become specialised for the permanent and selective exchange of materials and messages, and those on the end walls for bulk transport of solutes (van Bel and Knoblauch, 2000). The plasmodesmata between SE and CC are responsible for the exchange of small solutes and macromolecules in the SE/CC complex (van Bel, 2003).

Protein transfer between these cells was demonstrated by Fisher *et al.* (1992) providing evidence for macromolecular transfer between SE and CC. SE are connected to each other through their end walls to form sieve plates with a number of large 'pores' (Evert, 1990). The plates originate during cytokinesis as ordinary cell walls traversed by plasmodesmata and the pores develop in loci where plasmodesmata are present (Esau and Thorsch, 1985).

SE contain two types of phloem-specific plastids: S-type plastids, which have small starch inclusions only, and P-type plastids, which have proteinaceous inclusions and may also have small starch grains (Evert, 1990). The function of these two types of plastid in SE remains to be elucidated. However, it has been hypothesized that they may function as storage organelles. Thus it might be expected that SE-plastids would contain fewer inclusions in times of nutritional shortage (van Bel, 2003).

The functional significance of the few usually dilated mitochondria that are detected in electron micrographs of mature SE has not been established.

Collection and analysis of phloem contents

Identification of solutes and macromolecules in phloem sap has relied on a range of techniques to sample exudates from severed sieve tubes. The most gentle means of sampling is the use of stylets of feeding aphids (Fisher *et al*., 1992; Peel, 1975) or other sap sucking insects (Aki *et al*., 2008). However, the amounts of exudate collected are generally small and the procedures required are technically very demanding and laborious. Thus, most data have come from analysis of exudates collected following incisions made to the vasculature. While exudate can be collected from incisions to the bark of many woody species (Zimmermann and Ziegler, 1975), very few herbaceous species 'bleed' freely from such wounds. In most cases the SE rapidly occludes with coagulated structural proteins to block sieve pores and prevent loss of the cell contents (Will and van Bel, 2006). By bathing the wound in a solution containing a chelator (like EDTA) to remove cations, including Ca^{2+} (Gaupels *et al.*, 2008c), or by treating the tissue cryogenically (Pate *et al*., 1984), occlusion of the sieve plates is retarded. However, there are a few species where SE

contents exude naturally from an incision in the vasculature of some tissues. These include a number of cucurbits (Yoo *et al.,* 2004), castor bean (Schobert *et al.,* 1995), the pedicels of developing wheat grains (Fisher *et al.,* 1992), the developing floral axis of *Brassica napus* (Giavalisco *et al.,* 2006) and members of the genus *Lupinus* (Pate *et al.,* 1974). Among the lupins, *L. angustifolius* (narrow-leafed lupin), *L. albus* (white lupin), *L. mutabilis* (pearl or Andean lupin) and *L. cosentinii* will exude readily, while other species, like *L. luteus* (yellow lupin) and *L. polyphyllus*, will not 'bleed' spontaneously (Pate *et al.,* 1974).

Phloem exudate collected from a single SE using aphid stylets might be relatively free of contaminants from surrounding cells. In contrast, wounds made to the vasculature by incision are likely to result in exudate that also includes the contents of cells other than the sieve tubes, as well as material from the surrounding apoplast. Similarly, solutes normally immobilised in the apoplast can be released into the phloem via ion exchange when a chelator is used to attenuate occlusion of sieve tubes. A number of authors have suggested criteria to assess the degree of contamination of exudates collected from incisions (Buhtz *et al*., 2008; Gaupels *et al*., 2008c; Giavalisco *et al*., 2006; Haywood *et al*., 2005; Yoo *et al*., 2004; Ruiz-Medrano *et al*., 1999). Most commonly the presence of chloroplast proteins, such as the subunits of Rubisco, has been regarded as a measure of contamination. In all cases, including aphid feeding, phloem exudation results from rapid pressure release with the possibility that macromolecules anchored to the parietal cytoplasm and plasma membrane of the SE, and not normally mobile in phloem, might be mobilised into exudate. These considerations have been discussed previously (Atkins and Smith, 2007) and will be raised in subsequent chapters in relation to the 'purity' of lupin phloem exudates collected from incisions. While the relative contents of the major solutes in phloem such as sucrose or the main amino acids are not likely to be changed significantly as a result of contamination, this is an important issue for minor constituents and especially macromolecules that are recovered in very small amounts and for which translocated regulatory roles are postulated.

Proteins in phloem exudate

A broad range of enzyme activities has been detected in phloem exudates collected from a number of woody and herbaceous species (Eschrich and Heyser, 1975) indicating that the exudates contained an arsenal of proteins. In cucurbit species the levels may be as high as 35-60 µg/µl (Walz *et al*., 2004) while in exudate collected with leaf hopper stylets from rice levels are typically 0.2 µg/µl (Hayashi *et al*., 2000). Early attempts to separate individual proteins (Hoffmann-Benning *et al*., 2002; Marentes and Grusak, 1998) established that a wide size range of polypeptides could be recovered and that some sequence data could be obtained using mass spectrometric techniques. The advent of proteomic analysis has proven to be a powerful tool in identifying a large number of proteins recovered from phloem exudates of both dicotyledonous and monocotyledonous species. Exudates collected from the stylets of sap-sucking insects (aphids and leaf hoppers) are regarded as providing the least contaminated spectrum of proteins most likely to be translocated systemically (Aki *et al*., 2008; Gaupels *et al* 2008a; Barnes *et al*., 2004; Fisher *et al*., 1992). Proteomic analyses of phloem exudates collected from incisions to the vasculature of a number of species that either 'bleed' spontaneously (e.g. castor bean [Barnes *et al*., 2004] or cucurbits [Haebel and Kehr, 2001]) or, in which exudation is aided by application of a chelator (e.g *Brassica* [Giavalisco *et al*., 2006]), have also shown a broad range of proteins, a number of which are common with those identified in stylet exudates. These include the phloem-specific proteins, phloem protein 1 (PP1) and phloem protein 2 (PP2) that are major constituents of cucurbit phloem and are involved in the sealing process following wounding (Read and Northcote, 1983). Others are concerned with sugar metabolism and transport, protein turnover, detoxification of reactive oxygen species, defence against insect feeding and pathogenesis (Giavalisco *et al*., 2006; Walz *et al*., 2004; Walz *et al*., 2002). These are reviewed extensively in Chapter 4. Proteomic data confirm that phloem contains a complex array of many hundreds of proteins that are potentially exchanged between the SE and CC along the translocation pathway (Giavalisco *et al*., 2006; Walz *et al*., 2004). Some of the proteins present within the phloem are likely to play a role in the maintenance of the SE system and so are not necessarily signalling molecules (Ruiz-Medrano *et al.,* 2001). Others, such as

the Flowering Locus T (FT) protein associated with the flowering signal, do indeed appear to be ‘messages’.

While it is clear that the phloem sap contains many proteins, it is not at all clear which of these are translocated and, more importantly, those whose function is dependent on long distance transport. Golecki *et al*. (1998) detected additional proteins in phloem exudate of *Cucumis sativus* scions grafted to *Cucurbita* spp stocks within 9-11 days of grafting, suggesting phloem translocation of proteins from the stock to the scion. Oparka and Santa Cruz, (2000) pointed out that unequivocal demonstration that translocated proteins are unloaded into sink tissues, where they are also shown to have a function, is essential before a role as a translocated signal can be assigned with any certainty.

The classic phloem mobile signal florigen has recently been identified as the Flowering Locus T protein (FT) in *Arabidopsis* (Corbesier *et al.,* 2007), *Cucurbita* (Lin *et al.,* 2007) and as Hd3a, the FT ortholog in rice (Tamaki *et al.,* 2007). Corbesier *et al.* (2007) demonstrated that in *Arabidopsis* an FT:GFP fusion protein could move across a graft union to induce flowering in the scion of a mutant that could not produce FT. Tamaki *et al.* (2007) used similar techniques to show that Hd3a in rice also induced flowering. Both studies showed that the mRNA that encodes these proteins and that had been suggested as the florigen signal (Huang *et al.,* 2005) was not mobile in phloem to any extent. The presence of FT protein in phloem exudate of *Cucurbita* sp was demonstrated by Lin *et al.* (2007) as well as its movement through a graft from flowering pumpkin (*Cucurbita maxima*) stocks to long-day-grown *Cucurbita moschata* scions to induce flowering. No evidence of *FT* mRNA crossing the graft union in the phloem translocation stream was found in this report either.

Certain phloem proteins could be involved in RNA transport within the plant forming translocatable ribonucleoprotein complexes with endogenous or pathogenic RNA (Gomez *et al.*, 2005). CmPP16-1 protein from *C. maxima* is an RNA binding protein with properties similar to viral movement proteins, in that it can interact with plasmodesmata and increase the size exclusion limit (SEL) (Xoconostle-Cázares *et al*., 1999). Microinjection and heterografting experiments support the theory that CmPP16-1 binds RNA, enters the sieve

tube system and moves through phloem into scion tissue (Xoconostle-Cázares *et al*., 1999). Aoki *et al.* (2005) demonstrated that CmPP16-1 moved as a complex with other proteins and that these proteins positively regulated its downward movement when introduced into rice phloem. Movement of CmPP16-1 upward in the shoot was by mass flow. A second protein, CmPP16-2, also interacted with these proteins but did not regulate its movement. These results suggest that although macromolecules may move with mass flow, there can also be directed movement of proteins in phloem. Hsc70 chaperones have been implicated in movement of macromolecules into SE from CC. Like CmPP16-1, these proteins act to increase the SEL of plasmodesmata, a property specific to the phloem localised members of this gene family (Aoki *et al.,* 2002). A motif was identified that was proposed to be responsible for cell-to-cell trafficking of the Hsc70 proteins.

A Phloem Small RNA Binding Protein1 (PSRP1) was identified by Yoo *et al*. (2004) in phloem exudate of *C. maxima*. PSRP1 binds small RNA species and could mediate the cell-to-cell trafficking of small single stranded (but not double stranded) RNA molecules. However, long-distance trafficking of small RNA in phloem was not demonstrated. Based on these results, a role for PSRP1 in the exchange of small single stranded RNA between CC and SE was suggested. PSRP1 may also be important for local small RNA transmission since small RNA molecules do not appear to move unaided between cells, not even through dilated plasmodesmata microchannels (Yoo *et al*., 2004). An ortholog of this protein has not been identified in any other plant species suggesting that its role may be specific to cucurbits.

RNA in phloem exudate

The long distance movement of RNA molecules was first demonstrated for plant viruses (Carrington *et al.,* 1996). Plant viruses exploit the cell-to-cell and systemic transport systems to allow the spread of infection throughout the plant (Jorgensen *et al.,* 1998; Carrington *et al.,* 1996). Viral movement proteins facilitate the cell-to-cell movement of viral nucleic acids through plasmodesmata by forming protein-RNA complexes, and increasing the SEL of plasmodesmata (Ding *et al.,* 1992). The maize *knotted1* (*Kn1*) homeobox gene encodes a

transcriptional regulator, KN1, that influences cell fate at the vegetative meristem. Its mRNA moves both cell-to-cell (Lucas *et al.,* 1995) and systemically (Kim *et al.,* 2001). Microinjection experiments in tobacco mesophyll cells revealed that the KN1 protein behaved like a viral movement protein, as it increases the SEL of plasmodesmata and moves between cells, facilitating the transport of its own mRNA (Lucas *et al*., 1995).

Numerous transcripts have been identified in phloem sap of rice (Sasaki *et al*., 1998), *Arabidopsis* (Deeken *et al*., 2008), melon (Omid *et al.,* 2007), *Ricinus communis* (Doering-saad *et al.,* 2006) and barley (Doering-Saad *et al.*, 2002; Gaupels *et al.*, 2008a). The functional analysis of the cDNA identified in transcriptome studies revealed transcripts involved in a wide range of processes including metabolism, plant responses to stresses, transport, DNA/RNA binding and protein turnover. The presence of transcripts in phloem exudate supports the prospect of an RNA-based signalling network that is believed to function in control of many plant processes (Lough and Lucas, 2006). Although transcripts have been identified in phloem exudate, there are few for which translocation has been demonstrated and the need for translocation established (Haywood *et al.,* 2005; Kim *et al*., 2001; Ruiz-Medrano *et al.*, 1999; Kühn *et al*., 1997). *In situ* localization experiments showed the movement of an endogenous SUCROSE TRANSPORTER-1 (*SUT1*) transcript from the CC (site of transcription) through the connecting plasmodesmata into the SE in Solanaceae (Kühn *et al*., 1997). Heterografting experiments showed phloem transport of *CmNACP* mRNA (a transcript containing a conserved NAC domain and present in the pumpkin phloem translocation stream) from pumpkin stock to cucumber scions and the accumulation of this transcript in cucumber scion apical tissues (Ruiz-Medrano *et al.*, 1999). The tomato *Mouse ears* (*Me*) mutation is characterized by octapinnate compound leaves in contrast with pinnate venation and acute lobes in the wild-type. The mouse ears phenotype was observed in wild-type tomato scions grafted onto *Me*-mutant stock (Kim *et al*., 2001). This change in the wild-type phenotype was correlated with the graft transmissibility of *Me* transcripts (*LeT6* and pyrophosphate-dependent phosphofructokinase (*PFP*) fusion transcripts) into wild-type scions, reflecting the ability of the transcript to be translocated through the phloem from the stock to the apical meristem of the scion. The fact that the translocated mutant mRNA

caused changes in leaf morphology of the wild type scions suggested that the RNA was functional (Kim *et al*., 2001). Other examples of movement of mRNA that cause changes in phenotype are the *gai* mRNA, which produced changes to leaf morphology in transgenic tomato lines (Haywood *et al.,* 2005), and *BEL5* mRNA, which controls tuber production in response to day-length in potato (Banerjee *et al.,* 2006). Movement of *gai* mRNA supports the idea of regulated movement of RNA in phloem (Haywood *et al.,* 2005). Although translocated *gai* RNA could be detected in the apex and floral buds it was not detected in developing fruits. These would have acted as a strong sink for photo assimilates, suggesting that processes other than mass flow determines the organs to which translocated RNA is delivered. Omid *et al.* (2007) used grafting experiments to demonstrate the long-distance trafficking of six transcripts, three of them associated with auxin signalling, identified in a cDNA library constructed from melon phloem exudate. This study also showed that this long-distance capability was neither general for all phloem transcripts nor associated with the abundance of the specific transcript in the phloem sap. These results also suggest that long-distance movement of mRNA molecules is both controlled and selective (Omid *et al.,* 2007).

Small RNA in phloem

Small RNA molecules have been identified in phloem exudate collected from *B. napus* (Buhtz *et al*., 2008); *L. albus (*Yoo *et al*., 2004; Jordan, 2004); *C. maxima*, *R. communis* and *Yucca filamentosa* (Yoo *et al*., 2004). The small RNA population includes microRNA (miRNA) and small interfering RNA (siRNA).

Small interfering RNA and miRNA control expression of genes through their ability to direct cleavage of RNA, control translation or mediate epigenetic silencing. Most siRNA act in defence of the genome from transposons and viruses while miRNA regulate endogenous target genes (Bartel, 2004). siRNA range in size from 21-24 nucleotides, are generated from long-double stranded RNA by the action of a ribonuclease III enzyme Dicer and are incorporated into a ribonucleotide protein complex known as the RNA induced silencing complex (RISC) (Mallory and Vaucheret, 2004; Bartel, 2004). Although siRNA often

derive from transposons, viruses, or heterochromatic DNA (Bartel, 2004), there are also two classes of endogenous siRNA. The first, trans-acting siRNA (ta-siRNA), are derived from a non-coding, single stranded precursor transcript after cleavage by a miRNA. The action of an RNA-dependent RNA polymerase (RDR6) produces double stranded RNA from the precursor and phased siRNA are produced by DCL4, with the phase determined by the site of miRNA cleavage (Allen *et al.,* 2005; Peragine *et al.,* 2004). The second, natural antisense transcript-derived siRNA (nat-siRNA), are produced as a result of cleavage of two convergent and partially overlapping transcripts. The first nat-siRNA discovered mediate responses to salt stress (Borsani *et al.,* 2005) and pathogen attack (Katiyar-Agarwal *et al.,* 2006).

miRNA are small (19-25 nucleotide), single stranded RNA molecules that function by targeting mRNA for cleavage or by blocking translation of their mRNA target (Mallory and Vaucheret, 2004). This process is mediated by base pairing of the miRNA to its target. In plants the target sites for miRNA binding have perfect or near perfect complementarity with the miRNA sequence (Bartel and Bartel, 2003). miRNA are evolutionarily conserved across plant species (Reinhart *et al.,* 2002).

miRNA biogenesis

miRNA are derived from a MIR gene that is transcribed through POLII to form a pri-miRNA that can fold into a stem-loop structure that is processed by the ribonuclease III enzyme Dicer DCL1 (Bartel, 2004). The results of studies on miRNA biogenesis in *Arabidopsis* indicated that three proteins, DCL1, HYL1, and the C2H2 Zn-finger protein SERRATE (SE), are required for the accurate processing of miRNA precursors in the plant cell nucleus (Dong *et al*., 2008). Dong *et al.* (2008) showed that recombinant DCL1 cleaves dsRNA, pri-miRNA and pre-miRNA in the nucleus to release short RNA of predominantly 21 nt, requiring only divalent cations and ATP for its activity. Both HYL1 and SE stimulate DCL1 activity on both pri- and pre-miRNA substrates and markedly increase the fidelity of cleavage (Figure 1.2) (Dong *et al.,* 2008). Yu *et al.* (2008) proposed recently that DDL interacts with DCL1 in miRNA biogenesis in *Arabidopsis* facilitating the recognition of pri-miRNA. HEN1 protein is also involved in miRNA biogenesis in plants and in post-transcriptional gene

silencing (PTGS) (Park *et al*., 2002). HEN1 methylates miRNA and siRNA (Yu *et al*., 2005). Methylation is believed to protect the 3′ ends of the small RNA from uridylation and degradation (Li *et al*., 2005). HASTY protein exports miRNA from the nucleus to the cytoplasm where it associates with Argonaute (AGO1) to direct cleavage and translational repression (Vaucheret *et al.,* 2004) (Figure 1.2).

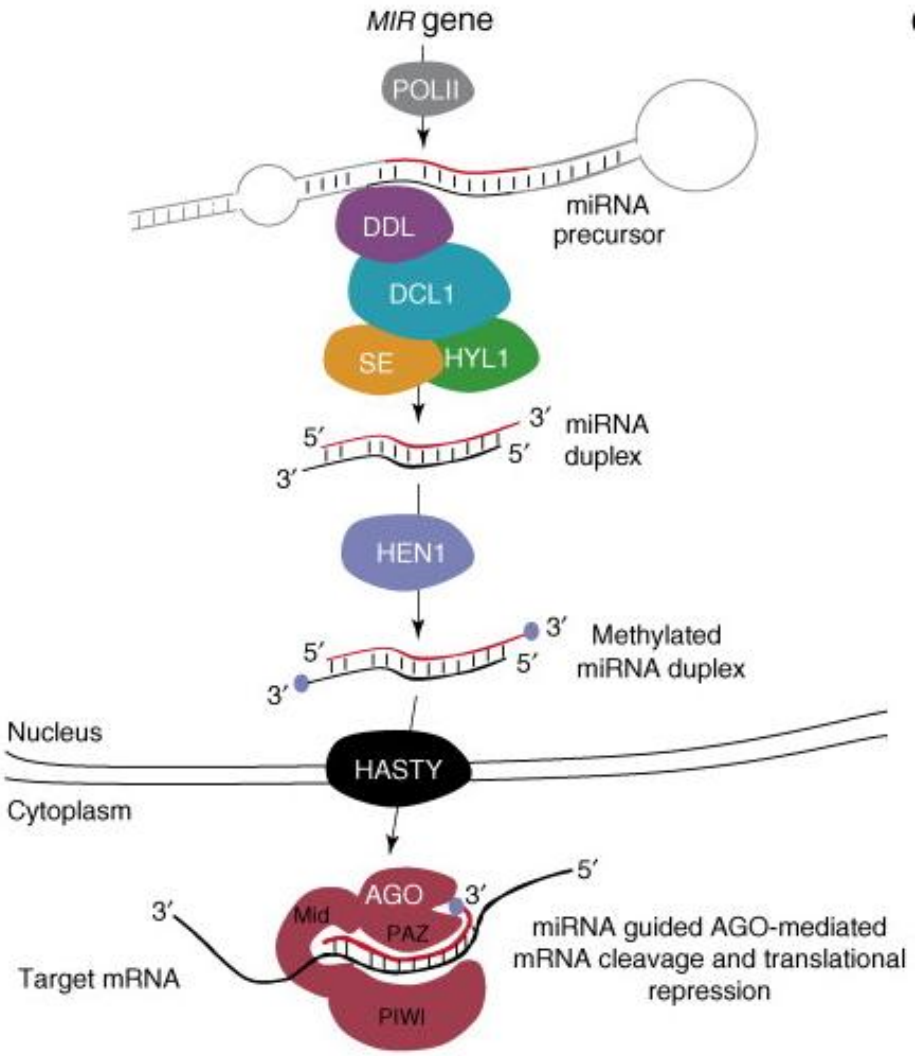

Figure 1.2. Simplified schematic representation of microRNA biogenesis in *Arabidopsis*. MIR gene is transcribed through POLII to form a pri-miRNA that can fold into a stem-loop structure that is processed by DCL1 apparently associated with HYL1, SE and DDL to generate a miRNA duplex. The miRNA is methylated by the action of HEN1, exported to the cytoplasm by HASTY and associated with Argonature (AGO1) to direct cleavage and translational repression. (Figure taken from Mallory *et al.,* 2008).

miRNA targets

A large number of miRNA target mRNA of transcription factors that regulate development or are related to genes with known developmental roles, suggesting that miRNA help to coordinate a wide range of cell division and cell fate decisions throughout the plant (Rhoades *et al.*, 2002). For example, miR165 targets the transcription factors *PHABULOSA (PHB)* and *PHAVOLUTA (PHV)* that regulate axillary meristem initiation and leaf development, while miR172 is predicted to target *AP2*, which specifies floral organ identity (Bartel and Bartel, 2003). Plant mutants that are defective in miRNA accumulation show altered developmental phenotypes that include defects in floral development and in leaf morphology (Mallory and Vaucheret, 2004; Vazquez *et al*., 2004; Park *et al.*, 2002). miRNA regulation is not limited to development but also has a role in environmental and hormone responses (Kidner and Martienssen, 2005; Sunkar and Zhu, 2004). Sunkar and Zhu (2004) identified miRNA whose accumulation was either induced or decreased by abiotic stresses.

Some miRNA such as miR395, miR398 and miR399 are involved in the coordination of nutrient homeostasis (Buhtz *et al*., 2008; Pant *et al*., 2007; Chiou *et al*., 2006; Bari *et al*., 2006; Fujii *et al*., 2005; Yamasaki *et al*, 2007). miR399 has been reported to control inorganic phosphorus (Pi) homeostasis by regulating the expression of UBC24 transcript that encodes a ubiquitin-conjugating E2 enzyme in *A. thaliana*. miR399 expression is induced by Pi starvation while accumulation of UBC mRNA is reduced (Chiou *et al*., 2006; Fujii *et al*., 2005). The down-regulation of UBC transcript appears to be important for the attenuation of primary-root elongation and for the induction of phosphate transporter genes (Fujii *et al*., 2005). miRNA395, predicted to target ATP sulphurylases (APS1, APS3 and APS4), is induced during sulphate starvation which results in the down-regulation of the corresponding target gene (Jones-Rhoades and Bartel, 2004). Yamasaki *et al*. (2007) suggested that miR398 is a key factor in copper homeostasis in plants and that it regulates the stability of mRNA of major copper proteins under copper-limited conditions. An increase in the levels of miR395, miR398 and miR399 in phloem exudate collected from *B. napus* plants grown under sulphate, copper and phosphate

deficiency conditions respectively was demonstrated recently by Buhtz *et al*. (2008).

miRNA translocation

Phloem mobility of small RNA has been suggested since the discovery of the systemic spread of post-transcriptional gene silencing. However, confirmation that siRNA actually constitute the phloem-translocated signal propagated during gene silencing is still to be confirmed (Buhtz *et al*., 2008). miR166 is involved in abaxial cell fate specification by restricting *hd-zipIII* expression to the adaxial side (Juarez *et al.,* 2004). miRNA166 initially accumulates immediately below the incipient leaf but subsequently in a progressively broader domain including the adaxial side (Juarez *et al.,* 2004). The progressively expanding expression pattern of miRNA166 during leaf development, and its accumulation in phloem, led Juarez *et al*. (2004) to suggest that miRNA166 may form a movable signal that emanates from a signalling centre below the incipient leaf. The presence of miRNA in phloem exudate has been interpreted as their having a role in long distance signalling to regulate gene expression (Buhtz *et al*., 2008; Pant *et al*., 2007). This systemic signalling would be important for the coordination of processes related to development, defence and nutrient allocation (Buhtz *et al*., 2008). Pant *et al*. (2007) suggested that miR399 is a phloem mobile molecule that increases in concentration in phloem exudate during Pi limitation. These authors studied miR399 translocation in *Arabidopsis* using micrografting experiments with a transgenic plant over-expressing miR399 under the control of the 35S promoter and grafted onto wild-type rootstock. Grafts were grown under Pi replete conditions. The authors reported that miR399 was efficiently translocated from Pi-replete transgenic shoots to wild type roots (Pant *et al*., 2007).

Aims of this study

To understand the molecular basis of the long distance communication pathway it is necessary to increase the knowledge of the component parts. To this end it is important to better define: a) genes specifically expressed within the plant vascular system b) transcripts present within the phloem translocation stream and c) the full complement of proteins that operate in it (Lough and Lucas,

2006). To date there is no information on these components in phloem of a legume. Lupins (*L. albus* and *L. angustifolius*) have provided a wealth of information on the long distance translocation of low molecular weight solutes and in establishing quantitative 'source-sink' relationships for C, N and other nutrients in a nodulated grain legume (Atkins and Smith, 2007). The ability to collect phloem exudates both, readily and in substantial volumes, without the use of a chelating agent, has been critical to these advances and provides an ideal tool to study the translocation of macromolecular species in a legume.

The aim of this study was to document the macromolecular components of lupin phloem exudate, in particular to identify proteins and RNA molecules. In addition, the role of one class of small RNA molecules, miRNA, identified in phloem exudate, was investigated to determine whether they were translocated and whether particular miRNA species were translocated in response to nutrient deprivation. Identification of these molecules in phloem exudate is the first step in the study of the potential components of a signalling network and will provide new insights into the potential role of these molecules in phloem.

CHAPTER 2

GENERAL METHODS

This chapter describes common methodologies used throughout this study to derive data sets.

Plant material and collection of phloem exudates

Seeds of *Lupinus albus* L. *cv*. Kiev mutant (white lupin) were planted in coarse river sand in pots maintained in a naturally lit glasshouse or in the field in a local sandy soil in late May and watered daily. Both the glasshouse- and field-grown plants were inoculated with *Bradyrhizobium* strain WU425 at sowing. Those in pots were fertilized twice per week with ¼ strength N-free nutrient solution containing 0.5 mM $MgSO_4$ $_7H_2O$, 0.62 mM K_2SO_4, 0.5 mM KH_2PO_4, 0.5 mM $CaSO_4$, 0.04 mM Fe-EDTA and micronutrients (46 µM H_3BO_3, 9 µM $MnCl_2$. $_4H_2O$, 0.8 µM $ZnSO_4$. $_7H_2O$, 0.3 µM $CuSO_4$ and 0.1 µM Na_2MoO_4. $_2H_2O$). Phloem sap exudate was collected by making shallow incisions in the lateral and dorsal sutures of fruits, inflorescence stalks and in some cases at other sites on the plant (clearly defined in later chapters) with sterile single sided razor blades. The first drop of exudate was discarded. All pipette tips used for collection and Eppendorf tubes used for storage were sterile and RNase-free and at all times hands were covered by laboratory gloves. Phloem exudate collected from different plants was bulked and stored immediately at -80°C to minimise degradation of proteins, mRNA and miRNA.

Deoxyribonucleic acid (DNA) techniques

Agarose gel electrophoresis

Agarose gel electrophoresis was used to visualise PCR products. PCR products were loaded onto 1% (w/v) agarose gels in 0.5x TBE buffer (0.045 M Tris-borate, 0.001 M EDTA [pH 8.0]). To visualise DNA, gel solutions contained 0.1 µg ethidium bromide per 100 ml TBE buffer. One volume of 5X loading dye

solution (0.25% [w/v] bromophenol blue, 0.25% [w/v] Xylene cyanol FF, 15% Ficoll Type 400) was added to 5 vol of PCR product and gels were run at 70 V in a Bio-Rad Wide Mini-Sub tank using 0.5X TBE as running buffer. To determine the size of the PCR products, 6 µl of 1kb DNA ladder (GeneRuler™, MBI Fermentas) was loaded next to the samples. DNA was visualised using a UV transilluminator (Nova-Line).

Agarose gels were photographed using a Kodak DC-40 digital camera and images downloaded onto a computer using the software accompanying the camera.

Purification of PCR products

After electrophoresis, PCR products were extracted using QIAquick Gel Extraction Kit (QIAGEN) following the instructions in the protocol provided by the manufacturer. Briefly, the DNA fragment of interest was excised from the gel with a sterile razor blade, dissolved in 3 vol of buffer QG (provided with kit, proprietary formulation) and incubated at 50°C for 10 min, vortexing the tube twice for 1 min during the incubation. One volume of isopropanol was added to the sample and mixed. The mixture was placed in a QIAquick spin column and centrifuged for 1 min at 12,000 *g*. The solution that flowed through was discarded and the column washed by adding 0.75 ml of buffer PE (provided with kit, proprietary formulation) followed by centrifugation for 1 min at 12,000 *g*. DNA was eluted by adding 30 µl sterile DI water to the centre of the membrane and centrifuging at 12,000 *g* for 1 min.

Ribonucleic acid (RNA) techniques

Isolation of total RNA from samples of tissue and phloem exudate

Total RNA was isolated from tissue and from phloem exudate samples using TRIzol® reagent (Invitrogen) following the instructions in the protocol provided by the manufacturer. Frozen tissue samples were ground to a fine powder in liquid nitrogen. Ten volumes of TRIzol® reagent was added and the mixture was incubated at 21°C for 5 min. Chloroform was then added at 0.2 ml per 1 ml of TRIzol® reagent used in the previous step. The samples were shaken by hand

for 30 sec and incubated at 21°C for 3 min followed by centrifugation at 12,000 *g* for 15 min at 4°C. The upper aqueous phase was transferred to a fresh RNase-free tube and RNA precipitated by adding 10 µg RNase-free glycogen (Roche) and 0.5 ml of isopropyl alcohol per 1 ml of TRIzol® reagent used at the start of the procedure. Samples were incubated at 21°C for 10 min and centrifuged at 12,000 *g* for 30 min at 4°C. After removing the supernatant the RNA pellet was washed with 75% ethanol. Samples were mixed by vortexing and centrifuged at 7,500 *g* for 5 min at 4°C. The ethanol was removed and the pellet briefly air dried and dissolved in diethylpyrocarbonate (DEPC)-treated water. The concentration of isolated RNA was determined using a NanoDrop ND-1000 Spectrophotometer (NanoDrop Technologies). For phloem exudate samples, 5 ml of TRIzol® was added to 1.5 ml of phloem exudate and total RNA isolated following the protocol described above.

DNA elimination from RNA preparations

DNA was digested from isolated total RNA using DNase I, Amplification Grade (Invitrogen). To a 0.2 ml microcentrifuge tube the following reagents were added: 0.5–1 µg RNA, 1 µl 10X DNase I Reaction Buffer, 1 µl DNase I, Amp Grade (1 U/µl) and DEPC-treated water to 10 µl total reaction volume. The sample was incubated for 15 min at 21°C. DNase I was inactivated by adding 1 µl of 25 mM EDTA solution and the sample heated for 10 min at 65°C.

Reverse transcription

Unless otherwise stipulated reverse transcription was performed using the iScript™ cDNA synthesis kit (Bio-Rad) and following the manufacturer's instructions. A reverse transcription reaction was set up by adding 4 µl 5x iScript reaction mix (containing the oligo (dT) primer), 1 µl iScript reverse transcriptase, nuclease-free water (to a 20 µl total reaction volume) and 1 µg total RNA to a 0.2 ml microcentrifuge tube. The complete reaction was mixed and briefly centrifuged, then incubated at 25°C for 5 min, 42°C for 30 min and finally 85°C for 5 min.

Real-time PCR

Real-time PCR analysis was carried out on a LightCycler 480 (Roche Diagnostics) using SYBR® green as the fluorescent dye. Reactions in 5 µl were

set up using 2x SYBR green master mix (Roche) and 0.5 µM final concentration of specific primers. RT-PCR conditions were: pre-incubation at 95°C for 10 min followed by 40 cycles of amplification at 95°C for 10 sec, 55°C for 10 sec and 72°C for 20 sec. For melting curve analysis, samples were heated at 95°C for 10 sec and cooled to 55°C for 30 sec. Fluorescence signals were collected continuously from 55ºC to 95ºC. A final cycle at 50ºC for 10 sec was added to allow cooling and the results were analysed using the LightCycler software (Roche).

CHAPTER 3

STRUCTURAL CHARACTERIZATION OF *Lupinus albus* TISSUE AT SITES OF PHLOEM EXUDATE COLLECTION

INTRODUCTION

In angiosperms, the phloem vascular tissue contains two main types of cells, the sieve elements (SE) and the companion cells (CC). The phloem translocation system makes use of a turgor gradient along the sieve tubes as the driving force for mass flow (van Bel, 2003). Developing fruits of lupin are a major 'sink' for assimilates and other nutrients and, while phloem exudates can be collected from other sites on the plant (Pate *et al.*, 1979), exudation from the fruits is more persistent and delivers greater volumes of exudate than elsewhere. In this study, phloem exudate was collected by making shallow incisions in the major veins along the dorsal and ventral sutures of *L. albus* pods. The accompanying photograph shows these sites of exudate collection together with a diagrammatic representation of the major and minor vasculature of a typical legume fruit (Figure 3.1A and 3.1B). Although the vasculature of the pod sutures are richer in phloem tissue than the vasculature at other sites (Pate *et al*., 1974) the exudate produced is expected to also contain the contents of other cells damaged by the wound. The morphology and structure of the vascular tissue of the pod sutures was studied to determine the distribution of phloem and xylem, and the nature of surrounding cells likely to be wounded as a result of incisions made to collect exudate. Sampling of pod tissue for microscopy required excising small sections of the suture vasculature presumably causing release of turgor pressure in the transport phloem and triggering the sealing process in the SE (Ehlers *et al*., 2000; van Bel, 2003). Because lupins 'bleed' spontaneously from wounds to the vasculature, it was of interest to extend the study to include aspects of the ultra-structure of the SE/CC complex, specifically to examine the consequences of turgor release. Subsequent chapters focus on the characterisation of macromolecules (proteins

and RNA including miRNA) present in phloem exudate collected mostly from wounds to the vasculature of developing fruits of *L. albus*.

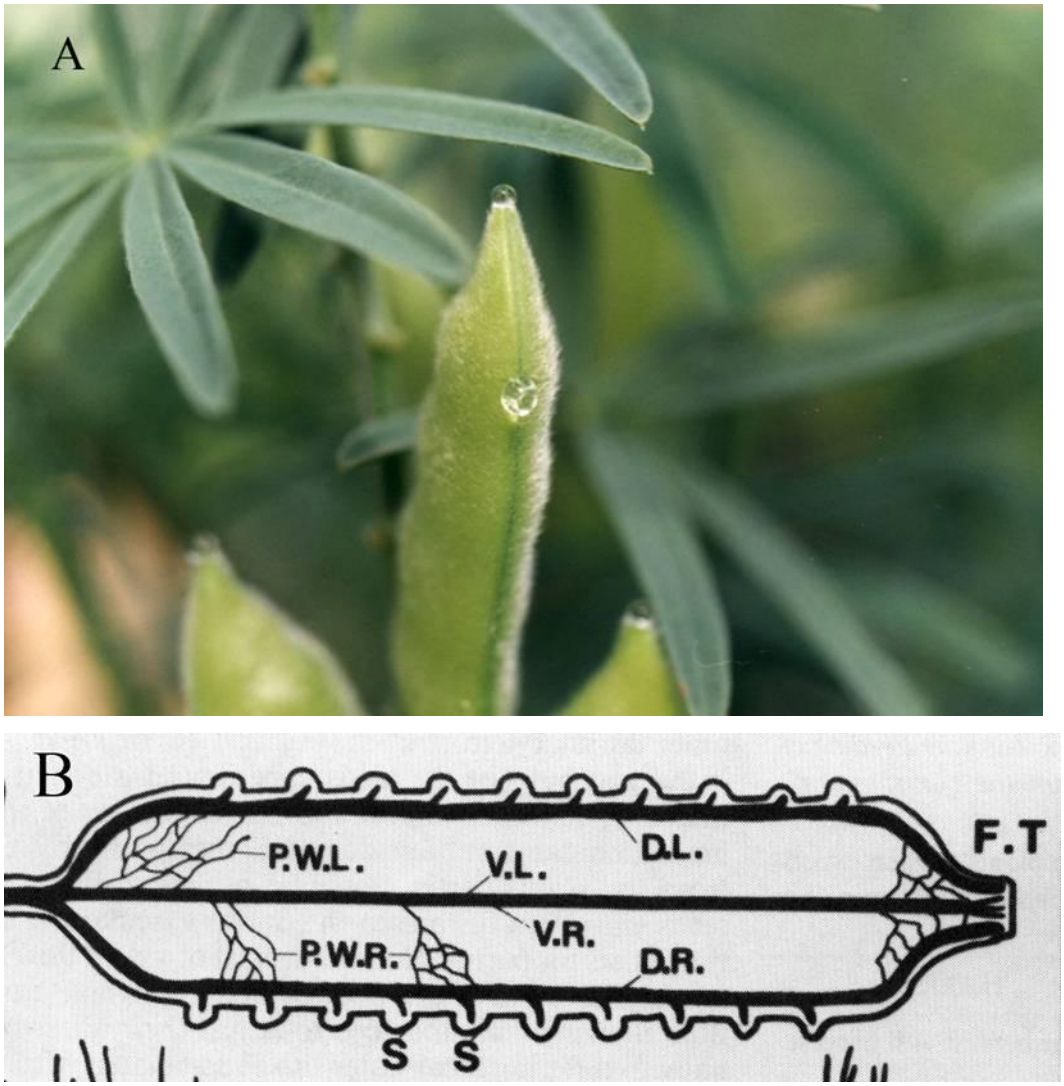

Figure 3.1. A). Phloem exudation from incisions to the ventral suture and the stylar tip of lupin fruits. B). Diagrammatic representation of a legume pod opened along its dorsal suture (DR and DL) and showing its vascular link to the seeds. The vasculature of the ventral suture (VR and VL), the pod wall vasculature (PWL and PWR) as well as the vasculature at the stylar tip of the fruit (FT) is also depicted. R and L refer to the right and left sides of the fruit respectively. The diagram is taken from Pate *et al.* (1985).

EXPERIMENTAL PROCEDURES

Preparation of tissue for microscopy

Tissue was prepared using a method modified from Pate *et al*. (1978). Small blocks of tissue about 4x4 mm were excised from the sutures of young fruits using a double-sided razor blade while the tissue was immersed in a fixative reagent containing 2.5% (w/v) glutaraldehyde in 0.05 M phosphate buffer (pH 7.3). Tissue was held in fixative for 3 h at room temperature, rinsed twice using 0.05 M phosphate buffer (pH 7.3) and then transferred to vials containing 1% (w/v) osmium tetroxide in the same phosphate buffer for 2 h at room temperature. The samples were then rinsed twice with 0.05 M phosphate buffer and passed through a graded series of ethanol solutions at room temperature over two days to dehydrate the tissue. After dehydration, a pre-infiltration step was conducted by placing the tissue samples in propylene oxide for 9 h. Propylene oxide was changed for fresh reagent and the samples held at room temperature overnight. Dehydrated tissue was embedded in Spurr's resin (Spurr, 1969). Blocks of resin-embedded tissue samples were trimmed before sectioning on an Ultra-Microtome (Leica). Semi-thin tissue sections (0.3 µm) were cut using glass knives with a water filled boat attached and stretched with chloroform vapour. The sections were mounted on glass slides, stained with 1% (w/v) Toluidine Blue (pH 9.0) and analysed under an optical microscope (Zeiss Axioplan 2) equipped with an Axiocam digital camera to provide low magnification images of the tissue.

Optical microscope images were also used to determine the optimum orientation of the tissue for further sectioning. Once the orientation of the resin-embedded tissue was clear, ultra-thin sections were cut to gold or silver interference colour (70-90 nm) using a diamond knife and stretched with chloroform vapour. These sections were mounted on ethanol-rinsed 200 square mesh Thin Bar Copper Grids (ProSciTech) and allowed to dry overnight at room temperature before imaging with a JEOL 2100 Transmission Electron Microscope (TEM) equipped with a Gatan Orius digital camera.

RESULTS

While the lupin pod tissue was not wounded prior to its being sampled for microscopy, cutting small 4 mm cube samples from the fruit sutures would have effectively 'wounded' the vasculature causing release of turgor pressure in the phloem. Thus both structural and ultra-structural features described below could reasonably be expected to be typical of tissues that were incised for phloem exudate collection.

Optical microscopy

Low magnification images obtained with the optical microscope provided a view of the vascular and surrounding tissue of the sutures of developing fruit of *L. albus* (Figure 3.2A). In Toluidine Blue stained sections, the whole tissue stained purple except the xylem that stained light blue/green due to the presence of lignin deposited on the cell walls (Figure 3.2B). The dense cytoplasmic content of CC shows a darker purple staining (Figures 3.2B and 3.2C). These cells also show the cell wall protrusions and cytoplasmic invaginations typical of transfer cells. A higher magnification view of the SE-CC complex in Figure 3.2C shows the thicker cell walls of the SE compared to the adjacent parenchyma cells. Each of the vascular bundles in the suture veins are associated with large parenchyma cells that constitute a bundle sheath tissue. It is the bundle sheath that gives the distinctive darker green colour to the sutures as it contains more chlorophyll than the surrounding pod walls (Figure 3.1A). Not surprisingly these bundle sheath cells have obvious chloroplasts which would have been damaged when the veins were incised for phloem exudate collection.

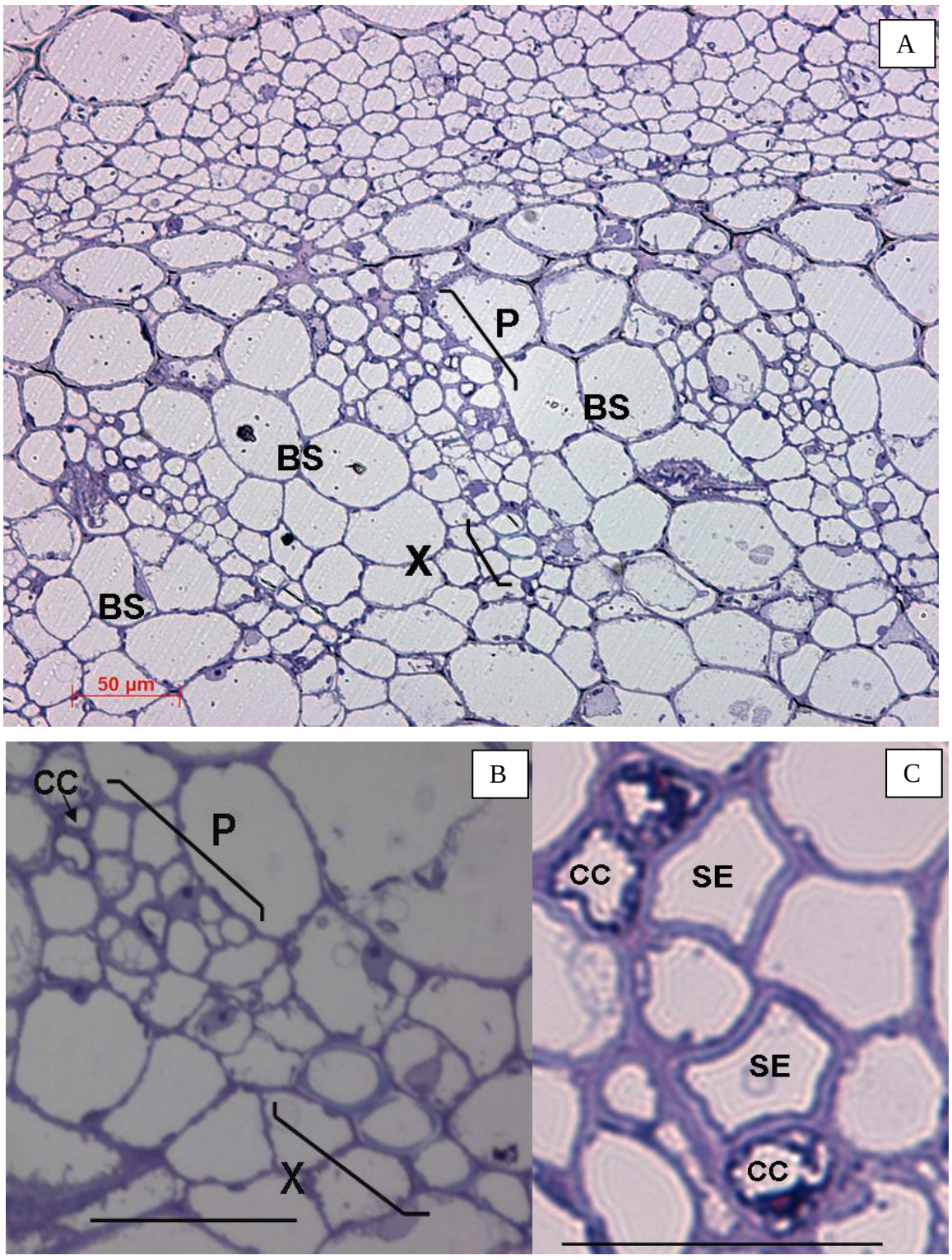

Figure. 3.2. Step-wise magnification of *L. albus* vascular tissue. Transverse semi-thin tissue section of the ventral suture of a developing lupin fruit stained with 1% (w/v) Toluidine Blue pH 9.0. A). Xylem and phloem vascular tissue are located adjacent to each other. Bundle sheath cells surround the vascular tissue. Three vascular bundles are observed. 20X. B). Phloem vascular tissue stains purple. Only xylem vessels stain light blue/green due to presence of lignin in cell walls. 40X. Bar line: 20 µm. C). SE/CC complex. CC are characterised by their dense protoplast. SE lumen looks devoid of contents. SE cell walls are thicker than cell walls from adjacent cells. 100X. Bar line: 10 µm. P, phloem; X, xylem vessels; BS, bundle-sheath cell; SE, sieve element; CC, companion cell.

Transmission Electron Microscopy

Ultrastructural features of *L. albus* phloem vascular tissue were observed using a JEOL 2100 Transmission Electron Microscope (TEM). The large bundle sheath cells surrounding the SE/CC files contained what appeared to be functional chloroplasts (some with small starch granules), nuclei (Figure 3.3) and large vacuoles with a tonoplast. The electron dense parietal cytoplasm of the CC contrasted with the very thin much less dense parietal cytoplasm of the SE. A higher magnification of the CC shows the clearly defined cell wall ingrowths into the parietal cytoplasm, which is rich in ribosomes and contains many mitochondria, golgi body, endoplasmic reticulum (ER) and a plastid with small protein inclusions (Figure 3.4). In some sections a number of mitochondria in the SE, in this case in the lumen of the cell, were recorded (Figure 3.5) while in others what appear to be structural proteins were seen also in the SE lumen (Figure 3.6). Both the mitochondria and the proteins could have been released from the parietal cytoplasm as a result of the sharp release of turgor in the SE on wounding.

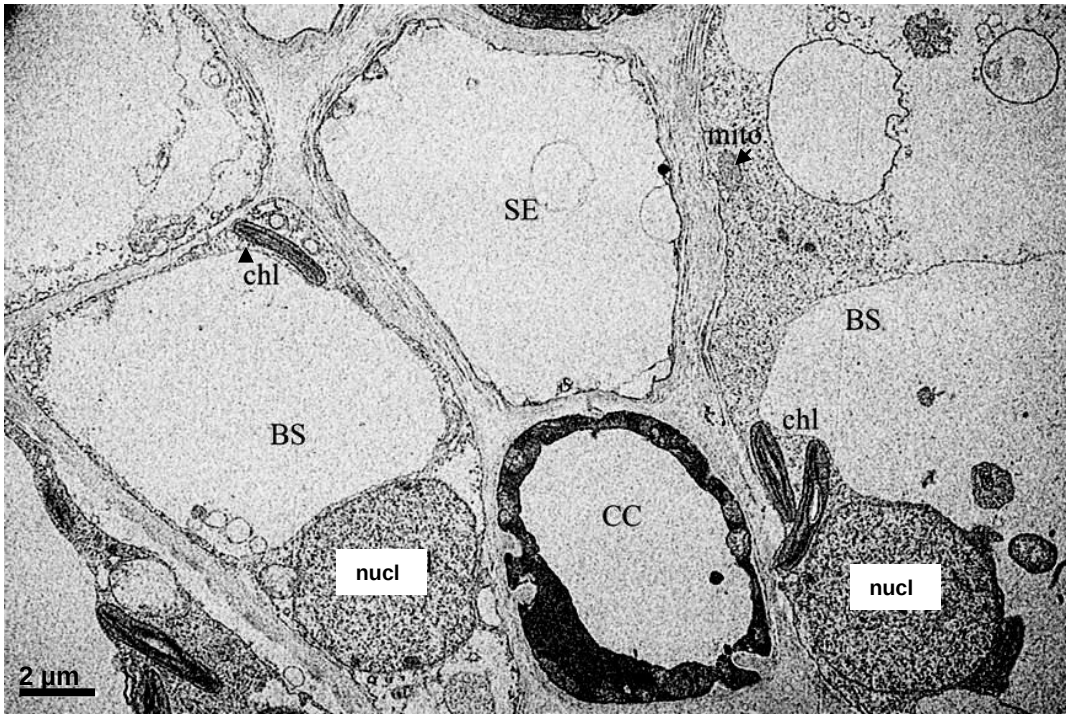

Figure 3.3. Low magnification TEM of a transverse section of fixed vascular tissue from the ventral suture of a developing lupin fruit. The bundle sheath cells (BS) adjoining the SE/CC complex show nuclear (nucl), mitochondrial (mito) and chloroplast (chl) components.

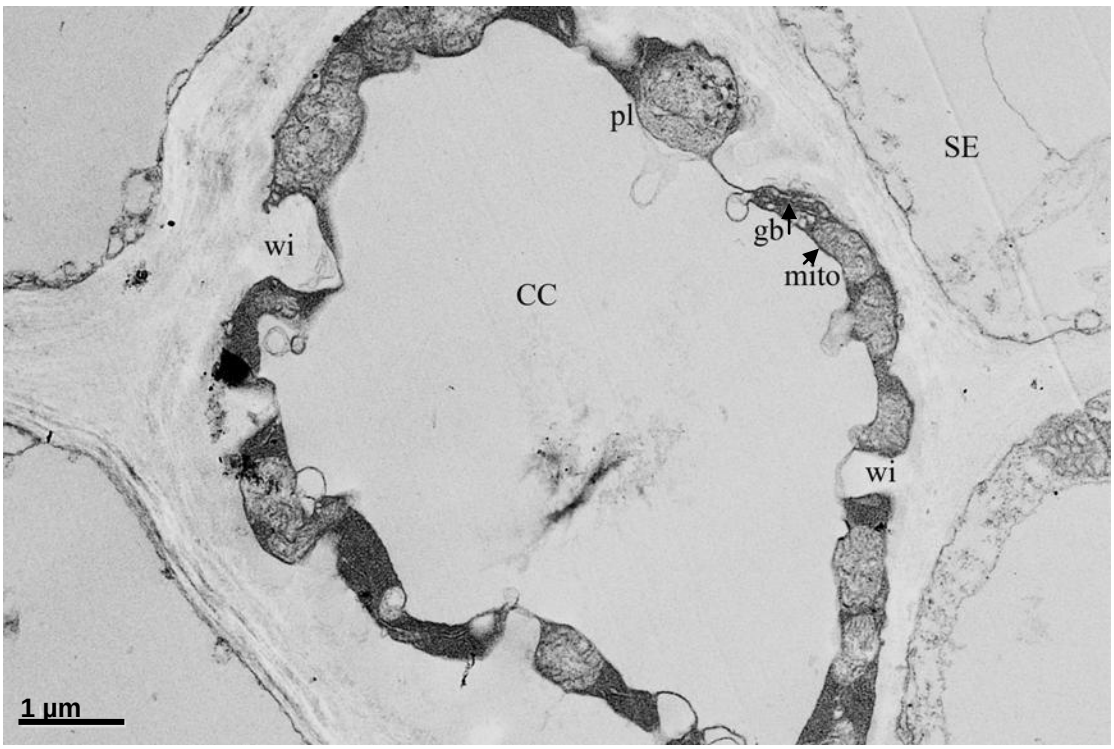

Figure 3.4. Higher magnification of a transverse section of a mature CC from the vasculature of the ventral suture of a developing lupin fruit. A dense parietal cytoplasm and cell wall ingrowths (wi) are characteristic of this type of cell. gb, golgi apparatus; mito, mitochondrion; pl, plastid.

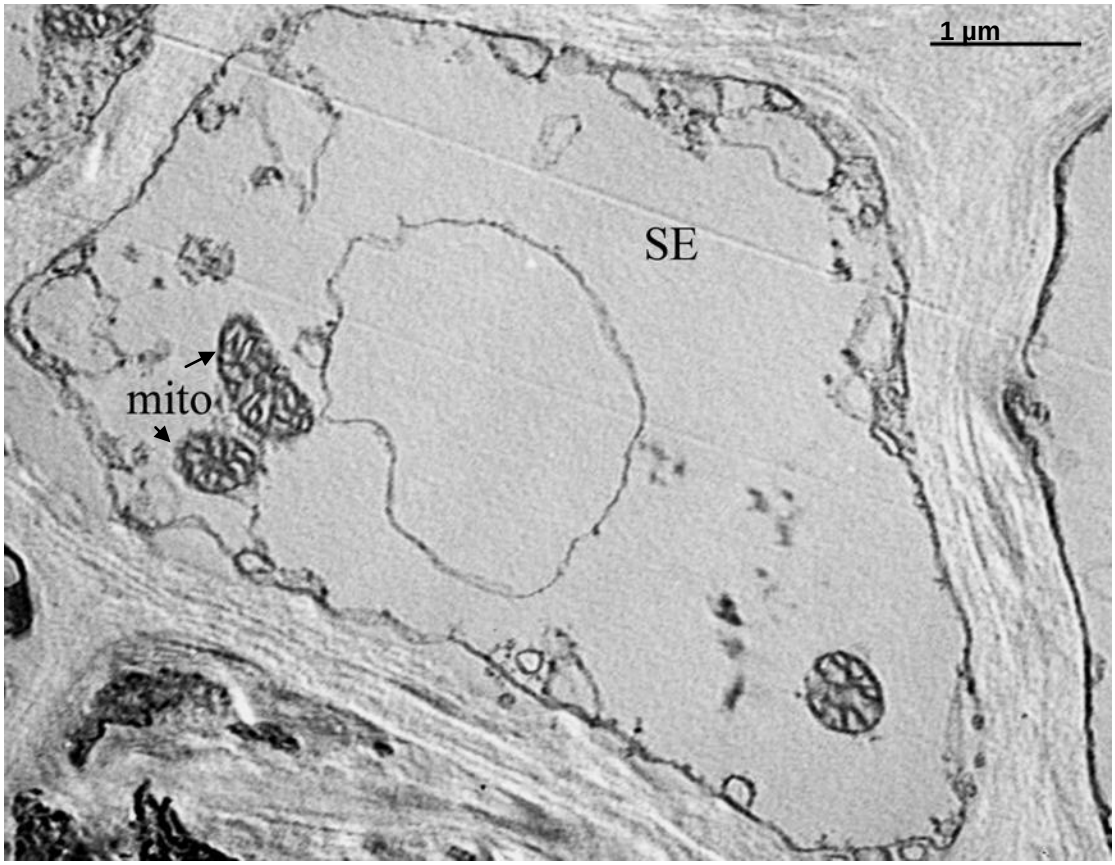

Figure 3.5. Transverse section of a sieve element (SE). Mitochondria (mito) are in the lumen apparently detached from the parietal cytoplasm.

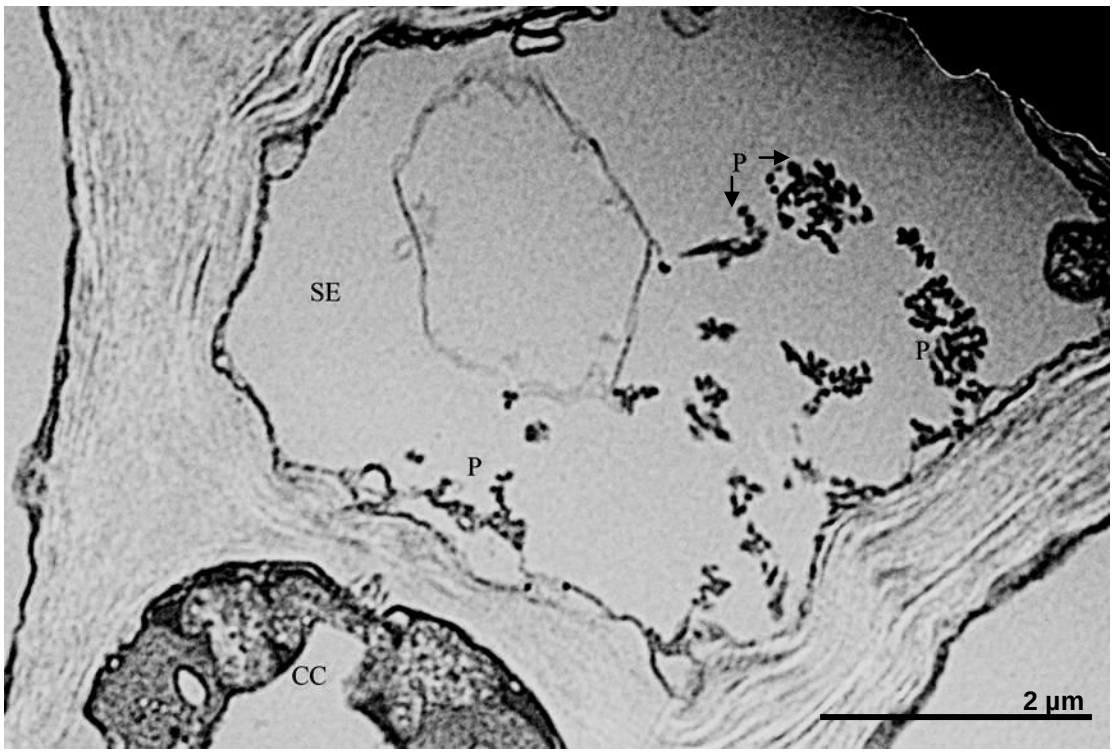

Figure.3.6. Transverse section of sieve element (SE)/ companion cell complex (CC). Structural proteins (P) are observed in the SE lumen with no homogenous distribution.

The SE/CC complex is connected by branched plasmodesmata presenting one pore on the SE side and several branches on the CC side (Figures 3.7 and 3.8). The plasmodesmatal pore unit (PPU) appears to be occluded by dispersed proteins and membranous components (Figures 3.7 and 3.8). Figure 3.7 shows a small double membrane-bound organelle in a parietal position, possibly a P-type plastid that appears to be releasing its contents probably as a result of turgor release during tissue preparation. Despite being disrupted, the SE plastid membrane stayed attached to the plasma membrane and the other membranes also appear to be attached. No connections between the SE/CC complexes with other cells were observed.

The files of SE were also connected by plasmodesmata to form pored sieve plates (Figures 3.9 to 3.11). Sieve pores were surrounded by callose collars and presumably structural proteins were observed on the sieve-plate walls and lumen. The sieve-plate lumen was filled by a dense filamentous material that was also located in front of the sieve pores, apparently occluding them.

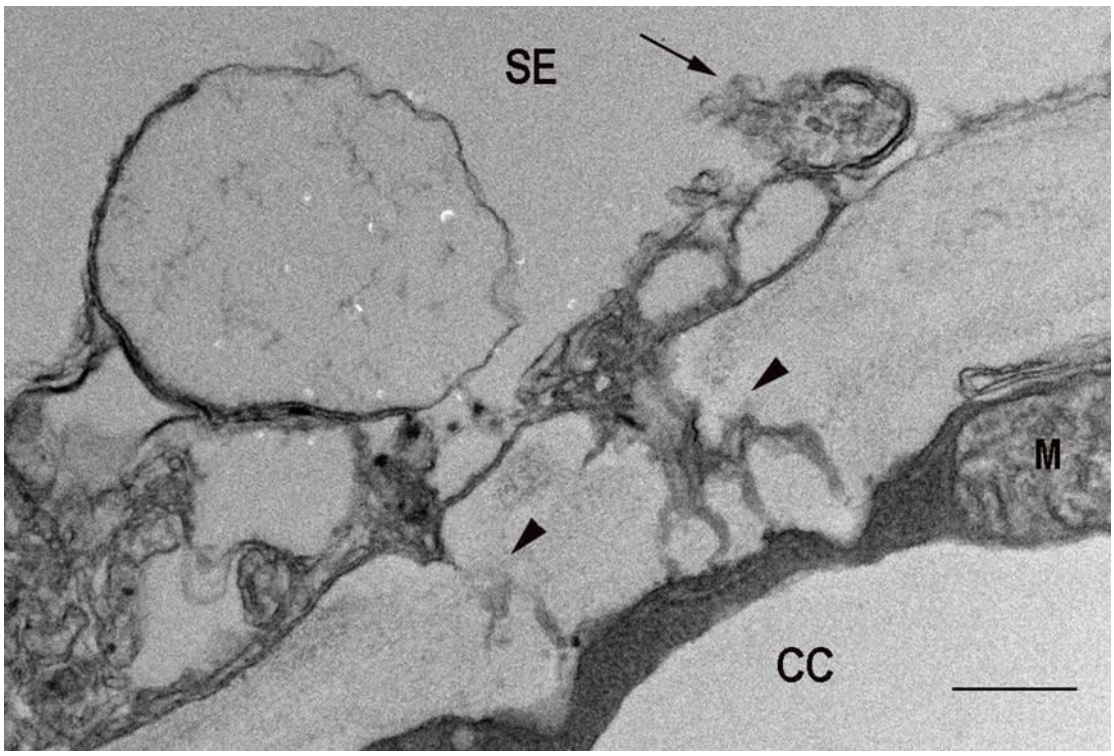

Figure 3.7. Transverse section of branched plasmodesmata (arrowheads) connecting a sieve element (SE) and a companion cell (CC). A presumable plastid located in a parietal position close to the pore (arrow) has released its contents probably as a result of turgor stress during tissue preparation. Structural proteins and membranous material appear to be occluding the pore. M mitochondrion. Bar line: 200 nm.

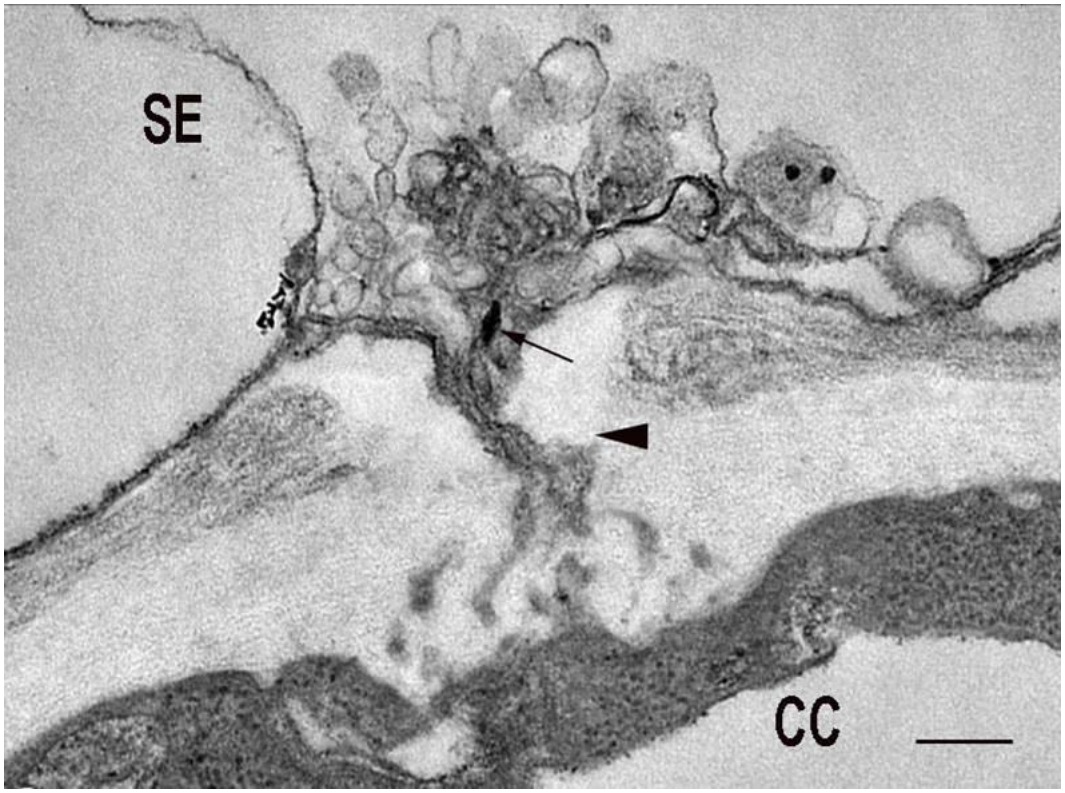

Figure 3.8. Transverse section of branched plasmodesmata (arrowhead) connecting a sieve element (SE) and a companion cell (CC). One pore is on the SE side and several branches on the CC side. Presumably structural proteins (arrow) and membranous material appear to be occluding the pore. Bar line: 200 nm.

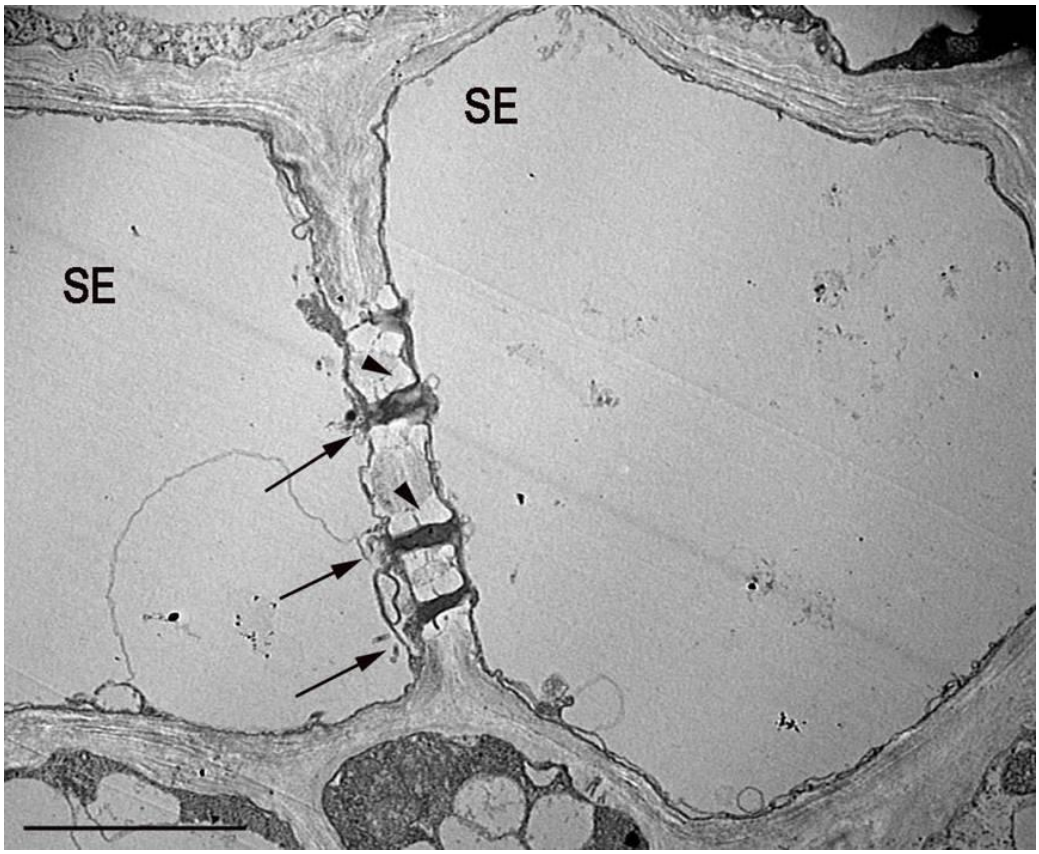

Figure 3.9. Transverse section of sieve elements (SE) connected by sieve-plates (arrows). Filamentous material is in front of the sieve-pores apparently occluding them. Sieve pores are surrounded by callose collars (arrowheads). Bar line: 2 µm

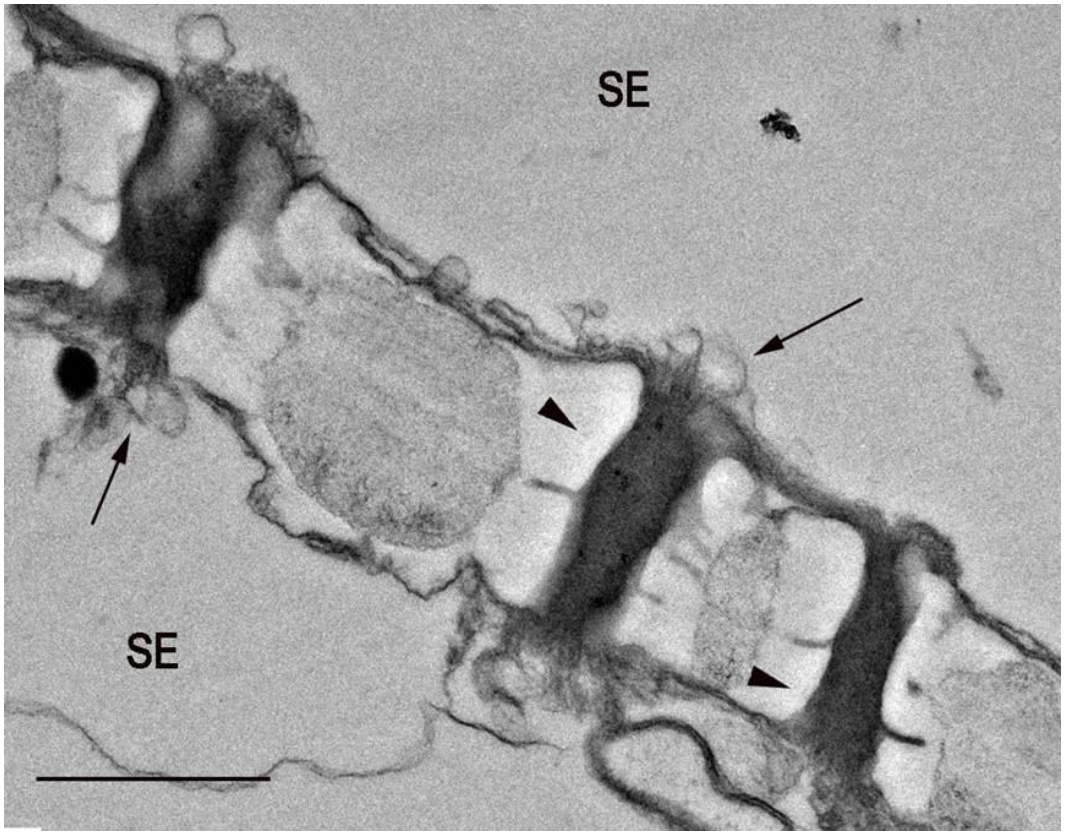

Figure 3.10. See legend for Figure 3.9. Bar line: 0.5 µm

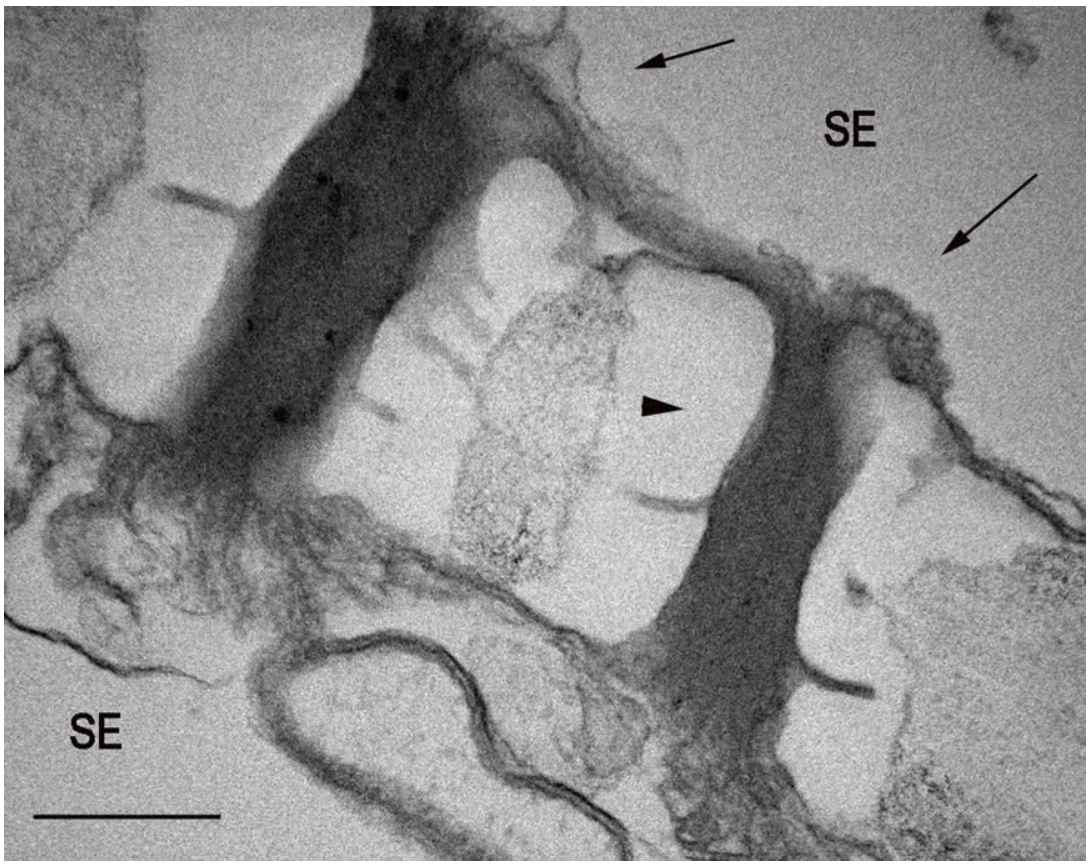

Figure 3.11. See legend for figure 3.9. Bar line: 200 nm

DISCUSSION

The structure of the vasculature within the sutures of the lupin fruit indicates that the incisions made to collect phloem exudate would have cut a range of cell types in addition to the SE. Of particular significance are the files of bundle sheath cells that are closely associated with the vasculature and contain numerous chloroplasts. Thus it seems inevitable that the phloem exudate forming at the wound would have contained both proteins and transcripts associated with photosynthesis. For example, chlorophyll a/b-binding protein and the large and small subunits of Rubisco could be expected to contaminate the exudate. While plastids were seen in some sections of SE and CC these would be most unlikely to provide functional photosynthetic proteins or transcripts. Mitochondria were also found in the SE, but these were dilated compared to those in the CC and surrounding parenchyma. Thus mitochondrial proteins and transcripts in exudate could have come from mitochondria released from a range of other cell types. Evert (1990) has suggested that the mitochondria in the SE may not be very active in view of the dilated appearance

of their cristae. While this may be the case, the significance of these mitochondria in SE functioning remains to be elucidated (van Bel and Knoblauch, 2000).

The structural features of the SE/CC complex found in the vasculature of the fruit sutures are in general consistent with what is known of the structure of translocating phloem in angiosperms, and particularly in other legumes (van Bel, 2003). The transfer cell structure of the CC with its dense protoplast observed in *L. albus* has been reported previously for other species (Pate *et al*., 1978) and has been recognised as a feature to identify CC. Evert (1990) states that unlike the SE member protoplast, which undergoes a selective autophagy and assumes a clear appearance during its ontogeny, the CC protoplast increases in density as it develops. Cell wall ingrowths were also observed in CC of *L. albus* (Figure 3.4) as described in *Vicia faba* and *Zinnia elegans* by Kempers *et al.* (1998). The thicker cell walls of SE have also been documented as a characteristic that aids in the recognition of the sieve-tube member (Evert, 1990). The SE lumen of *L. albus* was observed free of organelles ensuring a low-resistance pathway for mass flow. Only structural proteins, some presumptive plastids and a few mitochondria were observed. The parietal position of SE components may prevent them from being dragged into the translocation stream by turbulence associated with mass flow (Ehlers *et al*., 2000).

A large crystalline P-protein body located in the SE lumen was described initially by Palevitz and Newcomb (1971), and has since been observed in many members of the Fabaceae (Fisher, 1975; Evert, 1990; van Bel and van Rijen, 1994; Ehlers *et al*., 2000). These structures were not seen in SE in this study. However, the tissue was damaged such that turgor release and dispersal of such crystalline protein bodies might have been expected to have occurred in most SE as part of the rapid sealing response. The only structural proteins observed in *L. albus* SE were dispersed throughout the lumen (Figure 3.6) and did not resemble the much larger structure described for other legumes (Knoblauch *et al.,* 2001). To obtain a closer insight into the *in vivo* structure of SE, more careful tissue preparation using the techniques employed by Knoblauch and van Bel (1998) to preserve SE is required. Ehlers *et al*. (2000)

observed that crystalline P-proteins of injured *V. faba* (broad bean) SE were dispersed to different degrees and perhaps the dispersed proteins seen in the wounded lupin tissue in this study, is an extreme example of this. Turgor release and a physical surge of the translocation stream in phloem during tissue preparation would have undoubtedly altered the ultra-structural features of SE (Ehlers *et al*., 2000). The occurrence of mitochondria in the SE lumen (Figure 3.5) and 'exploded' plastids releasing their contents (Figure 3.7) were likely consequences of turgor release in this study.

Plugged sieve pores were a feature of the SE in this study of *L. albus* and in this respect closely resembled the 'injured' phloem in *V. faba* described by Ehlers *et al*. (2000). The dense fibrillar-like deposits within the sieve pores (Figures 3.9-3.11) have been ascribed to dispersed crystalline proteins (Ehlers *et al*., 2000; van Bel, 2003). Knoblauch and van Bel (1998) point out that a likely consequence of the surge produced by turgor release is that parietal proteins are torn away or detached from the SE plasma membrane building a covering layer on the developing plug. Substances released from disrupted P-plastids along with parietal proteins detached from the plasma membrane and dispersed crystalline P-proteins have been observed to form a conglomerate that plugs the sieve-pores in injured SE (Knoblauch and van Bel, 1998; van Bel *et al*., 2002). The pores, especially those between SE and CC, were also occluded by membranous material that could not be ascribed to any of the organelles but which may part of the 'normal' response to turgor release. Although ER with a parietal position has been observed in SE of many species, in some cases aggregated with parietal P-proteins (Ehlers *et al*., 2000), none was obvious in *L. albus* SE. However, it could be that turgor release caused displacement of the ER from a parietal location towards the pores, becoming part of the occlusion.

The fact that membranes of disrupted P-type plastids in SE were apparently still attached to the plasma membrane (Figure 3.7) is consistent with the idea that P-plastids or SE components in general are anchored in some way to the walls. Ehlers *et al*. (2000) found small, clamp-like structures connecting the SE plasma membrane and the outer membranes of plastids, mitochondria or parietal ER cisternae. Anchorages were also observed to occur between the

outer membranes of the SE organelles and the ER cisternae. It is thought that these structures may be responsible for the strictly parietal positioning of the cytoplasm (Ehlers *et al*., 2000). Clamp-like structures could then explain why the outer membrane of *L. albus* SE presumably plastids remained adhered to the plasma membrane after plastid disruption due to turgor pressure release.

No plasmodesmatal connections were seen between the SE/CC complex and adjacent cells of the bundle sheath in *L. albus*. In yellow lupin (*L. luteus*), van Bel and van Rijen (1994) observed that a phloem mobile dye did not move between the SE/CC complex and the adjoining phloem parenchyma cells. They suggested that the SE/CC complexes are symplasmically isolated from the phloem parenchyma cells in phloem of *L. luteus* and perhaps this is a feature of the genus *Lupinus*.

CHAPTER 4

PROTEOMIC ANALYSIS OF *Lupinus albus* PHLOEM EXUDATE

INTRODUCTION

The phloem long-distance translocation system of plants functions both as a nutrient delivery system and as an information pathway by which signal molecules are disseminated around the plant. These signals include not only known signalling factors, such as growth-regulators or bioactive peptides but also proteins and RNA (Lough and Lucas, 2006; Gomez *et al.*, 2005; Yoo *et al.*, 2004; Dinant *et al.*, 2003; Ruiz-Medrano *et al*., 2001; Oparka and Santa Cruz, 2000). Establishing the functional significance of macromolecules in the phloem translocation stream and the roles they play in the integration of whole plant signalling processes is the focus of a number of recent studies (Kehr and Buhtz, 2008; Lough and Lucas, 2006).

Although mature sieve elements (SE) lack ribosomes and nuclei, and are thus not equipped for transcription and translation, a large number of polypeptides have already been identified in phloem exudate collected by stylectomy and from incisions to the vasculature. These proteins are likely to have been synthesized in the companion cells (CC) and transported to SE via plasmodesmata (van Bel, 2003; Oparka and Santa Cruz, 2000). Using ^{35}S-labelled methionine supplied to wheat leaves Fisher *et al*. (1992) recovered rapidly labelled proteins in exudate collected by aphid stylets; consistent with the idea that currently expressed proteins are transferred from the CC. It is thought that many of the proteins found in phloem exudate are likely to be anchored in the parietal cytoplasmic layer *in vivo* but are released by the sudden loss of turgor resulting from incisions to the SE (Walz *et al*., 2004). Others may be washed out of damaged CC and parenchyma by the exudate collected at the wound site. These considerations were discussed earlier

(Chapter 1) and must be taken into account when interpreting the possible functions of proteins in exudates collected from wounded vasculature. Nevertheless, characterisation of proteins present in phloem could provide greater insight into the functions of the vascular system including identification of peptide/protein signalling components that may participate in long distance communication between distantly located organs (Lough and Lucas, 2006). There is now no doubt that some proteins are indeed translocated. Golecki *et al.* (1999) demonstrated the long distance movement of structural phloem proteins (P proteins) across a graft union consisting of *Cucurbita* stocks and *Cucumis sativus* scions. These proteins are associated with the wound response in SE and were long regarded as immobile in phloem (Cronshaw, 1981). In a series of elegant experiments Aoki *et al.*, (2005) labeled and injected two isolated pumpkin phloem proteins into the vasculature of intact rice plants through severed leaf hopper stylets to provide evidence for specificity in protein translocation. Interaction of one of the proteins, CmPP16-1, with other phloem proteins appeared to positively regulate translocation of this protein to the roots.

Proteomic analysis of phloem exudate collected from cucurbits (Lin *et al*., 2008; Walz *et al*., 2004; Haebel and Kehr, 2001), castor bean (*Ricinus communis)* (Barnes *et al*., 2004)*, Brassica napus* (Giavalisco *et al*., 2006), rice (*Oryza sativa)* (Aki *et al*., 2008) and lupin (Marentes and Grusak, 1998) has identified a complex population of proteins. These plant species are convenient for the study of phloem contents since they exude significant amounts of phloem after incisions are made in the vasculature (except for rice that has been sampled using leaf hopper stylets). These analysis have revealed a range of proteins involved in different processes such as antioxidant defence including thioredoxin-h and peroxidase, structural and maintenance components including phloem protein 1 (PP1) and phloem protein 2 (PP2), proteinase inhibitors including trypsin and chymotrypsin inhibitors and RNA binding proteins (Aki *et al*., 2008; Giavalisco *et al*., 2006; Walz *et al*., 2004; Yoo *et al*., 2004; Walz *et al*., 2002;). FLOWERING LOCUS T (FT), which is considered to be the long distance signal that regulates flowering (‘florigen’), has also been identified in phloem exudate (Aki *et al*., 2008; Giavalisco *et al*., 2006).

Mass spectrometric approaches have been used for analysis of the phloem proteome (Gaupels *et al*., 2008a; Giavalisco *et al*., 2006; Barnes *et al*., 2004; Hoffmann-Benning *et al*., 2002; Haebel and Kehr, 2001; Marentes and Grusak, 1998). Marentes and Grusak (1998) identified and characterized a number of low molecular weight proteins ranging from 2 to 10 kDa in exudate of *Lupinus albus* and *Pisum sativum* using matrix-assisted laser desorption/ionization time-of-flight mass spectrometry (MALDI-TOF-MS). Later, Hoffmann-Benning *et al*. (2002), combined high-performance liquid chromatography (HPLC) and MALDI-TOF-MS to compare peptides and small protein contents of the phloem exudate from flowering and non-flowering plants of *Perilla ocymoides* as well as from *L. albus*. The combination of these techniques allowed them to identify more peptides than those previously reported by Marentes and Grusak (1998); more than 100 molecules between 1 and 15 kDa. The techniques used in the studies described above have permitted identification and characterisation of some proteins present in phloem exudate of different plant species. However, MALDI-TOF-MS cannot provide a complete description in species like *L. albus* for which there is little genome sequence information. The identification of proteins by homology in plants like *L. albus* requires partial sequence determination using MS/MS. In this technique, a given parent (precursor) ion is selected from a mass spectrum and then 'broken up' to obtain product or daughter ion spectra (Standing, 2003). The series of product ions contains sufficient information to determine the peptide sequence and this in turn provides a means to assign an identity to the protein using protein database information (Standing, 2003).

While proteomic analysis of phloem exudates has been applied successfully to a number of dicotyledon species and, with the aid of sap sucking insects, for rice and barley, similar detailed analyses of proteins over a wide mass range for legume species have not been reported. In this study, partial sequence determination by MS/MS and subsequent protein database searches were used to identify proteins separated using 2D electrophoresis from *L. albus* phloem exudate collected from developing fruits and the inflorescence raceme. The likely function of the proteins identified within lupin phloem exudate is discussed in relation to their possible translocation.

EXPERIMENTAL PROCEDURES

Measurement of total protein concentration in phloem exudate

Phloem exudate was collected from *L. albus* plants as described in 'General Methods' (Chapter 2). Total protein concentration in phloem exudate was determined using the Bradford assay (Bradford, 1976) as described in the micro-assay protocol supplied with Biorad Dye concentrate. Six dilutions of bovine serum albumin (BSA) protein standard were prepared in water to a final volume of 800 µl. 200 µl of dye reagent concentrate was added to each standard and phloem protein sample, which were then incubated at room temperature for 15 min. The absorbance of each standard and sample was measured at 595 nm.

In cases where protein was dissolved in buffers incompatible with the Bradford method, such as buffers containing urea and/or high concentrations of detergent, the Peterson-Lowry method was used (Peterson, 1983). 10 µl of concentrated phloem protein was diluted to 400 µl using double distilled water. 0.05 mg soluble yeast RNA and 400 µl 72% (w/v) trichloroacetic acid (TCA) were added followed by incubation at 4˚C overnight. The sample was centrifuged at 12,000 *g* for 20 min at 4˚C. The supernatant was discarded and 500 µl cold (-20°C) acetone added to the pellet followed by incubation at -20˚C for 10 min. The sample was centrifuged at 12,000 *g* for 10 min and at 4˚C, the supernatant discarded and the pellet dried under vacuum for approximately 10 min. Six dilutions of BSA protein standards were prepared in water in a final volume of 400 µl. Once dried, the pellet was resuspended in 400 µl reagent A containing 25% CTC reagent (4 mM $CuS0_4.5H_20$, 0.9 M Na_2CO_3, 7 mM $KNaC_4H_4O_6.4H_2O$), 2.5% (w/v) SDS and 0.2 M NaOH. Reagent A (400 µl) was also added to each standard. 400 µl double distilled water was added to the samples followed by incubation at 21°C for 10 min. 200 µl of 17% Folin-Ciocalteu reagent in water was added to each standard and protein sample and they were incubated at room temperature for 30 min. The absorbance of each standard and sample was measured at 750 nm.

Preparation of a protein fraction from phloem exudate

A number of methods for concentration of the protein in phloem extract were tested to determine which resulted in the best recovery and provided material most suitable for subsequent analysis by one and two dimensional electrophoresis.

i. Phloem exudate was diluted 1:1 using 20% (w/v) trichloroacetic acid (TCA) followed by incubation of the sample for 20 min on ice. Samples were centrifuged at 12,000 *g* for 15 min at 4°C. The supernatant was removed and the resultant pellet washed twice with 500 µl cold 70% ethanol. The pellet was dried and resuspended in Tris buffered saline (TBS) containing 10 mM Tris (pH 7.2) and 500 mM NaCl.

ii. Phloem exudate was diluted in three volumes of cold (-20°C) acetone followed by incubation at -20°C overnight. The proteins were collected by centrifugation at 12,000 *g* for 15 min and the pellet dried and resuspended in TBS.

iii. Ammonium sulphate precipitation used 6.9 g of finely ground ammonium sulphate powder that was added in small portions to 10 ml of phloem exudate under constant agitation. Salts were allowed to dissolve before adding the next portion. The sample was incubated at 4°C for approximately 6 h to allow precipitation and pH was checked regularly and maintained close to neutral using 1 M Tris. The suspension was centrifuged in a Beckman JA-20 rotor at 12,000 *g* for 30 min and at 4°C and the pellet resuspended in 200 µl of TBS. This sample was dialysed overnight at 4°C against TBS using the Mini Dialysis Kit with an 8kDa cut-off (Amersham, Biosciences) following the manufacturer's instructions. Protein concentration was determined by Bradford assay as described above and samples were run on a 12% SDS-polyacrylamide gel.

iv. 10 ml aliquots of phloem exudate were concentrated on a Centriprep® Centrifugal Filter Device (Ultracel YM-3, 3000MWCO, Millipore) in a Beckman Swinging-bucket rotor at 4˚C for 6 h at 3,000 *g*. The final volume of the concentrated protein sample was approximately 1 ml. Protein concentration was

determined by Bradford Assay and the sample was run on a 12% SDS-PAGE. Phloem protein concentrated using the filter was subsequently used for 2D-electrophoresis.

Following column concentration, 700 µl of concentrated phloem sample was precipitated using 9 vol of cold (-20˚C) methanol. The sample was incubated overnight at -80˚C and then centrifuged at 12,000 *g* for 30 min in a Beckman JA-20 rotor at 4˚C. The resultant pellet was air dried at room temperature and resuspended in 600 µl 2-D lysis buffer containing 9 M Urea and 2% (w/v) CHAPS (3-[(3-cholamidopropyl)dimethyl-ammonio]-1-propanesulfonate).

One dimensional sodium dodecylsulphate polyacrylamide gel electrophoresis (SDS-PAGE)

SDS-PAGE was performed according to the procedure described by Laemmli (1970) and following the protocol described in the QIAexpress® detection and assay handbook from QIAGEN. A 0.75mm thick 12% (w/v) acrylamide/0.12% (w/v) bis-acrylamide (BioRad) mini-gel containing 40% 2.5x separating gel buffer (1.87 M Tris-HCl, pH 8.9 and 0.25% (w/v) SDS), 0.0005% (v/v) TEMED and 0.15% (w/v) ammonium persulfate was poured between assembled gel plates. A 4% (w/v) acrylamide/0.04% (w/v) bisacrylamide stacking gel containing 20% 5x stacking gel buffer (0.3 M Tris-phosphate, pH 6.7 and 0.5% (w/v) SDS), 0.0006% (v/v) TEMED and 0.15% (w/v) ammonium persulfate was poured on top of the separating gel. 5x SDS sample buffer (0.06 M Tris-HCl pH 6.8, 0.1% (v/v) glycerol, 2% (w/v) SDS, 0.05% (v/v) β-mercaptoethanol and 0.001% (w/v) bromophenol blue) was added to the sample to a final concentration of 1X. The sample was denatured by heating at 95°C for 5 min before loading onto the gel. BenchMark^{TM} pre-stained protein ladder (5.7kDa – 170.8 kDa) was run next to the samples. Gels were run for approximately 2.5 h at 15 mA in the Mini Protean II (BioRad) system using 1x electrophoresis buffer (0.1 M glycine, 25 mM Tris and 0.1% (w/v) SDS).

Gels were stained using Coomassie brilliant blue R250 (Sigma) solution (0.25% (w/v) Coomassie brilliant blue R250, 45% (v/v) methanol and 10% (v/v) acetic acid). Gels were incubated for 30 min in the staining solution with constant

gentle agitation and destained overnight in Coomassie blue destaining solution (40% (v/v) methanol, 10% (v/v) glacial acetic acid, 3% (v/v) glycerol).

Two-dimensional Polyacrylamide Gel Electrophoresis (2D-PAGE)

2-D gels were run according to the "2-D Electrophoresis Principles and Methods" handbook from Amersham Biosciences.

First-dimension Isoelectric Focusing (IEF)

IEF of protein extracts used 13 cm, pH 3-10 non linear immobilised pH gradient (IPG) strips (Immobiline^{TM} DryStrip, GE Healthcare) on a Multiphor II system (Pharmacia). 2% (v/v) IPG buffer pH 3-10 NL (Amersham Biosciences), 1% (w/v) 1,4-dithiothreitol (DTT) and 0.002% (w/v) bromophenol blue were added to concentrated phloem protein dissolved in 2-D lysis buffer (described above). Each strip was rehydrated overnight at 21ºC using 250 µl (approximately 1000 µg protein) of this solution. An Immobiline DryStrip Reswelling Tray (GE Healthcare) was used to hold the IPG strips during rehydration. Strips were focused at a total of 17kVh at 20˚C. Focused IPG strips were stored at -80˚C when the second dimension was not run immediately.

Second dimension SDS-PAGE

SDS-PAGE was performed as above, except that gels were 16 x 18 x 0.5 cm and contained 12.5% (w/v) acrylamide. Immediately prior to the second-dimension run, focused IPG strips were incubated in 10 ml of equilibration buffer (2% (w/v) SDS, 50 mM Tris-HCl pH 8.8, 6 M Urea, 30% (v/v) glycerol and 0.002% (w/v) bromophenol blue) containing 100 mg DTT at room temperature for 15 min, followed by a second incubation in 10 ml of equilibration buffer containing 250 mg iodoacetamide (IAA) and at room temperature for 15 min. An equilibrated IPG strip was placed between the glass plates on the surface of the second-dimension gel. 20 µl of Benchmark^{TM} Pre-stained protein ladder (5.7-170.8 kDa, Invitrogen) was applied to a piece (0.5 x 0.5 mm) of electrode strip IEF (Amersham Biosciences) and placed on the surface of the gel next to the acidic end of the IPG strip. The electrophoresis conditions were 15 mA/gel for 30 min followed by 30 mA/gel for approximately 4.5 h at 4˚C in a Hoefer SE600 unit (BioRad).

After electrophoresis, gels were stained using colloidal Coomassie Brilliant Blue G-250 following the protocol described by Rabilloud and Charmont (2000). Gels were fixed in 30% (v/v) ethanol and 2% (v/v) phosphoric acid for 30 min. The fixation was repeated twice. Then gels were rinsed in 2% (v/v) phosphoric acid 3 times for 20 min each. Gels were equilibrated for 30 min in a solution containing 2% (v/v) phosphoric acid, 18% (v/v) ethanol and 15% (w/v) ammonium sulphate. After this time, 1% (v/v) of a 2% Brilliant Blue G solution was added to the equilibration mix. Gels were stained for three days and rinsed with double distilled water, then digitally imaged using a GS-800 calibrated scanner. Gels were sealed in a plastic bag and stored at 4˚C.

Protein analysis by mass spectrometry

Protein digestion

Protein spots were excised from stained 2D gels using sterile scalpel blades and placed in low protein binding 1.5 ml tubes (LoBind Tubes, Eppendorf). Spots were destained in a solution containing 40% (v/v) acetonitrile (ACN) and 12 mM ammonium bicarbonate. This step was repeated until all dye had been removed. Destained gel spots were dehydrated by rinsing twice with 100% ACN. Gel spots were then dried by vacuum centrifugation for 15 min. 15 µl of 12 ng/µl of sequencing grade Trypsin (Promega) in 50 mM ammonium bicarbonate was added to the dried gel spots and samples were incubated at 4˚C for 1 h. Excess of trypsin was removed after incubation and 15 µl of 20 mM ammonium bicarbonate added. Samples were incubated at 37˚C overnight.

N-terminal derivatisation

N-terminal derivatisation of the protein samples was done using 4-sulphophenyl isothiocyanate (SPITC reagent, Sigma). 8 µl of SPITC was added to an equal volume of trypsin-digested sample followed by incubation at 55°C for 30 min. After incubation, triflouroacetic acid (TFA) was added to a final concentration of 0.3%.

MALDI MS/MS

After derivatisation, samples were desalted and concentrated with PerfectPure C-18 Tips (Eppendorf) to increase MS spectra quality following the manufacturer's instructions. Protein samples were eluted using 10 mg/ml of matrix (α-cyano-4-hydroxycinnamic acid, Sigma) solution containing 0.1% (v/v) TFA and 70% (v/v) ACN directly onto a MALDI target plate.

Samples were processed using a quadrupole time-of-flight hybrid mass spectrometer (QSTAR XL mass spectrometer) running with the oMALDI ionisation source. The instrument was calibrated with the fragmentation spectrum of Glu-Fibrinogen B (Sigma, molecular weight 1570.67). After obtaining the MALDI MS spectra, individual peptide ions with a higher number of counts and mass/charge (m/z) values were selected for further fragmentation to obtain product or daughter ion spectra. Partial amino acid sequences were derived manually from the product spectra. These partial sequences were subsequently used for protein database searches using the short, nearly exact matches BLAST algorithm (Expect threshold: 20000; word size: 2; matrix: PAM30) at the National Center for Biotechnology Information (NCBI) database. In the cases where no similar proteins could be found, further searches in the EST database were performed using the tblastn algorithm also at NCBI. Additional searches were done in an in-house lupin database containing unpublished ESTs kindly provided by collaborators at the Australian Commonwealth Scientific and Research Organization (CSIRO) and on ESTs from lupin phloem exudate obtained in this study (see Chapter 5). Matches were considered significant when identity was greater than 85%.

RESULTS

Preparation of a protein fraction from phloem exudate

Phloem exudate protein concentration determined by Bradford assay was on average 0.26 mg/ml. This was too low to permit visualisation of separated

proteins with PAGE, so a number of methods were investigated to concentrate the protein and remove sucrose which may interfere with electrophoresis.

Following precipitation with either TCA or cold acetone the protein pellet proved difficult to re-solubilise, possibly due to the high concentration of sucrose (10-20% w/v) in samples. Ammonium sulphate precipitation permitted better recovery of the protein pellet. The protein concentration after precipitation was on average 2.3 mg/ml. However, despite the acceptable yield of protein obtained with this method, the salt content present in the ammonium sulphate precipitated sample, even after dialysis, precluded effective 2-D electrophoresis.

Good protein recovery was also obtained using column filters. A final concentration of 2.25 mg/ml was determined by Bradford Assay. As these samples also had low salt concentration they were suitable for 2D-electrophoresis and this method for protein concentration was used for all further work. A typical 1D separation of phloem proteins of *L. albus* is shown in Figure 4.1.

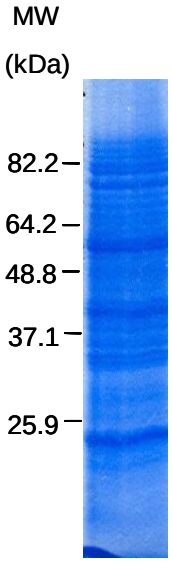

Figure 4.1. SDS-PAGE separation of *L. albus* phloem exudate proteins after column concentration. Phloem protein was concentrated using Centriprep® Centrifugal Filter Devices (3000MWCO) at 4°C for 6 h. The concentrated sample was run on a 12% SDS-PAGE. Protein gel was stained using Coomassie brilliant blue R250. Molecular mass markers are shown to the left of the figure.

De novo peptide sequencing by MS/MS

Phloem exudate was collected from fruits and inflorescence stems of *L. albus* plants as described earlier. Approximately 1 mg phloem protein was used for protein separation on 2D gels permitting resolution of more than 200 different protein spots (Figure 4.2). Of these, 130 were collected and partially sequenced

by MS/MS with 83 identified by their high level of similarity to sequences in protein databases (Table 4.1). These identified proteins matched 56 unique accession numbers as some of the identified proteins were present in more than one spot. Of the sequenced proteins, 37% were classified as 'unknown' (Figure 4.3). This group (see Appendix 1) included 9 spots that contained peptides either at too low concentration or that exhibited adverse fragmentation behaviour resulting in poor spectra that were difficult to interpret, and 38 spots showing no significant homology to any protein in the database or that matched proteins of an unknown function. Some of the more prominent protein spots (4, 8, 9, 10, 11, 13 and 16 in Figure 4.2) were in this latter category.

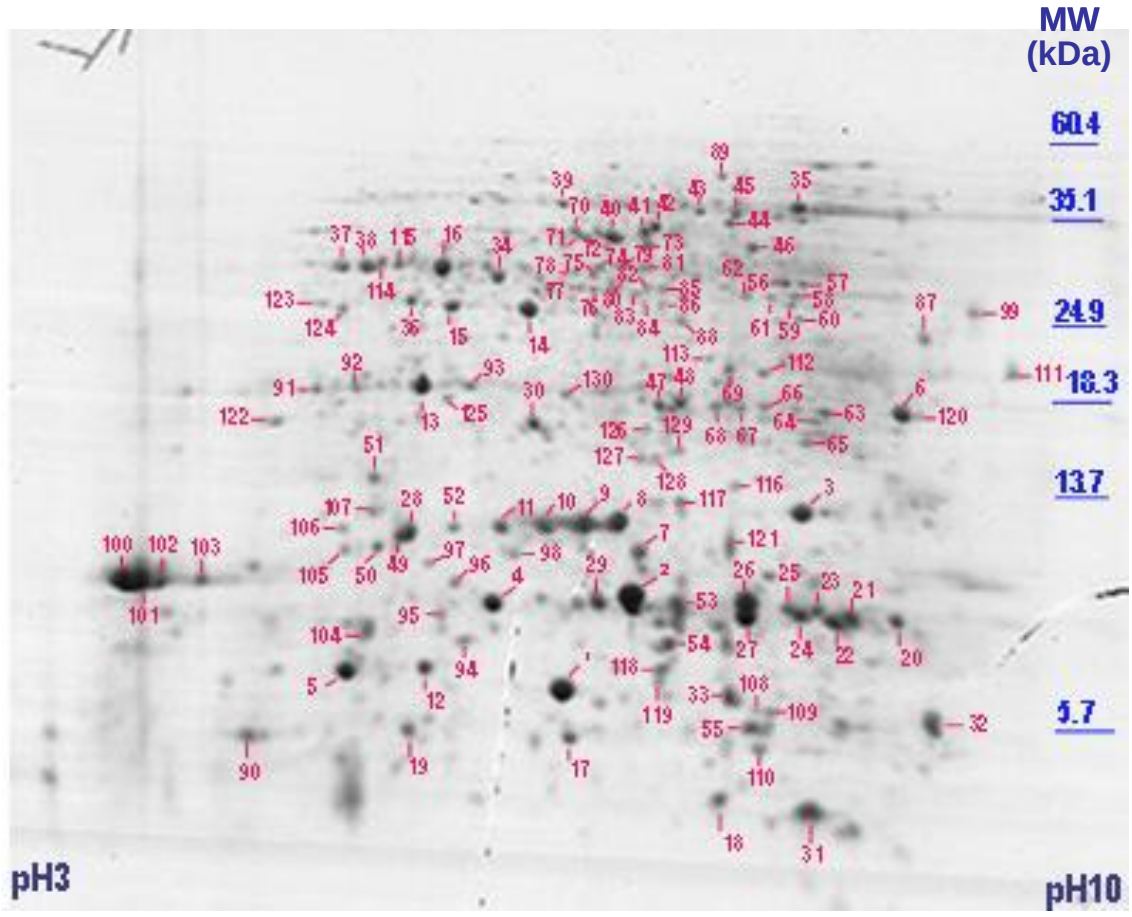

Figure 4.2. 2D gel electrophoresis separation of polypeptides in *L. albus* phloem exudate. Phloem exudate was collected from the vasculature of developing fruits and the inflorescence raceme. 1 mg of protein was separated and stained using colloidal Coomassie Brilliant Blue G250. Protein spots were excised, digested with trypsin and analysed by partial sequence determination by MS/MS and subsequently by using database searches. Molecular mass markers are shown to the right of the figure.

Proteins that were identified by homology in the database searches (Table 4.1) were grouped by putative function (Figure 4.3) into proteins involved in stress

and defence response, redox regulation, energy metabolism, general metabolism, protein synthesis and turnover, nucleic acid binding, cell wall synthesis, photosynthesis and signalling. The largest group of identified proteins comprised those involved in metabolism (10% general metabolism and 12% energy metabolism), followed by redox regulation (13%), protein synthesis and turnover (9%), cell wall synthesis (6%), with fewer numbers in the other groups.

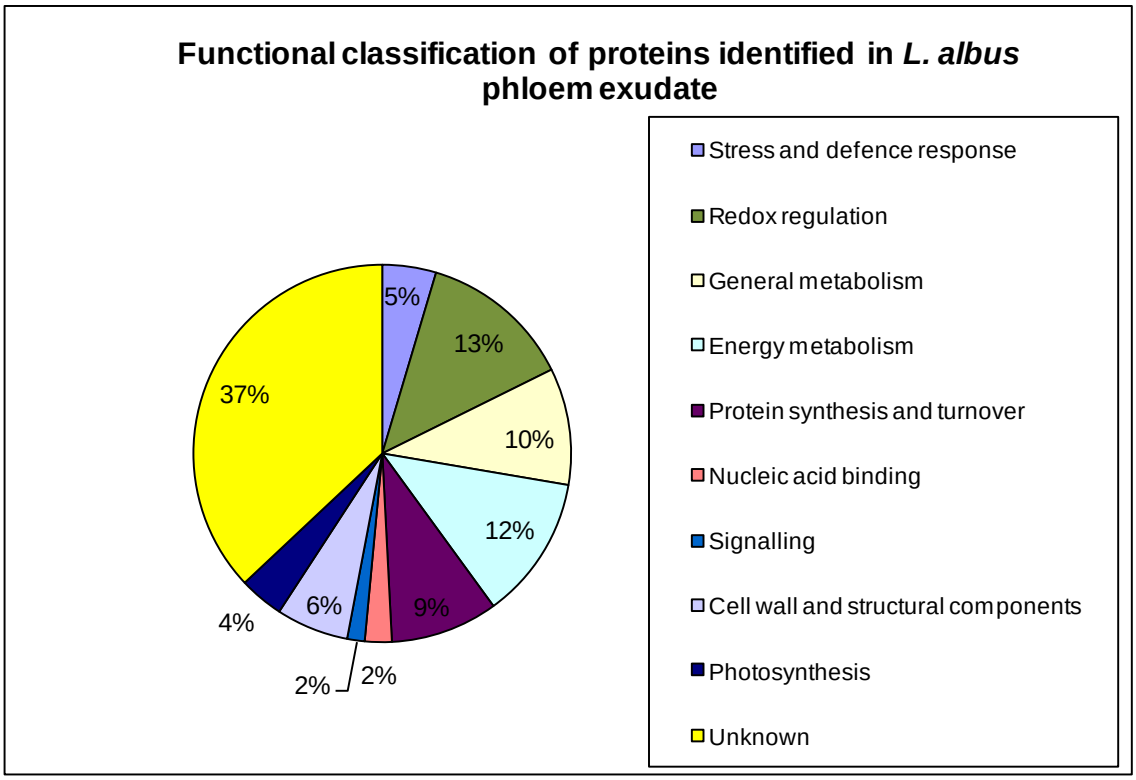

Figure 4.3. Functional categorisation of proteins identified in *L. albus* phloem exudate.

Table 4.1. Peptide sequences identified from *L. albus* phloem exudate protein spots separated by 2D gel electrophoresis and results from Blast searches. Phloem proteins were separated by 2D-electrophoresis and analysed by partial sequence determination by MS/MS. Although Isoleucine (I) and leucine (L) are not distinguishable by mass spectrometry these are shown as present in the database sequences.

Spot No.	Observed protein MW (kDa)	Partial aminoacid sequences that matched in blast search	Protein identification	Acc no.	Organism
STRESS AND DEFENCE RESPONSE					
1	6	EIAGNQNSLEIDGLAR QNALLEFGR	Narrow leaf lupin normalized cDNA library. Lupinus angustifolius cDNA similar to cysteine proteinase inhibitor	DV468746.1	Lupinus angustifolius
2	9	VEVLEYEKVPEYNNR	phloem specific protein	ABN41201.1	Pisum sativum
14	19	ALFNKEEDIGTYTIR FFPSEFGNDVDR	putative NAD(P)H oxidoreductase, isoflavone reductase	AAL85023.1	Arabidopsis thaliana
15	19	FFPSEFGNDVDR KVDVVISTVGHLL	pterocarpan reductase	BAF34843.1	Lotus japonicus
21	8	GIFTFEDESTSTVAPAR	pathogenesis-related 10	BAB63949.1	Lupinus albus
22	8	GIFTFEDESTSTVAPAR	pathogenesis-related 10	BAB63949.1	Lupinus albus
53	8	VEVLEYEKVPEYNNR	phloem specific protein	ABN41201.1	Pisum sativum
120	14.5	TFGNGQTLLLNLAGHSR FNDIQTGYSDRR	class III chitinase	CAA76203.1	Lupinus albus
REDOX REGULATION					
3	11	FLVDKEGNVVER	glutathione peroxidase 1	AAP69867.1	Lotus japonicus
33	6	KLIVVDFTASWCGPCNR SVAQDWAVEAMPTF	thioredoxin h	CAC36986.1	Pisum sativum
48	15	YAADEDAFFADYTEA HSEGLAHNADNGLDIAVR LPTDTALLSDPVFKLPVER	cytosolic ascorbate peroxidase 1	ABR18607.1	Gossypium hirsutum
55	5	LIVVDFTASWCGGPCGR	thioredoxin h	CAC36986.1	Pisum sativum
63	14.5	EFAEQLLSHLDTFL LLGWIEEVNKIDAYTQTR LYISYLCGPFAQR	glutathione S-transferase	BAC81649.1	Pisum sativum
73	29	TVEEYDYLPYFYSR YVLIGGGVSAGYAAR	monodehydroascorbate reductase I	AAU11490.1	Pisum sativum
108	5.7	LIVVDFTASWCGGPGCR TLEADWGVEAMPTF	thioredoxin h	CAC36986.1	Pisum sativum
109	5.7	LIVVDFTASWCGGPGCR	thioredoxin h	CAC36986.1	Pisum sativum

Spot No.	Observed protein MW (kDa)	Partial aminoacid sequences that matched in blast search	Protein identification	Acc no.	Organism
REDOX REGULATION					
117	11.5	ATVGAPNVLGDGCPFSQR	dehydroascorbate reductase	AAL71857.1	Nicotiana tabacum
122	14	LQPFGKVPAFQDDDLSLFESR	glutathione transferase	NP_191835.1	Arabidopsis thaliana
129	13	AAADAPNVLGDGCPFSQR	dehydroascorbate reductase	AAL71857.1	Nicotiana tabacum
PROTEIN SYNTHESIS AND TURNOVER					
7	10	TFPQQAGTIR	P deficient normal and proteoid roots 7 and 10 days after emergence Lupinus albus cDNA clone similar to eIF-4D	CA411198.1	Lupinus albus
31	4	TITLEVESSDTIDNAR LTIQDKEGIPPDQQR	ubiquitin extension protein	CAA80333.1	Lupinus albus
60	19	VDDHIGVAIAGLTADGR NQYDTDVTTWSPAGR INYCFTYESPLPVGR	20S proteasome subunit PAF1	AAM61575.1	Arabidopsis thaliana
82	23.5	NLPLVGEVGLGADLVR	globulin-like protein	AAM65577.1	Arabidopsis thaliana
86	21	AYLPVNESFGFSSQLR	elongation factor EF-2	AAF02837.1	Arabidopsis thaliana
95	7.5	LVTEPAPGISASPSEENMR NTDKWSPALQIR	ubiquitin-conjugating enzyme 1 like protein	ABI84266.1	Arachis hypogaea
97	9	GIGDGTVSYGMDDGDDIYMR SWTGTIIGPHNTVHEGR TLGSGGSSVVVPR	protein binding/ubiquitin-protein ligase	NP_566968.1	Arabidopsis thaliana
100	8	IVMELYADTTPR VFFDMAIGGSPVGR	Cyclophilin	O49886	Lupinus luteus
101	8	VFFDMAIGGSPVGR PRIVSEYADTTPR	Cyclophilin	O49886	Lupinus luteus
102	8	IVMELYADTTPR VFFDMAIGGSPVGR	Cyclophilin	O49886	Lupinus luteus
103	8	IVMELYADTTPR VFFDMAIGGSPVGR	Cyclophilin	O49886	Lupinus luteus
106	10	IVIGLYGDDVPQTVENFR	peptidylprolyl isomerase-like protein	AAM65904.1	Arabidopsis thaliana
PHOTOSYNTHESIS					
5	6	VDYLEFELEHGFVYR	ribulose bisphosphate carboxylase	CAA42617.1	Phaseolus vulgaris

Spot No.	Observed MW (kDa) protein	Partial aminoacid sequences that matched in blast search	Protein identification	Acc no.	Organism
PHOTOSYNTHESIS					
12	6.2	RWIPCLEFELEHGFVYR ELDEAKTEYPNSFIR EHNSSPGYYDGR	ribulose-1,5-bisphosphate carboxylase small subunit rbcS3	AAG24884.1	Glycine max
20	8	DTDILAAFR	ribulose 1,5-biphosphate carboxylase large subunit	CAA93923.1	Lupinus angustifolius
36	19	TFQGPPHGIQVER	ribulose 1,5-biphosphate carboxylase large subunit	CAA93923.1	Lupinus angustifolius
126	14	EYYFLSVLTR SKEVEYVGQVLR	23kDa polypeptide of the oxygen evolving complex of photosystem II	ABQ41909.1	Sonneratia alba
NUCLEIC ACID BINDING					
24	8	GFGFVTFANEQSMR	putative glycine-rich RNA-binding protein	BAF34340.1	Dianthus caryophyllus
26	8.5	GFGFVTFANEQSMR NITVNEAQSR	putative glycine-rich RNA-binding protein	BAF34340.1	Dianthus caryophyllus
27	8	GFGFVTFANEQSMR DAIEGLNGKDLDGR	putative glycine-rich RNA-binding protein	BAF34340.1	Dianthus caryophyllus
SIGNALLING					
28	10.5	TFYTLVMVDADAPSPSNPFLR NFAEINNLLPAAAVYFNCGQR FTLFYESPQPSEGIHR	Flowering locus T-like 1 protein	ABV56568.1	Chenopodium rubrum
107	11	EDCELYNLGSPVSAVYFNLQR	FTL1	ABR20498.1	Cucurbita moschata
CELL WALL AND STRUCTURAL COMPONENTS					
29	8.5	KLGSPQGYDDFAASLPADECGR	Actin-depolymerizing factor (ADF)	P30174	Brassica napus
32	5.7	YMVIQGEPGVVIR	profilin	ABG88188.1	Glycine max
46	29	DLYGNIVLSGGSTMFPGIADR SYELPDGQVITIGAER IWHHTFYNELR	actin	AAB40076.1	Glycine max
74	25	KLIGPAMYFGLMGDGQPIGR VPEGFDYELYNR	UDP-glucose:protein transglucosylase	O04300	Pisum sativum
81	25	GPAMYFGLMGDGQPIGR VPEGFDYELYNR NLSPSFFFNTNYDMER	UDP-glucose:protein transglucosylase	O04300	Pisum sativum
83	23	LISQIISSLTTSLR	tubulin A	AAX86047.1	Glycine max
96	8.5	LGENAQGYEDFTASLPADECGR YAVYDFEYLTEGNV IFFIAWSPDTSR	actin depolymerizing factor-like protein	ABC49719.1	Arachis hypogaea

Spot No.	Observed protein MW (kDa)	Partial aminoacid sequences that matched in blast search	Protein identification	Acc no.	Organism
CELL WALL AND STRUCTURAL COMPONENTS					
121	10	HCDGIQNELQATDPTEMDLDVFR IFFIAWGCPDTAR	ACTIN DEPOLYMERIZING FACTOR 1	NP_001078247.1	Arabidopsis thaliana
ENERGY METABOLISM					
TCA Pathway					
34	23	VLVTGAAGQIGYALVPMIAR IVQGLGIDEFSR	malate dehydrogenase	AAO15574.1	Lupinus albus
85	23.5	PLVTGAAGQIGYALVMNIAR	malate dehydrogenase	AAO15574.1	Lupinus albus
Glycolysis					
35	35	GNPTVEVDLTLSDGTFAR AAVPSGASTGIYEALELR	enolase	CAB75428.1	Lupinus luteus
37	24	GILGYTEDDVVSTDFIGDNR LVSWYDNEWGYSTR VPTVDVSVVDLTVR	glyceraldehyde-3-phosphate-dehydrogenase	CAI83772.1	Lupinus albus
38	24	GILGYTEDDVVSTDFIGDNR LVSWYDNEWGYSTR VPTVDVSVVDLTVR	glyceraldehyde-3-phosphate-dehydrogenase	CAI83772.1	Lupinus albus
39	35	GNPTVEVDVTLSDGTFAR AAVPSGASTGVYEALELR	enolase	CAB75428.1	Lupinus luteus
47	14.5	VIACIGETLEQR WLHENVSADVAASVR KVTPQAQEVHADQLR	triosephosphate isomerase	ABA86966.1	Glycine max
66	14.5	WIHENVSADVAASVR VIACGIGETLEQR	triosephosphate isomerase	AAT46998.1	Glycine max
68	14.5	VIQCIGETLEQR	triosephosphate isomerase	AAT46998.1	Glycine max
75	24	EPSELAIHENAYGLAR VAPEVVAEHTVR	fructose-bisphosphate aldolase	NP_001118453.1	Arabidopsis thaliana
76	23	LVSWYDNEWGYSTR TEDDVVSTDFIGDNR VPTVDVSVVDLTVR	glyceraldehyde-3-phosphate-dehydrogenase	CAI83772.1	Lupinus albus
77	23	GILGYTEDDVVSTDFIGDNR LVSWYDNEWGYSTR VPTVDVSVVDLTVR	glyceraldehyde-3-phosphate-dehydrogenase	CAI83772.1	Lupinus albus
84	21	SIGNSNYDVFLTR	putative NADPH dependent mannose 6-phosphate reductase	AAM64779.1	Arabidopsis thaliana
115	24	NVSWYDNEWGYSTR VPTVDVSVVDLTVR	glyceraldehyde-3-phosphate-dehydrogenase	CAI83772.1	Lupinus albus

Spot No.	Observed MW (kDa) protein	Partial aminoacid sequences that matched in blast search	Protein identification	Acc no.	Organism
GENERAL METABOLISM					
Aminoacid					
40	30	FVIGGPHGDAGLTGR	S-adenosylmethionine synthase	AAT40304.1	Medicago sativa
41	30	FVIGGPHGDAGLTGR	S-adenosylmethionine synthase	AAT40304.1	Medicago sativa
42	31	FVIGGPHGDAGLTGR TALADGEYYNENGAMVPVR	S-adenosylmethionine synthase	AAT40304.1	Medicago sativa
44	32	FVIGGPHGDAGLTGR	S-adenosylmethionine synthase	AAT40304.1	Medicago sativa
51	12	YFQTGGEIGFDTYFSMAR	methionine synthase	AAQ08403.1	Glycine max
70	30	FVIGGPHGDAGLTGR TQVTVEYYNSR	S-adenosylmethionine synthase	AAT40304.1	Medicago sativa
71	30	FVIGGPHGDAGLTGR	S-adenosylmethionine synthase	AAT40304.1	Medicago sativa
72	30	FVIGGPHGDAGLTGR	S-adenosylmethionine synthase	AAT40304.1	Medicago sativa
Sugars and polysaccharides					
43	33	ATSDLLLVQSDLYTLQDGFVAR VQLLEIAQVPDEHV VLQLETAAGAAIR	UDP-glucose pyrophosphorylase	O64459	Pyrus pyrifolia
45	33	YLTNSNEIHTFNQSKYPR VLQLETAAGAAIR	Udp-Glucose Pyrophosphorylase	2ICX_A	Arabidopsis thaliana
59	21	VFHYGSISLIVEPGCR IVDDQSILEDEPR LPLWPSPEEAR	fructokinase-like protein	CAD31714.1	Cicer arietinum
114	24	ILVTGGAGFIGSHLVDR VPTVDVSVVDLTVR SGFCYVSDLVDGLIR	UDP-D-glucuronate carboxy-lyase	BAB40967.1	Pisum sativum
123	19	SKKLQDLLELAR	aldo/keto reductase family protein	NP_001031505.1	Arabidopsis thaliana
Nucleotide					
56	24	VLPYMDYVFGNETEAR YNVEYIAGGATQNS ANCYAANVIIQR	adenosine kinase isoform 2S	AAU14833.1	Nicotiana tabacum
57	24	ALAYTDFLFGNETEAR VDYMNLSAPFVSEFFR ANCYAANVIIQR	adenosine kinase isoform 1S	AAU14832.1	Nicotiana tabacum
94	7	IIGATNPSQSEPGTIR VSICIKPDGVQR	nucleoside diphosphate kinase	AAN77500.1	Glycine max
Secondary metabolism. Phenylpropanoids/phenolics					
112	16.5	SWAVSDDLYEYILETSVYPR	caffeoyl-CoA 3-O-methyltransferase	ABE41833.1	Brassica rapa

Spot No.	Observed protein MW (kDa)	Partial aminoacid sequences that matched in blast search	Protein identification	Acc no.	Organism
UNKNOWN					
4	8.5	VHEGDWHTAGSVR	P deficient proteoid roots 12 and 14 days after emergence Lupinus albus cDNA clone	CA410380.1	Lupinus albus
61	23	SPFPFSQTVEAFSYLETGR VGDEVYGDINR	auxin-induced protein	AAA87182.1	Vigna radiata
62	23	SPFPFSQTVEAFSYLETGR FQVGDEVYGDINR	auxin-induced protein	AAA87182.1	Vigna radiata
64	14.3	LYTSYIGCPFAQR	P deficient proteoid roots 12 and 14 days after emergence Lupinus albus cDNA clone	CA410500.1	Lupinus albus
65	13.5	NFFEEHLHTDEEIR GGMIILPAGIYHR LAELGVLSWR FAAAGSGYFDVR	acireductone dioxygenase	ABW34717.1	Solanum tuberosum
80	24	IWPHSFEFR	unknown protein	ABK23804.1	Picea sitchensis
124	18	FSPNNLQPTIVSASWDR YQSLNAGSIIHSLCGFSPNR DVLSVAFSVDNR	LeArcA2 protein	BAA76896.1	Solanum lycopersicum
127	12.5	YYYNETQAR	U_NA-080222_Plates1_4m23.b1		Lupinus albus
128	12.5	LLNQPHPEGGFYTETFR	P deficient proteoid roots 12 and 14 days after emergence Lupinus albus cDNA clone	CA409832.1	Lupinus albus

DISCUSSION

In this study proteins isolated from *L. albus* phloem exudate were identified by a combination of 2D electrophoresis and peptide sequencing by MS/MS analysis. Proteins involved in metabolism, protein synthesis and turnover, cell redox homeostasis, synthesis of cell wall and structural components, stress and defence response, long distance signalling and nucleic acid binding were identified. The most abundant were cyclophilin (spots 100 and 101), a glycine-rich RNA-binding protein (spots 26 and 27), a proteinase inhibitor (spot 1) and phloem-specific protein (spot 2). Some of these might have been expected from analyses of phloem exudates from other species (Gaupels *et al*., 2008a; Aki *et al*., 2008; Giavalisco *et al*., 2006; Yoo *et al*., 2004; Barnes *et al*., 2004*;* Walz *et al*., 2002 and 2004; Haebel and Kehr, 2001; Marentes and Grusak, 1998). Prominent protein spots that showed no significant homology to any protein in the database (spots 8, 9 and 16 for example) could be unique to lupin phloem exudate. For example, spot 4 was also prominent and matched a *L. albus* cDNA library clone constructed from proteoid roots that also showed no significant similarity to any protein in the database. Some could also have been classed as 'unidentified' because they represent proteins where high conservation of sequence is not required for function. Since an identity greater than 85% was used for considering a match significant, proteins with low sequence conservation could have been overlooked during identification.

In a number of cases different spots were identified as the same protein e.g. thioredoxin h (spots 33, 55, 108, and 109). This might be a result of post-translational modifications of products of the same gene or that they originate from highly similar genes of a gene family (Giavalisco *et al*., 2006). The first possibility raises the question of whether these proteins are being modified in CC and transported into the SE in the modified form, or that they are modified in the SE; a possibility that would require the modifying factors (enzymes and substrates) to be present in the SE (Walz *et al*., 2004). Gaupels *et al*. (2008b) have shown that nitric oxide (NO) synthesis in vascular cells and specifically in CC is induced in response to stress- and pathogen defence-related compounds like hydrogen peroxide (H_2O_2) and salicylic acid. In cucurbit

phloem exudate these treatments resulted in a sharp increase in nitrated/nitrosylated proteins (Gaupels *et al*., 2008b). The authors suggested that NO-binding proteins serve to translocate the NO signal in phloem. Similarly, phloem proteins could be modified by a host of other post-translational modifications such us methylation, glycosylation and phosphorylation (Nakamura *et al.*, 1993; Hayashi *et al.*, 2000).

Protein synthesis and turnover

The lack of functional ribosomes in SE suggests that the proteins in SE are translated in and transferred from adjoining CC. Fisher *et al*. (1992) used ^{35}S-methionine labelling in wheat SE exudate collected by aphid stylectomy to show that recently synthesised proteins were present in SE, suggesting that there is significant protein turnover in phloem.

In this study, proteins with chaperone activity, such as cyclophilins (spots 100-103), were identified as very prominent spots. Cyclophilin has also been suggested to play a role in signal processing during development (Gasser *et al*., 1990) and in protein phosphorylation (Schobert *et al*., 1998), known to occur in SE (Nakamura *et al*., 1993).

Ubiquitin and various molecular chaperones, including cyclophilin, were detected in the phloem exudate from *R. communis* and it was suggested that these may be involved in protein transport through plasmodesmata (Schobert *et al*., 1995). Protein exchange between CC and SE seems to be tightly controlled and selective; some proteins destined for SE are capable of dilating plasmodesmata to increase the SEL (Ishiwatari *et al*., 1998). It has been proposed that phloem proteins with chaperone activity are involved in unfolding, cell-to-cell protein trafficking and refolding of polypeptides on the SE side after import from CC via plasmodesmata (Schobert *et al*., 1995 and 1998; Balachandran *et al*., 1997).

Ubiquitin extension protein (spot 31), ubiquitin conjugating enzyme-like protein (spot 95) and ubiquitin protein ligase (spot 97) have been identified in this study. Each of these could be involved in the transport of proteins synthesized in the

CC to the SE in *L. albus*. Therefore, they could be playing an important role in the maintenance of the enucleate SE. Ubiquitin and ubiquitin conjugating enzyme were also reported in phloem exudate from *B. napus* (Giavalisco *et al*., 2006) and *C. maxima* (Lin *et al.*, 2008).

Schobert *et al*. (1998) studied the soluble proteins present in phloem exudate collected from seven monocotyledon and dicotyledon plants (*R. communis* L., *Triticum aestivum* L., *O. sativa* L., *Yucca filamentosa* L., *C. maxima* Duch., *Robinia pseudoacacia* L. *and Tilia platyphyllos* L). Molecular chaperones such as cyclophilin, as well as ubiquitin were detected in the phloem exudate of all species examined. It is assumed that chaperones and ubiquitin are required for the maintenance of SE function (Schobert *et al*., 1995). Interestingly, ubiquitin was estimated to represent up to 10% of the total proteins in phloem exudate from *R. commmunis* (Schobert *et al*., 1995) but this does not appear to be the case in lupin phloem.

Since SE undergo profound proteolysis during maturation, Schobert *et al*. (1995) studied whether components of the ubiquitin-dependent protein-degradation system were present in the phloem exudate of castor bean seedlings. Although substantial amounts of ubiquitin were found, the absence of proteasome-related proteins led Schobert *et al*. (1995) to conclude that the ubiquitin-dependent proteasome-mediated proteolytic pathway was not functional in SE. This feature may be important in keeping the functioning proteins stable in the enucleated SE (Hayashi *et al*., 2000). This study has identified a proteasome subunit (spot 60) and is consistent with recent reports of proteasome subunits in phloem exudate from *B. napus* (Giavalisco *et al*., 2006) and *C. maxima* (Lin *et al.,* 2008). Giavalisco *et al*. (2006) suggested that a ubiquitin-dependent protein sorting function might be attributed to these proteins in phloem rather than a simple proteolytic activity function.

While proteins involved in protein synthesis were not identified, spots 74 and 81 indicated a UDP glucose;protein transglycosylase in the exudate. Such activity could lead to post-translational modification in phloem and might account for the multiple spots on gels that were found for some of the proteins. It would be

interesting to assess the degree to which glycosylated proteins occurred in these exudates.

Redox regulatory proteins

As noted above, *in vivo* synthesis of NO has been demonstrated in CC of *Vicia faba* vascular bundles in response to salicylic acid and H_2O_2 (Gaupels *et al.,* 2008b). Each of these compounds has been linked in a response pathway to pathogen attack or other stress responses. Thus a very complex relationship between such a pathway and antioxidant defence mechanisms involving glutathione (GSH), for example, must exist in phloem.

Although long-lived enucleate SE are generally exposed to O_2 concentrations lower than the air/aqueous solvent equilibrium value, and thus might be expected to be less prone to generate potentially toxic reactive oxygen species (ROS) (Raven, 1991), the presence and functionality of a complete antioxidant defence mechanism in the phloem has been suggested in previous studies (Walz *et al*., 2002; Haebel and Kehr, 2001; Ishiwatari *et al*., 1995). Walz *et al*. (2002) showed that antioxidant defence enzymes in phloem exudate are active in *in vitro* assays and that their level of activity increases markedly during drought stress. As a general reaction to stress and pathogen attack, plants produce ROS. To avoid damage to endogenous components, antioxidant defence proteins and metabolites are essential to maintain cellular functions (Walz *et al*., 2004).

Proteins involved in cell redox homeostasis, such as glutathione peroxidase (spot 3), ascorbate peroxidase (spot 48), monodehydroascorbate reductase (spot 73) and dehydroascorbate reductase (spot 117, 129), were all identified in this study, consistent with the existence of an effective ascorbate-glutathione cycle in phloem (Figure 4.4). The protein that is required to reduce oxidised glutathione, glutathione reductase, was not detected in lupin exudate and it is notable that it was also not detected by Walz *et al.* (2004). This is surprising as Alosi *et al*. (1988) found high levels of activity for this enzyme in the squash exudates they assayed. Lin *et al.* (2008) also identified this reductase recently in exudate of *C. maxima*. Thioredoxin h, also identified in this study (spots 33,

55, 108, 109), would serve to repair proteins that have been damaged by ROS formed as a result of oxidative stress (Ishiwatari *et al*., 1995). Proteins involved in cell redox homeostasis may play a role in phloem protein stability under stress and in maintenance of SE integrity by removing ROS over the prolonged life of the SE/CC complex (Raven, 1991). Critical to the functioning of this cyclic scavenging mechanism is the provision of reductant (NADPH). It is possible that reduced thioredoxin could provide a source of electrons but it is not clear how oxidised thioredoxin is reduced. Similarly, the substrates glutathione and ascorbate are required in the SE if this cycle functions there. Alosi *et al*. (1988) showed mM concentrations of glutathione in *Cucurbita* phloem exudates. In adittion, presence of L-Ascorbic acid in phloem exudates collected from *A. thaliana* by aphid stylectomy and its long distance transport was demonstrated by Franceschi and Tarlyn (2002). Glutathione S-transferase (GST) (spot 63, 122) was present in lupin exudate. This enzyme catalyses a reaction between the thiol group of cysteine in the tripeptide to form a conjugate with xenobiotic molecules (toxins, herbicides etc) rendering them inactive/non-toxic. Perhaps GST functions to conjugate and translocate xenobiotics or endogenous toxins that enter the SE/CC complex. It should be noted that while glutathione is potentially important for these various 'protection' functions it is also a significant form of translocated S in plants (Pate, 1965) and is believed to be the long distance signal in phloem that regulates sulphate ion uptake in roots (Lappartient *et al.,* 1999). GSH is also likely to react with NO formed in CC (Gaupels *et al.,* 2008b) to form S-nitrosoglutathione (GSNO) a potent inducer of defence related genes and possible long-distance systemic signal (van Bel and Gaupels, 2004).

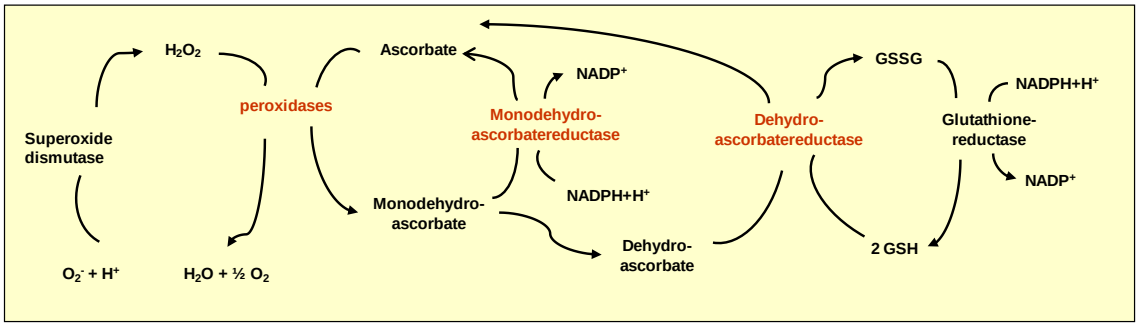

Figure 4.4. Antioxidants defence enzymes and metabolites. Proteins involved in the antioxidant defence system that were identified in *L. albus* phloem exudate are printed in red. Redox regulatory proteins have been proposed to be essential for the maintenance and longevity of the enucleate SE. The figure is modified from Walz *et al.* (2002).

Thioredoxin h represented a considerably larger proportion of phloem sap proteins in rice than of total proteins from leaves, roots, and seeds (Ishiwatari *et al.*, 1995). Thioredoxins are ubiquitous low-molecular-mass proteins that function to reduce disulfide bonds on target proteins. Reduced thioredoxin h can regenerate proteins that have been inactivated by oxidative stress. By repairing damaged proteins, thioredoxin may be important in overcoming the difficulties inherent in the transportation of newly synthesized replacement proteins from CC to SE (Ishiwatari *et al.*, 1995). Thioredoxin h might be expected to be reduced by NADPH but the ultimate source of reductant in SE remains a matter of speculation. A putative NAD(P)H oxidoreductase, isoflavone reductase (spot 14) was identified in *L. albus* phloem exudate and this activity, given the availability of reduced substrate in SE, could serve to reduce thioredoxin h.

Redox regulatory systems and scavenging agents have been proposed to be essential for the maintenance and longevity of the enucleate SE (Schobert *et al*., 1998) and the collective data from proteomic analyses, including those reported in this study, support the idea.

Stress and defence response

A number of studies have identified individual proteins in phloem exudate that are thought to be involved in stress and, particularly, defence-related responses in plants. Among these are proteinase inhibitors (Walz *et al*., 2004; Giavalisco *et al*., 2006; Schobert *et al*., 1998; Christeller *et al*., 1998) that, in addition to defending against herbivores and pathogens, might also influence the stability

of proteins in the phloem (Giavalisco *et al.,* 2006). The partial degradation of the SE cytoplasm during differentiation must be under tight regulatory control to inhibit the process at the appropriate developmental stage. Phloem-specific proteinase inhibitors could exert temporal control of selective autophagy during SE differentiation (Dannenhoffer *et al*., 2001). The presence of proteinase inhibitors translocated in phloem suggests an additional role in regulating protein turnover in the SE-CC complex (Dannenhoffer *et al.,* 2001).

One of the prominent spots in gels of lupin exudate proteins was a cysteine proteinase inhibitor (spot 1). Cysteine inhibitors have also been identified in phloem exudate from *B. napus* (Giavalisco *et al*., 2006), *R. communis* (Barnes *et al.*, 2004; Schobert *et al*., 1998) and *C. maxima* (Lin *et al.*, 2008; Haebel and Kehr, 2001).

Ultra-structural studies of SE from a range of species have described parietal proteins along the plasma membrane known collectively as P-proteins (phloem proteins) and identified from proteomic studies as PP1 and PP2. These proteinaceous structures begin to accumulate in differentiating SE and persist in mature translocating phloem (Golecki *et al*., 1999). The structures were also a feature of the parietal cytoplasm in lupin SE (Chapter 3) and a phloem specific protein was identified in the present proteomic analysis (spots 2 and 53). These proteins seem to play an important role in sealing the wounded SE (Hayashi *et al*., 2000) and possibly in response to stress and pathogens (Walz *et al*., 2004). It appears likely that polymerized and unpolymerized P proteins exist in dynamic equilibrium within SE, where the concentration of each is responsive to physiological change within the vascular system (Golecki *et al*., 1999). A change in the redox state of the phloem sap, in part by the activity of glutathione reductase, has been proposed as one mechanism to regulate gel-sol transitions between P protein subunits and filaments (Alosi *et al*., 1988). Golecki *et al*. (1999) demonstrated that PP1 and PP2 are capable of long-distance movement in the phloem of grafted cucurbit plants, but a functional role that relies on their translocation has not been investigated. While the P proteins are most abundant in SE they have also been described from immuno-histological studies in CC and phloem parenchyma (Cronshaw, 1981).

The identification of a pathogenesis-related-protein (PRP) (spots 21 and 22) suggests an active defence reaction mechanism in the phloem of *L. albus*. It is not clear whether the presence of this protein is constitutive or whether it indicates that the plants from which phloem exudate was collected were responding to a pathogen attack. Although phloem exudate was collected from field-grown plants that looked healthy, the possibility that pathogens had infected the plants without producing visible symptoms cannot be excluded. In this regard, it may be significant that lupin exudate was found to harbour a number of transcripts identified as those for bean yellow mosaic virus (see Chapter 5), a common disease of lupins in Western Australia. On the other hand, Regalado and Ricardo (1996) found that PRP were present in the intercellular fluid of healthy *L. albus* leaves and there are reports of these proteins in the apoplast and xylem of a number of species (Aki *et al.,* 2008; Alvarez *et al.,* 2006). Similarly, a chitinase protein (spot 120), not previously reported in phloem exudate, was also identified in this study. Chitinase was found in xylem exudate in rice (Aki *et al*., 2008) but not in phloem collected from leaf hopper stylets. Xylem is regarded to be under negative pressure so that after incision, phloem exudate could conceivably enter xylem vessels rather than xylem contents flowing into the exudate. However, sugar-rich phloem exudate bathing the wound would certainly attract water and solutes from the tissue apoplast and perhaps this was the source of these proteins. There is also a possibility that chitinase is a true SE component of *L. albus*. In this case, the protein could play a role in defence against pathogens and wounding, further supporting the existence of a defence reaction mechanism in phloem.

Spots 14 and 15 are quite prominent and were identified as isoflavone reductase and pterocarpan (or pterocarpin) reductase respectively. These two proteins are NADP-linked oxidoreductases involved in the synthesis of isoflavonoid phytoalexins in legumes (Blount *et al.,* 1992). Phytoalexins are also likely to be part of the plant's defences against microbial and herbivore attack but whether or not these defence molecules are present in and translocated by phloem is not known.

Cell wall and structural components

Plant cells contain a dynamic network of cytoskeletal elements that remodel cytoplasmic architecture in response to external and internal stimuli (Staiger *et al.*, 1997). Actin reorganization is likely to be modulated by the spatial distribution and activity of a plethora of actin-associated proteins. There is increasing evidence that the small actin binding proteins, profilin and actin-depolymerizing factor, regulate actin dynamics in plant cells (Staiger *et al.,* 1997). Analysis of phloem exudate of *R. communis* revealed that profilin, a potent regulator of actin polymerization, was present along with actin (Schobert *et al*., 2000) but in 15-fold molar excess compared to actin. The high profilin content within the translocation stream may prevent formation of microfilaments (Schobert *et al*., 2000). At high concentrations, profilin prevents the polymerization of actin, whereas it enhances polymerization at low concentrations (Barnes *et al*., 2004). The high profilin levels detected in *R. communis*, *R. pseudoacacia L. and T. platyphyllos* phloem exudate may attenuate wound-induced actin polymerization yielding a phloem system with a propensity to 'bleeding'. However, further characterization of profilin properties and actin dynamics, within SE, is needed to test this hypothesis (Schobert *et al*., 1998). In this study structural component proteins such as actin (spot 46), actin depolymerizing factors (spots 29, 96 and 121) and profilin (spot 32) have been identified in phloem exudate of lupin.

Microinjection studies provided direct evidence that profilin can move through plasmodesmata (Schobert *et al*., 2000). Schobert *et al*. (2000) demonstrated that actin and profilin are constantly delivered into the SE and carried along in the translocation stream. Actin and profilin were also found in phloem exudate from a number of monocotyledon and dicotyledon species (Giavalisco *et al*., 2006; Schobert *et al.,* 1998). Whether or not actin participates in anchoring organelles in the parietal cytoplasm of SE (see Chapter 3) needs to be investigated but it is tempting to think that these proteins function in SE in this way.

The regulation of actin depolymerizing factors (ADF)-actin interactions probably occurs by phosphorylation and changes in pH. At pH <7.4, ADF primarily bind to the polymer and at pH >8.0 they cause extensive depolymerization

(Staiger *et al*., 1997). Therefore, basic pH values usually found in phloem (Pate *et al.,* 1974) should lead to a rapid reduction of polymerized actin (Giavalisco *et al.,* 2006).

In this study tubulin (spot 83) was also identified. Schobert *et al*., (1998) reported the absence of tubulin in phloem exudate collected from a variety of species. Their results were consistent with previous microscopic studies in which microtubules were not detected within mature SE (Evert, 1990). Interestingly, Lin *et al.* (2008) has recently identified tubulin in *C. maxima* phloem exudate suggesting that tubulin could indeed be present in SE. Kulikova *et al.* (2003) reported a faint signal for tubulin in the *Cucurbita pepo* phloem exudate using specific antibodies to the protein. Immunolocalisation with anti-tubulin antibodies on tissue sections containing SE could be used to confirm the presence of tubulin in phloem of lupin, but was beyond the scope of this study.

Metabolism

General metabolism

The vast majority of the proteins identified in lupin phloem exudate were associated with metabolism. These results are consistent with previous studies on rice phloem exudate collected by stylectomy (Aki *et al*., 2008).

A group of seven spots were identified as S-adenosylmethionine (SAM) synthase (spots 70-72, 40-42 and 44), and a single small spot (spot 51) was identified as methionine synthase. The identification of these proteins in phloem exudate suggests the synthesis of ethylene in the SE. In plants, methionine is the only known precursor for ethylene biosynthesis. Ethylene is synthesized from methionine through the intermediates SAM and aminocyclopropane-carboxylate (ACC) (Chen *et al*., 1991). Therefore, activities of ACC synthase and ACC oxidase would also be required for the production of ethylene in SE. Although, ACC oxidase was not identified in *L. albus* phloem exudate, it is common to almost all plant tissues and perhaps it corresponds to one of the spots that could not be identified or was not sequenced. There are two other

metabolic fates for SAM, one is in the biosynthesis of polyamines and the second is the source of methyl groups for the methylating reactions that take place in plants. The identification of a methyltransferase (spot 112) would support the role of SAM synthase in providing methyl groups for methylation reactions in SE, possibly associated with post-translational modification of proteins. However, further studies are needed to test this hypothesis.

This analysis identified two of the phosphotransferases involved in purine metabolism, nucleoside diphosphate kinase (spot 94) and adenosine kinase (spot 56, 57) in lupin phloem exudate. Each of these spots was small and faint and while this does not preclude their occurrence in SE they could just be contaminants. Whether or not nucleotide metabolism and specifically ATP formation in SE occurs remains an interesting question. If glycolysis persists in SE, as the following section suggests, then substrate phosphorylation potential may be important in SE functioning. ATP utilisation would then require enzymes to transfer phosphate groups and, in the case of the diphosphate kinase, to metabolise pyrophosphate. Perhaps significantly, two protein spots (43 and 45), were identified in lupin as UDP-glucose pyrophosphorylase.

Energy metabolism

The major solutes in phloem exudate (10-20 % w/v) and no doubt in phloem contents *in vivo* are the main products of photosynthetic C reduction, sugars (Ziegler, 1975). Thus the SE/CC complex has an abundant potential source of energy and, while the content of hexoses (glucose and fructose) in exudate from lupins is usually very low, there appears to be some very limited hydrolysis (2%) of the disaccharide (Pate *et al.,* 1974). Whether hydrolysis occurs during passage to the SE or in phloem has not been determined. Sucrose synthase (SuSy) has been localised to CC in zones of both loading and unloading of phloem (Nolte and Koch, 1993). Interestingly, neither SuSy nor invertase and hexokinase were identified in exudate collected from rice by stylectomy (Aki *et al.,* 2008), from incisions in *Brassica napus* (Giavalisco *et al.,* 2006) or from lupin in this study. UDP-glucose pyrophosphorylase protein (spots 43 and 45) was identified in lupin exudate but its functional significance for sucrose metabolism in the absence of SuSy is not clear.

Phloem exudate collected from *R. communis* was found to contain a full complement of glycolytic intermediates (Geigenberger *et al*., 1993) and in a number of proteomic analyses of exudates glycolysis pathway proteins have been identified. These data have led to the generalisation that glycolysis may be involved with carbohydrate metabolism in SE/CC complexes to produce ATP for phloem loading and glucose for callose formation (Hayashi *et al*., 2000). However, it is important to note that some glycolytic enzymes may be multifunctional proteins involved in processes other than carbohydrate metabolism (Plaxton, 1996). Glycolysis is also directly involved in many biochemical adaptations of plant and non-plant species to environmental stresses such as nutrient limitation, osmotic stress, drought, cold/freezing, and anoxia (Plaxton, 1996). In lupin, exudate proteins involved in glycolysis including fructose-bisphosphate aldolase (spot 75), enolase (spots 35 and 39), glyceraldehyde-3P dehydrogenase (spots 37, 38, 76, 77, 115), triosephosphate isomerase (spots 47, 66 and 68) and fructokinase (spot 59) were identified. While a number of these were small faint spots, some like enolase and glyceradlehyde-3P-dehydrogenase, were quite prominent. Nevertheless, a complete glycolytic pathway was not found and this was also the case for rice phloem collected by stylectomy (Aki *et al.,* 2008).

A number of other proteins involved in carbohydrate metabolism were also identified from lupin exudate including mannose 6P reductase (spot 84), UDP-D-glucuronate carboxy-lyase (spot 114) and as noted earlier a UDP-glucose;protein transglycosylase. Other enzymes of glucuronate metabolism were not identified but it could be significant that D-glucuronate is a precursor for ascorbate synthesis.

The only protein of the Kreb's cycle identified in lupin exudate was malate dehydrogenase (spots 34, 85) and, interestingly, this was also the case for the rice leaf hopper stylet exudate collected by Aki *et al.* (2008). This suggests that mitochondria in SE do not serve ATP-generation and then CC must act as ATP-generators for SE function.

Photosynthesis

Large and small subunits of Rubisco were identified from four relatively prominent gel spots (5, 12, 20 and 36) in lupin phloem exudate. The most prominent were spots 5 and 12 that were due to the large subunit. There was no ultra-structural evidence that mature SE contained chloroplasts (see Chapter 3) but that the parenchyma, and particularly the cells of the adjacent bundle sheaths that were wounded by incisions to the suture vasculature, were rich in chloroplasts. Thus the presence of these proteins in phloem exudate is likely due to contamination from neighbouring cells and any other chloroplast-containing cells opened at the wound and bathed in exudate as it formed. Despite the fact that Rubisco subunits were represented in the exudate by relatively prominent spots, it should be remembered that this protein constitutes the majority of all proteins in a photosynthetic tissue, so that even a small degree of contamination will provide a significant level of Rubisco to the exudate. The analysis also identified a 23 kDa polypeptide from photosystem II of the thylakoid membrane structure of chloroplasts (spot 126). Compared to Rubisco on 2D gels, this protein was a very small faint spot (Figure 4.2) giving a better idea of the extent of contamination. Not surprisingly, analyses of exudates collected by stylectomy contained no photosynthesis-related proteins (Barnes *et al.,* 2004; Aki *et al.,* 2008; Gaupels *et al.,* 2008a) while Rubisco polypeptides have been identified in exudate collected by incision from *B. napus* (Giavalisco *et al*., 2006) and pumpkin (Lin *et al.,* 2008).

While the photosynthetic protein in lupin exudate is most likely due to contamination, other sources could be considered. These proteins could also represent remnants of the SE differentiation process and are no longer functional. SE in a less differentiated state probably still have nuclei and active chloroplasts. These less differentiated SE could be contributing a small but still significant proportion of the photosynthetic proteins found in exudate collected after wounding. If SE plastids function as storage units (van Bel, 2003) then perhaps non-functional remnants of photosynthetic proteins could have been retained during the SE maturation process and are released as a result of turgor loss during phloem collection. In this study, disrupted SE plastids of *L. albus* were observed releasing their contents as a result of turgor loss during tissue preparation (see Chapter 3). Interestingly, the observed mass of Rubisco small

subunit in spot 5 (ca 6 kDa) and spot 12 (ca 6.2 kDa) is lower than the theoretical molecular weight of their closest match which is 15kDa for Rubisco small subunit of *P. vulgaris* protein (spot 5) and 20kDa for Rubisco small subunit from *G. max* (spot 12). Giavalisco *et al*. (2006) also observed smaller Rubisco small subunit proteins in phloem exudate of *B. napus.* The authors suggested that this phloem polypeptide could be proteolytically trimmed or catabolised, consistent with the idea of non-functional photosynthesis-related proteins in phloem exudate. A number of the proteins identified and described above as being involved in glycolysis such as glyceraldehyde-3P-dehydrogenase are also known to function in photosynthesis.

Long distance signalling

In addition to acting at their site(s) of synthesis and entry into the sieve-tube system, proteins within the SE may play a role in long-distance signalling (Schobert *et al*., 1998). Some SE proteins, synthesized at the site of loading in a leaf, may be delivered to distant sink organs, such as the shoot and/or root apices, where they act on cellular processes in CC, the surrounding parenchyma and beyond (Schobert *et al*., 1998; Balachandran *et al*., 1997).

Nakamura *et al*. (1993) suggested that certain signals might be transduced by phosphorylation and dephosphorylation reactions in the sieve tube of rice plants. Indeed several proteins in rice phloem exudate, collected by stylectomy, were found to be phosphorylated *in vivo* suggesting the possibility of a signal transport system (Nakamura *et al*., 1993). The inhibition of protein phosphorylation by a protein kinase inhibitor *in vitro* was consistent with protein kinases existing in the phloem sap of rice plants in a soluble form (Nakamura *et al*., 1993). No protein kinases were identified in *L. albus* phloem exudate in this study.

One of the prominent spots identified on gels of phloem exudate of lupin contained a protein that showed high homology to Flowering Locus T-like 1 protein from *Chenopodium rubrum* (spot 28) while a second, less prominent spot, contained a protein that showed high homology to Flowering Locus T (FT) protein from *Cucurbita moschata* (spot 107). Because lupin exudate was

collected from fruits on plants where flowers were still developing on secondary and tertiary inflorescences, the presence of FT in phloem might have been expected. These results are consistent with the reported presence of FT proteins in exudate collected from *B. napus* (Giavalisco *et al*., 2006), *C. maxima* (Lin *et al.,* 2008) and by stylectomy from rice (Aki *et al*., 2008). FT proteins and their orthologs have been shown to act as non-cell-autonomous signals that regulate flowering, and are now believed to act as the long-distance signal ('florigen') that induces flowering in *Arabidopsis* (Corbesier *et al*., 2007) and rice (Tamaki *et al.,* 2007). Introduction of a gene construct encoding the FT protein fused to green fluorescent protein (GFP), *FT:GFP*, into *Arabidopsis ft-7* mutants resulted in earlier flowering of these plants. Grafting experiments confirmed that FT:GFP protein could move over long distances. Transgenic *SUC2:FT:GFP ft-7* plants that expressed FT:GFP only in the CC were grafted onto *ft-7* mutants. After grafting, FT:GFP protein was detected across the graft junction and in the vasculature of *ft-7* mutant rootstock. No *FT:GFP* mRNA could be detected in the *ft-7* rootstocks, consistent with the flowering signal being the protein rather than the transcript (Corbesier *et al*., 2007). Grafting studies also demonstrated transmission of a florigenic signal from flowering *C. maxima (*pumpkin) stocks to long day grown *C. moschata* scions (species responsive only to inductive short-day photoperiods) (Lin *et al*., 2007). While mass spectrometric analysis revealed the presence of FT protein in phloem exudate collected from flowering *C. maxima* stocks and from florally induced *C. moschata* scions, *FT* transcripts were not detected using real-time RT-PCR on phloem exudate collected from the flowering *C. maxima* stocks. These studies and a third in rice (Tamaki *et al,* 2007) indicate that FT is functioning as a 'florigenic' signal and not its transcript, as had been initially thought (Huang *et al.*, 2005). Phloem translocation of FT in lupin has not been proven but it seems very likely based on the results from other plants.

Nucleic acid binding

Two of the more prominent spots (26 and 27) on gels of lupin phloem exudates proteins were identified as containing a glycine-rich RNA-binding protein. Other proteomic analyses of exudates have also identified glycine-rich RNA-binding proteins in *R. communis* (Barnes *et al*., 2004), *B. napus* (Giavalisco *et al.*, 2006), *C. maxima* (Lin *et al.,* 2008) and *O. sativa* (Aki *et al*., 2008). It has been

suggested that some members of this family may be involved in stress responses, as their mRNA levels change following exposure to cold, wounding, hormone treatments and water stress in both plants and animals (Nomata *et al*., 2004; Zchut *et al*., 2003). However, the physiological function of these proteins is still not clear. Carpenter *et al*. (1994) found that expression of *Ccr1* and *Ccr2,* two gene members of a class of *A. thaliana* glycine-rich RNA-binding proteins, was influenced by cold treatment and circadian rhythm and hypothesized that CCR1 could stabilize mRNA species during conditions of cold and in response to other environmental stresses. Other possible functions of these types of protein include pre-mRNA processing, mRNA translation and stability, mRNA repression and/or protein turnover (Ludevid *et al*., 1992). Although it is quite tempting to speculate that these proteins could be forming ribonucleotide complexes and translocating RNA as has been reported for some other RNA binding proteins, to date there are no reports of RNA translocation properties attributed to this group of glycine-rich proteins.

Glycine-rich RNA-binding proteins (GRP) also appear to have a role in floral transition in *A. thaliana* specifically in regulation of flowering time (Streitner *et al*., 2008). The loss of function mutant, *At*GRP7, exhibits a delay in the transition to flowering, whereas the gain of function through ectopic over-expression of *At*GRP7 promotes flowering. *At*GRP7 apparently affect flowering time by influencing levels of FLOWERING LOCUS C (*FLC*); a key repressor of flowering (Streitner *et al*., 2008).

CONCLUSION

Proteins identified in phloem exudates of lupin in this study provide a basis to investigate their likely functional roles in SE and possibly in long distance movement and signalling. It is also clear that more extensive analysis in lupin is needed to fully explore this potential. Lin *et al.,* (2008) have identified some 1200 proteins in phloem exudate collected from the stems of pumpkin suggesting that the data represented here for lupin is not complete. In addition to using PAGE, Lin *et al.* (2008) separated groups of proteins by ion exchange as a means to increase resolution. Perhaps one of the emerging proteomic technologies such as ‘isobaric tags for relative and absolute quantitation’ (iTRAQ), followed by 2D-LC-MS/MS (Glen *et al.,* 2008) could be used to extend

the spectrum of identified proteins in lupin exudate and, importantly, provide quantitative data. This latter might be a means to study potential protein ‘signals’ in lupin phloem that can be collected from many different ‘source’ and ‘sink’ sites on the plant.

CHAPTER 5

TRANSCRIPTOME ANALYSIS OF *Lupinus albus* PHLOEM EXUDATE

INTRODUCTION

A number of mRNA molecules have been identified in the vascular tissue of *Arabidopsis* (Deeken *et al*., 2008), *Plantago major* (Pommerrenig *et al*., 2006) and *Apium graveolens* (Vilaine *et al*., 2003). Transcripts have also been identified in phloem exudates from *Arabidopsis* (Deeken *et al*., 2008), *R. communis* (Doering-Saad *et al.,* 2006) and melon (Omid *et al.,* 2007). These analyses used exudate collected from incisions to the vasculature. mRNA has also been recovered from exudates collected by stylectomy from rice (Sasaki *et al.,* 1998) and barley (Doering-Saad *et al.*, 2002; Gaupels *et al.*, 2008a), providing strong evidence that these mRNA are true components of the SE. Sasaki *et al.* (1998) identified mRNAs for thioredoxin h, oryzacystatin-I and actin using RT-PCR. The selection of these transcripts was based on their expressed proteins being prominent in the rice exudate. Doering-Saad *et al.* (2002) used the same approach to detect the transcripts for H^+/sucrose co-transporter SUT1, aquaporin and a H^+ ATPase. More recently, Gaupels *et al*. (2008a) have developed a method for collection of exudate from a series of aphid stylets, allowing collection of a much greater volume (around 5-10 µl) available for analysis. Thus Gaupels *et al.* (2008a) were able to use a cDNA-based differential display technique to detect mRNA in barley phloem. Their study identified eight transcripts related to metabolism, signalling and pathogen defence, none of which had previously been detected in stylet exudates. There are no data for transcripts in stylet exudate from a dicotyledon species.

Omid *et al.* (2007) constructed a cDNA library from mRNA extracted from melon phloem sap collected by incision. Their study identified 986 unique transcripts

corresponding to 1830 expressed sequence tags (ESTs). About 37% of the transcripts were related to 'cellular response to hormone and stress'. The most abundant stress-response genes were those encoding phloem filaments, heat-shock proteins, and metallothioneins. More than 15% of transcripts were related to signal transduction (Omid *et al.* 2007). Doering-Saad *et al.* (2006) identified 158 transcripts present in phloem exudate collected from *R. communis*. Functional analysis revealed mRNA encoding proteins involved in transport, DNA/RNA binding and protein turnover, response to stress, metabolism and cell wall structure. As is the case for proteomic analysis of phloem exudates (see Chapter 4), some of these transcripts would have resulted from contamination of the exudates by the contents of damaged cells. Despite this uncertainty, cDNA libraries based on exudate collected from incisions to the vasculature provide a more complete inventory of potential phloem-specific transcripts. The presence of transcripts in phloem exudate has been interpreted as supporting the idea of an RNA-based systemic signalling network (Haywood *et al.,* 2005).

Since mature SE lack nuclei and ribosomes, neither transcription nor translation is expected to occur in SE, and any mRNA recovered from phloem is likely to have been transported there from CC. Nevertheless, studies using exudates collected from incisions to the vasculature, e.g. from castor bean seedlings (Doering-Saad *et al.,* 2006) and pumpkin (Ruiz-Medrano *et al.,* 2007), have identified a significant number of short ribosomal RNA species. Buhtz *et al*. (2008) suggest that these are simply remnants of differentiating SE but their origin is more likely to be adjacent CC. Plants have evolved a highly robust mechanism for the exchange of information macromolecules between the CC and the sieve tube system (Ruiz-Medrano *et al*., 2007). Ruiz-Medrano *et al*. (2007) studied the effect of cucumber mosaic virus (CMV) infection on the phloem sap mRNA population in *C. maxima.* Their results revealed that CMV infection caused only a minor change to the overall population of 'phloem-mobile' mRNA species, supporting the notion that the transport of mRNA into the functional phloem is a robust process in which the viral movement protein (MP) fails to significantly alter the targeting of endogenous mRNA (Ruiz-Medrano *et al*., 2007). There is a body of evidence for phloem-specific expression of a number of genes identified using *in situ* localisation techniques and, more recently, specific cell sampling methods based on laser capture

micro dissection and flow cytometric separation of cells and nuclei (Nelson *et al.,* 2008; Brady *et al.,* 2007; Zhang *et al.,* 2008). Zhang *et al.* (2008) identified a spectrum of expressed genes specific to the CC in *Arabidopsis* roots and a number of these have been detected in phloem exudates.

Long distance transport of mRNA through graft junctions has been demonstrated (Kim *et al*., 2001; Ruiz-Medrano *et al*., 1999). Omid *et al*. (2007) assessed the long distance translocation ability from melon stocks to pumpkin scions of 43 transcripts identified in phloem exudates of melon. Six of these transcripts, three of them associated with auxin-signal transduction, were found to be translocated from melon to pumpkin (Omid *et al*., 2007). Although the level of transcript for some of these 'signalling' genes was low in exudate, other more prominent mRNA were not translocated. This is consistent with the idea that the transport to and translocation of mRNA in the SE is selective; a necessary prerequisite if these phloem-mobile transcripts have systemic regulatory roles.

In this study, a cDNA library was constructed from mRNA isolated from phloem exudate of *L. albus* plants. A total of 1063 clones were sequenced and their identity established using genomic database information. A functional analysis of the identified transcripts revealed a great diversity of encoded proteins, with the most abundant involved in metabolism and in protein synthesis and turnover. A small group of transcripts was identified as having potential signalling functions. Potential contamination of *L. albus* phloem exudates, with transcripts derived from neighbouring cells, was assessed using real-time RT-PCR to compare the levels of eight different transcripts in phloem exudate to the pod tissue surrounding the vasculature from which phloem exudate was collected. The overall aim of this study was to give a global insight into the mRNA composition of *L. albus* phloem exudate with a view to identifying transcripts associated with biochemical processes in SE and as potential signalling macromolecules. This is the first transcriptomic analysis of phloem exudate for a species in the legume family.

EXPERIMENTAL PROCEDURES

Phloem exudate collection

Phloem exudate was collected from *L. albus* plants as described in 'General Methods' (Chapter 2).

mRNA isolation from phloem exudate

Total RNA was isolated from phloem exudate as described in 'General Methods' (Chapter 2). mRNA was isolated from total RNA using a Dynabeads® mRNA DIRECT™ kit (DYNAL BIOTECH) following the manufacturer's instructions. Briefly, 4 vol of Lysis/Binding buffer (supplied with the kit) was added to the phloem exudate total RNA sample. Dynabeads were added to the phloem/Binding buffer mix and incubated with continuous mixing for 10 min at 21°C. After incubation, the sample tube was placed on a magnet (DYNAL) and the supernatant removed. The bead/mRNA complex was washed with the buffers supplied in the kit and mRNA eluted in 10 µl of 10 mM Tris-HCl. Beads were separated from the solution using the magnet.

cDNA library construction

A cDNA library was constructed from mRNA using the CloneMiner cDNA Library Construction Kit (Invitrogen) following the manufacturer's instructions. Briefly, a first strand of cDNA was synthesized using Biotin-*att*B2-oligo(dT) primer and SuperScript™ II Reverse Transcriptase (Invitrogen). A second strand was synthesized using *Escherichia coli* DNA polymerase I. *att*B1 adapter was ligated to the 5' end of the double-stranded cDNA followed by size fractionation using column chromatography. *att*B-flanked cDNA was cloned into pDONR222™ vector (Invitrogen) (Figure 5.1) by recombination and transformed into *E. coli* ElectroMAX™ DH10B™ T1 Phage-Resistant Competent Cells (Invitrogen).

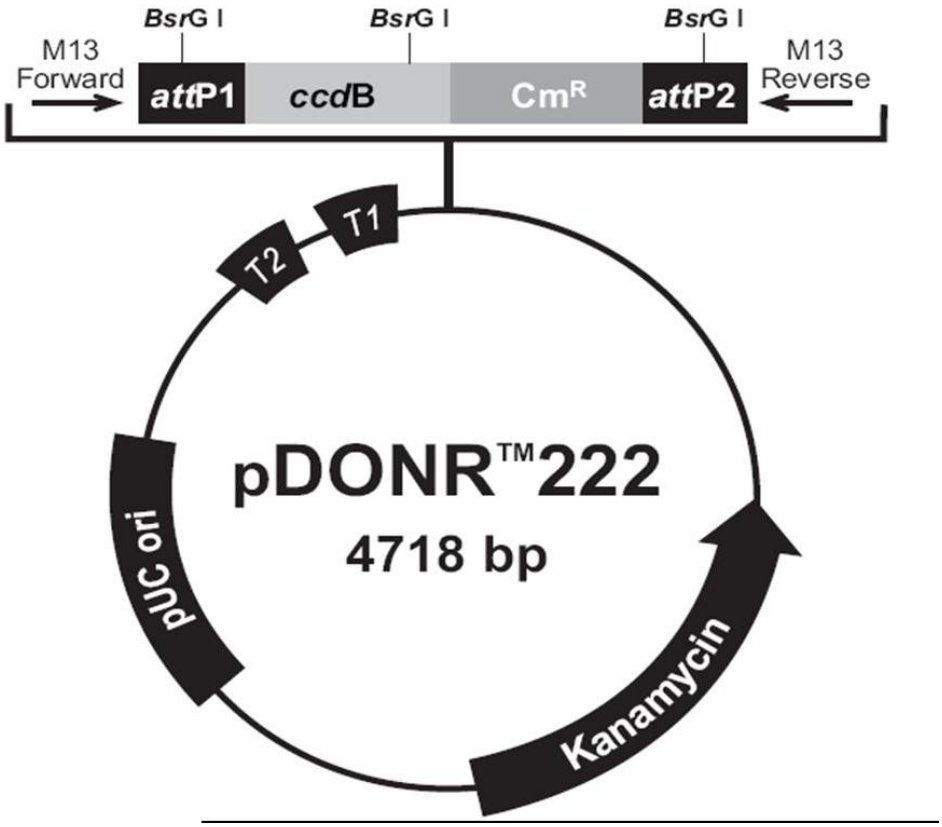

Figure 5.1. Vector map of pDONR™222. T2: transcription termination sequence: bases 58-85(c); T1: transcription termination sequence: bases 217-260 (c); M13 forward priming site: bases 327-342; *att*P1: bases 360-591; *Bsr*G I restriction sites: bases 442, 1232, 2689; *ccd*B gene: bases 987-1292(c); Chloramphenicol resistance gene (Cm^R): bases 1612-2295 (c); *att*P2: bases 2543-2774(c); M13 reverse priming site: bases 2816-2832; kanamycin resistance gene: bases 2899-3714(c); pUC origin: bases 4045-4718; (c)= complementary strand. The figure was taken from the CloneMiner™ cDNA library construction kit handbook, Invitrogen.

Plasmid DNA isolation

Plasmids grown in transformed *E. coli* were isolated using the UltraClean™ mini plasmid prep kit™ (MO BIO Laboratories, Inc.) following the manufacturer's instructions. Bacterial cells were grown on 2 ml Luria-Bertani (LB) broth medium (in 1L: 5 g yeast extract, 10 g tryptone, 10 g NaCl) containing 50 µg/ml kanamycin at 37°C overnight with vigorous shaking. To pellet the cells, bacterial cultures were centrifuged for 1 min at 12,000 *g*. The supernatant was removed and 50 µl resuspension buffer added to the pellet followed by vortexing at the highest speed. 100 µl lysis buffer was added to the resuspended cells. Samples were mixed gently by inverting the tubes once. Neutralising buffer (325 µl) was added to the sample and mixed gently by inverting the tubes followed by centrifugation for 1 min at 12,000 *g*. The supernatant was transferred to a spin filter unit provided with the kit and centrifuged for 30 sec to bind the plasmid

DNA to the filter membrane. Wash buffer (300 µl) was added to the spin filter and centrifuged for 30 sec at 12,000 *g*. Plasmid DNA was eluted by adding 50 µl of sterile water and centrifuging for 30 sec at 12,000 *g*.

Determination of average insert size and EST sequencing

Average insert size was determined by agarose gel electrophoresis. Sixty randomly-selected single colonies were picked from LB agar plates and cultured overnight in 2 ml LB broth medium containing 50 µg/ml kanamycin as described above. Plasmid DNA was isolated and the insert amplified by PCR using M13 forward and reverse primers (Table 5.1). PCR products were visualised on 1% (w/v) agarose gels as described in 'General Methods' (Chapter 2). and insert size estimated using 1kb DNA ladder (GeneRuler^{TM}, MBI Fermentas). The inserts of 1063 randomly-selected clones were sequenced using M13 primers (Table 5.1). The sequences were subjected to BLASTN and BLASTX searches against the NCBI database. Matches with a threshold *E* value of 10^{-10} were considered significant.

Table 5.1. DNA oligonucleotide sequences used to determine average insert size and as sequencing primers to sequence inserts in entry clones derived from recombination with pDONR^{TM}222 vector.

Primer	DNA oligonucleotide sequence
M13 Forward	5'-GTAAAACGACGGCCAG-3'
M13 Reverse	5'-CAGGAAACAGCTATGAC-3'

Levels of transcripts in phloem exudate and tissues

Levels of S-adenosylmethionine (SAM) synthase, Rubisco Small Subunit, aquaporin, flowering locus T, chlorophyll a/b binding protein, actin, ubiquitin and sucrose synthase transcripts (all identified in *L. albus* phloem exudate), were estimated in phloem exudate using real-time RT-PCR and compared with levels in pod, flower, stem and leaf tissue that had been sampled from the same plants at the same time. Isolation of total RNA and real-time RT-PCR were performed as described in 'General Methods' (Chapter 2). The primers used for real-time RT-PCR are shown in Table 5.2. To ensure maximum specificity and

efficiency during PCR amplification, primers were designed using the Roche website:

https://www.roche-applied-science.com/sis/rtpcr/upl/acenter.jsp?id=030000

Table 5.2. DNA oligonucleotide sequences used as specific primers in real-time RT-PCR. Specific primers were used in a final concentration of 0.5 µM in 5 µl real-time PCR reactions.

	DNA oligonucleotide sequences	
	Forward	**Reverse**
S-adenosylmethionine synthase	AGGAAGGAAGATCATCATTGACA	TCCTTTCCGGAGAAAGCAC
Rubisco Small Subunit	CATGGATTCGTGTACCGTGA	TGTCCAGTAGCGTCCATCAT
Aquaporin	AAATTGTTGGCACCTTCGTC	AATCTCTGGCGCTACGTTTG
Flowering locus T	TTCTACACACTGGTTATGGTGGA	GCAAGTATTCCCTCAAGAAAGG
Chlorophyll a/b binding protein	TGGTGACTATGGTTGGGACA	CTCACGGTTCTTGGCAAAAG
Actin	GTTCCGTTGCCCAGAAGTC	ATTCCAGGCGCTTCCATAC
Ubiquitin	AATCAACCCTCCACCTCGT	GGTGAGGGTTTTGACGAAGA
Sucrose synthase	TGGTTTGGTAGAAAGCTATGCTAAG	GCCAGCTACAACGACAAGGT

Primers were required to have melting temperatures of 60ºC±1ºC and to amplify products around 60-70bp. Results were analysed using the LightCycler software (Roche). Three biological replicates with two technical replicates were measured per sample. Standard curves for absolute quantification were prepared for each gene by amplifying the appropriate inserts in the plasmids (using M13 primers in Table 5.1) and using a dilution series of gel purified PCR products (see 'general methods' Chapter 2). After gel purification, DNA was quantified using the NanoDrop ND-1000 Spectrophotometer (NanoDrop Technologies) and number of molecules calculated. Standards were diluted to 6.023^{10} molecules µL-1. From this stock, a series of 7-fold dilutions were made.

RESULTS

cDNA library of phloem exudate

Insert size was determined by agarose gel electrophoresis. Analysis of the transformants showed an average insert size of approximately 1198 bp, and of 60 clones analysed, all contained inserts. Figure 5.2 shows the analysis of 18 randomly-selected clones to determine the size of the cDNA inserts. A total of 1063 clones were sequenced, 192 sequences were excluded based on the quality of the sequence and 144 ESTs did not show significant similarity to any sequence in the databases searched. A total of 609 unique transcripts corresponding to 727 ESTs were identified. Redundant sequences were assembled into 67 contigs corresponding to 176 ESTs with an average of 2.6 ESTs per contig (Table 5.3).

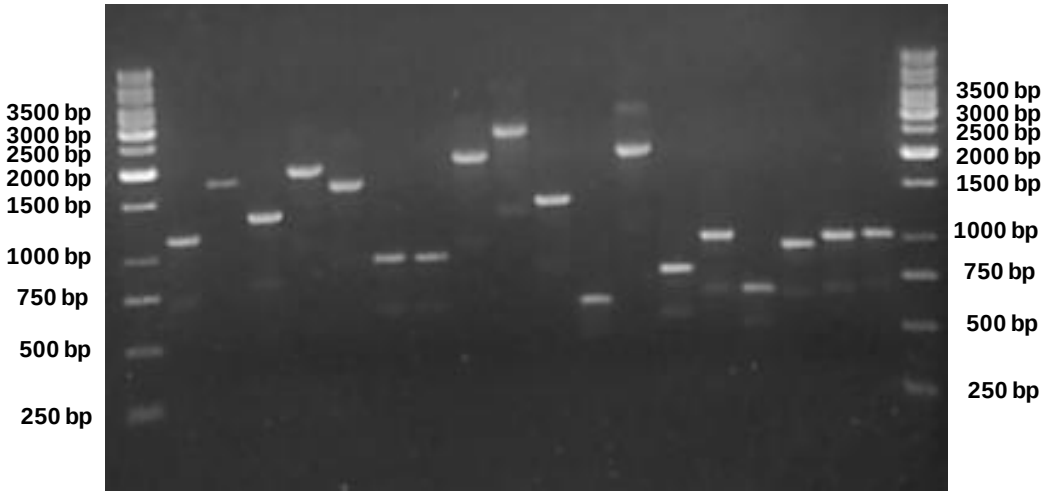

Figure 5.2. Analysis of transformants. Insert size was determined by agarose gel electrophoresis. Single bacterial colonies were picked from LB agar plates and cultured overnight in LB broth containing 50 µg/ml kanamycin. Plasmid DNA was isolated and the insert amplified by PCR using M13 primers. PCR products were visualised on 1% (w/v) agarose gels. 1kb DNA ladder was run alongside the samples to determine the size of the PCR products.

The most abundant transcripts (Table 5.3) coded for a pathogenesis related protein (7 sequences, Ac No. BAB63949.1), chlorophyll a/b-binding protein (6 sequences, Ac No. AAA50172.1), polyprotein from white lupin/bean yellow mosaic virus (6 sequences, Ac No. ABG33691.1), a peptidyl-prolyl cis-trans

isomerase (cyclophilin) (5 sequences, Ac No. O49886) and a drought-induced protein (5 sequences, Ac No. AAK73280.1).

Functional categorisation showed that transcripts coding for proteins with unknown functions (Appendix 2) formed the largest category (282 sequences, 39% of all ESTs). All proteins with insufficient functional information were classified in this category. The largest groups of transcripts coding for proteins with known functions were metabolism with 16% of all ESTs (12% general metabolism and 4% energy metabolism), protein synthesis and turnover with 11% of all ESTs, and redox regulation, signalling and stress response and defence related with 5% of all ESTs each (Figure 5.3). The smaller categories of ESTs were grouped under photosynthesis, cell wall and structural components and transport with 3% each. A group of 23 ESTs (3% of all ESTs) classified as viral proteins was also observed. Transcripts encoding proteins with multiple or unclear function were grouped as 'unclassified' (3% of all ESTs) (Figure 5.3).

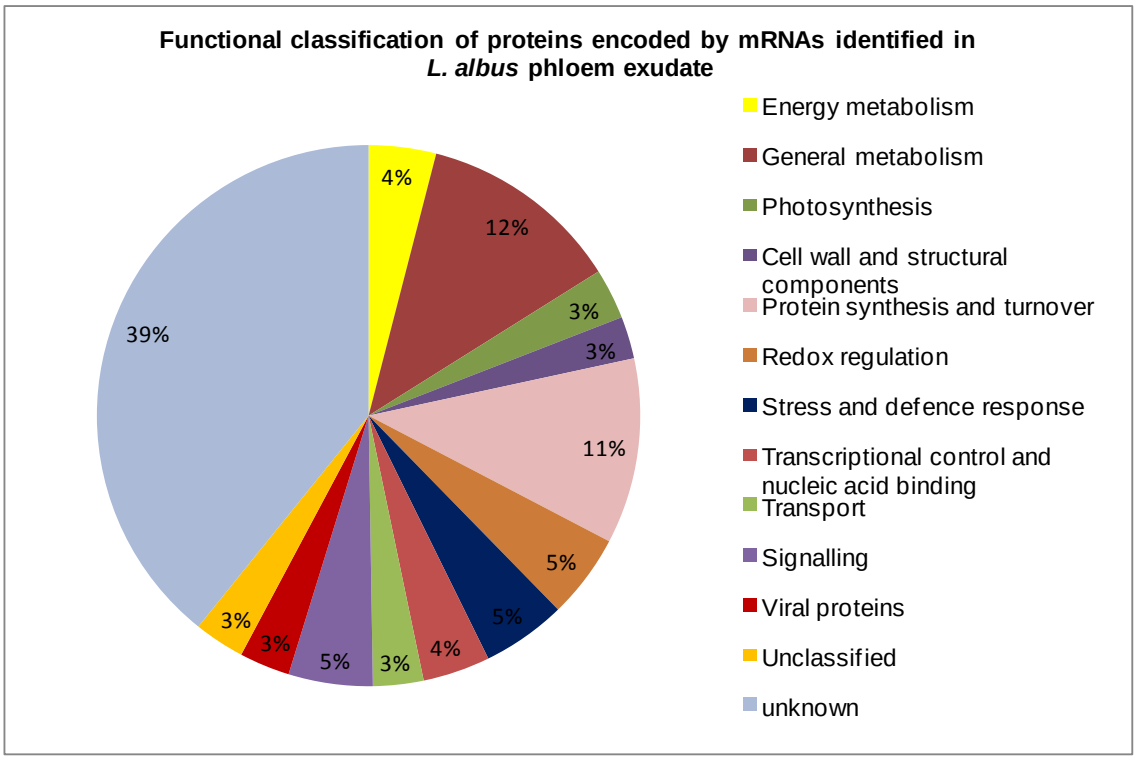

Figure 5.3. Functional categorisation of proteins encoded by mRNA identified in *L. albus* phloem exudate collected by the incision method.

Table 5.3. Results of BLASTX search and functional classification of *L. albus* phloem exudate ESTs. A cDNA library was constructed from mRNA isolated from phloem exudate collected from *L. albus* plants. Clones were sequenced and their identity established using genomic database information. “Unclassified” transcripts had multiple or unclear functions.

Accession number	Similarity	Score (bits)	E-value	ESTs per mRNA
ENERGY METABOLISM				
ABB46862.2	Enolase, putative, expressed [Oryza sativa (japonica cultivar-group)]	543	1.00E-153	1
BAC77064.1	NADP-specific isocitrate dehydrogenase [Lupinus albus]	528	1.00E-148	1
BAA77604.1	plastidic aldolase NPALDP1 [Nicotiana paniculata]	514	1.00E-144	1
AAL66290.1	adenosine 5'-phosphosulfate reductase [Glycine max]	500	1.00E-140	1
NP_001078275.1	pyruvate kinase, putative [Arabidopsis thaliana]	473	1.00E-132	1
O65735	Fructose-bisphosphate aldolase, cytoplasmic isozyme [Cicer arietinum]	471	1.00E-131	2
CAA56354.1	NADP dependent malic enzyme [Phaseolus vulgaris]	465	1.00E-129	1
O24301	Sucrose synthase 2 (Sucrose-UDP glucosyltransferase 2) {Pisum sativum]	461	1.00E-128	1
AAO15574.1	malate dehydrogenase [Lupinus albus]	394	1.00E-123	1
ABA86966.1	triosephosphate isomerase [Glycine max]	424	1.00E-117	2
CAI83772.1	glyceraldehyde-3-phosphate-dehydrogenase [Lupinus albus]	413	1.00E-114	2
P80269	NADH dehydrogenase [ubiquinone] [Solanum tuberosum]	363	5.00E-99	1
AAF01037.1	NADH ubiquinone oxidoreductase PSST subunit [Lupinus luteus]	337	4.00E-91	1
ABA07956.1	glyceraldehyde-3-dehydrogenase C subunit [Glycine max]	311	2.00E-83	1
ABD28700.1	ATP binding , related [Medicago truncatula]	306	1.00E-81	1
BAC81652.1	short-chain alcohol dehydrogenase A [Pisum sativum]	297	4.00E-79	2
Q42961.1	Phosphoglycerate kinase, chloroplast precursor [Nicotiana tabacum]	248	3.00E-64	3
AAY85660.1	cytosolic glucose-6-phosphate isomerase [Helianthus annuus]	220	4.00E-56	1
AAT46998.1	triosephosphate isomerase [Glycine max]	202	1.00E-50	1
CAI53675.1	pyruvate kinase [Glycine max]	147	5.00E-34	1
YP_001648758.1	ATP synthase subunit 6 [Mycosphaerella graminicola]	135	3.00E-30	1
1F3Y|A	Chain A [Lupinus Angustifolius L.]	102	1.00E-20	1

Accession number	Similarity	Score (bits)	E-value	ESTs per mRNA
GENERAL METABOLISM				
AAA98603.1	mitochondrial aspartate aminotransferase [Glycine max]	525	1.00E-147	1
AAL33919.1	UDP-glucose pyrophosphorylase [Amorpha fruticosa]	523	1.00E-147	3
BAB40967.1	UDP-D-glucuronate carboxy-lyase [Pisum sativum]	514	1.00E-144	1
ABO77438.1	S-adenosyl-L-methionine synthetase [Medicago sativa subsp. falcata]	503	1.00E-141	2
CAJ01707.1	putative S-adenosylhomocystein hydrolase 2 [Hordeum vulgare subsp. vulgare]	504	1.00E-141	1
Q9SP37	Adenosylhomocysteinase [Lupinus luteus]	495	1.00E-138	2
AAA74441.1	phosphatidylinositol-specific phospholipase C [Glycine max]	478	1.00E-136	1
CAB61752.1	dTDP-glucose 4-6-dehydratase [Cicer arietinum]	484	1.00E-135	2
AAU89742.1	serine/threonine protein kinase-like [Solanum tuberosum]	479	1.00E-134	1
Q43785	Glutamine synthetase (Glutamate--ammonia ligase) [Medicago sativa]	477	1.00E-133	1
CAC05439.1	glucose-6-phosphate 1-dehydrogenase [Arabidopsis thaliana]	463	6.00E-129	1
P51850	Pyruvate decarboxylase isozyme 1 (PDC) [Pisum sativum]	461	1.00E-128	1
ABO80948.1	S-adenosylmethionine synthetase [Medicago truncatula]	456	1.00E-127	3
AAO23063.1	ent-kaurenoic acid oxidase [Pisum sativum]	410	1.00E-122	1
1803516A	glycolate oxidase [Lens culinaris]	437	1.00E-121	1
AAW21273.1	glutamine synthetase [Saccharum officinarum]	434	1.00E-120	1
ABO61376.1	serine hydroxymethyltransferase [Populus tremuloides]	434	1.00E-120	1
ABC74567.1	acetoacetyl-CoA thiolase [Picrorhiza kurrooa]	435	1.00E-120	1
CAA53078.1	3-ketoacyl-CoA thiolase B [Mangifera indica]	432	1.00E-119	1
NP_188498.1	aspartate/glutamate/uridylate kinase family protein [Arabidopsis thaliana]	430	1.00E-119	1
AAT58365.1	GMPase [Medicago sativa]	427	1.00E-118	1
BAA82130.1	acid phosphatase [Lupinus albus]	417	4.00E-115	1
AAC50014.1	aspartate aminotransferase [Glycine max]	407	1.00E-115	1
ABA54865.1	putative 3-deoxy-D-arabino-heptulosonate 7-phosphate synthase 3 [Fagus sylvatica]	413	1.00E-114	1
AAK52082.1	nuclease [Nicotiana tabacum]	416	1.00E-114	1
Q9FR44.1	Phosphoethanolamine N-methyltransferase 1 [Arabidopsis thaliana]	408	1.00E-112	1
AAT40304.1	S-adenosylmethionine synthase [Medicago sativa]	402	1.00E-110	1

Accession number	Similarity	Score (bits)	E-value	ESTs per mRNA
GENERAL METABOLISM				
Q96423	Trans-cinnamate 4-monooxygenase (Cinnamic acid 4-hydroxylase) [Glycyrrhiza echinata]	397	1.00E-109	1
ABD33275.2	progesterone 5-beta-reductase, putative [Medicago truncatula]	398	1.00E-109	1
ABN08096.1	Galactose mutarotase-like [Medicago truncatula]	377	1.00E-103	1
CAC10212.1	putative mitochondrial glyoxalase II [Cicer arietinum]	375	1.00E-102	1
AAR13305.1	phytochelatin synthetase-like protein [Phaseolus vulgaris]	372	1.00E-101	1
BAA25187.1	ARG10 [Vigna radiata]	368	1.00E-100	2
AAM60857.1	dihydrolipoamide S-acetyltransferase, putative [Arabidopsis thaliana]	365	2.00E-99	2
ABB29942.1	S-adenosyl methionine synthase-like [Solanum tuberosum]	360	5.00E-98	2
AAX84672.1	aldo/keto reductase AKR [Manihot esculenta]	353	5.00E-96	1
CAO48819.1	D-alanine--D-alanine ligase family [Arabidopsis thaliana]	350	8.00E-95	1
ABC94943.1	squalene epoxidase [Medicago sativa]	316	8.00E-85	1
NP_195815.3	ATP binding / kinase/ protein serine/threonine kinase [Arabidopsis thaliana]	319	1.00E-85	1
BAB33421.1	putative senescence-associated protein [Pisum sativum]	307	4.00E-82	4
AAL74418.2	ATP sulfurylase [Glycine max]	306	1.00E-81	1
CAA74101.1	laccase [Populus trichocarpa]	301	4.00E-80	1
ABD28680.1	Rubber elongation factor [Medicago truncatula]	301	2.00E-80	1
BAC10552.1	nine-cis-epoxycarotenoid dioxygenase4 [Pisum sativum]	288	2.00E-76	1
ABW34717.1	acireductone dioxygenase [Solanum tuberosum]	281	4.00E-74	1
AAO49473.1	putative serine/threonine kinase [Vitis vinifera]	274	4.00E-72	1
P28002	Caffeic acid 3-O-methyltransferase [Medicago sativa]	268	2.00E-70	1
AAB03852.1	alpha-carboxyltransferase aCT-1 precursor [Glycine max]	257	6.00E-67	1
AAG28503.1	hexokinase [Citrus sinensis]	246	2.00E-63	2
ABQ81923.1	aminotransferase 2 [Cucumis melo]	241	2.00E-62	1
NP_195242.1	O-methyltransferase family 2 protein [Arabidopsis thaliana]	241	4.00E-62	3
NP_187342.1	MFP2 (MULTIFUNCTIONAL PROTEIN); enoyl-CoA hydratase [Arabidopsis thaliana]	241	2.00E-62	1
BAA88226.1	thiamin biosynthetic enzyme [Glycine max]	239	6.00E-62	2
P43280	S-adenosylmethionine synthetase 1 [Solanum lycopersicum]	238	2.00E-61	1

Accession number	Similarity	Score (bits)	E-value	ESTs per mRNA
GENERAL METABOLISM				
AAK63009.1	heme oxygenase 3 [Glycine max]	238	1.00E-61	1
Q04593	Phenylalanine ammonia-lyase 2 [Pisum sativum]	238	2.00E-61	1
BAD94178.1	putative myo-inositol 1-phosphate synthase [Arabidopsis thaliana]	219	8.00E-56	2
BAF49299.1	putative glycosyltransferase [Clitoria ternatea]	195	1.00E-48	1
NP_194843.1	glycosyl hydrolase family 17 protein [Arabidopsis thaliana]	192	2.00E-47	1
AAL91002.1	asparagine synthetase [Securigera parviflora]	179	4.00E-44	1
BAB33422.1	putative senescence-associated protein [Pisum sativum]	175	2.00E-42	1
NP_565701.1	lipase class 3 family protein [Arabidopsis thaliana]	169	9.00E-41	1
NP_190412.1	hydrolase, alpha/beta fold family protein [Arabidopsis thaliana]	160	4.00E-38	1
CAA63598.1	glyoxysomal beta-ketoacyl-thiolase [Brassica napus]	156	5.00E-37	1
AAY86360.1	cinnamoyl-CoA reductase [Acacia mangium x Acacia auriculiformis]	149	9.00E-35	1
ABU62755.1	4,5-DOPA dioxygenase extradiol [Nicotiana benthamiana]	147	2.00E-34	1
AAS79665.1	cryptochrome 2A apoprotein [Pisum sativum]	137	5.00E-31	1
AAL89723.1	S-adenosylmethionine decarboxylase [Glycine max]	136	4.00E-31	2
AAC70779.1	granule-bound glycogen (starch) synthase [Astragalus membranaceus]	128	2.00E-28	1
ABW89464.1	glutamine synthetase [Gossypium hirsutum]	119	8.00E-26	1
ABN06032.1	Galactose-binding like [Medicago truncatula]	111	2.00E-23	1
ABO77440.1	S-adenosylmethionine decarboxylase [Medicago sativa subsp. falcata]	72.4	2.00E-11	2
AAB96761.1	ferredoxin-dependent glutamate synthase [Glycine max]	72.8	1.00E-11	1
PHOTOSYNTHESIS				
AAA50172.1	photosystem II type I chlorophyll a/b-binding protein [Glycine max]	514	1.00E-144	6
AAR10886.1	chlorophyll a/b binding protein [Trifolium pratense]	442	1.00E-122	3
AAD27878.1	chlorophyll a/b binding protein CP29 [Vigna radiata]	432	1.00E-119	1
P27521.1	Chlorophyll a-b binding protein 4 [Arabidopsis thaliana]	357	7.00E-97	1
ABQ63097.1	photosystem I subunit PsaD [Glycine max]	342	1.00E-92	1
AAA33866.1	ribulose 1,5-bisphosphate carboxylase small subunit [Malus x domestica x Pyrus communis]	300	5.00E-80	1

Accession number	Similarity	Score (bits)	E-value	ESTs per mRNA
PHOTOSYNTHESIS				
P08927	RuBisCO large subunit-binding protein subunit beta [Pisum sativum]	298	3.00E-79	1
O65100	Ferritin-3, chloroplast precursor [Vigna unguiculata]	283	8.00E-75	1
BAD97359.1	PsbQ [Nicotiana tabacum]	204	3.00E-51	1
ABI84258.1	photosystem I psaH protein [Arachis hypogaea]	202	2.00E-50	1
ABC46708.1	chloroplast photosystem II [Arachis hypogaea]	196	7.00E-49	2
P10690	Photosystem II 10 kDa polypeptide [Spinacia oleracea]	156	5.00E-37	1
CAB53034.1	photosystem I subunit XI precursor [Arabidopsis thaliana]	153	4.00E-36	1
CAA96570.1	CP12 [Pisum sativum]	148	3.00E-34	1
P14226	Oxygen-evolving enhancer protein 1 [Pisum sativum]	89.7	5.00E-17	1
CELL WALL AND STRUCTURAL COMPONENTS				
Q39445	Tubulin beta chain (Beta-tubulin) [Cicer arietinum]	546	1.00E-154	1
AAF03692.1	actin [Picea rubens]	487	1.00E-136	1
P37392	Tubulin beta-1 chain (Beta-1-tubulin) [Lupinus albus]	469	1.00E-134	1
NP_187818.1	ACT11 (ACTIN-11) [Arabidopsis thaliana]	451	1.00E-125	1
AAB40079.1	actin [Glycine max]	429	1.00E-119	1
ABN08645.1	Tubulin binding cofactor C [Medicago truncatula]	405	1.00E-111	1
P12459.1	Tubulin beta-1 chain (Beta-1-tubulin) [Glycine max]	394	3.00E-108	1
BAD29243.1	dTDP-D-glucose 4,6-dehydratase-like [Oryza sativa]	390	1.00E-107	1
AAV83799.1	putative actin 1 [Chorispora bungeana]	367	1.00E-100	3
ABX57816.1	alpha tubulin [Picea wilsonii]	306	6.00E-82	1
ABB16985.1	profilin-like protein [Solanum tuberosum]	248	2.00E-64	1
AAU81921.1	profilin [Arachis hypogaea]	221	4.00E-56	1
CAD33929.1	microtubule associated protein [Cicer arietinum]	208	2.00E-52	1
ABA81885.1	profilin-like [Solanum tuberosum]	207	5.00E-52	1
Q941H7	Profilin (Minor allergen Lit c 1) [Litchi chinensis]	158	1.00E-37	1
ABV55999.1	alpha-tubulin 7 [Populus tremuloides]	151	2.00E-35	1
NP_566316.1	kelch repeat-containing protein [Arabidopsis thaliana]	73.6	6.00E-12	1
PROTEIN SYNTHESIS, TURNOVER AND SORTING				
ABA12220.1	translation elongation factor 1A-4 [Gossypium hirsutum]	518	1.00E-145	1
ABA12221.1	translation elongation factor 1A-5 [Gossypium hirsutum]	497	1.00E-139	1
ABE91931.1	Proteasome component region PCI [Medicago truncatula]	485	1.00E-135	1

Accession number	Similarity	Score (bits)	E-value	ESTs per mRNA
PROTEIN SYNTHESIS, TURNOVER AND SORTING				
AAY67798.1	14-3-3 protein [Manihot esculenta]	468	1.00E-130	1
CAC20221.1	ribosomal protein L2 [Glycine max]	466	1.00E-130	2
Q96453	14-3-3-like protein D (SGF14D) [Glycine max]	459	1.00E-127	3
AAB36545.1	ubiquitin-like protein [Phaseolus vulgaris]	444	1.00E-123	2
P35100	ATP-dependent Clp protease ATP-binding subunit clpC homolog [Pisum sativum]	435	1.00E-120	2
ABD32840.1	Peptidase C1A, papain [Medicago truncatula]	430	1.00E-119	1
ABF18679.1	cysteine protease [Medicago sativa]	415	1.00E-114	1
AAN72085.1	putative aminopeptidase [Arabidopsis thaliana]	391	1.00E-107	1
CAA83548.1	PsHSC71.0 [Pisum sativum]	371	1.00E-103	1
NP_178234.1	60S ribosomal protein L7 (RPL7B) [Arabidopsis thaliana]	370	1.00E-101	1
AAD56020.1	elongation factor-1 alpha 3 [Lilium longiflorum]	369	1.00E-101	2
ABE79560.1	Chaperone DnaK [Medicago truncatula]	358	3.00E-97	1
ABA46772.1	RUB1-conjugating enzyme-like protein [Solanum tuberosum]	353	9.00E-96	2
O65731	40S ribosomal protein S5 [Cicer arietinum]	347	3.00E-94	1
ABE80155.1	Peptidylprolyl isomerase, FKBP-type [Medicago truncatula]	342	2.00E-92	1
CAA04447.1	DnaJ-like protein [Medicago sativa]	335	2.00E-90	2
NP_565477.1	AtRPN1a/RPN1A (26S proteasome regulatory subunit S2 1A); binding [Arabidopsis thaliana]	227	4.00E-90	1
AAR83877	60S ribosomal protein L19 [Capsicum annuum]	330	5.00E-89	2
ABD28502.1	Cyclin-like F-box [Medicago truncatula]	329	1.00E-88	1
CAD29823.2	putative ubiquitin-conjugating enzyme [Populus x canadensis]	325	2.00E-87	1
AAK02067.1	cyclophilin-40 [Arabidopsis thaliana]	322	1.00E-86	1
ABA40437.1	40S ribosomal protein S7-like protein [Solanum tuberosum]	311	3.00E-83	2
O49886	Peptidyl-prolyl cis-trans isomerase (PPIase) (Rotamase) (Cyclophilin) [Lupinus luteus]	312	1.00E-83	5
ABM53472.1	eIF5A [Rosa chinensis]	307	5.00E-82	2
NP_564011.1	UBC36; ubiquitin-protein ligase [Arabidopsis thaliana]	309	2.00E-82	1
AAR83868.1	60S ribosomal protein L12 [Capsicum annuum]	279	2.00E-73	1
P48724	Eukaryotic translation initiation factor 5 (eIF-5) [Phaseolus vulgaris]	275	3.00E-72	1

Accession number	Similarity	Score (bits)	E-value	ESTs per mRNA
PROTEIN SYNTHESIS, TURNOVER AND SORTING				
AAD34458.1	Skp1 [Medicago sativa]	266	8.00E-70	1
CAA80333.1	ubiquitin extension protein [Lupinus albus]	264	4.00E-69	1
ABR25690.1	60S ribosomal protein l7a [Oryza sativa (indica cultivar-group)]	257	3.00E-67	1
ABN08266.1	Poly(ADP-ribose) polymerase, catalytic region [Medicago truncatula]	254	5.00E-66	1
ABF93903.1	60S ribosomal protein L21, putative [Oryza sativa (japonica cultivar-group)]	245	2.00E-63	1
NP_565053.1	SNF7 family protein [Arabidopsis thaliana]	240	6.00E-62	1
ABG27020.1	SKP1-like b [Medicago truncatula]	234	7.00E-60	1
AAS57912.1	70 kDa heat shock cognate protein 1 [Vigna radiata]	228	3.00E-58	1
O22584	40S ribosomal protein S14 [Lupinus luteus]	223	8.00E-57	1
NP_173692.1	PFL (POINTED FIRST LEAVES) [Arabidopsis thaliana]	222	2.00E-56	1
Q9M5L0	60S ribosomal protein L35 [Euphorbia esula]	219	7.00E-56	2
NP_195162.2	protease-related [Arabidopsis thaliana]	145	7.00E-54	1
ABJ91230.1	CBL-interacting protein kinase 24 [Populus trichocarpa]	202	6.00E-51	1
ABB55398.1	40S ribosomal protein S10-like [Solanum tuberosum]	206	2.00E-51	1
1909359A	ribosomal protein S19 [Solanum tuberosum]	194	3.00E-48	1
AAP72960.1	putative ribosomal protein L31 [Lactuca sativa]	188	2.00E-46	3
Q06445	Cysteine proteinase inhibitor (Cystatin) [Vigna unguiculata]	171	2.00E-41	1
CAA10612.1	ribosomal protein S14 [Pisum sativum]	156	1.00E-36	1
ABA46751.1	eukaryotic initiation factor 5A4-like protein [Solanum tuberosum]	141	2.00E-32	1
ABY60454.1	putative polyubiquitin [Adonis aestivalis var. palaestina]	133	3.00E-30	1
O04287	Peptidyl-prolyl isomerase FKBP12 (12 kDa FK506-binding protein) [Vicia faba]	127	2.00E-28	1
O22518	40S ribosomal protein SA (p40) [Glycine max]	111	1.00E-23	1
AAC15418.1	14-3-3 protein homolog [Maackia amurensis]	109	6.00E-23	1
AAL91663.1	60s acidic ribosomal protein [Prunus dulcis]	100	5.00E-20	1
NP_187595.1	CDC48 (CELL DIVISION CYCLE 48); ATPase [Arabidopsis thaliana]	101	1.00E-20	1
AAB88458.1	ribosomal protein S12 [Lupinus albus]	98.6	4.00E-19	1
P25866	Ubiquitin-conjugating enzyme [Triticum aestivum]	94.4	4.00E-18	1

Accession number	Similarity	Score (bits)	E-value	ESTs per mRNA
PROTEIN SYNTHESIS, TURNOVER AND SORTING				
ABY56104.1	ribosomal protein [Cucumis sativus]	92.8	6.00E-18	1
ABC69274.2	putative DnaJ protein [Camellia sinensis]	89.7	1.00E-16	1
ABD32395.1	Histone-fold/TFIID-TAF/NF-Y [Medicago truncatula]	80.9	4.00E-14	1
REDOX REGULATION				
ABQ41114.1	monodehydroascorbate reductase [Vitis vinifera]	507	1.00E-142	1
CAI56334.1	TPA: isoflavone reductase-like protein 5 [Vitis vinifera]	450	1.00E-125	1
AAO13838.1	peroxidase 2 [Lupinus albus]	420	1.00E-116	1
AAG22740.1	allergenic isoflavone reductase-like protein [Betula pendula]	414	1.00E-114	2
ABM45856.1	cytosolic ascorbate peroxidase [Arachis hypogaea]	382	1.00E-104	1
NP_181836.1	AT-P4H-1 (A. THALIANA P4H ISOFORM 1); oxidoreductase [Arabidopsis thaliana]	370	1.00E-101	1
P32110	Probable glutathione S-transferase (Heat shock protein 26A) (G2-4) [Glycine max]	347	5.00E-94	2
CAM57107.1	Rieske iron-sulphur protein precursor [Glycine max]	345	2.00E-93	1
CAE12168.2	formate dehydrogenase [Quercus robur]	343	8.00E-93	1
ABX79343.1	dehydroascorbate reductase [Vitis vinifera]	340	5.00E-92	1
ABD32912.1	Ferric reductase-like transmembrane component [Medicago truncatula]	341	2.00E-92	1
ABI84254.1	thioredoxin fold [Arachis hypogaea]	291	2.00E-77	2
CAD31838.1	putative quinone oxidoreductase [Cicer arietinum]	290	5.00E-77	1
ABF51006.1	Cu-Zn superoxide dismutase [Arachis hypogaea]	259	1.00E-67	1
AAC83463.1	cationic peroxidase 2 [Glycine max]	236	1.00E-60	2
P49332	Probable glutathione S-transferase parC [Nicotiana tabacum]	235	2.00E-60	1
CAM57109.1	Rieske iron-sulphur protein precursor [Zantedeschia aethiopica]	231	2.00E-59	1
BAA10929.1	cytochrome P450 like_TBP [Nicotiana tabacum]	187	6.00E-46	4
T02955	probable cytochrome P450 monooxygenase [Zea mays]	144	3.00E-41	1
BAA76419.1	ascorbate peroxidase [Cicer arietinum]	144	2.00E-33	1
CAJ43614.1	monodehydroascorbate reductase [Plantago major]	141	4.00E-32	2
CAA10132.1	superoxide dismutase [Cicer arietinum]	125	2.00E-27	1
BAD18377.1	type 2 metallothionein [Glycine max]	105	2.00E-21	1
ABQ44281.1	metallothionein type 2 [Sesbania drummondii]	93.6	4.00E-18	2
CAJ38394.1	cytochrome b5 reductase [Plantago major]	77.4	3.00E-13	1

Accession number	Similarity	Score (bits)	E-value	ESTs per mRNA
STRESS AND DEFENCE RESPONSE				
NP_188317.2	chitinase [Arabidopsis thaliana]	498	1.00E-139	2
CAO41879.1	leucine-rich repeat resistance protein-like protein [Gossypium hirsutum]	369	1.00E-100	1
BAB63949.1	pathogenesis-related 10 [Lupinus albus]	313	7.00E-84	7
BAD86819.1	hypersensitive-induced response protein [Lotus japonicus]	329	9.00E-89	1
AAF15296.2	lipoxygenase [Phaseolus vulgaris]	309	1.00E-82	2
P16148	Protein PPLZ12- Lupinus polyphyllus	236	1.00E-60	1
AAO33591.1	putative early light induced protein [Arachis hypogaea]	220	6.00E-56	1
AAT06600.2	dehydrin [Lupinus albus]	203	8.00E-51	3
AAD50376.1	ripening related protein [Glycine max]	203	1.00E-50	4
CAB44031.1	lectin [Glycine max]	191	4.00E-47	1
CAA03926.1	PR-10 protein [Lupinus albus]	158	1.00E-37	1
AAK73280.1	drought-induced protein [Retama raetam]	144	5.00E-33	5
AAB18970.2	lipoxygenase [Phaseolus vulgaris]	117	3.00E-25	2
AAP23944.1	leucine-rich repeat protein [x Citrofortunella mitis]	108	1.00E-22	1
ABB29467.1	salt-tolerance protein [Glycine max]	96.3	7.00E-19	1
NP_190693.1	senescence/dehydration-associated protein-related [Arabidopsis thaliana]	74.3	2.00E-12	1
AAZ85353.1	putative submergence induced protein 2-like [Solanum ochranthum]	75.1	3.00E-12	1
CAB85628.1	putative ripening-related protein [Vitis vinifera]	75.1	2.00E-12	1
BAE48663.1	Pm52 [Prunus mume]	71.2	4.00E-11	1
AAR26524.1	abscisic stress ripening-like protein [Glycine max]	71.2	8.00E-11	1
TRANSCRIPTIONAL CONTROL AND NUCLEIC ACID BINDING				
ABN09109.1	Helicase, C-terminal [Medicago truncatula]	492	1.00E-137	1
NP_564150.1	F-box family protein [Arabidopsis thaliana]	475	1.00E-132	1
ABD32851.1	Helicase, C-terminal; Zinc finger [Medicago truncatula]	452	1.00E-125	1
AAG10600.1	MYB-related transcription factor PHAN1 [Pisum sativum]	384	1.00E-105	1
P48513	Transcription initiation factor IIB [Glycine max]	382	1.00E-104	1
AAX13298.1	MADS box protein SEP3 [Lotus corniculatus var. japonicus]	327	4.00E-88	2
NP_172336.3	ATRX/CHR20; ATP binding / DNA binding / helicase [Arabidopsis thaliana]	286	8.00E-76	1
ABH02875.1	MYB transcription factor MYB123 [Glycine max]	247	8.00E-64	2
O49289	Putative DEAD-box ATP-dependent RNA helicase 29 [Arabidopsis thaliana]	246	1.00E-63	1
NP_001078676.1	RNA and export factor-binding protein, putative [Arabidopsis thaliana]	238	3.00E-61	1
ABS18448.1	WRKY55 [Glycine max]	221	6.00E-56	1

Accession number	Similarity	Score (bits)	E-value	ESTs per mRNA
TRANSCRIPTIONAL CONTROL AND NUCLEIC ACID BINDING				
ABN06047.1	Zinc finger, RING-type; Transcription factor jumonji, jmjC [Medicago truncatula]	216	1.00E-54	1
NP_186796.1	ATHB-1 (Homeobox-leucine zipper protein HAT5) [Arabidopsis thaliana]	211	6.00E-53	1
NP_180427.1	ATP binding / ATP-dependent helicase/ nucleic acid binding [Arabidopsis thaliana]	204	6.00E-51	1
ABI34666.1	bZIP transcription factor bZIP124 [Glycine max]	200	1.00E-49	1
CAL25353.1	ACBF-like dna binding protein [Platanus x acerifolia]	190	7.00E-47	1
AAA82062.1	eukaryotic release factor 3 [Ricinus communis]	189	1.00E-46	1
AAG13810.1	PSTVd RNA-binding protein Virp1a [Lycopersicon esculentum]	181	3.00E-44	1
BAE71188.1	BEL1-like homeodomain transcription factor [Trifolium pratense]	179	2.00E-43	1
P26585	HMG1/2-like protein (Protein SB11) [Glycine max]	164	5.00E-39	1
AAA88792.1	nucleosome assembly protein 1 [Glycine maxima]	117	4.00E-38	1
NP_974373.1	MIF2 (MINI ZINC FINGER 2); DNA binding [Arabidopsis thaliana]	130	4.00E-29	1
ABD28504.1	Nucleosome assembly protein (NAP) [Medicago truncatula]	117	8.00E-25	1
AAZ86071.1	MADS-box protein [Glycine max]	111	2.00E-23	1
AAQ96342.1	putative ethylene response factor ERF3b [Vitis aestivalis]	102	3.00E-20	1
NP_190149.1	RNA recognition motif (RRM)-containing protein [Arabidopsis thaliana]	103	1.00E-20	2
NP_177360.1	PATL1 (PATELLIN 1); transporter [Arabidopsis thaliana]	90.9	9.00E-17	1
ABH02837.1	MYB transcription factor MYB81 [Glycine max]	79	2.00E-13	1
TRANSPORT				
AAL58570.1	vacuolar processing enzyme 2 [Glycine max]	483	1.00E-135	1
NP_200125.1	CNGC1 (CYCLIC NUCLEOTIDE GATED CHANNEL 1) [Arabidopsis thaliana]	454	1.00E-126	1
CAA11025.1	aquaporin [Lupinus albus]	446	1.00E-123	3
AAL66293.1	phosphate transporter [Glycine max]	425	1.00E-117	1
Q9FY14	Probable aquaporin TIP-type (MtAQP1) [Medicago truncatula]	392	2.00E-107	2
NP_569004.1	nucleotide-sugar transporter family protein [Arabidopsis thaliana]	313	1.00E-100	1
ABB02396.1	temperature-induced lipocalin [Medicago truncatula]	339	1.00E-91	1

Accession number	Similarity	Score (bits)	E-value	ESTs per mRNA
TRANSPORT				
CAD56216.1	transportin-like protein [Cicer arietinum]	324	4.00E-87	1
CAA98170.1	RAB7C [Lotus japonicus]	313	6.00E-84	1
AAF21428.2	salt-induced AAA-Type ATPase [Mesembryanthemum crystallinum]	298	4.00E-79	1
BAA25753.1	Ca2+/H+ exchanger [Vigna radiata]	258	2.00E-67	1
NP_177419.1	ATTIM23-2 (Arabidopsis thaliana translocase inner membrane subunit 23-2); protein translocase	158	3.00E-37	1
ABE68718.1	putative aquaporin [Arachis hypogaea]	149	1.00E-34	1
ABD32809.1	Vacuolar (H+)-ATPase G subunit; KH, prokaryotic type [Medicago truncatula]	121	3.00E-26	1
ABD33158.1	Syntaxin, N-terminal [Medicago truncatula]	102	1.00E-20	1
NP_182033.1	SEC61 BETA (suppressors of secretion-defective 61 Beta); protein transporter [Arabidopsis thaliana]	85.9	1.00E-15	1
SIGNALLING				
BAA92699.1	type 2A protein phosphatase-3 [Vicia faba]	555	1.00E-157	1
ABC61505.1	AGO4-2 [Nicotiana benthamiana]	510	1.00E-143	3
Q9SWF9	Zinc finger CCCH domain-containing protein ZFN-like [Pisum sativum]	475	1.00E-132	1
NP_190753.2	CPK13 (calcium-dependent protein kinase 13) [Arabidopsis thaliana]	461	1.00E-128	1
AAA53276.1	GTP-binding protein [Pisum sativum]	436	1.00E-121	1
NP_192169.1	ATMLO1/MLO1 (MILDEW RESISTANCE LOCUS O 1); calmodulin binding [Arabidopsis thaliana]	431	1.00E-119	1
Q39817	Calnexin homolog precursor [Glycine max]	413	1.00E-114	1
BAA02113.1	GTP-binding protein [Pisum sativum]	414	1.00E-114	1
P51139	Glycogen synthase kinase-3 homolog MsK-3 [Medicago sativa]	404	1.00E-111	1
AAQ72787.1	putative GTP-binding protein [Cucumis sativus]	398	1.00E-109	1
NP_191645.1	guanine nucleotide exchange family protein [Arabidopsis thaliana]	366	1.00E-100	1
AAC33305.1	fiber annexin [Gossypium hirsutum]	344	2.00E-93	1
BAA92697.1	type 2A protein phosphatase-1 [Vicia faba]	313	4.00E-84	1
ABJ74170.1	histidine kinase 1 [Lupinus albus]	306	1.00E-81	1
NP_190767.1	protein kinase family protein [Arabidopsis thaliana]	303	1.00E-81	1
Q5J907	Translationally-controlled tumor protein homolog (TCTP) [Elaeis guineensis]	303	7.00E-81	4

Accession number	Similarity	Score (bits)	E-value	ESTs per mRNA
SIGNALLING				
AAM12880.1	GTP-binding protein [Helianthus annuus]	285	1.00E-75	1
AAM83095.1	SOS2-like protein kinase [Glycine max]	253	8.00E-66	2
AAM65586.1	receptor protein kinase-like protein [Arabidopsis thaliana]	248	3.00E-64	1
BAD01612.1	flowering locus T [Populus nigra]	228	3.00E-58	1
NP_174810.1	ANNAT1 (ANNEXIN ARABIDOPSIS 1) [Arabidopsis thaliana]	206	1.00E-51	1
ABJ91228.1	CBL-interacting protein kinase 22 [Populus trichocarpa]	197	7.00E-49	1
CAC24474.1	GTP binding protein [Cichorium intybus x Cichorium endivia]	194	4.00E-48	1
AAP72282.2	calcium-dependent calmodulin-independent protein kinase [Cicer arietinum]	186	8.00E-46	1
NP_198992.2	cell cycle control crn (crooked neck) protein-like [Arabidopsis thaliana]	168	4.00E-40	1
P54766	GTP-binding nuclear protein Ran1B [Lotus japonicus]	147	2.00E-34	1
ABN08208.1	Remorin, C-terminal region [Medicago truncatula]	97.4	3.00E-19	1
VIRAL PROTEINS				
AAB97459.1	nuclear inclusion B [bean yellow mosaic virus]	562	1.00E-159	4
P17765	Genome polyprotein [Bean yellow mosaic virus]	532	1.00E-150	2
AAF00522.1	polyprotein [bean yellow mosaic virus]	529	1.00E-148	3
AAB37237.1	polyprotein [Bean yellow mosaic virus]	513	1.00E-144	3
ABG33691.1	polyprotein [White lupin mosaic virus]	508	1.00E-142	6
BAE96599.1	polyprotein [Bean yellow mosaic virus]	491	1.00E-137	1
AAF00524.1	polyprotein [bean yellow mosaic virus]	487	1.00E-136	1
ABM69145.1	coat protein [Bean yellow mosaic virus]	371	1.00E-101	1
NP_734173.1	P1 protein [Bean yellow mosaic virus]	212	1.00E-53	1
CAO02584.2	polyprotein [Bean yellow mosaic virus]	106	4.00E-22	1
UNCLASSIFIED				
CAE45585.1	coatomer alpha subunit-like protein [Lotus japonicus]	464	1.00E-129	1
NP_001062159.1	Os08g0500700 [Oryza sativa (japonica cultivar-group)]	355	2.00E-96	1
BAE71192.1	putative Asp1 [Trifolium pratense]	336	1.00E-90	1
NP_001046690.1	Os02g0321900 [Oryza sativa (japonica cultivar-group)]	322	2.00E-86	1
NP_001064799.1	Os10g0465800 [Oryza sativa (japonica cultivar-group)]	312	1.00E-83	2
CAA72315.1	putative 21kD protein precursor [Medicago sativa subsp. x varia]	281	3.00E-74	1
AAM21317.1	auxin-regulated protein [Populus tremula x Populus tremuloides]	267	6.00E-70	2
NP_189128.2	SEC14 cytosolic factor [Arabidopsis thaliana]	253	8.00E-66	1
NP_001046972.1	Os02g0519900 [Oryza sativa (japonica cultivar-group)]	251	3.00E-65	1

Accession number	Similarity	Score (bits)	E-value	ESTs per mRNA
UNCLASSIFIED				
NP_179889.1	casein kinase II alpha chain, putative [Arabidopsis thaliana]	385	1.00E-105	1
CAH66528.1	H0502B11.8 [Oryza sativa (indica cultivar-group)]	232	2.00E-59	1
NP_001065830.1	Os11g0163100 [Oryza sativa (japonica cultivar-group)]	217	6.00E-55	1
NP_172636.1	pentatricopeptide (PPR) repeat-containing protein [Arabidopsis thaliana]	214	5.00E-54	1
ABC70464.1	CASTOR protein [Glycine max]	212	2.00E-53	1
NP_001045723.1	Os02g0122000 [Oryza sativa (japonica cultivar-group)]	201	3.00E-50	1
BAB82450.1	PBng143 [Vigna radiata]	142	6.00E-33	1
AAM62421.1	Drm3 [Pisum sativum]	126	8.00E-28	2
ABW74471.1	auxin-repressed protein [Paeonia suffruticosa]	81.3	6.00E-26	1
ABR25977.1	osiaa30-auxin-responsive [Oryza sativa (indica cultivar-group)]	114	2.00E-24	1
AAD32146.1	Nt-iaa28 deduced protein [Nicotiana tabacum]	114	5.00E-24	1
ABN08340.1	ZIM [Medicago truncatula]	166	2.00E-39	1
AAD09514.1	GMFP5 [Glycine max]	159	3.00E-37	1
AAG33924.1	auxin-repressed protein [Robinia pseudoacacia]	66.6	5.00E-10	1

Levels of transcripts in pod tissue and phloem exudate

The level of S-adenosylmethionine (SAM) synthase, Rubisco Small Subunit, aquaporin, flowering locus T, chlorophyll a/b binding protein, actin, ubiquitin and sucrose synthase, transcripts identified in the *L. albus* phloem exudate cDNA library, were measured by real-time RT-PCR in samples of exudate, and also in tissue samples from pods, flowers, stems and leaves. Only data for levels in pod tissue sampled adjacent to the suture veins that were incised and the level in exudate are presented here (Figure 5.4); the complete data set for all tissues and exudate is presented in Appendix 3. All transcripts analysed showed higher expression in pod tissue compared to the levels found in phloem exudate.

Dissociation curves, with single peaks for all genes analysed, confirmed the specificity of PCR products (see Appendix 4).

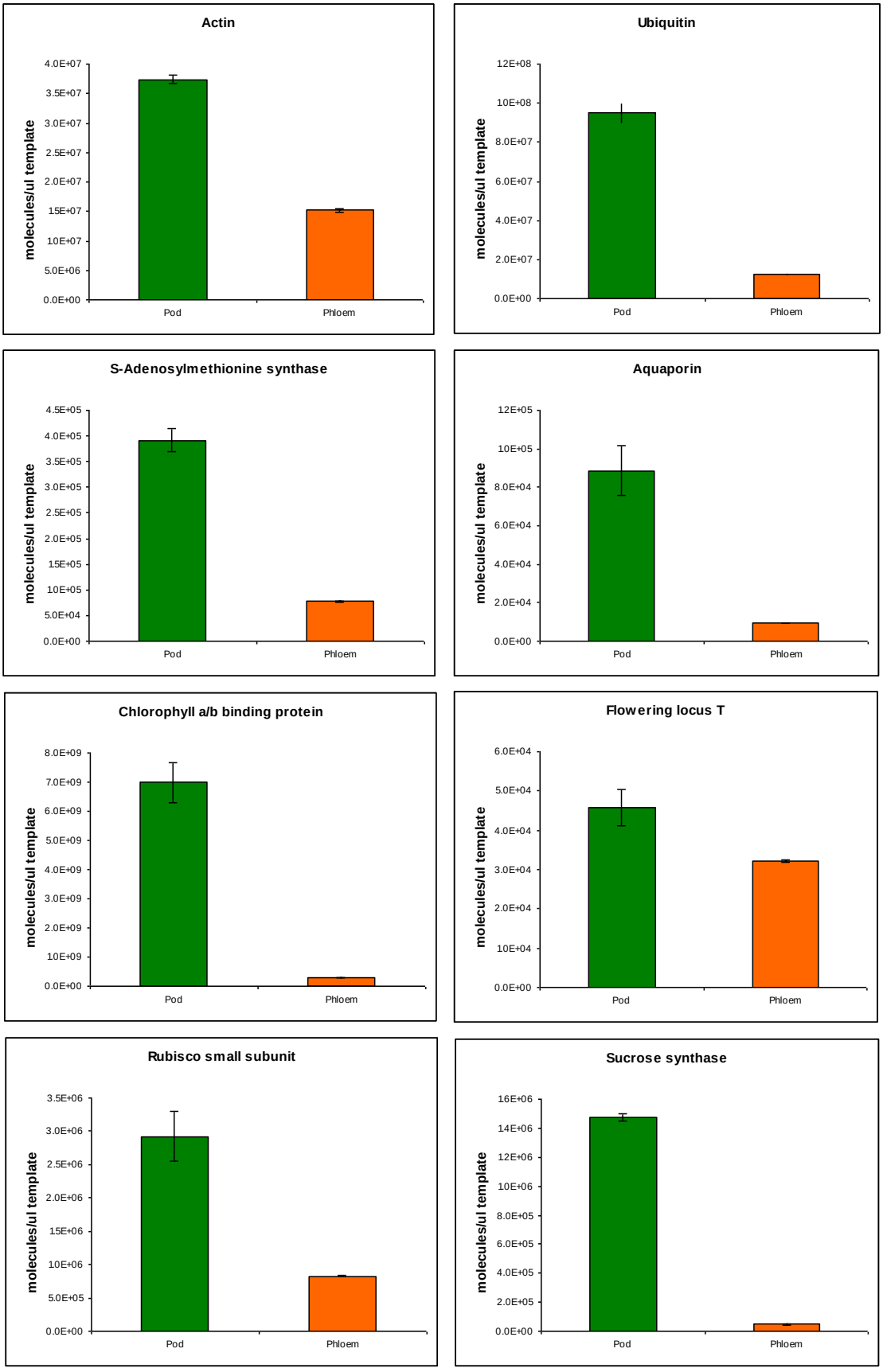

Figure 5.4. Absolute quantification of transcripts in *L. albus* phloem exudate and pod tissue. 1 µg of total RNA isolated from pod tissue and phloem exudate was reverse transcribed followed by real-time PCR analysis performed on a LightCycler480 (Roche Diagnostics) using SYBR® green as the fluorescent dye. Data are the mean ± standard error of three biological replicates with two technical replicates each.

To assess the likely levels of contamination of the *L. albus* phloem exudates collected in this study, a comparison of the transcript levels for each of the genes measured by real-time RT PCR (Figure 5.4) was made by setting expression in the pod tissue to 1.0 and expressing the level in exudate as a proportion of 1.0 (Figure 5.5).

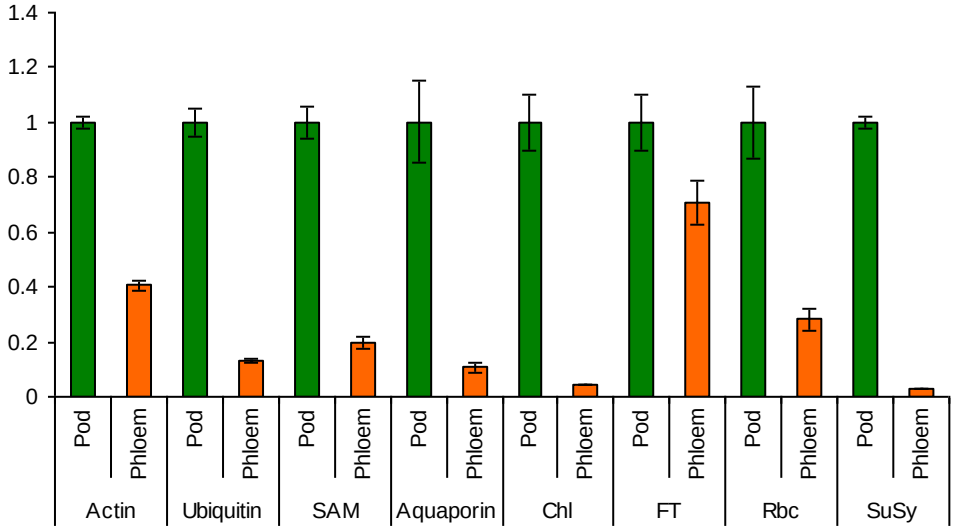

Figure 5.5. Relative levels of transcripts in *L. albus* phloem exudate. 1 µg of total RNA isolated from pod tissue and phloem exudate was reverse transcribed followed by real-time PCR analysis performed on a LightCycler480 (Roche Diagnostics) using SYBR® green as the fluorescent dye. Data is expressed as a ratio with pod tissue expression set at 1. Data are the mean ± standard error of three biological replicates with two technical replicates each. SAM, S-Adenosylmethionine synthase; Chl, chlorophyll a/b binding protein; FT, flowering locus T; Rbc, Rubisco Small Subunit; SuSy, sucrose synthase.

DISCUSSION

The transcriptome profile for phloem exudate of *L. albus* identified 609 unique transcripts with the most abundant encoding proteins involved in metabolism, protein synthesis and turnover, redox regulation and signalling, with 73% of all ESTs corresponding to singletons. A similar analysis for exudate from melon by Omid *et al*. (2007) reported that almost 80% of the identified transcripts in exudate were also singletons. These authors proposed that the high percentage of singletons indicates that phloem exudate must contain at least several thousand transcripts. Even though insect stylectomy is generally regarded as a method that provides 'pure' phloem samples (Gaupels *et al*., 2008a; Sasaki *et*

al., 1998; Fisher *et al*., 1992), a comparison with transcript analysis using stylet exudate is not possible since cDNA libraries have not been generated for these exudates.

The largest group of transcripts identified in this study encoded proteins involved in metabolism (Energy and General Metabolism, Table 5.3). Interestingly, proteins involved in metabolism also formed the largest group of proteins identified in *L. albus* phloem exudate (Chapter 4). The transcripts in this category comprised a diverse range of proteins involved in carbohydrate (particularly sugar) metabolism, the synthesis and breakdown of organic acids, amino acids and other N-containing substrates, fatty acid and secondary metabolite synthesis, the synthesis of ethylene and in ATP/adenylate metabolism as well as a host of transferase enzymes. Transcripts encoding proteins associated with metabolism have been identified in phloem exudate collected from barley by stylectomy (Gaupels *et al*., 2008a), but the analysis was limited and progress in determining which of these transcripts are in SE awaits detailed cDNA library analysis of stylet exudate. One of the transcripts in barley stylet exudate was identified as glycosyl transferase (Gaupels *et al.,* 2008a), also found in lupin exudate in this study. This enzyme might potentially glycosylate secondary metabolites involved in pathogen response (Gachon *et al.,* 2005), and may be responsible for post-translational modification of proteins in the SE (Taoka *et al.,* 2007). One of the most important enzymes involved in sugar metabolism, SuSy, has been localised to phloem and immunological studies have shown specific localisation to CC (Nolte and Koch, 1993). Although the proteomic analysis of lupin exudate did not detect SuSy (Chapter 4), a relatively low level of a transcript encoding the protein (3% compared to levels in pod tissue, Figure 5.5) was observed. Doering-Saad *et al*. (2006) also identified a transcript for this enzyme in phloem exudate collected from castor bean, but in the monocotyledons sampled by stylectomy neither the protein nor its transcript have been documented (Gaupels *et al.,* 2008a).

The second largest group of transcripts identified in lupin phloem exudate encoded proteins involved in protein synthesis and turnover such as ubiquitin, cyclophilin, 14-3-3 protein and a number of proteolytic enzymes, as well as a

proteasome component. Many of the proteins encoded by this group of transcripts were also identified in *L. albus* phloem exudate by proteomic analysis (Chapter 4) and some have been detected in phloem exudate collected by stylectomy in rice (Sasaki *et al*., 1998). While the presence of these protein degrading enzymes might be expected in SE either in relation to protein turnover (Fisher *et al.,* 1992) or in protecting the phloem against pathogen or insect attack, the presence of their transcripts would not be required unless they had some other role in SE. Perhaps some of these are part of the long distance signalling pathway with a range of as yet unknown functions. Omid *et al*. (2007) found that a substantial percentage of transcripts in phloem exudate collected from melon were related to proteinase-inhibitor activity and the ubiquitin–ligase complex, which was also the case for lupin exudate. Transcripts encoding heat shock proteins were also identified in *L. albus* phloem exudate which is consistent with this transcript been detected in melon exudate (Omid *et al*., 2007). Heat shock proteins are known for their chaperon function; being involved in folding, unfolding and trafficking of proteins through the plasmodesmata from CC to SE (Aoki *et al*., 2002; Schobert *et al*., 1995). Despite the presence of heat shock protein transcripts in lupin exudate, the protein was not found in the proteome (Chapter 4). Heat shock proteins have been identified in phloem exudate of *C. maxima* (Lin *et al.*, 2008); *B. napus* (Giavalisco *et al*., 2006) and *R. communis* (Schobert *et al*., 1995).

Transcripts encoding proteins involved in redox regulation represented the third largest group of transcripts identified with known function. Within this category, the encoded proteins were also identified in the proteomic analysis (Chapter 4). These included thioredoxin, peroxidase and monodehydroascorbate reductase. Thioredoxin mRNA has also been identified in phloem exudate collected from rice by stylectomy (Sasaki *et al*., 1998), and a role in phloem protein stability under stress and in maintenance of SE has been attributed to the protein (Raven, 1991) (see Chapter 4).

A closely related category of transcripts was that encoding proteins likely to be involved in responses to stress and in defence against pathogens and insect attack. These transcripts encoded proteins including pathogenesis related proteins (PRP), enzymes such as SAM synthetase and those likely to be part of

a reaction to ROS, metallothioneins and other defence-related response proteins, some of which were detected also in the proteomic analysis of lupin exudate. While not related directly to this group, ten transcripts were found that encoded components of the polyprotein of the bean yellow mosaic virus (BYMV). BYMV is a major pathogen of all lupin species world wide and is prevalent in *L. angustifolius* and *L. albus* crops in Western Australia (Sweetingham *et al.,* 1998). The virus is transmitted through seed but also non-persistently by aphids. In this study phloem exudates were collected from both glasshouse and field-grown plants that in some cases showed some symptoms of BYMV infection. Thus it is not surprising that the transcripts for the BYMV polyprotein were detected in the phloem exudates used in this study. This observation raises the possibility that some of the defence and stress-related proteins and their transcripts found in lupin exudate, were in part a response to a persistent low level of BYMV infection and perhaps also as a response to aphid feeding. Divol *et al*. (2005) dissected the phloem from celery petioles and were able to clone 1187 ESTs for 891 non-redundant genes from the mRNA. These authors compared mRNA from plants with and without feeding aphids and found transcripts increased in those with aphids for 126 genes. These included genes involved in cell wall modification (expansin, pectin esterases and glucosyl transferases), aquaporins, enzymes of vitamin synthesis, carbonic anhydrase, glycolate oxidase, a number of metallothionens, catalase, GSH peroxidase, SAM synthetase and a number of ribosomal proteins. Given that the lupin plants used in this study were exposed to both aphids and virus infection, it is not surprising that many of the transcripts identified by Divol *et al.* (2005) were also present in the exudate from lupin.

Calcium ion has a central role in the physiology of phloem and particularly in the sealing mechanisms in SE following damage or stress (van Bel, 2003). Thus it seems reasonable to expect that Ca^{2+}-dependant regulatory functions might be a normal component of SE biochemistry. Components with this function included protein kinases and calmodulin, both of which were found among the transcripts in lupin exudate, although neither protein was detected in the proteomic analysis (Chapter 4). Protein kinases were present in exudate collected from rice by stylectomy (Nakamura *et al*., 1995). Nakamura *et al*. (1993) demonstrated that protein phosphorylation occurs in sieve tubes of rice

plants *in vivo,* and that the phosphorylation of proteins occurs in a calcium-dependent manner *in vitro*. A transcript encoding a protein kinase family protein was also identified by Gaupels *et al*. (2008a) in phloem exudate collected from barley by stylectomy. Thus it seems very likely that protein kinase transcripts and also the enzyme are components of SE *in vivo*. Nakamura *et al.,* (1995) have speculated that post-translational protein phosphorylation is part of the systemic signalling mechanism but this relationship is yet to be confirmed.

Another transcript encoding a protein involved in signalling identified in *L. albus* phloem exudate in this study was Flowering locus T (*FT*). Huang *et al*. (2005) originally reported that *FT* mRNA in *Arabidopsis* was an important component of the floral stimulus that moves from leaf to shoot. However, in a little less than two years Huang *et al.*'s (2005) paper proposing the *FT* mRNA hypothesis was retracted. Recently, FT protein, but not *FT* mRNA, was shown to migrate from leaves to the apical meristem as explained in Chapter 4 (Lin *et al.,* 2007; Corbesier *et al*., 2007). Lin *et al*. (2007) did not detect *FT*-like mRNA in phloem exudates collected from flowering pumpkin plants suggesting that, in pumpkin, *FTL* mRNA is not a component of the phloem long-distance signalling system involved in floral induction. The relatively high level of *FT* transcript in *L. albus* phloem exudates compared to the surrounding pod tissue (70% of that in pod tissue, Figure 5.5) and compared to the low expression of chlorophyll a/b binding protein, or even Rubisco small subunit, would suggest that *FT* is a true component of SE in lupin and not due to contamination from neighbouring cells. Therefore, probably in lupin, some movement of *FT* transcript from CC to SE is possible. However, it is important to emphasise that the presence of *FT* in phloem exudate of lupin does not imply its translocation. The other report of *FT* transcript in phloem exudate has been provided by Deeken *et al*. (2008) in exudate of *Arabidopsis* collected into a bathing solution containing EDTA. Although this method facilitates phloem exudation by chelating Ca^{2+} to prevent the SE sealing after wounding, facilitated exudation using the chelator can enhance contamination (Gaupels *et al*., 2008c) making it difficult to be certain about the source of the transcript.

A transcript encoding Argonaute4 (AGO4) protein, thought to be involved in RNA silencing, was also identified in this study. It has been suggested that

AGO4 along with siRNA directs histone and DNA methylation (Zilberman *et al*., 2003). This is the first time AGO4 has been identified in phloem exudate and its presence could suggest that AGO4 transcript is a mobile signal that is translocated in phloem to be translated in other parts of the plant where it acts in RNA silencing.

The question about the source of each of the mRNA species that are detected in phloem exudate sampled by incision of the vasculature requires consideration. Identification of 15 transcripts representing 23 ESTs encoding proteins involved in photosynthesis in *L. albus* phloem exudate (Table 5.3), clearly indicates contamination of the exudate by transcripts derived from neighbouring photosynthetic cells. These transcripts included proteins involved in the thylakoid-based light reactions, as well as both large and small subunits of Rubisco. Similarly, eight sequences for ribosomal proteins and for other proteins associated with translation were also detected (Table 5.3), again not regarded as likely to be in SE *in vivo*, unless they have some role other than protein synthesis.

Figure 5.5 shows that for the two transcripts associated with photosynthesis, Rubisco small subunit and chlorophyll a/b binding protein levels in phloem were 30% and 4% respectively of those in the surrounding pod tissue. It is difficult to know which of these truly reflects the level of contamination at the wound. If it is assumed that the chlorophyll a/b binding protein transcripts in exudate were all derived from the surrounding tissue then in absolute terms the level of contamination was relatively low. On this basis, it may be concluded that each of the other transcripts (except SuSy) were to some extent derived from SE. On the other hand, the level of Rubisco small subunit transcripts was much higher in exudate indicating more substantial contamination. If this latter reflects contamination then flowering locus T (FT) and perhaps actin (Figure 5.5) were the only transcripts that could be ascribed, at least in part, to SE. On the other hand, if the level of SuSy is taken as indicator of contamination then a rough estimate of contamination could be obtained by dividing Susy's ratio (0.03) through the highest ratio observed, in this case flowering locus T (FT)'s ratio (0.70), whose high ratio would be suggesting that this transcript is indeed present in phloem exudates of *L. albus*. This analysis would suggest a possible

level of contamination of 4%. Doering-Saad *et al.* (2006) generated cDNA libraries from *R. communis* phloem exudate collected 15 and 120 min after incision and compared the annotated transcripts in each as a way to assess the degree of contamination from damaged cells at the incision site (reasoning that contamination would be greater in the initial exudate collected). Based on the idea that photosynthetic proteins were the most likely contaminants, they concluded that as 12% of the transcripts analysed in the 15 min library were related to photosynthesis compared to only 2% in the 120 min library, there was much lower contamination in the phloem exudates used to construct the latter. Therefore, considering that in this study the first drop of exudate from incisions to the vasculature in lupin was discarded, and that the cDNA library was prepared only from mRNA in the subsequent exudate, it is reasonable to assume that the contamination of the cDNA library with non-phloem transcripts was minimised.

Detailed transcriptomic studies may facilitate the identification of potential mobile mRNAs that are part of a long distance communication network in phloem. However, specific source-sink relationships for transcripts, just as is the case for proteins or any other potential systemic signal, must be experimentally demonstrated before assigning them a function as translocated signalling molecules. The availability of these comprehensive phloem transcript profiles will facilitate reverse-genetic studies and forward-genetic screens for phloem and long-distance RNA signalling mutants (Deeken *et al*., 2008).

CHAPTER 6

microRNA IN PHLOEM AND THEIR LONG DISTANCE TRANSPORT

INTRODUCTION

Plant microRNA (miRNA) have conserved regulatory functions in development as well as in environmental and hormone responses (Kidner and Martienssen, 2005; Sunkar and Zhu, 2004; Jones-Rhoades and Bartel, 2004). Sunkar and Zhu (2004) observed that the expression of some miRNA was responsive to abiotic stresses. miR393 was strongly induced by cold, dehydration, NaCl, and ABA treatments. miR397b and miR402 were slightly induced by all the stress treatments, whereas miR319c appeared to be induced only by cold but not dehydration, NaCl, or ABA. Other miRNA, such as miR395, miR398 and miR399, have been implicated in coordination of nutrient homeostasis (Buhtz *et al*., 2008; Valdés *et al.,* 2008; Pant *et al*., 2008; Yamasaki *et al*, 2007; Chiou *et al*., 2006; Bari *et al*., 2006; Fujii *et al*., 2005). Detection of a number of miRNA in phloem exudate of cucurbits (Yoo *et al*., 2004), *Lupinus albus* (Jordan 2004; Yoo *et al*., 2004) and *Brassica napus* (Buhtz *et al*., 2008) has led to the idea that these regulatory molecules may be translocated and serve as long-distance signals.

Jordan (2004) cloned 700 small RNA from seedling tissues and phloem exudate collected from *L. albus*. Around 300 of the clones (18-25 nt in length) from phloem were sequenced and nine identified as miRNA by homology to those found in *Arabidopsis* (miR159, miR164, miR165/166, miR168, miR169, miR395, miR398 and miR399). Northern blot analysis showed that some of these, miR399 for example, while present in vegetative tissues, were more prominent in phloem. More recently Buhtz *et al*. (2008) identified 32 annotated miRNA

sequences in phloem exudate from *B napus*. Unfortunately, there has been no data published for miRNA in exudates collected by stylectomy and the same technical reservations, outlined earlier in relation to protein and mRNA (Chapters 4 and 5), of relying on analysis of exudate collected from incisions to the vasculature applies equally to miRNA. Thus it was important to measure the accumulation of miRNA species in exudate and compare it to that of lupin pod tissue that surrounded the area where exudate was collected.

If miRNA in phloem have a diversity of regulatory roles in development, gene silencing or nutrient allocation (Kehr and Buhtz, 2008), it is reasonable to expect that their spectrum in phloem at different 'sink' organs will differ among sites of exudation. This study has exploited this feature of phloem exudation in lupins to test the idea. Among the miRNA that have been recovered in phloem exudates, miR166 and miR399 have been suggested to be 'phloem-mobile' (Juarez *et al*., 2004; Pant *et al*., 2008). There is now a body of evidence suggesting that miR399 controls inorganic phosphate (Pi) homeostasis in plants by regulating the expression of a component of the proteolysis machinery (Chiou *et al.*, 2006; Fujii *et al.,* 2005). Upon Pi starvation, miR399 is induced in *A. thaliana,* and its target gene, a ubiquitin-conjugating (UBC) E2 enzyme, is inhibited (Chiou *et al*., 2006; Fujii *et al*., 2005). The inhibition of UBC E2 appears important for the attenuation of primary-root elongation and for the induction of the phosphate transporter gene *AtPT1* (Fujii *et al*., 2005). Regulation of E2 gene expression by miR399 affects Pi acquisition, Pi allocation between roots and shoots, and Pi remobilisation within leaves. Thus precise control of miR399 expression and its interaction with E2 mRNA appears to be critical to the maintenance of Pi homeostasis (Chiou *et al.*, 2006). Bari *et al*. (2006) showed, by map-based cloning, that *PHO2* encodes the UBC E2-conjugase that is modulated by the Pi-dependent miR399 and that primary transcripts for this miRNA are strongly induced by low Pi and rapidly repressed after Pi addition. *PHO2* transcript changes reciprocally to miR399 transcripts in Pi deprived plants and in miR399 over-expressers (Bari *et al*., 2006). Increase in miR399 accumulation in response to Pi deficiency has also been recently demonstrated in roots of *Phaseolus vulgaris* (Valdés *et al.,* 2008).

Buhtz *et al*. (2008) demonstrated increased levels of miR395, miR398 and miR399 in phloem exudate from *B. napus* in response to sulphate, copper and phosphate starvation respectively. A similar response by miR399 to Pi starvation has also been reported in the phloem exudate of pumpkin (Pant *et al*., 2008). Overall these responses strongly suggest a role for miRNA in systemic information transfer in relation to nutrient allocation (Buhtz *et al*., 2008). Some support for this idea comes from Pant *et al*. (2008) who studied miR399 translocation in micro-grafting experiments with *Arabidopsis*. Their results showed that chimeric plants constitutively over-expressing miR399 in the shoot accumulate mature miR399 species to very high levels in their wild-type roots under Pi replete conditions. Corresponding primary transcripts were virtually absent in roots. They concluded that miR399 is efficiently translocated from transgenic shoots to wild-type roots and that miR399 itself might act as a long-distance Pi starvation signal in *Arabidopsis*. Lupins respond to limiting Pi supply by changing the allocation of dry matter to favour vegetative growth and restrict reproductive development (Ma *et al*., 2002). Despite these changes phloem exudation at developing lupin fruits persists providing an experimental system to test the effects of Pi nutrition on the levels of miR399 in phloem.

The biogenesis of miRNA seems to require various enzyme-catalyzed steps to form mature molecules. The HUA ENHANCER 1 (HEN1) protein has been involved in miRNA biogenesis in *Arabidopsis*. *hen1* single mutants in *Arabidopsis* exhibit developmental defects such as reduced organ size, altered rosette leaf shape, reduced plant height, reduced carpel fusion, delayed flowering and reduced fertility with mature siliques approximately ¼ to ½ the length of a wild-type silique (Chen *et al*., 2002). The *HEN1* gene was first identified because of its role in organ identity specification in the flower (Chen *et al*., 2002) and was subsequently shown to control the accumulation of endogenous miRNA (Park *et al*., 2002). Boutet *et al*. (2003) showed that HEN1 also has an effect on the accumulation of transgene siRNA involved in sense posttranscriptional gene silencing (S-PTGS), suggesting that HEN1 functions in both the miRNA and the siRNA pathways. HEN1 has putative nuclear localization signal (Park *et al*., 2002) suggesting that its action on miRNA biogenesis occurs in the nucleus.

A significant reduction in miRNA accumulation was observed in *hen1* mutants and Vazquez *et al*. (2004) confirmed that the marked decreased in miRNA accumulation observed in these mutants reduces mRNA cleavage. The HEN1 protein has an N-terminal putative double-stranded RNA–binding motif and a C-terminal region that is conserved among many bacterial, fungal, and metazoan proteins (Park *et al*., 2002). The precise role of HEN1 in miRNA biogenesis was not clear until Yu *et al*. (2005) showed that plant miRNAs have a naturally occurring methyl group on the ribose of the last nucleotide and that HEN1 protein is a methyltransferase that recognizes and methylates miRNA/miRNA* duplexes. Li *et al*. (2005) showed that a previous reported size increase of small RNAs in the *hen1* mutant (Vazquez *et al*., 2004) was due to the addition of one to five U residues to the 3′ ends of the small RNAs. Li *et al*. (2005) concluded that a novel uridylation activity targets the 3′ ends of unmethylated miRNA and siRNA in *hen1* mutants. Therefore, 3′-end methylation must be a common step in miRNA and siRNA metabolism in plants and most likely protects the 3′ ends of the small RNA from the uridylation activity. HEN1 appears to maintain the correct size as well as the normal levels of miRNA (Li *et al*., 2005). In addition to the uridylation activity, a 3′-to-5′ exonuclease activity is apparently counteracted by the 3′ methylation. The methylation of miRNA and siRNA by HEN1 may also prevent RNA-dependent RNA polymerases (RdRP) from using the small RNA as primers. However, this assumption still needs to be experimentally evaluated (Li *et al*., 2005). The lack of methylation in *hen1* mutants would explain the reduced abundance or even undetectable levels of some miRNA.

The presence of miRNA in phloem exudate suggests a possible role in signalling. However, direct evidence for the biological relevance of long-distance transport of miRNA is still missing (Kehr and Buhtz, 2008). miRNA in phloem could play a role in long-distance transport of information in response to external inputs like nutrient availability. The *hen1* mutant in *Arabidopsis* offers a potential experimental tool to test the idea that miRNA might be translocated. In this study, grafting experiments were used to test whether naturally occurring miRNA are translocated through a graft junction from *Arabidopsis* wild-type to *hen1* mutant plants under both nutrient replete and S deficiency conditions.

EXPERIMENTAL PROCEDURES

Plant material, growth conditions and phloem collection

An analysis of the miRNA profile in lupin phloem exudate collected from different sites of the plant was carried out. Field-grown *Lupinus albus* L. *cv* Kiev mutant plants were used for collection of phloem exudates as described in the General Methods (Chapter 2). In addition to incisions made at the fruit suture vasculature, exudate was also collected from incisions close to the apex of inflorescence branches prior to flowering and to the base of the stem below the lowest leaf (Figure 6.1). These collections at diverse sites were made on the same plants and at the same time. Small RNA was isolated from the phloem exudate and accumulation of miRNA detected by northern blot analysis.

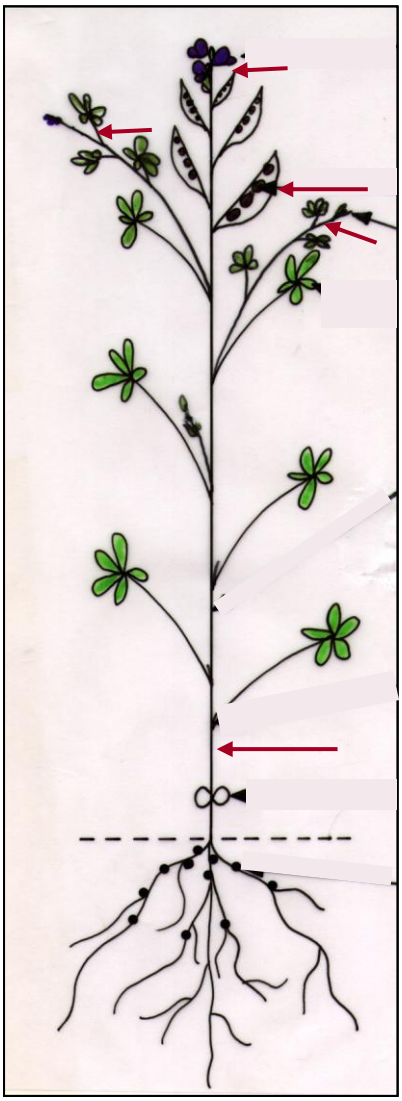

Figure 6.1. Sites of phloem exudate collection from incisions to the vasculature of field-grown *L. albus* plants. Phloem exudate was collected by making shallow incisions at the fruit suture vasculature, base of the stem below the lowest leaf and at the proximity of the apex of the inflorescence branches (red arrows). Diagram courtesy of *C. Atkins*.

In order to study the effects of Pi nutrition on the levels of miR399 in phloem exudate and leaf tissue, *L. albus* plants were grown as described in General Methods (Chapter 2) with a complete (N-free) nutrient solution in pots containing coarse sand under greenhouse conditions during autumn and winter. Leaf tissue and phloem exudate collected from the inflorescence raceme were obtained. After this first collection, the pots were washed through with water followed by Pi-free nutrient solution. This nutrient solution was maintained in the pots over four weeks by frequent addition. Leaf tissue and phloem exudates were collected again from the inflorescence raceme and pod suture vasculature 2, 3 and 4 weeks after Pi deprivation. Small RNA was isolated and accumulation of miR399 in phloem and leaf tissue was studied using northern blot assays. Accumulation of miR168, not known to be affected by Pi levels, served as control.

miRNA translocation through a graft junction was tested using *Arabidopsis thaliana* wild-type and *hen1-6* mutant seedlings. *hen1-6* (SALK_090960) T-DNA insertional mutant (ecotype Columbia Col-0) (Alonso *et al*., 2003) was obtained from the *Arabidopsis* Biological Resource Center (ABRC). Wild-type *Arabidopsis* (ecotype Columbia Col-8) and *hen1-6* seeds were surfaced-sterilized by agitation in a 5% (v/v) NaOCl solution containing 0.01% (v/v) Tween 20 for 5 min followed by a number of rinses in sterile double distilled water. Seeds were germinated in Petri dishes in the growth medium described by Lincoln *et al*. (1990) containing 5 mM KNO_3, 2.5 mM KPO_4 (pH 5.5), 2 mM $MgSO_4$, 2 mM $Ca(NO_3)_2$, 50 µM Fe-EDTA, 70 µM H_3BO_3, 14 µM $MnCl_2$, 0.5 µM $CuSO_4$, 1 µM $ZnSO_4$, 0.2 µM Na_2MoO_4, 10 µM NaCl, 0.01 µM $CoCl_2$., 0.7% (w/v) agar and 1% (w/v) sucrose. Seeds in agar plates were stratified for 3 d at 4˚C in the dark before being transferred to a growth chamber under fluorescent illumination at approximately 120 µE m^{-2} sec^{-1} with a constant temperature of 23˚C and photoperiod of 16 h.

Propagation of *hen1-6* homozygous mutant

In order to identify homozygous *hen1-6* mutant lines, the presence of the T-DNA insertion was first confirmed by PCR analysis. Genomic DNA was isolated from 3 or 4 leaves collected from individual seedlings using

phenol/chloroform/iso-amyl alcohol extraction. Leaves were ground in liquid nitrogen and 120 µl of DNA extraction buffer (pH 8.5) containing 1% (w/v) sarkosyl, 100 mM Tris-HCl, 100 mM NaCl and 10 mM EDTA was added. 120 µl of phenol/chloroform/iso-amyl alcohol was added to the samples and tubes shaken vigorously for 30 sec followed by incubation at room temperature for 5 min. Samples were centrifuged for 10 min at 5,000 *g*, the aqueous phase collected and the phenol/chloroform/iso-amyl alcohol and centrifugation steps repeated. 1/10 vol 3 M sodium acetate (pH 4.8) and 1 vol isopropanol was added to the aqueous phase and samples centrifuged for 5 minutes at 5,000 *g*. The resultant pellet was washed with 100 µl 70% (v/v) ethanol and resuspended in 10 µl R40 buffer (40 µg/mL RNase A in TE buffer (10 mM Tris-HCl, 1 mM EDTA (pH 8.0)).

Isolated DNA was amplified by PCR using the following primers:

* Left (LP) 5'-TCCAATCTTTCCTGATCGTTG-3'
* Right (RP) 5'-ATGCATTTTTCCTTCGGAGTC-3' and
* T-DNA insertion primer (TP) 5'-TGGTTCACGTAGTGGGCCATCG-3'.

PCR was set up as TP+RP for the identification of homozygous mutants and LP+RP for the identification of wild-type (Figure 6.2). For heterozygous mutants both PCR products were expected. Standard 25 µl reactions were set up using Taq DNA polymerase and following the protocol described by Qiagen (*Taq* PCR handbook). PCR was carried out in a Hybaid PCR Express thermal cycler and comprised an initial denaturation step at 94˚C for 3 min followed by 30 cycles of melting at 94˚C for 30 sec, annealing at 58˚C for 30 sec and extension at 72˚C for 1 min. Reactions were subsequently analysed by agarose gel electrophoresis (Figure 6.3) performed as described in General Methods (Chapter 2). Homozygous *hen1-6* lines were propagated to be used in miRNA translocation studies.

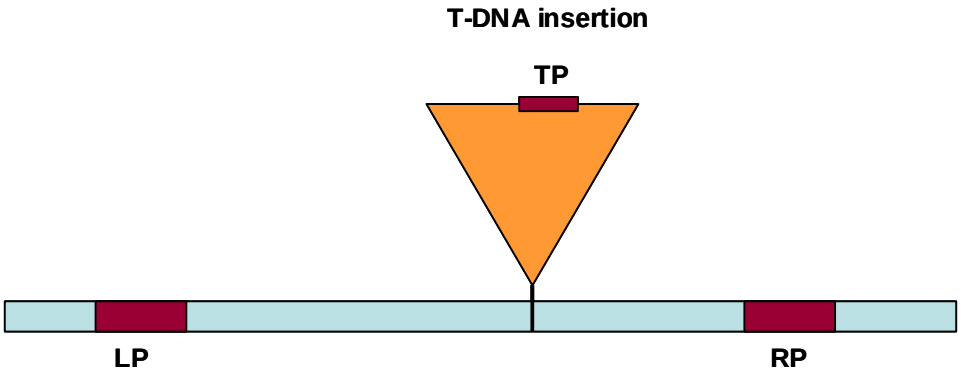

Figure 6.2. Primers for genotyping *hen1* T-DNA insertion mutant. T-DNA insertion in *hen1-6* lines was confirmed by PCR. For homozygous *hen1-6* mutants, a PCR product was obtained only using the T-DNA insertion (TP) and right (RP) primers combination. For wild-type, a PCR product was obtained using only the left (LP) and right (RP) primers combination. For heterozygous *hen1* mutant, PCR products were obtained with both primer combinations. Homozygous *hen1* lines were propagated and used in miRNA translocation studies.

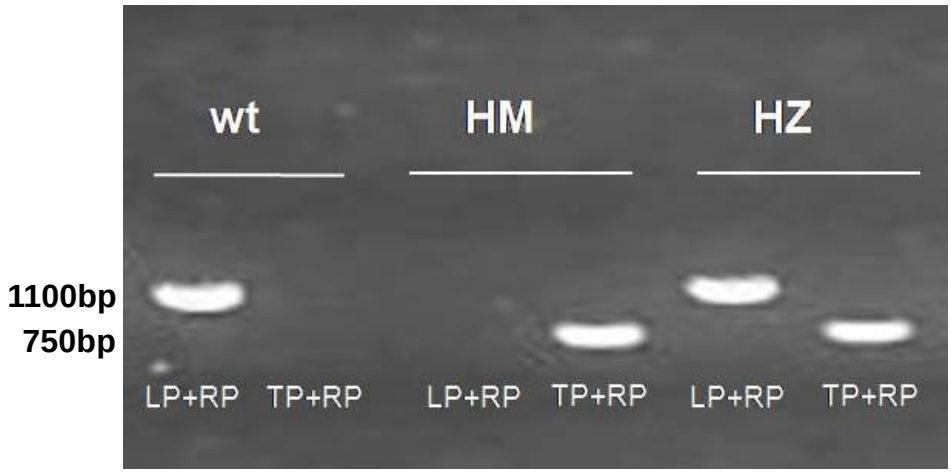

Figure 6.3. T-DNA insertion in *hen1-6* mutants. Genomic DNA was isolated from *Arabidopsis* leaves and amplified by PCR. PCR products were visualised on a 1% (w/v) agarose gel. For *Arabidopsis* wild-type (wt), a PCR product (1100 bp) was obtained using left (LP) and right (RP) primers. For the homozygous (HM) *hen1-6* mutant, a PCR product (750bp) was obtained using T-DNA insertion (TP) and right (RP) primers. For heterozygous (HZ) *hen1-6* mutant, PCR products were obtained for both primer sets.

Accumulation of miRNA in *Arabidopsis* wild-type and *hen1-6* mutant

In order to study the accumulation of miR164, miR159, miR156, miR168 and miR166 in *Arabidopsis* wild-type and *hen1-6* mutant seedlings, small RNA was isolated and microRNA accumulation analysed by northern blot assays.

Grafting experiments

Grafting of mature plants

A. thaliana wild-type and *hen1-6* homozygous mutant seeds were surface sterilized and sown in square petri dishes. Grafting was carried out as described by Haywood *et al.* (2005) using approximately four week-old *Arabidopsis* ecotype Columbia (Col-8) wild-type plants and homozygous *hen1-6* mutant lines. Growth conditions were as described above. Silicone tubing (Medical grade tubing 0.63mm ID x 1.19mm OD, Biolab) was slit longitudinally and then cut into approximately 0.7-1.0 cm lengths, sterilized in 70% (v/v) ethanol and rinsed in sterile double distilled water. The primary inflorescence of the wild-type rootstock plant was excised approximately 5 mm above the rosette and a piece of tubing inserted over the base of the cut rootstock. A drop of sterile distilled water was pipetted on top of the cut rootstock within the tubing to avoid dehydration of the cut tissue. The primary inflorescence of the *hen1-6* scion plant was excised to be approximately 3 cm long and then inserted into the tubing already fitted to the wild-type rootstock (Figure 6.4). As a control, wild-type inflorescences were grafted onto wild-type rootstocks and *hen1-6* inflorescences onto *hen1-6* rootstocks. Grafted plants were transferred to sterilised potting mix (42% (w/w) vermiculite, 17% (w/w) perlite, 21% (w/w) coco peat, 0.1% (w/w) dolomite lime and 0.1% (w/w) complete Osmocote fertilizer) and covered with plastic for one week to maintain relative humidity near 100%. Plants were maintained in a growth chamber under fluorescent illumination at approximately 120 µE m^{-2} sec^{-1}, constant temperature of 23˚C and photoperiod of 16 h for approximately 6 weeks. Small RNA was isolated and accumulation of miRNAs in *hen1-6* and wild-type scions studied by northern blot assays.

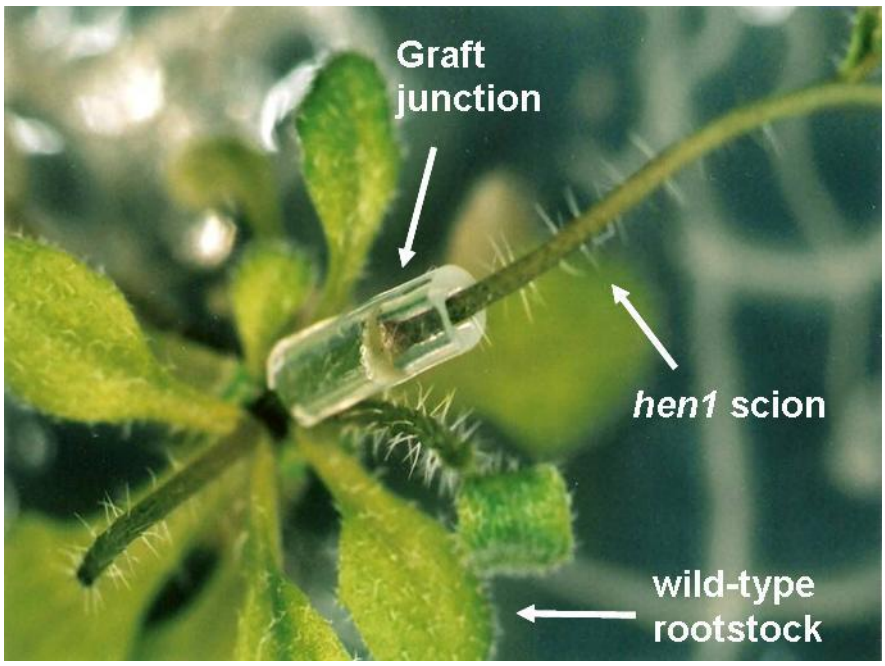

Figure 6.4. Homozygous *hen1-6* mutant inflorescence grafted onto *Arabidopsis* wild-type rootstock. The primary inflorescence of approximately 4 week-old *hen1-6* scions was grafted onto wild-type rootstocks. Sterile silicone tubing was used to keep the graft in place during healing.

Micrografting

Micrografting was performed as described by Turnbull *et al*. (2002). *A. thaliana* wild type and *hen1-6* homozygous mutant seeds were surface sterilized and sown in square Petri plates as described previously. Plates were placed at 4˚C in the dark for 3 d and then transferred to a growth chamber at 21˚C with a 16 h photoperiod (120 µE m^{-2} sec^{-1}) for further 3 d. Plates were oriented vertically with lighting from above to minimize scion bending. The temperature was then increased to 27˚C, the light intensity decreased to 60 µE m^{-2} sec˙1 and photoperiod reduced to 8 h. Seedlings were maintained under these conditions for another 4 d before grafting. Silicone tubing (Medical grade tubing 0.3 mm internal diameter, Biolab) was slit longitudinally and then cut into approximately 1.5 mm lengths, sterilized in 70% (v/v) ethanol and rinsed in sterile distilled water. Micrografting was done under the dissecting microscope. The *hen1-6* rootstock donor was cut perpendicular to the hypocotyl using a No. 11 scalpel blade and a length of tubing placed over the cut hypocotyl of the rootstock. The wild type scion was excised and inserted into the other end of the tubing until it touched the rootstock. As a control, wild-type scions were grafted onto wild-type rootstocks and *hen1-6* scions grafted onto *hen1-6* rootstocks. Grafted plants

were grown under hydroponics conditions in sterile ¼-strength nutrient solution containing 0.75 mM $MgSO_4.7H_2O$, 1.5 mM $Ca(NO_3)_2.4H_2O$, 1.25 mM KNO_3, 0.5 mM KH_2PO_4 and 0.04 mM Fe-EDTA. The following micronutrients were added: 46 µM H_3BO_3, 9 µM $MnCl_2.4H_2O$, 0.8 µM $ZnSO_4.7H_2O$, 0.3 µM $CuSO_4$ and 0.1 µM Na_2MoO_4. $2H_2O$ and pH was adjusted to 5.5 with KOH. Nutrient solution was added to a previously autoclaved Magenta GA7 box (Sigma) containing a foam plug (Sigma) placed in the centre of a Osmotek Float Unit (Austratec Pty Ltd) as described by Arteca and Arteca (2000). The foam plugs were thoroughly wetted with nutrient solution and a single grafted plant was placed on each plug (Figure 6.5). Grafts in magenta boxes were maintained in the growth chamber at 27˚C with a 16 h photoperiod and light intensity of 120 µE m^{-2} sec^{-1}, provided by cool white fluorescent lamps, for approximately one week until the graft junction had healed. After this time, the temperature was reduced to 23˚C and the light intensity reduced to 97 µE m^{-2} sec^{-1}. Grafts were visually assessed daily under a dissecting microscope from 3 d after grafting and for approximately 2 weeks. Any adventitious roots were immediately excised. Nutrient solution was replaced twice per week. The lid covering the magenta vessel was removed gradually over a period of one week. Small RNA was isolated and translocation of microRNA analysed by northern blot assays four weeks after grafting.

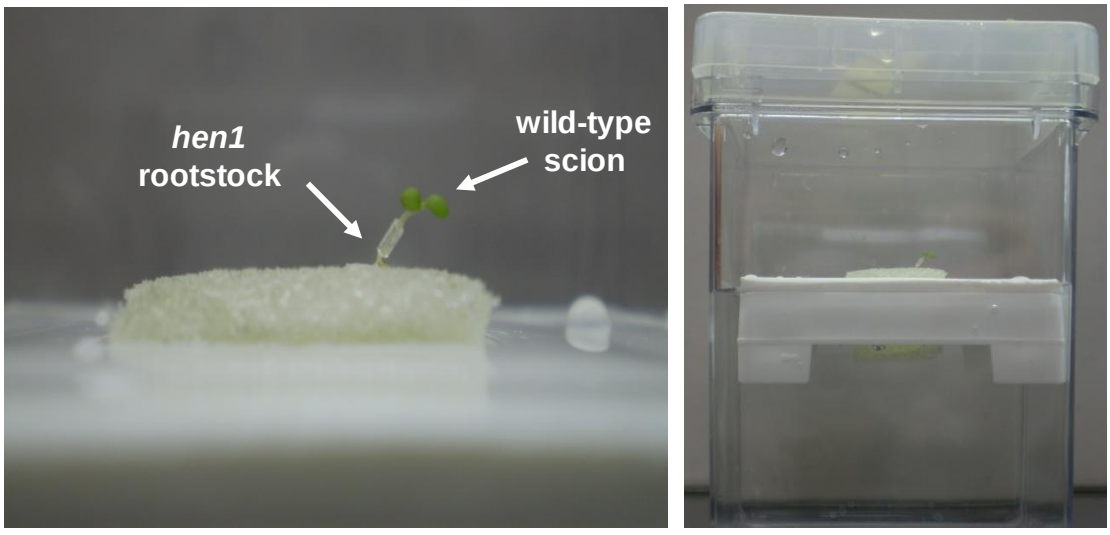

Figure 6.5. Wild-type scion grafted onto *hen1-6* mutant rootstock. Micrografted plants were grown under hydroponics conditions in Magenta boxes. Micrografted plants were placed on a foam plug fitted in the centre of a float unit and this assembly placed in the Magenta box. Nutrient solution was changed twice per week.

Demonstration of grafting functionality

The surface of two rosette leaves of an *Arabidopsis* wild-type rootstock having *hen1-6* mutant as scion, were scarified using fine forceps and a 0.5 µl drop of ^{32}P-ATP (7000ci/mmol; 100mci/mL) applied to the damaged surface. The radioisotope was allowed to translocate for 10 min under direct light. The treated leaves were excised and discarded and the plants dried between paper sheets in the oven at 80°C for 4.5 h. Once dried, plants were exposed to X-ray film for approximately 1 h at -80°C.

Assessment of miR395 translocation under sulphur deficiency

In order to determine whether miR395 is translocated in response to sulphur deficiency, wild-type scions were grafted onto *hen1-6* rootstocks and *hen1-6* scions grafted onto wild-type rootstocks. As control, wild-type scions were grafted onto wild-type rootstocks and *hen1-6* scions onto *hen1-6* rootstocks. Micrografts were maintained in full nutrient solution for two weeks. After this time, grafts were transferred to a sulphur deficient medium in which $MgSO_4$ was replaced by 0.5 mM $Mg(NO_3)_2.6H_2O$, and the micronutrient components, $ZnSO_4$ and $CuSO_4$, replaced by 1 µM $ZnCl_2$ and 1 µM $CuCl_2$. Micrografted plants were maintained in S-free medium for 2 weeks. Total RNA was isolated from scions and rootstocks using TRIzol reagent (Invitrogen) (see 'General Methods' Chapter 2) and 0.5 µg total RNA reverse transcribed using specific stem-loop reverse transcription primers. Levels of expression of miR395 in scions and in rootstocks under full nutrient and sulphur deficiency conditions were assessed by real-time RT-PCR. Expression of miR168 was used as control.

Small RNA isolation

Small RNA was isolated using a *mir*Vana^{TM} miRNA isolation kit (Ambion) following instructions from the manufacturer. Briefly, tissue was ground in liquid nitrogen and 10 vol of lysis/binding buffer (containing guanidinium thiocyanate) and 1/10 vol of miRNA homogenate additive added. Samples were incubated on ice for 10 min. One vol of acid-phenol:chloroform was added followed by vortexing and centrifugation at 10,000 *g* in a Beckman JA-20 rotor for 5 min at room temperature. The aqueous phase was collected and 1/3 vol of absolute

ethanol added. The sample was passed through a filter cartridge (supplied with the isolation kit) to immobilize large RNA. Absolute ethanol (2/3 vol) was added to the filtrate (containing small RNA) which was passed through a second filter to immobilize the small RNA. The filter was washed twice using the wash solutions supplied with the kit and small RNA were eluted from the filter into RNase-free tubes using 70 µl of diethylpyrocarbonate (DEPC)-treated water and stored at -80˚C.

Small RNA concentration was assessed using a Varian, Cary 3-UV visible spectrophotometer. 3.3 µl of eluate was added to 1 ml of DEPC-treated water and optical density (OD) measured at 260 and 280 nm. The conversion 1 A260 unit = 33 µg/ml of single stranded small RNA was used to calculate the RNA concentration.

Northern blot analysis

RNA was separated on a 15% (w/v) denaturing polyacrylamide gel (16 X 18 X 0.15 cm, Bio-Rad) containing 48% (w/v) urea, 1 X TBE, 15% acrylamide:bis acrylamide 19:1, 0.05% (w/v) ammonium persulfate and 0.1% (v/v) TEMED. Before loading the samples gels were pre run at 20 mA for 1 h in a PROTEAN II gel electrophoresis unit (Bio-Rad) in 1 x TBE running buffer (90 mM Tris base, 89 mM boric acid and 2 mM EDTA). Samples of RNA (5 µg) were diluted in an equal volume of gel loading buffer containing 95% (v/v) formamide, 18 mM EDTA, 0.025% (w/v) SDS, xylene cyanol and bromophenol blue (Ambion). The samples were incubated at 95˚C for 3 min, briefly centrifuged and loaded onto the gel. RNA size markers of 18, 21 and 24 nucleotides were end labelled with ^{32}P and run on the gel with the samples. Electrophoresis was performed at 20 mA for approximately 3 h. The section of the gel containing the labelled markers was excised, sealed in plastic and exposed to X-ray film overnight at -80˚C. The rest of the gel was stained using ethidium bromide in 0.5X transfer buffer (0.05 M Tris base, 0.05 M boric acid and 0.001 M EDTA) and visualised under UV light.

RNA was transferred overnight to a Hybond-N^+ nylon membrane (Amersham Biosciences) at 4˚C and at 25 V using a trans-blot cell (Bio-Rad) according to

the manufacturer's instructions. Following RNA transfer, the membrane was UV cross-linked for 5 min and baked at 80˚C for 2 h to fix the RNA to the blot.

End-labelling of RNA markers and DNA oligonucleotide probes

DNA oligonucleotides complementary to microRNA miR164, miR168, miR159, miR156, miR166 and miR399 (Table 6.1), previously found in phloem exudate (Jordan, 2004 and Yoo *et al*., 2004), were used to probe Northern blots. RNA sequences of 18, 21 and 24 nucleotides were used as size markers. DNA probes and RNA markers were ^{32}P end-labelled using the KinaseMax^{TM} Kit (Ambion) following the manufacturer's instructions. Briefly, 25 pmol of oligonucleotides was mixed with 13.5 µl Nuclease-Free water, 1 µl of γ ^{32}P ATP (6000-7000 Ci/mmol), 2 µl of 10X Kinase Buffer (Promega) and 10U of T4 Polynucleotide Kinase enzyme (Promega). The reaction was incubated at 37˚C for 1 h and stopped by heating at 95˚C for 2 min.

To remove unincorporated nucleotides from radiolabelled probes the reaction mix was passed through NucAway Spin Columns (Ambion) following the manufacturer's instructions.

Table 6.1. DNA oligonucleotides complementary to miR164, miR168, miR159 and miR156, miR166 and miR399 were used as probes in northern blots assays for detection of the corresponding microRNA. N indicates either A, T, G or C; H indicates A, C or T and Y indicates C or T. T_m is the melting temperature of the probe.

MicroRNA	MicroRNA sequence	DNA oligonucleotide probe sequence (Tm)
miR164	UGGAGAAGCAGGGCACGUGCA	TGCACGTGCCCTGCTTCTCCA(58)
miR168	UCGCUUGGUGCAGGUCGGGAA	TTCCCGAYCTGCACCAAGCGA(57)
miR159	UUUGGAUUGAAGGGAGCUCUA	TAGAGCTCCCTTCAATCCAAA(50)
miR156	UGACAGAAGAGAGUGAGCAC	GTGCTCACTCTCTTCTGTCA (52)
miR166	UCGGACCAGGCUUCAUUCCCC	GGGGAATGAAGCCTGGTCCGA(58)
miR399	UGCCAAAGGAGAUUUGCCCUG	CNGGGCAAHTCTCCTTTGGCA(56)

Probing northern blots

The membrane was prehybridized at the melting temperature of the DNA oligonucleotide probe (Table 6.1) for 1 h in 20 ml freshly prepared hybridization buffer containing 5x SSPE, 1% (w/v) SDS, 10% (w/v) dextran sulphate and

0.5% (w/v) Blotto milk powder. This buffer was then replaced with 7 ml hybridization buffer containing the radiolabelled oligonucleotide. The membrane was hybridized overnight at the melting temperature of the probe. Unbound probe was removed by washing the membrane in 3x SSC for 5 min followed by a wash in 3x SSC, 0.1% (w/v) SDS for 15 min at 30˚C and then another wash in pre-heated 2x SSC, 0.1% (w/v) SDS at 10°C below the melting temperature of the probe. A final wash of the membrane was done in 1x SSC, 0.1% (w/v) SDS at room temperature for 10 min. The membrane was monitored using a Morgan series 900 mini-monitor after additional washes.

The membrane was sealed in a plastic bag and exposed to a phosphor imager plate overnight and then to X-ray film at -80˚C for approximately 2 weeks before being developed.

Levels of miRNA in pod tissue and phloem exudate of *L. albus*

In order to study the levels of miR168, miR399, miR395 and miR164 in lupin phloem exudate compared to pod tissue, samples were collected from approximately 3 month old *L. albus* plants grown under greenhouse conditions. Total RNA was isolated using TRIzol reagent (Invitrogen) (see 'General Methods' Chapter 2.) and 0.5 µg total RNA reverse transcribed using specific stem-loop reverse transcription primers. Levels of miRNA were analysed by real-time RT- PCR.

Real-time RT-PCR analysis

Synthesis of cDNA

In order to quantify mature miRNA, total RNA was reverse transcribed using SuperScript III reverse transcriptase (200 units/µl) (Invitrogen) following the pulsed reverse transcription protocol described by Varkonyi-Gasic *et al*. (2007). 0.5 µg total RNA was mixed with 1 µl 10 mM dNTP mix, 0.4 µl 10 µM miRNA-specific stem-loop primer (highly specific for mature miRNA) (Table 6.2) and nuclease-free water to a final volume of 13 µl. This mixture was incubated at 65°C for 5 min and chilled on ice. 4 µl 5X first-strand buffer, 1 µl 0.1M DTT, 40 units RNase inhibitor RNaseOUT^{TM} (Invitrogen) and 200 units SuperScript III

were added. The reaction was incubated for 30 min at 16°C, followed by 60 cycles at 30°C for 30 sec, 42°C for 30 sec and 50°C for 1 sec. Reverse transcriptase was inactivated by incubation at 85°C for 5 min.

Table 6.2. DNA oligonucleotide sequences used as miRNA-specific-stem-loop reverse transcription primers. The last six nucleotides at the 3' end of the specific stem-loop primer is a reverse complement of the last six nucleotides at the 3' end of the corresponding miRNA.

MicroRNA	Stem-loop reverse transcription primer
miR399d	5'-GTCGTATCCAGTGCAGGGTCCGAGGTATTCGCACTGGATACGACCGGGGCAAA-3'
miR164c	5'-GTCGTATCCAGTGCAGGGTCCGAGGTATTCGCACTGGATACGACCGCACG-3'
miR395a	5'-GTCGTATCCAGTGCAGGGTCCGAGGTATTCGCACTGGATACGACGAGTTC-3'
miR168	5'-GTTGGCTCTGGTGCAGGGTCCGAGGTATTCGCACCAGAGCCAACTCCCGA-3'

Real-time RT-PCR

Real-time RT-PCR was performed as described in 'General Methods' (Chapter 2.) using miRNA-specific forward primers and a universal reverse primer designed according to Pant *et al.* (2008) (Table 6.3).

Table 6.3. DNA oligonucleotide sequences used as miRNA-specific forward and universal reverse primers in a real-time RT-PCR. Specific forward primers exclude the last six nucleotides at the 3' end of the miRNA. 5-7 nucleotides were added randomly to the 5' end of each forward primer to increase the melting temperature.

MicroRNA	Real-time PCR forward primer
miR399d	5'-CGACGTGCCAAAGGAGATTTG-3'
miR164c	5'-CACGTGGAGAAGCAGGGCA-3'
miR395a	5'-CGACGCTGAAGTGTTTGGGG-3'
miR168	5'-TGTGGTTCGCTTGGCGCAGG-3'
	Real-time PCR universal reverse primer
miR399, miR164, miR395	5'-CCAGTGCAGGGTCCGAGGT-3'
miR168	5'-GTGCAGGGTCCGAGGT-3'

Standard curves were prepared for each miRNA from a dilution series of the experimental sample that in a pilot PCR run had shown the highest expression of each microRNA. PCR products of that sample were gel purified (see 'General Methods' Chapter 2.), quantified using a Nanodrop ND-1000 Spectrophotometer (NanoDrop Technologies) and the number of molecules calculated. Standards were diluted to 6.023^{10} molecules μl^{-1}. From this stock, a series of 7-fold dilutions were made. Results were analysed using the LightCycler software (Roche). Two or three biological replicates with two technical replicates were measured per sample.

RESULTS

MicroRNA in phloem exudate collected from *L. albus*

Accumulation of miRNA in phloem exudate collected from different sites of the plant

MicroRNA profile in exudate collected at different sites on the plant could provide information about differential expression of miRNA in CC at different sites and/or specificity in phloem loading. Lupins offer the possibility of making collections from a number of ‘source’ and ‘sink’ locations and this has been exploited in this study by making collections from pods, from the apices of inflorescence branches and from the base of the stem below the lowest leaf.

Northern blot analysis showed two of the miRNA assayed, miR156 and miR168, to have comparable accumulation in exudate at each of the sites sampled (Figure 6.6). However, miR164 had the highest accumulation in phloem exudate collected from pods with relatively little in exudates from the base of the stem and from branch apices while miR159 and miR166 showed highest accumulation in exudate collected from the base of the stem and pods.

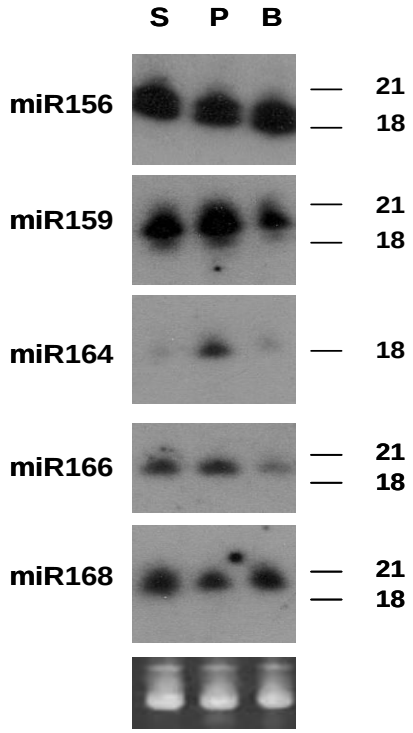

Figure 6.6. Northern blot assays of 5 µg small RNA extracted from phloem exudate collected from base of the stem (S), pods (P) and branches (B) of field-grown *L. albus* plants. RNA samples were separated on a 15% denaturing polyacrylamide gel, transferred to Hybond-N^+ nylon membrane and hybridized to specific ^{32}P end-labelled DNA oligonucleotide probes complementary to miR156, miR159, miR164, miR166 and miR168. Low molecular weight RNA was visualized by ethidium bromide staining to serve as loading control.

Accumulation of miR399 in phloem exudate and leaf tissue under Pi deficiency conditions

There is strong evidence from other plant species supporting the idea that miR399 is associated with nutrient status, specifically the level of Pi (Pant *et al*., 2008; Chiou *et al.*, 2006; Fujii *et al.,* 2005), and that it seems to be mobile in phloem (Pant *et al*., 2008). If miR399 acts as a signal to allow the plant to respond to Pi deficiency, an increase in the miRNA in phloem in response to low Pi might be expected. Northern blot analysis was used to determine the change in miR399 levels in phloem and leaves of lupin under Pi deficiency conditions. Plants were grown in pots under greenhouse conditions and fertilised with a complete (N-free) nutrient solution until flowering, followed by fertilisation with Pi-free nutrient solution. Elemental analysis confirmed that Pi levels in leaves of these plants decreased over time (Figure 6.7A). No analysis for Pi in phloem exudate was made as insufficient volume of exudate was available. miR399 accumulated in exudate and in leaves as plants were subjected to progressive Pi withdrawal (Figures 6.7B and 6.7C) but was not detected either in exudate or leaves collected from plants fertilized with full nutrient solution. The Increase in miR399 under Pi deficiency was greater in

phloem exudate than in leaves and increased with time. Levels of control miR168 did not change during Pi limitation (Figures 6.7D-G).

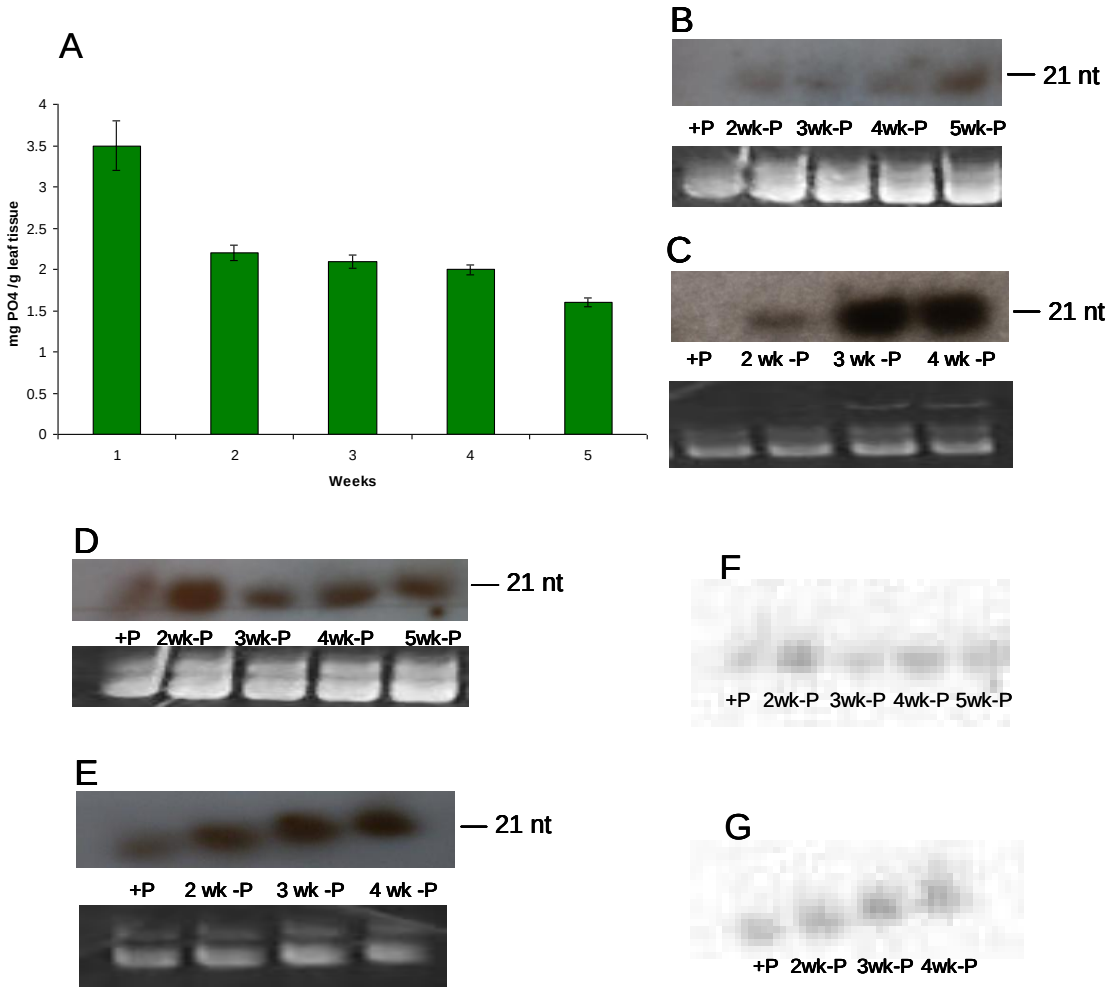

Figure 6.7. Accumulation of miR399 in *L. albus* phloem exudate and in leaf tissue in response to Pi deficiency. A) Phosphate analysis performed on leaf tissue the first week of sampling (+P) and 2, 3, 4 and 5 weeks after Pi was omitted from the nutrient solution. Data are mean values ± SE (n=5). B-E) Northern blot of 5 µg small RNA extracted from *L. albus* leaf tissue (B and D) and phloem exudate (C and E) collected from plants that had been fertilised using a full nutrient solution (+P). Phloem exudate was collected 2, 3 and 4 weeks and leaf tissue 2, 3, 4 and 5 weeks after Pi was omitted from the nutrient solution and RNA was isolated from the samples. RNA samples were separated on a 15% denaturing polyacrylamide gel, transferred to Hybond-N^+ nylon membrane and hybridised to specific ^{32}P end-labelled DNA oligonucleotide probes complementary to miR399 (B and C) and miR168 (D and E). Low molecular weight RNA was visualized by ethidium bromide staining and serves as loading control. F and G) Phosphoimaging of blot hybridised to specific probe complementary to miR168. F) leaf tisse, G) phloem exudate.

Levels of miRNAs in pod tissue and phloem exudate

In order to assess whether miRNA detected in lupin phloem were there as a result of contamination of exudate from damaged neighbouring cells during the period of sampling, levels of miR164, miR168, miR399 and miR395 in phloem

exudate were compared to those in the neighbouring tissue surrounding the site from which the exudate was collected. Each of these miRNA had been identified previously in phloem exudate from lupin fruits (Jordan, 2004). This analysis used real-time RT-PCR and showed that the level of miR164 was 4.5 fold higher in pod tissue than in phloem exudate (Figure 6.8). However, the levels of miR168, miR395 and miR399 were significantly higher in phloem exudate (52-fold, 132-fold and 39-fold respectively) compared to pod tissue (Figure 6.8) making it unlikely that their presence in phloem was the result of contamination from neighbouring cells damaged in the process of collecting exudates.

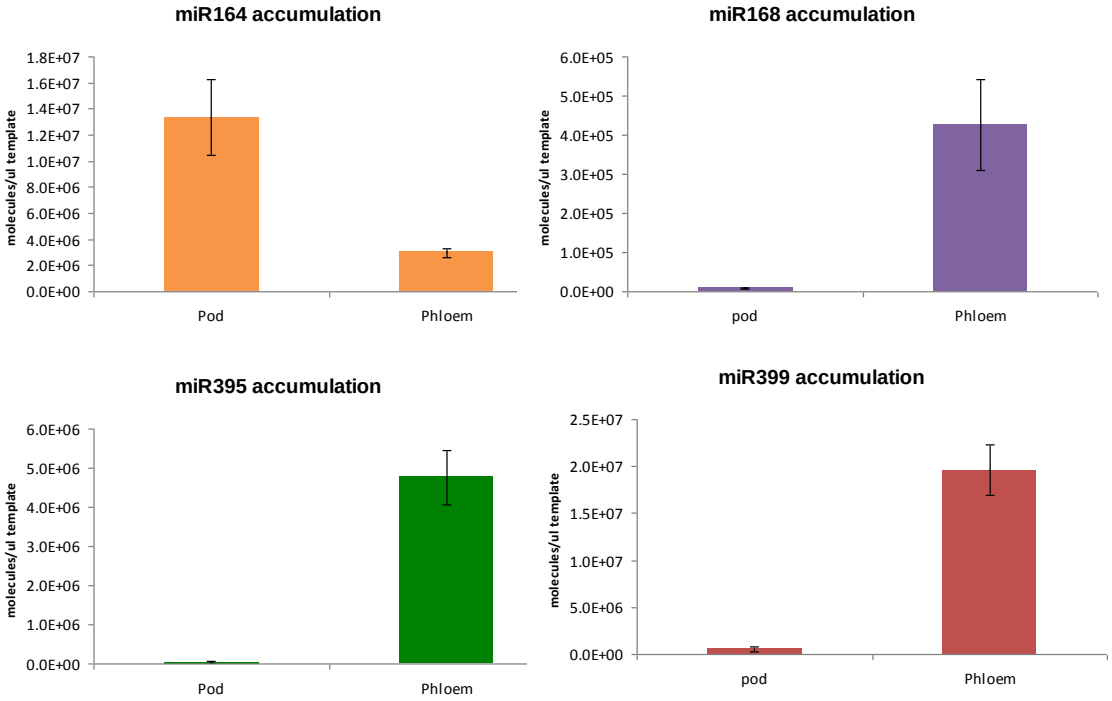

Figure 6.8. Absolute quantification of miRNAs in *L. albus* phloem exudate and pod tissue. 0.5 µg of total RNA isolated from pod tissue and phloem exudate was reverse transcribed using miRNA-specific stem-loop primers followed by real-time PCR analysis performed on a LightCycler480 (Roche Diagnostics) using SYBR® green as the fluorescent dye. Data are the mean ± standard deviation of three biological replicates with two technical replicates each.

Dissociation curves with single peaks for miR399, miR395, miR164 and miR168 confirming the specificity of PCR products are shown in Appendix 5.

Investigation of translocation of miRNA in *Arabidopsis*

Homozygous *hen1-6* mutant exhibited developmental defects including reduced leaf size, reduced plant height and altered leaf shape as it has been described

for some other *hen1* mutants (Vazquez *et al.,* 2004; Park *et al.,* 2002). Each of the miRNA assayed in lupin exudate collected at different sampling sites on the plant were also measured in extracts of seedlings of wild-type and homozygous *hen1-6* mutants of *Arabidopsis*. All analysed miRNA were detected in the wild-type (Figure 6.9). However, miR166, miR168 and miR156 were below detectable levels in *hen1-6* and miR164 was close to the detection limit in the mutant (Figure 6.9). In addition there was a second band of higher molecular weight (24 nt) for miR159 in the mutant seedlings that was not present in the wild-type.

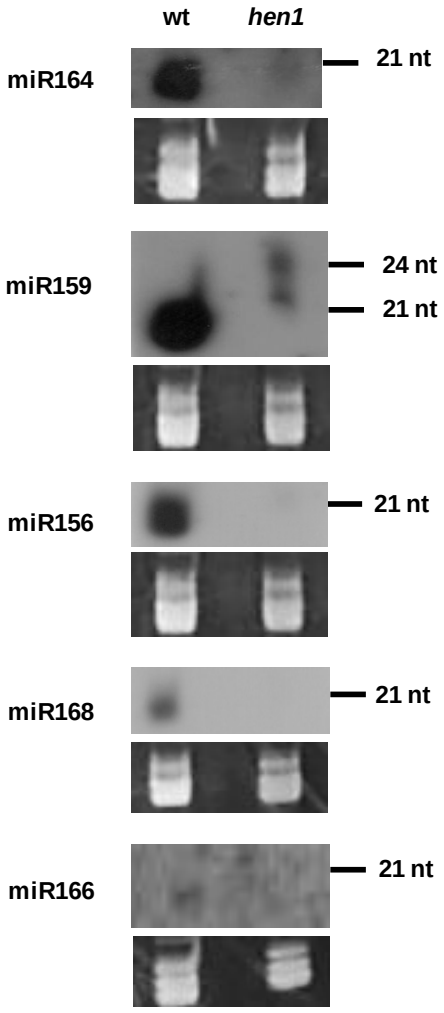

Figure 6.9. MicroRNA accumulation in *Arabidopsis* wild-type and *hen1-6* mutant plants. Northern blot assays of 5 µg small RNA extracted from *Arabidopsis* wild-type and *hen1-6* mutant seedlings (both in Columbia ecotype). RNA samples were separated on a 15% denaturing polyacrylamide gel, transferred to Hybond-N^+ nylon membrane and hybridized to specific ^{32}P end-labelled DNA oligonucleotide probes complementary to miR164, miR159, miR156, miR168, miR166. Blot initially hybridised to miR159 probe was stripped and rehybridised to miR156 probe. Low molecular weight RNA was visualised by ethidium bromide staining and serves as loading control en each case

To assess the possibility that any of these miRNA in *Arabidopsis* were translocated in phloem, a series of grafting experiments were carried out using wild-type and *hen1-6* mutant plants. In the first experiments, the rootstocks were rooted rosettes comprising a number of mature and developing leaves, and the scions were the developing inflorescence (see Figure 6.4). Figure 6.10 indicates that the graft was functional. In this case the primary inflorescence of an approximately 4 week old *hen1-6* mutant was grafted onto the rooted rosette of wild-type plants. The movement of ^{32}P from the rosette leaves indicates phloem translocation in both upward and downward directions.

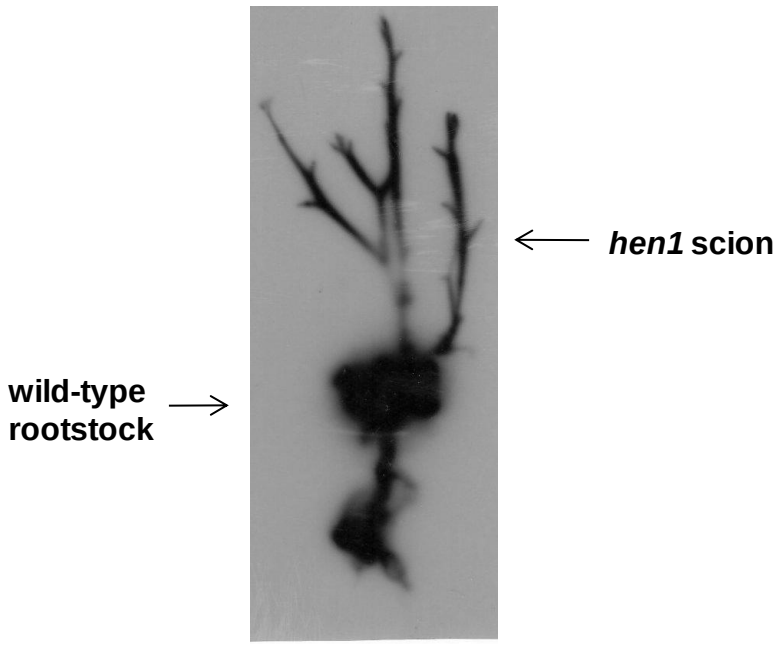

Figure 6.10. Grafting functionality. Two rosette leaves of *Arabidopsis* wild-type rootstock having *hen1-6* mutant as scion were scarified and ^{32}P ATP applied to the damaged surface. The radioisotope was allowed to translocate for 10 min, the graft dried and exposed to X-ray film for approximately 1 h.

Because the constitutive level of expression of each of the miRNA was so low in the *hen1-6* mutant, any translocation of the miRNA in phloem from the rosette of the wild-type rootstock should be readily detected in the mutant scion. Despite the presence of the wild-type rootstock there was no increase in any of the miRNA recovered from the *hen1-6* scions (Figure 6.11). In *hen1-6* mutant scions, most of the miRNA were below detectable levels and an additional band of higher molecular weight was still observed for miR159 as it was in intact plants. The pattern of miRNA levels in *hen1-6* scions grafted onto wild-type rootstocks was similar to the one in *hen1-6* scions grafted onto *hen1-6*

rootstocks. There was no change to the phenotype of *hen1-6* scion as a consequence of grafting onto a wild-type rootstock. These results indicate that the miRNA tested were not translocated from the rosettes to inflorescence tissue, and that if others are, they do not alter the phenotype of the *hen1-6* mutant.

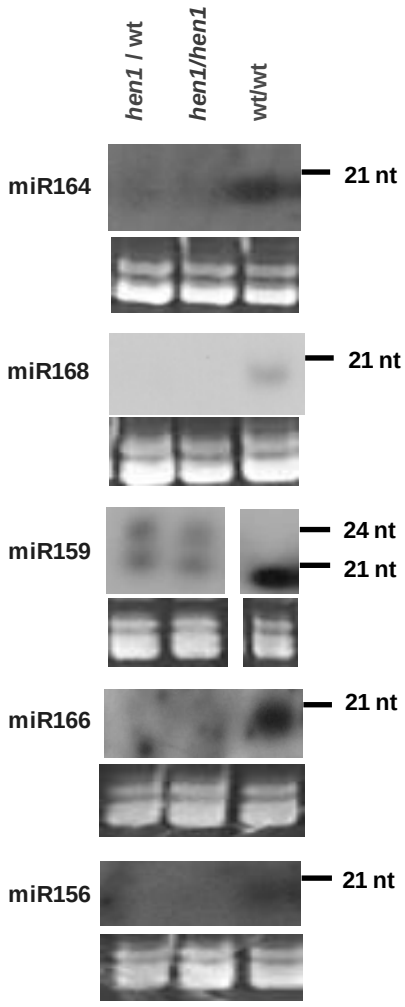

Figure 6.11. MicroRNA accumulation in grafted *Arabidopsis* wild-type and *hen1-6* scions. Northern blot assays of 5 µg small RNA extracted from *Arabidopsis* wild-type and *hen1-6* scion tissues in a grafting system. RNA samples were separated on a 15% denaturing polyacrylamide gel, transferred to Hybond-N^+ nylon membrane and hybridised to specific ^{32}P end-labelled DNA oligonucleotide probes complementary to miR164, miR168, miR159, miR166 and miR156. Low molecular weight RNA was visualised by ethidium bromide staining to serve as loading control. Abb: *hen1* scion grafted onto wild-type rootstock (*hen1*/wt); *hen1* scion grafted onto *hen1* rootstock (*hen1*/*hen1*); wild-type scion grafted onto wild-type rootstock (wt/wt).

To assess the possibility that miRNA in phloem might be translocated in a downward direction, micrografting was carried out using *hen1-6* mutant rootstocks with wild-type scions. Accumulation of miRNA in mutant rootstocks grafted to wild-type scions was comparable to that of *hen1-6* rootstocks grafted to *hen1-6* scions, with most of the miRNA undetectable and an additional band

of higher molecular weight for miR159 in *hen1* rootstocks (Figure 6.12). For each of the miRNA the pattern in wild-type/wild-type grafted plants was similar to that of ungrafted plants (Figures 6.9). These results indicate that the naturally occurring miRNA assayed were not translocated in the downward phloem stream.

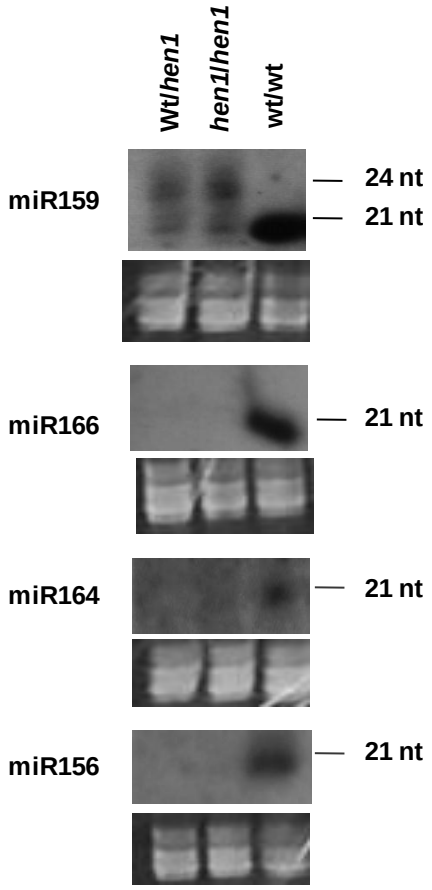

Figure 6.12. MicroRNA accumulation in micro-grafted *Arabidopsis* wild-type and *hen1-6* rootstocks. Northern blot assays of 5 µg small RNA extracted from *Arabidopsis* wild-type and *hen1-6* rootstock tissues in a micrografting system. RNA samples were separated on a 15% denaturing polyacrylamide gel, transferred to Hybond-N^+ nylon membrane and hybridised to specific ^{32}P end-labelled DNA oligonucleotide probes complementary to miR159, miR166, miR164 and miR156. Low molecular weight RNA was visualised by ethidium bromide staining to serve as loading control. Abb: wild-type scion grafted onto *hen1* rootstock (wt/*hen1*); *hen1* scion grafted onto *hen1* rootstock (*hen1*/*hen1*); wild-type scion grafted onto wild-type rootstock (wt/wt).

Since the miRNAs studied with *Arabidopsis* did not appear to be translocated under normal conditions of nutrient sufficiency, it was of interest to assess the movement of miR395 which has been associated with plant responses to S deficiency (Buhtz *et al.,.* 2008; Jones-Rhoades and Bartel, 2004). Micrografting was used to investigate whether miRNAs were translocated in *Arabidopsis* grafted plants grown under S deficiency. These plants showed a distinctive pink to purple coloration towards the apex of inflorescence branches (Figure 6.13).

Figure 6.13. Wild-type *A. thaliana* scion grafted onto a wild-type rootstock grown on S deficient nutrient solution. White arrows show a pink to purple coloration close to the inflorescences.

Quantitative RT-PCR showed that miR395 levels increased in wild-type and *hen1-6* grown under S deficiency (Figure 6.14). A large increase (4380-fold) of miR395 levels was observed in wild-type scion grafted onto wild-type rootstock. An increase of miR395 levels in wild-type rootstock having wild-type as scion (491-fold) and wild-type rootstock having *hen1-6* as scion (536-fold) was observed under S deficiency as well. A strong 125-fold increase of miR395 levels in *hen1-6* rootstock having wild-type as scion was also found under S deficiency. However, miR395 levels in the wild-type scion of this graft did not increase. A 1.5 fold increase in miR168 in wild-type scion grafted onto wild-type rootstock grown under S-deficiency was observed (Figure 6.15), but it was not significant.

The RT PCR data were not ‘normalised’. Normalisation is used to correct for differences in quantity or quality caused by factors such us variations in nucleic acid recovery and in cDNA synthesis efficiency. Two *Arabidopsis* genes, expressed protein (*At*2g32170) and UBC9 (*At*4g27960) have been reported to

be stably expressed under nutrient stress conditions (Czechowski *et al.*, 2005) and these were tested as possible reference genes. However, neither was constant in this experiment (data no shown) and for this reason the data could not be normalised. Thus it is not possible to judge how much of the differences in expression found have contributed to the results. Given this, it will be important in future studies to investigate a larger number of reference genes to identify one that shows stable expression in nutrient deprivation so that the results can be validated.

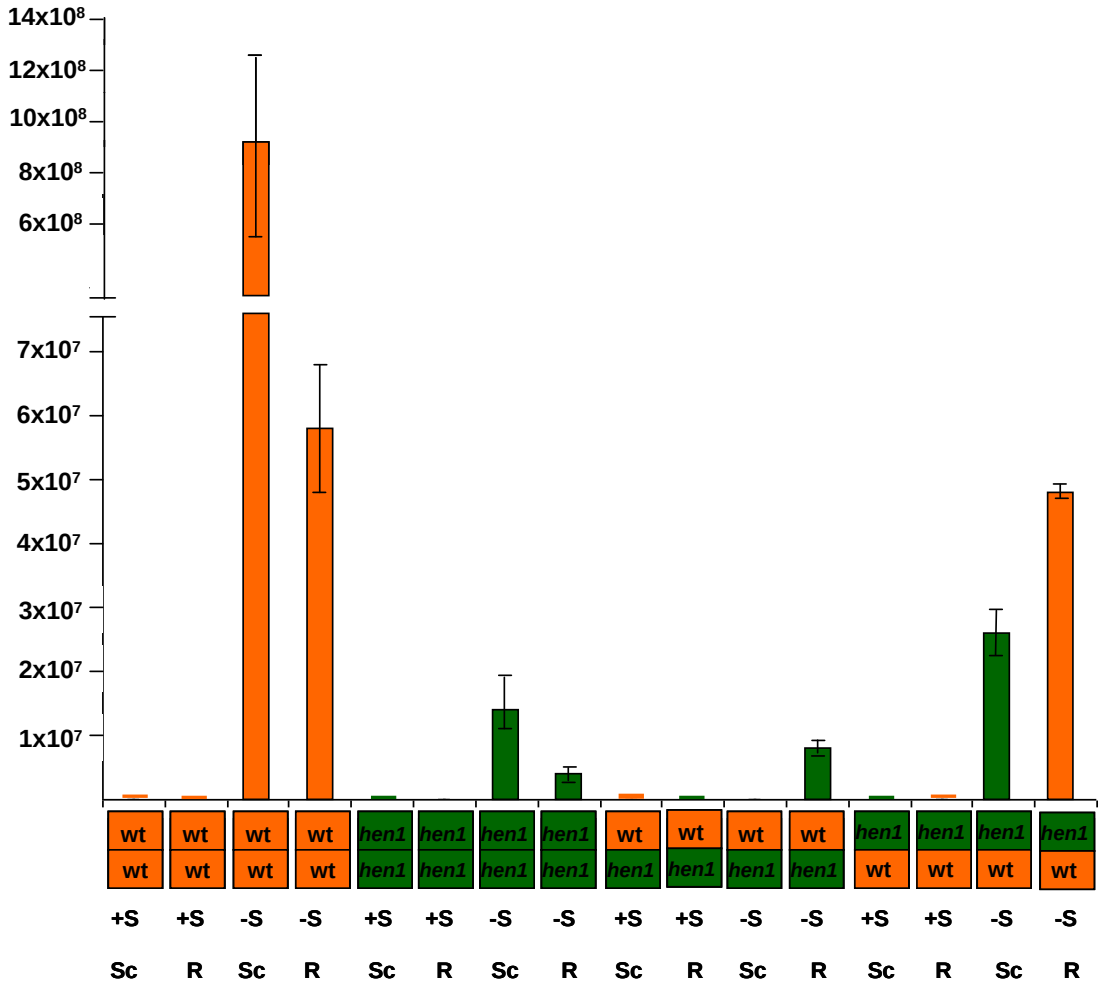

Figure 6.14. Accumulation of miR395 in micro-grafted *Arabidopsis* wild-type and *hen1-6* mutant under nutrient replete and S deficiency growing conditions. Micrografted Wild-type (orange) and *hen1-6* (green) were grown under nutrient replete (+ S) and S-deficiency (- S) conditions. 0.5 µg of total RNA isolated from scions and rootstocks was reverse transcribed using miRNA-specific stem-loop primers followed by real-time PCR analysis performed on a LightCycler480 (Roche Diagnostics) using SYBR® green as the fluorescent dye. Data are the mean ± SE of 3 biological replicates with two technical replicates each. Scion wild-type grafted onto *hen1-6* rootstock and scion *hen1-6* grafted onto wild-type rootstock, both grown under nutrient replete conditions, had only 2 biological replicates. Scions (Sc) and rootstocks (R) genotypes are depicted below the graphs indicating to what the column correspond to.

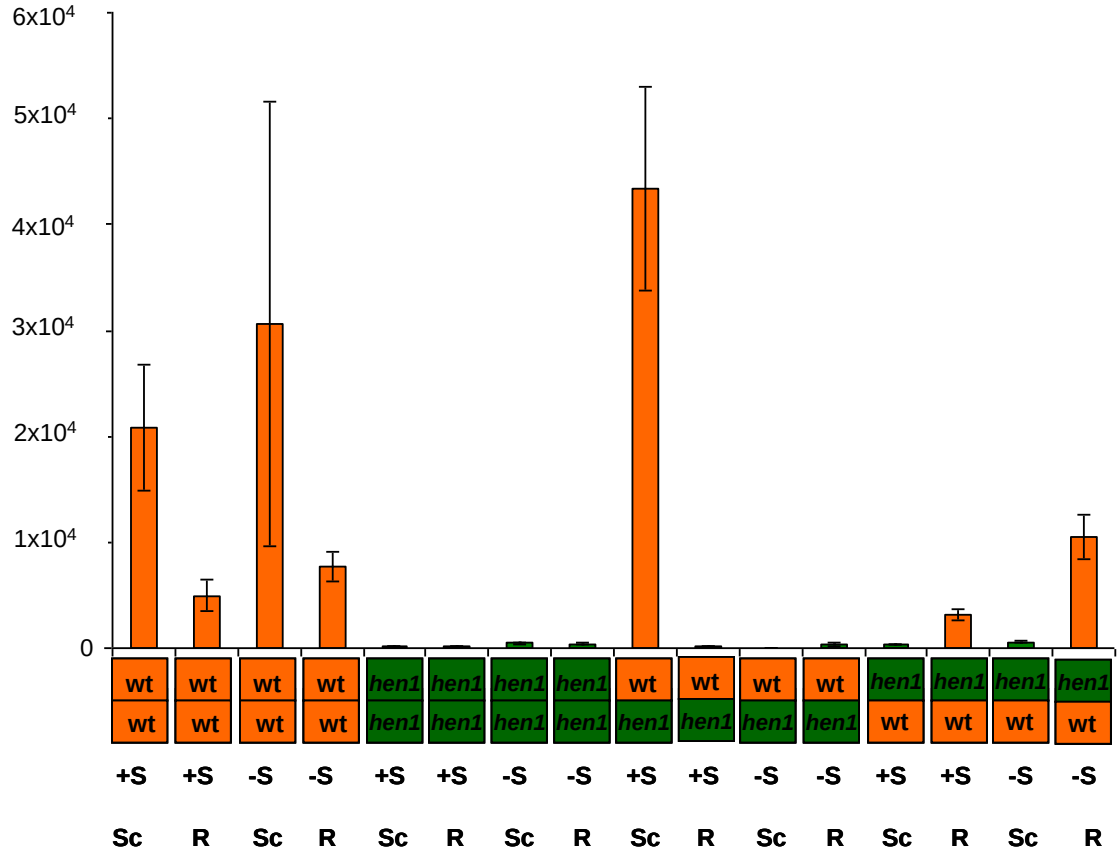

Figure 6.15. Absolute quantification of miR168 in micro-grafted *Arabidopsis* wild-type and *hen1-6* mutant under nutrient replete and S deficiency growing conditions. Micrografted Wild-type (orange) and *hen1-6* (green) were grown under nutrient replete (+ S) and S-deficiency (-S) conditions. 0.5 µg of total RNA isolated from scions and rootstocks was reverse transcribed using miRNA-specific stem-loop primers followed by real-time PCR analysis performed on a LightCycler480 (Roche Diagnostics) using SYBR® green as fluorescent dye. Data are the mean ± SE of 3 biological replicates with two technical replicates each. Scion wild-type grafted onto *hen1-6* rootstock and scion *hen1-6* grafted onto wild-type rootstock, both grown under nutrient replete conditions, had only 2 biological replicates. Scions (Sc) and rootstocks (R) genotypes are depicted below the graphs indicating to what the column correspond to.

Dissociation curves with single peaks for miR168 and miR395 under full nutrient and sulphur deficiency conditions, confirming the specificity of PCR products, are shown in Appendix 6.

DISCUSSION

Following the initial findings of miRNA in phloem exudate from cucurbits (Yoo *et al*., 2004) and *Lupinus albus* (Jordan, 2004; Yoo *et al*., 2004), a number of studies have led to the suggestion that these small RNA species might be phloem-mobile and may have a long-distance signalling role (Buhtz *et al*., 2008; Pant *et al*., 2008). Systemic signalling might reasonably be expected to be involved in a range of 'source-sink relationships' whether these relate to the partitioning of assimilates, nutrient allocation or in the coordination of development processes, defence or responses to abiotic stress (reviewed in Lough and Lucas, 2006).

Although the question of contamination due to the mode of phloem sampling in lupin applies also to miRNA, as discussed earlier for proteins and gene transcripts detected in exudates (Chapters 4 and 5), the data gathered here for four miRNA in exudate versus the surrounding pod tissue (Figure 6.8) clearly indicates that three of those assayed were highly enriched in phloem. It thus seems likely that miR168, miR395 and miR399 are indeed normal constituents of the SE in lupin.

The most reasonable explanation for the presence of miRNA in phloem is that they are transported from the adjacent CC. Thus, the fact that the pattern for five miRNA in exudate collected at three different sites on the lupin plant (Figure 6.6) was not the same suggests either differential expression of miRNA in CC at different sites and/or specificity in phloem loading. If miRNA serve as translocated signals it is not too surprising that the downward-moving and upward-moving phloem streams showed different compositions. It would be interesting to further exploit the ability to collect phloem exudates from different parts of the phloem stream in lupin, by extending the range of miRNA assayed to include the many more that have been identified in exudates (Buhtz *et al*., 2008; Jordan, 2004). The five miRNA studied in lupin exudates at different sites were also examined in grafting experiments with *Arabidopsis* plants (Figures 6.11 and 6.12). The *hen 1-6* mutant grafted as a means to report translocation of miRNA from wild-type roots or scions failed to show evidence of translocation

in either upward or downward moving phloem streams under nutrient replete conditions. This negative result does not preclude movement of other miRNA in phloem. Pant *et al*. (2008) have inferred movement of miR399, from the shoot to the root, in grafted *Arabidopsis* grown under nutrient replete conditions in which the scion over-expressed the miRNA and the rootstock showed virtually no expression of the primary transcript for the miR399 gene. miR399 is involved in Pi nutrition, regulating the expression of genes involved in Pi transport. Perhaps it is this particular class of miRNA, i.e. those involved in nutrient uptake and allocation, that are mobile in phloem and that may only move long distances in response to specific internal or external factors such as developmental inputs or stress conditions like nutrient availability. Other miRNA, though found in exudate, may in fact be expressed in a cell autonomous fashion and have very limited cell to cell movement (Yoo *et al.,* 2004). While there seems little doubt that miR399 is present in phloem it is not yet clear whether or not the primary transcript is expressed in CC. The most recent data that provides a global analysis of transcription in CC comes from nuclei isolated by flow cytometry from CC in the roots of *Arabidopsis* (Zhang *et al.*, 2008). Among the 237 genes that were enriched more than 1.5 fold compared to nuclei from non-CC, none were identified as primary transcripts for miRNA. Interestingly transcripts for some of the Pi responsive genes that interact with miR399 (*pho1* together with *pht1* and *pht2)* were identified (Zhang *et al.,* 2008, supplemental data Table 1).

The most compelling case for translocation of miRNA is that of miR399 which increases sharply in both, leaf tissue and phloem exudate, in response to Pi starvation in pumpkin and rapeseed (Pant *et al.,* 2008). A similar response of miR399 to Pi withdrawal was demonstrated here for *L. albus* (Figure 6.7). The PCR analysis showed abundant levels of transcript for miR399 and miR395 in lupin exudate even though the plants were not deliberately exposed to nutrient deficiency (Figure 6.8). However, the local field soils used for growing lupins in this study have characteristically low levels of nutrients and it was quite likely that plants were deficient in Pi and S, explaining the very high levels of miR399 and miR395 observed. In this respect, it should be noted that Buhtz *et al*. (2008), showed these miRNA in exudate of *B. napus* from plants grown in full nutrients suggesting it is possible that these miRNA are present at low level in

phloem, even when plants are not under nutrient stress. As noted above, lupins offer the possibility of sampling exudate from phloem translocating to the upper organs of the shoot and to the root system separately, and it will be interesting to examine the status of miR399 in these streams under a range of nutrient limitations.

This study aimed initially to develop experiments on the translocation of miR399 in *Arabidopsis* using the *hen 1-6* mutant. However, as a study on translocation of miR399 was recently published (Pant *et al*., 2008), this aspect was abandoned and the focus changed to translocation of another of the miRNA involved in nutrient acquisition and allocation, miR395. Levels for this miRNA in phloem exudates are responsive to the status of S in *B. napus* (Butz *et al*., 2008) and offer another candidate miRNA for studies of long distance movement. In this study, a strong increase in the level of miR395 in wild-type scions grafted to wild-type root-stocks grown under S-deficiency conditions was observed. A strong increase in miR395 also in *hen1-6* grafted material was obtained under S-deprivation. Although *hen1-6* accumulates low levels of miRNA that are short lived due to the lack of methylation (Li *et al*., 2005), miRNA are still likely to be synthesised. The real-time RT-PCR method would have detected methylated and unmethylated miRNA. Transcription of the miR395 gene would thus be stimulated under S-deficiency and the increased level of non-functional miR395 detected in *hen1-6* mutant. An increase in miR395 in wild-type rootstock and in its *hen1-6* scion was observed under S-deficiency. On the other hand, although miR395 levels in *hen1-6* rootstock having wild-type as scion increased under S deficiency, levels of miR395 in this wild-type scion did not increase. These results could suggest that *hen1-6* rootstock has responded to S deficiency by producing miR395, but that the lack of methylation results in miRNA being degraded probably making *hen1-6* rootstock unable to communicate the information about S deficiency to its wild-type scion. This assumption would be supported by an increase of miR395 level in *hen1-6* scion grafted to wild-type rootstock suggesting that in this case, functional miR395 in wild-type are able to send the information about nutrient deficiency to the *hen1-6* scion which in turn responds by increasing the levels of miR395 which is likely to be short lived. These speculations need to be treated with caution as where a *hen1-6* scion was grafted to a *hen1-6* rootstock there

was an increase in miR395 in the scion. The increase of miR395 levels in wild-type and *hen1-6* rootstocks under S-deficiency suggests that expression of miR395 is taking place in roots. In fact, recently, Kawashima *et al.* (2008) provided evidence that 5 of the 6 loci for *MIR395* are expressed both in roots and leaves of *Arabidopsis,* being localised to the vascular tissue. Even though the low affinity SO_4 transporter *(SULTR2;1*) is down-regulated by miR395, expression of both, miRNA and target, increases in roots during S deficiency. The authors (Kawashima *et al.*, 2008) suggest that this results from the expression of *MIR395* being localised to CC while for the SO_4 transporter expression is restricted to xylem parenchyma. However, the study by Zhang *et al.* (2008) of transcript abundance in CC from roots of *Arabidopsis* did not identify any of the MIR395 loci but did find transcripts for a number of sulphurylase genes and the SO_4 transporter.

It is important to note that this data have not been normalised and samples have not been corrected for differences in quantity or quality caused by factors such as variations in nucleic acid recovery and variations in cDNA synthesis efficiency. It is not clear how much of these differences are contributing to the results. Given this it will be important to investigate a larger number of reference genes to identify one that shows stable expression in sulphur deprivation so that the results can be validated.

The data in this study, together with those of Kawashima *et al*. (2008), could be interpreted to indicate that the S-deficiency signal moves from the root system in xylem. A number of 'signals' have been found to move in xylem while others have been inferred from physiological experiments but have yet to be identified (reviewed in Atkins and Smith, 2007). A critical analysis of xylem exudates for small RNA species has not been reported. There is also the possibility that miR395 is not the signal itself but that it activates the signal that transmits the information of S-deficiency to the scion through xylem. Of course this same consideration could apply to miRNA and the actual 'signals' translocated in phloem. While cell-to-cell movement through a symplastic route has been reported for small RNA (Yoo *et al*. 2004) it seems unlikely that this process could possibly transfer macromolecules, even though miRNA are quite small, from root to shoot; even in very small *Arabidopsis* plants over a significant

period of time. In fact, microinjection studies showed that small RNA cannot move unaided through plasmodesmata (Yoo *et al*., 2004). Thus there must be a protein or set of proteins being expressed also in CC that bind the miRNA and facilitate diffusion through plasmodesmata into the SE.

Clearly a more extensive analysis of a range of miRNA need to be assessed in grafting experiments to establish which if any is translocated. Similarly, there is a need to determine where in the vasculature of both roots and shoots miRNA encoding genes are expressed. It is also to be hoped that the labelling and flow cytometric tools employed in Zhang *et al.* (2008) studies can be extended to other organs. The studies of Kawashima *et al*. (2008) provide an example of where *in situ* hybridisation might be used to advantage. The unique ability of lupins to exude phloem contents at a number of sites offers an exciting possibility. It has proved possible to collect sufficient volumes of exudate from the midrib veins of leaflets and from the petiole (Atkins *et al.*, 1983) providing access to the ‘source’ of signals and to the ‘sink’ sites at the flowers, developing fruits as well as at stem segments towards the root system (Pate *et al.*, 1979).

CHAPTER 7

GENERAL DISCUSSION

While the essential role of phloem in translocation of assimilated C and other nutrients to the growing organs of a plant is widely documented, systemic transport of ‘signals’ is not so well understood. The identification of macromolecules like proteins and RNA, including small RNA in phloem exudates has led to the idea that some of these might be mobile, and perhaps function as signals to form part of a communication system that regulates plant development and responds to both internal and external cues such as photoperiod, temperature, water, nutrient availability and pathogen attack (Lough and Lucas, 2006). In general, the identification of such macromolecules has relied on analysis of phloem exudates collected either by incisions to the vasculature in species that do not readily seal wounded phloem or from aphid stylets. Phloem collection by stylectomy is regarded to yield ‘pure; exudates and so provides insight into the true composition of SE. While contamination of exudates collected from wounded vasculature is likely to be inconsequential for major translocated solutes (sugars, amino acids and inorganic macronutrients), this is not the case for solutes that are present in trace amounts, and particularly for macromolecular species. Unfortunately, analyses of exudates collected by stylectomy has been done only for a few monocotyledon species, thus limiting comparisons with the exudate composition for species that ‘bleed’ from incisions (cucurbits, castor bean, oilseed rape and some legumes, including species of the genus *Lupinus*). Nevertheless, it is important that a detailed inventory for proteins and RNA species in phloem exudates is collected so that potential signals can be identified and their role(s) studied.

The presence of macromolecules in phloem exudates raises important questions regarding their source and translocation:

1. Have macromolecules identified in phloem exudate moved from adjacent CC or have they resulted from contamination from neighbouring cells during phloem sampling?

2. Are these macromolecules translocated?
3. Is translocation essential for their function?

While the data for protein, mRNA and microRNA in phloem exudate from *Lupinus albus* collected in this study cannot answer these questions, they do nevertheless provide a basis from which to develop experimental approaches that will further our understanding of the signalling role(s) of phloem translocation.

In this study phloem exudates, collected from incisions mainly to the sutures of developing fruits of *L. albus*, were used to identify proteins, mRNA and miRNA that might be part of the translocation stream *in vivo*. Proteomic analysis identified 83 proteins by their high level of similarity to sequences in protein databases from 130 protein spots collected from 2D gels and partially sequenced by MS/MS. These identified proteins matched 56 unique accession numbers as some of the identified proteins were present in more than one spot on the 2D gels (Table 4.1). The more prominent proteins identified, cyclophilin, a proteinase inhibitor, a glycine-rich RNA-binding protein and a phloem specific protein, have also been reported in stylet exudate from cereals (Aki *et al.,* 2008; Gaupels *et al.,* 2008). Transcriptomic analysis of *L. albus* phloem exudate identified a total of 609 unique transcripts corresponding to 727 ESTs (Table 5.3). The largest group of transcripts and proteins identified in this study were involved in metabolism suggesting some metabolic activity in SE. Proteins and transcripts encoding proteins involved in protein synthesis, turnover and sorting was also a significant group possibly fulfilling a function in the transport of macromolecules from CC to SE.

In this study, an analysis of the levels of four miRNA, previously found in lupin phloem exudate (Jordan, 2004), showed higher levels of miR399, miR395 and miR168 in phloem exudate compared to pod tissue from which the exudate had been collected (Figure 6.8). These results suggested that these miRNA were specifically localised to phloem. A role in nutrient homeostasis has been attributed to miR399, miR395 and miR398 (Buhtz *et al*., 2008; Pant *et al.*, 2008; Yamasaki *et al.,* 2007; Chiou *et al.,* 2006; Fujii *et al.,* 2005). In this study an increase of miR399 in *L. albus* tissue and phloem exudate was observed in

response to Pi deficiency (Figure 6.7) which is in accordance with the increased in miR399 observed by Buhtz *et al*. (2008) in phloem exudate from *B. napus* under Pi deficiency conditions.

The results outlined above provide the first set of analyses for macromolecules in phloem exudate from a legume. It is reassuring that many of the proteins and transcripts as well as miRNA have also been documented in exudates collected from a number of cucurbits (Lin *et al.*, 2008; Walz *et al*., 2004;), *Ricinus communis* (Doering-Saad *et al.,* 2006; Barnes *et al*., 2004), *B. napus* (Buhtz *et al*. 2008; Giavalisco *et al*., 2006), and *Oryza sativa* (Aki *et al*., 2008; Sasaki *et al.,* 1998). However, the question of their origin remains to be addressed. It has been assumed that mature translocating SE are enucleate and lack the biochemical machinery for protein synthesis; the structure of the phloem tissue in *L. albus* from which exudate was collected confirms this view (Chapter 3). Similarly, it has also been assumed that proteins and transcripts in SE would have to be transported there from the adjacent CC through plasmodesmata. Again, the ultra-structure of *L. albus* phloem tissue confirms the close association of SE with CC characterised by the presence of wall ingrowths and dense cytoplasm. An early study by Fisher *et al*. (1992), using ^{35}S-methionine to label newly synthesised proteins in wheat, showed that some proteins are indeed transferred from CC to phloem exudate collected, in the case of that study, through aphid stylets.

The belief that mature SE are unable to synthesise proteins has recently been challenged. In a proteomic analysis of pumpkin phloem exudate, Lin *et al*. (2008) identified 1,121 proteins that were annotated from GenBank and BLAST search analyses against *Arabidopsis*, rice and poplar (*Populus trichocarpa*). The authors reported that contamination from the cut surface of the pumpkin stem was negligible as only three unique peptides for Rubisco subunits were recovered. Their study identified proteins involved with RNA-binding, mRNA translation, ubiquitin-mediated proteolysis and macromolecular and vesicle trafficking. Lin *et al.* (2008) concluded that protein synthesis and turnover processes are likely to occur within the phloem translocation stream. Experimental confirmation for this view is lacking but if protein synthesis in SE can be demonstrated, then the long held assumptions about the source of

macromolecules in phloem might have to be revised. A proteasome- related and components of a ubiquitin- dependant protein degradation pathway were found in this study in *L. albus* exudate, and had been previously reported in *B. napus* exudate (Giavalisco *et al.,* 2006).

Although exudates collected by incision are undoubtedly contaminated to some extent with the contents of neighbouring cells, other consequences of the technique should be considered in this context. The osmotic potential of a 20% sucrose solution is ca 17 ATM so that whether the SE is opened by an incision or by a stylet the sudden release of pressure is likely to have significant physical effects on both sieve tubes and CC. It is important to realise the extent to which such physical impacts might occur in the vasculature that is cut.

It is difficult to know how many SE were severed when the suture vasculature was cut. Pate *et al.* (1978), counted approximately 1200 SE in transverse sections of 6 week old fruit stalks of *L. albus*. If the data for a comparably aged *L albus* fruit suture can be used, then three times the number recorded as entering the fruit from the stalk or 1200 x 3 = 3600 SE seems a reasonable estimate for the number of SE in the pod sutures sampled in this study. This is simply based on the fact that the dorsal and ventral sutures of the fruit comprise 3 major veins that develop from and are connected directly to the vasculature of the fruit stalk (Pate *et al.,* 1974). Typical SE in the fruit stalk are ca 150 μm^2 in cross-sectional area (ca 15 µm in diameter) and ca 200 µm in longitudinal section (Pate *et al*., 1978) and probably SE in the fruit vasculature are similar. Assuming a cylinder, this gives 30,000 μm^3 or 0.03 nl as the volume of 1 SE. The parietal cytoplasm accounts for some of this cell volume but it is only a small proportion (Figure 3.7) and could be ignored. Thus 1 µl exudate represents the contents of ca 33,300 SE. Exudate samples ranged from 10-50 µl and, on this basis, would have accumulated the contents of 0.33-1.65 million SE. If there are 3600 linear arrays of SE in transverse sections and if all were cut then the length of the vascular sutures contributing to the exudate would range from 18 to 92 mm. The specific mass transfer rates estimated by Pate *et al.* (1978) for the fruit stalk of lupin were based on the C economy of the fruits as they developed and so apply equally to the vasculature within the sutures. These ranged from ca 5 to more than 22 $cm.h^{-1}$

and if these rates of flow were maintained following incision, then for (say) a 10 min period of exudation, the supporting phloem could be expected to traverse ca 1-4 cm along the translocation pathway. Because this rate of flow is accommodated by three major vascular bundles in the sutures of the fruit, then 1/3 or 30-130 mm would be traversed by phloem contents during the period of exudation. These two estimates (i.e 18-92 mm based on SE number and 30-130 mm based on mass transfer rates) of the length of suture vasculature that contributed to the exudate are similar and in each case suggest a substantial amount of tissue. The first conclusion from these considerations is that if the physical effects on CC that result from an incision causes more than 'normal' transfer of macromolecules to SE then potentially the impact on phloem exudate composition could be massive. The second is that it is reasonable to suppose that the volume of other cells damaged by the sampling method was, by comparison, relatively small and that the contamination due to their contents is minimal.

Recent conclusions about protein synthesis in SE aside (Lin *et al.,* 2008), any macromolecule identified in phloem exudate must have been transported from CC. Thus, information on the transcripts that can be associated with or recovered from CC is important. Transcriptomic analysis of isolated cell types, including CC protoplasts (Brady *et al.,* 2007) or nuclei specific to CC (Zhang *et al.,* 2008) provide a global picture of localised gene expression. In the latter, *Zhang et al.* (2008) used a nuclear-targeted version of GFP under the control of the *SULPHATE TRANSPORTER2;1* (*SULTR2;1*) promoter and purified fluorescent nuclei from homogenates of transgenic *Arabidopsis* roots by fluorescence-activated sorting with a flow cytometer. RNA isolated from these nuclei was then used as a target for microarray hybridisation. The study provides a comprehensive analysis of transcripts enriched in CC nuclei of roots and identified a set of 237 nuclear-enriched phloem companion cell (NPCC) genes. While the extensive list of transcripts available from the study by Zhang *et al.* (2008) provides a basis from which to assess CC as a source of transcripts found in phloem exudates, in this case the comparison might be restricted to roots. Some of the genes that have been localised by others to CC by *in situ* methods (two subunits of glutamate dehydrogenase and glutamine synthetase for example, Kichey *et al*., 2005) were not identified by Zhang *et al.*

(2008) and the authors concluded that these were found in aerial tissue of *Arabidopsis* and that the CC of phloem in roots and shoots have tissue-specific patterns of gene expression. The sorts of analyses described above need to be extended to aerial tissues of *Arabidopsis* and if possible to species from which phloem exduates have been collected so that a more comprehensive inventory of genes expressed in CC can be assembled. Such a database would be invaluable in further studies aimed at identifying macromolecular signals in phloem.

The second important question posed above (are these macromolecules translocated?) is difficult to answer. The present study did not attempt to determine if any of the proteins or transcripts found in phloem exudate from *L. albus* was translocated. The evidence for the 'florigenic' signalling protein, Flowering Locus T (FT), being translocated systemically is compelling (Corbesier *et al.,* 2007; Tamaki *et al.,* 2007; Lin *et al.*, 2007) and in this study both the protein and its transcript were found in exudate from flowering lupin plants. Similarly infection of lupins by the bean yellow mosaic virus (BYMV) results in systemic spread of the symptoms and it is likely that transcripts for the BYMV polyprotein identified in phloem were indeed translocated. It should be stressed that any conclusions about translocated macromolecules need to be carefully tested and proven before proteins and transcripts can be assigned systemic signalling roles.

Arabidopsis and its *hen1-6* mutant, in which miRNA methylation and so stability is compromised, provided a realistic experimental system to test the translocation of a group of miRNA that had been identified earlier in *L. albus* exudate. Grafting of four week old *Arabidopsis* plants and micro-grafting of seedlings was used as means to identify miRNA translocated from the wild-type tissues to those of the *hen1-6* mutant. The grafts were generated to assess translocation in both upward and downward directions. However, no evidence of translocation under normal nutrient replete conditions of any of the miRNA included in this analysis was obtained (Figures 6.11 and 6.12). This result may simply reflect the fact that none of the tested miRNA are phloem mobile or that they only move in response to specific external or internal inputs not tested during this study.

The most compelling data for mobility of miRNA in phloem come from studies in which miR399 increases sharply in phloem exudate as a response to Pi deprivation (Pant *et al.,* 2008) and similar features appear to be the case for other nutrient limitations including for S (Buhtz *et al.,* 2008). This latter was the basis for a study of translocation of miR395 using *Arabidopsis* wild-type and its *hen1-6* mutant under S-limitation. Conclusive evidence for phloem mobility was not obtained but some evidence for root-to-shoot movement (Figure 6.14), perhaps in xylem, of a signal related to the response of miR395 was indicated. These data are preliminary and require more detailed experimentation to establish the form and translocation path for the S-deficiency signal. In any case, it is becoming obvious that the picture is far more complex than the initial observation of increased miR395 level in phloem exudate in response to S and perhaps this realisation also applies to the 'apparent' translocation of other miRNA species.

It is important that the cellular site(s) for miRNA transcription and synthesis in vascular tissue is established. Interestingly, the detailed transcriptomic analysis of nuclei isolated from CC of *Arabidopsis* root (Zhang *et al.,* 2008) failed to identify any transcripts for miRNA or for enzymes associated with their synthesis. Even though the complement of expressed genes might be different to that from other sites of the plant it seems remarkable that no miRNA transcripts were found. Similarly none of the proteins associated with miRNA synthesis were detected in the current proteomic study of *L.albus* exudate or in the more than 1000 peptides found in pumpkin exudate by Lin *et al.* (2008).

The third question posed above is the most important of all in establishing the connection between macromolecules in phloem and their possible role(s) as systemic signals involved in regulating plant development or conditioning responses. This study did not extend to a consideration of this question. Nevertheless, the data for proteins and RNA in lupin phloem exudate provides a starting point from which potential candidates for systemic signalling functions can be considered. Questions about the origin of each and every protein or transcript in exudate remain but in general the picture emerging from a wide range of species for which exudates have been analysed is consistent. The

phloem appears to contain a group of proteins responsible for SE maintenance and so the maintenance of translocation processes. There also appears to be specific metabolic components, like glycolysis, that might also function to support the SE and a wide range of proteins that appear to be involved in ‘defence’ (either for the plant generally or the phloem in particular). The phloem also carries a variety of enzymes involved in protein modification and turnover. How these relate specifically to either phloem function or systemic signalling is yet to be studied. The analyses also reveal a remarkably diverse group of macromolecules that have very specific metabolic functions in cells but which cannot yet be connected to phloem functions or to signalling roles. The encoding genes for these proteins will provide targets from which knockout mutants and genetic screens can be assembled broadening the range of tools available to address the important question raised above. No doubt with these powerful genetic tools new systemic signals can be identified.

REFERENCES

Aki, T., Shigyo, M., Nakano, R., Yoneyama, T. and Yanagisawa, S. (2008) **Nano scale proteomics revealed the presence of regulatory proteins including three FT-Like proteins in phloem and xylem saps from rice.** Plant Cell Physiol. 49: 767–790.

Allen, E., Xie, Z., Gustafson, A.M. and Carrington, J.C. (2005) **microRNA-directed phasing during trans-acting siRNA biogenesis in plants.** Cell 121: 207–221.

Alonso, J.M., Stepanova, A.N., Leisse, T.J., Kim, C.J., Chen, H., Shinn, P., Stevenson, D.K., Zimmerman, J., Barajas, P., Cheuk, R., Gadrinab, C., Heller, C., Jeske, A., Koesema, E., Meyers, C.C., Parker, H., Prednis, L., Ansari, Y., Choy, N., Deen, H., Geralt, M., Hazari, N., Hom, E., Karnes, M., Mulholland, C., Ndubaku, R., Schmidt, I., Guzman, P., Aguilar-Henonin, L., Schmid, M., Weigel, D., Carter, D.E., Marchand, T., Risseeuw, E., Brogden, D., Zeko, A., Crosby, W.L., Berry, C.C. and Ecker, J.R. (2003) **Genome-wide insertional mutagenesis of *Arabidopsis thaliana*.** Science 301: 653-657.

Alosi, M.C., Melroy, D.L. and Park, R.B. (1988) **The regulation of gelation of phloem exudate from *Cucurbita* fruit by dilution, glutathione, and glutathione reductase.** Plant Physiol. 86: 1089-1094.

Alvarez, S., Goodger, J.Q., Marsh, E.L., Chen, S., Asirvatham, V.S. and Schachtman, D.P. (2006) **Characterization of the maize xylem sap proteome.** J. Proteome Res. 5: 963–972.

Aoki, K., Suzui, N., Fujimaki, S., Dohmae, N., Yonekura-Sakakibara, K., Fujiwara, T., Hayashi, H., Yamaya, T. and Sakakibara, H. (2005) **Destination-selective long-distance movement of phloem proteins.** Plant Cell 17: 1801-1814.

Aoki, K., Kragler, F., Xoconostle-Cázares, B. and Lucas, W.J. (2002) **A subclass of plant heat shock cognate 70 chaperones carries a motif that facilitates trafficking through plasmodesmata.** Proc. Natl. Acad. Sci. USA 99: 16342-16347.

Arteca, R.N. and Arteca, J.M. (2000) **A novel method for growing *Arabidopsis thaliana* plants hydroponically**. Physiol. Plant. 108: 188-193.

Atkins, C.A. and Smith, P.M.C. (2007) **Translocation in legumes**: **assimilates**, **nutrients**, **and signaling molecules.** Plant Physiol. 144: 550-561.

Atkins, C.A. (1999) **Spontaneous phloem exudation accompanying abscission in *Lupinus mutabilis* (Sweet)**. J. Exp. Bot. 50: 805-812.

Atkins, C.A., Pate, J.S., Peoples, M.B. and Joy, K.W. (1983) **Amino acid transport and metabolism in relation to the nitrogen economy of a legume leaf.** Plant Physiol. 71: 841-848.

Balachandran, S., Xiang, Y., Schobert, C., Thompson, G.A. and Lucas, W.J. (1997) **Phloem sap proteins from *Cucurbita maxima* and *Ricinus communis* have the capacity to traffic cell to cell through plasmodesmata**. Proc. Natl. Acad. Sci. USA 94: 14150–14155.

Banerjee, A.K., Chatterjee, M., Yu, Y., Suh, S.-G., Miller, W.A. and Hannapel, D.J. (2006) **Dynamics of a mobile RNA of potato involved in a long-distance signaling pathway.** Plant Cell 18: 3443–3457.

Bari, R., Pant, B.D., Stitt, M. and Scheible, W.-R. (2006) **PHO2, micro RNA399 and PHR1 define a phosphate signalling pathway in plants.** Plant Physiol. 141: 988-999.

Barnes, A., Bale, J., Constantinidou, C., Ashton, P., Jones, A. and Pritchard, J. (2004) **Determining protein identity from sieve element sap in *Ricinus communis* L. by quadrupole time of flight (Q-TOF) mass spectrometry.** J. Exp. Bot. 55:1473–1481.

Bartel, B. and Bartel, D.P. (2003) **MicroRNAs: at the root of plant development?** Plant Physiol. 132: 709-717.

Bartel, D.P. (2004) **MicroRNAs: genomics, biogenesis, mechanism, and function.** Cell 116: 281-297.

Blount, J.W., Dixon, R.A. and Paiva, N.L. (1992) **Stress responses in alfalfa (*Medicago sativa* L.) XVI. Antifungal activity of medicarpin and its biosynthetic precursors, implications for the genetic manipulation of stress metabolites.** Physiol. Mol. Plant Pathol. 41: 333-349.

Borsani, O., Zhu, J., Verslues, P.E., Sunkar, R. and Zhu, J-K. (2005) **Endogenous siRNAs derived from a pair of natural cis-antisense transcripts regulate salt tolerance in *Arabidopsis*.** Cell 123: 1279-1291.

Bradford, M.M. (1976) **A rapid and sensitive method for the quantitation of microgram quantities of protein utilizing the principle of protein-dye binding.** Anal. Biochem. 72: 248-254.

Brady, S.M., Orlando, D.A., Lee, J.Y., Wang, J.Y., Kock, J., Dinneny, J.R., Mace, D., Ohler, U. and Benfey, P.N. (2007) **A high-resolution root spatiotemporal map reveals dominant expression patterns.** Science 318: 801-806.

Boutet, S., Vazquez, F., Liu, J., Beclin, C., Fagard, M., Gratias, A., Morel, J.B., Crete, P., Chen X. and Vaucheret, H. (2003) ***Arabidopsis* HEN1: a genetic link between endogenous miRNA controlling development and siRNA controlling transgene silencing and virus resistance.** Curr. Biol. 13: 843–848.

Buhtz, A., Springer, F., Chappell, L., Baulcombe, D., and Kehr, J. (2008) **Identification and characterization of small RNAs from the phloem of *Brassica napus*.** Plant J. 53: 739-749.

Carpenter, C.D., Kreps, J.A. and Simon, A.E. (1994) **Genes encoding glycine-rich Arabidopsis thaliana proteins with RNA-binding motifs are influenced by cold treatment and an endogenous circadian rhythm.** Plant Physiol. 104: 1015–1025.

Carrington, J.C., Kasschau, K.D., Mahajan, S.K. and Schaad, M.C. (1996) **Cell-to-cell and long distance transport of viruses in plants**. Plant Cell 8: 1669-1681.

Chen, X., Liu, J., Cheng, Y. and Jia, D. (2002) ***HEN1* functions pleiotropically in *Arabidopsis* development and acts in C function in the flower.** Development 129: 1085–1094.

Chen, S.L., Chen, C.T. and Kao, C.H. (1991) **Polyamines promote the biosynthesis of ethylene in detached rice leaves.** Plant Cell Physiol. 32: 813-817.

Chiou, T.J., Aung, K., Lin, S.I., Wu, C.C., Chiang, S.F. and Su, C.L. (2006) **Regulation of phosphate homeostasis by microRNA in *Arabidopsis*.** Plant Cell 18: 412-421.

Christeller, J.T., Farley, P.C., Ramsay, R.J., Sullivan, P.A. and Laing, W.A. (1998) **Purification, characterization and cloning of an aspartic proteinase inhibitor from squash phloem exudate.** Eur. J. Biochem. 254: 160-167.

Corbesier, L., Vincent, C., Jang, S., Fornara, F., Fan, Q., Searle, I., Giakountis, A., Farrona, S., Gissot, L., Turnbull, C. and Coupland, G. (2007) **FT protein movement contributes to long-distance signalling in floral induction of *Arabidopsis*.** Science 316: 1030-1033.

Cronshaw, J. (1981) **Phloem structure and function.** Ann. Rev. Plant Physiol. 32: 465-484.

Czechowski, T., Stitt, M., Altmann, T., Udvardi, M.K. and Scheible, W-R. (2005) **Genome-wide identification and testing of superior reference genes for transcript normalization in *Arabidopsis*.** Plant Physiol. 139: 5-17.

Dannenhoffer, J.M., Suhr, R.C. and Thompson, G.A. (2001) **Phloem-specific expression of the pumpkin fruit trypsin inhibitor.** Planta 212: 155-162.

Deeken, R., Ache, P., Kajahn, I., Klinkenberg, J., Bringmann, G. and Hedrich, R. (2008) **Identification of *Arabidopsis thaliana* phloem RNAs provides a search criterion for phloem-based transcripts hidden in complex datasets of microarray experiments.** Plant J. 55: 746–759.

Dinant, S., Clark, A.M., Zhu, Y., Vilaine, F., Palauqui, J.C., Kusiak, C. and Thompson, G.A. (2003) **Diversity of the superfamily of phloem lectins (phloem protein 2) in angiosperms.** Plant Physiol. 131: 114-128.

Ding, B., Itaya, A. and Qi, Y. (2003) **Symplasmic protein and RNA traffic: regulatory points and regulatory factors.** Curr. Opin. Plant Biol. 6: 596-602.

Ding, B., Haudenshield, J.S., Hull, R.J., Wolf, S., Beachy, R.N. and Lucas, W.J. (1992) **Secondary plasmodesmata are specific sites of localization of the tobacco mosaic virus movement protein in transgenic tobacco plants.** Plant Cell 4: 915–928.

Divol, F., Vilaine, F., Thibivilliers, S., Amselem, J., Palauqui, J.C., Kusiak, C. and Dinant, S. (2005) **Systemic response to aphid infestation by *Myzus persicae* in the phloem of *Apium graveolens*.** Plant Mol. Biol. 57: 517–540.

Doering-Saad, C., Newbury, H.J., Couldridge, C.E., Bale, J.S. and Pritchard, J. (2006) **A phloem-enriched cDNA library from *Ricinus*: insights into phloem function.** J. Exp. Bot. 57: 3183-3193.

Doering-Saad, C., Newbury, H.J., Bale, J.S. and Pritchard, J. (2002) **Use of aphid stylectomy and RT–PCR for the detection of transporter mRNAs in sieve elements**. J. Exp. Bot. 53: 631–637.

Dong, Z., Han, M.-H. and Fedoroff, N. (2008) **The RNA-binding proteins HYL1 and SE promote accurate *in vitro* processing of pri-miRNA by DCL1.** Proc. Natl. Acad. Sci. USA. 105: 9970-9975.

Ehlers, K., Knoblauch, M. and van Bel, A.J.E. (2000) **Ultrastructural features of well-preserved and injured sieve elements: minute clamps keep the phloem transport conduits free for mass flow.** Protoplasma 214: 80–92.

Esau, K. and Thorsch, J. (1985) **Sieve plate pores and plasmodesmata, the communication channels of the symplast: ultrastructural aspects and developmental relations.** Am. J. Bot. 72: 1641-1653.

Eschrich, W. and Heyser, W. (1975) **Biochemistry of phloem constituents.** In: Zimmermann, M.H., Milburn, J.A. (Eds.), Encyclopedia of Plant Physiology, vol. 1: Transport in Plants. I. Phloem Transport. Springer, Berlin, pp. 101–136.

Evert, R.F. (1990) **Dicotyledons.** In: Behnke, H.-D., Sjölund, R.D. (Eds.), Sieve elements. Comparative structure, induction and development. Springer-Verlag, Berlin, pp. 103-137.

Fisher, D.B., Wu, K. and Ku, M.S.B. (1992) **Turnover of soluble proteins in the wheat sieve tube.** Plant Physiol. 100: 1433-1441.

Fisher, D.B. (1975) **Structure of functional soybean sieve elements**. Plant Physiol. 56: 555-569.

Franceschi, V.R. and Tarlyn, N.M. (2002) **L-Ascorbic acid is accumulated in source leaf phloem and transported to sink tissues in plants**. Plant Physiol. 130: 649-656.

Fujii, H., Chiou, T-J., Lin, S.-I., Aung, K. and Zhu, J.-K. (2005) **A miRNA involved in phosphate-starvation response in *Arabidopsis***. Curr. Biol. 15: 2038-2043.

Gachon, C.M.M., Langlois-Meurinne, M. and Saindrenan, P. (2005) **Plant secondary metabolism glycosyltransferases: the emerging functional analysis.** Trends Plant Sci. 10: 542–549.

Gasser, C.S., Gunning, D.A., Budelier, K.A. and Brown, S.M. (1990) **Structure and expression of cytosolic cyclophilin/peptidyl-prolyl cis-trans isomerase of higher plants and production of active tomato cyclophilin in *Escherichia coli*.** Proc. Natl. Acad. Sci. USA. 87: 9519-9523.

Gaupels, F., Buhtz, A., Knauer, T., Deshmukh, S., Waller, F., van Bel, A.J.E., Kogel, K.-H. and Kehr, J. (2008a) **Adaptation of aphid stylectomy for analyses of proteins and mRNAs in barley phloem sap.** J. Exp. Bot. 59: 3297-3306.

Gaupels, F., Furch, A.C.U., Will, T., Mur, L.A.J., Kogel, K.-H. and van Bel, A.J.E. (2008b) **Nitric oxide generation in *Vicia faba* phloem cells reveals them to be sensitive detectors as well as possible systemic transducers of stress signals.** New Phytol. 178: 634–646.

Gaupels, F., Knauer, T. and van Bel, A.J.E (2008c) **A combinatory approach for analysis of protein sets in barley sieve-tube samples using EDTA-facilitated exudation and aphid stylectomy.** J. Plant Physiol. 165: 95-103.

Geigenberger, P., Langenberger, S., Wilke, I., Heineke, D., Heldt, H.W. and Stitt, M. (1993) **Sucrose is metabolised by sucrose synthase and glycolysis within the phloem complex of *Ricinus communis* L. seedlings**. Planta 190: 446–453.

Giavalisco, P., Kapitza, K., Kolasa, A., Buhtz, A. and Kehr, J. (2006) **Towards the proteome of *Brassica napus* phloem sap**. Proteomics 6: 896-909.

Glen, A., Gan, C.S., Hamdy, F.C., Eaton, C.L., Cross, S.S., Catto, J.W.F., Wright, P.C. and Rehman, I. (2008) **iTRAQ-facilitated proteomic analysis of human prostate cancer cells identifies proteins associated with progression.** J Proteome Res 7: 897–907.

Golecki, B., Schulz, A., Carstens-Behrens, U. and Kollmann, R. (1998) **Evidence for graft transmission of structural phloem proteins or their precursors in heterografts of Cucurbitaceae**. Planta 206: 630–640.

Golecki, B., Schulz, A. and Thompson, G.A. (1999) **Translocation of structural P proteins in the phloem**. Plant Cell 11:127–140.

Gomez, G., Torres, H. and Pallás, V. (2005) **Identification of translocatable RNA-binding phloem proteins from melon, potential components of the long-distance RNA transport system.** Plant J. 41: 107-116.

Haebel, S. and Kehr, J. (2001) **Matrix-assisted laser desorption/ionization time of flight mass spectrometry peptide mass fingerprints and post source decay: a tool for the identification and analysis of phloem proteins from *Cucurbita maxima* Duch. separated by two-dimensional polyacrylamide gel electrophoresis.** Planta 213: 586-593.

Hayashi, H., Fukuda, A., Suzui, N. and Fujimaki, S. (2000) **Proteins in the sieve element–companion cell complexes: their detection, localization and possible functions.** Aust. J. Plant Physiol. 27: 489–496.

Haywood, V., Kragler, F. and Lucas, W.J. (2002) **Plasmodesmata: pathways for protein and ribonucleoprotein signaling.** Plant Cell. 14 Suppl: 303-325.

Haywood, V., Yu, T.S., Huang, N.C. and Lucas, W.J. (2005) **Phloem long-distance trafficking of GIBBERELLIC ACID-INSENSITIVE RNA regulates leaf development**. Plant J. 42: 49-68.

Hoffmann-Benning, S., Gage, D.A., McIntosh, L., Kende, H. and Zeevaart, J.A.D. (2002) **Comparison of peptides in the phloem sap of flowering and non-flowering *Perilla* and lupine plants using microbore HPLC followed by matrix-assisted laser desorption/ionization time-of-flight mass spectrometry.** Planta 216: 140-147.

Huang, T., Bohlenius, H., Eriksson, S., Parcy, F. and Nilsson, O. (2005) **The mRNA of the *Arabidopsis* gene *FT* Moves from leaf to shoot apex and induces flowering.** Science 309: 1694-1696.

Ishiwatari, Y., Fujiwara, T., McFarland, K.C., Nemoto, K., Hayashi, H., Chino, M. and Lucas, W.J. (1998) **Rice phloem thioredoxin h has the capacity to mediate its own cell-to-cell transport through plasmodesmata.** Planta 205: 12-22.

Ishiwatari, Y., Honda, C., Kawashima, I., Nakamura, S., Hirano, H., Mori, S., Fujiwara, T., Hayashi, H. and Chino, M. (1995) **Thioredoxin h is one of the major proteins in rice phloem sap**. Planta 195: 456-463.

Jones-Rhoades, M.W. and Bartel, D.P. (2004) **Computational identification of plant microRNAs and their targets, including a stress induced miRNA**. Mol. Cell 14: 787-799.

Jordan, M. (2004) **MicroRNA in *Lupinus albus* (L.)** Honours Thesis. The University of Western Australia. School of Plant Biology.

Jorgensen, R.A., Atkinson, R.G., Forster, R.L. and Lucas, W.J. (1998) **An RNA-based information superhighway in plants**. Science 279: 1486–1487.

Juarez, M.T., Kui, J.S., Thomas, J., Heller, B.A. and Timmermans, M.C.P. (2004) **MicroRNA-mediated repression of rolled leaf1 specifies maize leaf polarity.** Nature 428: 84–88.

Katiyar-Agarwal, S., Morgan, R., Dahlbeck, D., Borsani, O., Villegas, A., Zhu, J-K., Staskawicz, B.J. and Jin, H. (2006) **A pathogen-inducible endogenous siRNA in plant immunity.** Proc. Natl. Acad. Sci. USA 103: 18002-18007.

Kawashima, C.G., Yoshimoto, N., Maruyama-Nakashita, A., Tsuchiya, Y.N., Saito, K., Takahashi, H. and Dalmay, T. (2008) **Sulphur starvation induces the expression of microRNA-395 and one of its target genes but in different cell types**. Plant J. DOI: 10.1111/j.1365-313X.2008.03690.x.

Kehr, J. and Buhtz, A. (2008) **Long distance transport and movement of RNA through the phloem.** J. Exp. Bot. 59: 85-92.

Kempers, R., Ammerlaan, A. and van Bel, A.J.E. (1998) **Symplasmic constriction and ultrastructural features of the sieve element/companion cell complex in the transport phloem of apoplasmically and symplasmically phloem-loading species.** Plant Physiol. 116: 271-278.

Kichey, T., Le Gouis, J., Sangwan, B., Hirel, B. and Dubois, F. (2005) **Changes in the cellular and subcellular localization of glutamine synthetase and glutamate dehydrogenase during flag leaf senescence in wheat (*Triticum aestivum* L.)**. Plant Cell Physiol 46: 964–974

Kidner, C.A., and Martienssen, RA. (2005) **The developmental role of microRNA in plants.** Curr. Opin. Plant Biol. 8: 38-44.

Kim, M., Canio, W., Kessler, S. and Sinha, N. (2001) **Developmental changes due to long-distance movement of a homeobox fusion transcript in tomato**. Science 293: 287-289.

Knoblauch, M., Peters, W.S., Ehlers, K. and van Bel, A.J.E. (2001) **Reversible calcium-regulated stopcocks in legume sieve tubes.** Plant Cell 13: 1221–1230.

Knoblauch, M. and van Bel, A.J.E. (1998) **Sieve tubes in action.** Plant Cell 10: 35–50.

Kühn, C., Franceschi, V.R., Schulz, A., Lemoine, R. and Frommer, W.B. (1997) **Macromolecular trafficking indicated by localization and turnover of sucrose transporters in enucleate sieve elements**. Science 275: 1298-1300.

Kulikova, A.L., Turkina, M.V. and Puryaseva, A.P. (2003) **Cytoskeletal proteins in the phloem tissues and phloem sap of higher plants.** Cell Biol. Int. 27: 223–224.

Laemmli, U.K. (1970) **Cleavage of structural proteins during the assembly of the head of bacteriophage T4.** Nature 227: 680-685.

Lappartient, A.G., Vidmar, J.J., Leustek, T., Glass, A.D.M. and Touraine, B. (1999) **Inter-organ signaling in plants: regulation of ATP sulfurylase and sulfate transporter genes expression in roots mediated by phloem-translocated compound**. Plant J. 18: 89-95.

Li, J., Yang, Z., Bin Yu, J.L. and Chen, X. (2005) **Methylation protects miRNAs and siRNAs from a 3-end uridylation activity in *Arabidopsis*.** Curr. Biol. 15: 1501–1507.

Lin, M-K., Lee, Y-J., Lough, T.J., Phinney, B.S. Lucas, W.J. (2008) **Analysis of the pumpkin phloem proteome provides functional insights into angiosperm sieve tube function.** Mol. Cell Proteomics. Published online: 20 Oct 2008. M800420-MCP200 PMID: 18936055

Lin, M-K., Belanger, H., Lee, Y-J., Varkonyi-Gasic, E., Taoka, K-I., Miura, E., Xoconostle-Cázares, B., Gendler, K., Jorgensen, R. A., Phinney, B., Lough, T.J. and Lucas, W.J. (2007) **FLOWERING LOCUS T protein may act as the long-distance florigenic signal in the Cucurbits.** Plant Cell 19: 1488-1506.

Lincoln, C., Britton, J.H. and Estelle, M. (1990) **Growth and development of the *axr1* mutants of *Arabidopsis*.** Plant Cell 2: 1071-1080.

Lough, T.J. and Lucas, W.J. (2006) **Integrative plant biology: role of phloem long-distance macromolecular trafficking.** Annu. Rev. Plant Biol. 57: 203–232.

Lucas, W.J., Yoo, B.-C. and Kragler, F. (2001) **RNA as a long-distance information macromolecule in plants.** Nat. Rev. Mol. Cell Biol. 2: 849–857.

Lucas, W.J., Bouché-Pillon, S., Jackson, D.P., Nguyen, L., Baker, L., Ding, B. and Hake, S. (1995) **Selective trafficking of KNOTTED1 homeodomain protein and its mRNA through plasmodesmata.** Science 270: 1980-1983.

Ludevid, M.D., Freire, M.A., Gómez, J., Burd, C.G., Albericio, F., Giralt, E., Dreyfuss, G. and Pagès, M. (1992) **RNA binding characteristics of a 16 kDa glycine-rich protein from maize.** Plant J. 2: 999-1003.

Ma, Q., Longnecker, N. and Atkins, C. (2002) **Varying phosphorus supply and development, growth and seed yield in narrow-leafed lupin.** Plant Soil 239: 79-85.

Mallory, A.C., Elmayan, T. and Vaucheret, H. (2008) **MicroRNA maturation and action—the expanding roles of ARGONAUTEs.** Curr. Opin. Plant Biol. 11: 560-566.

Mallory, A.C. and Vaucheret, H. (2004) **MicroRNAs: something important between the genes**. Curr. Opin. Plant Biol. 7: 120-125.

Marentes, E. and Grusak, M.A. (1998) **Mass determination of low-molecular-weight proteins in phloem sap using matrix-assisted laser desorption/ionization time-of-flight mass spectrometry**. J. Exp. Bot. 49: 903-911.

Nakamura, S.-I., Hayashi, H., Mori, S. and Chino, M. (1995) **Detection and characterization of protein kinases in rice phloem sap.** Plant Cell Physiol. 36: 19-27

Nakamura, S.-I., Hayashi, H., Mori, S. and Chino, M. (1993) **Protein Phosphorylation in the Sieve Tubes of Rice Plants.** Plant Cell Physiol. 34: 927-933.

Nelson, T., Gandotra, N. and Tausta, S.L. (2008) **Plant cell types: reporting and sampling with new technologies.** Curr. Opin. Plant Biol. 11: 567-573.

Nolte, K.D. and Koch, K.E. (1993) **Companion-cell specific localization of sucrose synthase in zones of phloem loading and unloading.** Plant Physiol. 101: 899-905.

Nomata, T., Kabeya, Y. and Sato, N. (2004) **Cloning and characterization of glycine-rich RNA-binding protein cDNAs in the moss *Physcomitrella patens.*** Plant Cell Physiol. 45: 48–56.

Omid, A., Keilin, T., Glass, A., Leshkowitz, D. and Wolf, S. (2007) **Characterization of phloem-sap transcription profile in melon plants**. J. Exp. Bot. DOI:10.1093/jxb/erm214.

Oparka, K.J. and Santa Cruz, S. (2000) **The great escape: phloem transport and unloading of macromolecules.** Annu. Rev. Plant Physiol. Plant Mol. Biol. 51: 323–347.

Palevitz, B.A. and Newcomb, E.H. (1971) **The ultrastructure and development of tubular and crystalline P protein in the sieve elements of certain papilionaceous legumes**. Protoplasma 72: 399–426.

Pant, B.D., Buhtz, A., Kehr, J. and Scheible, W. (2008) **MicroRNA399 is a long-distance signal for the regulation of plant phosphate homeostasis.** Plant J. 53: 731-738.

Park, W., Li, J., Song, R., Messing, J. and Chen, X. (2002) **CARPEL FACTORY, a Dicer homolog, and HEN1, a novel protein, act in microRNA metabolism in Arabidopsis thaliana.** Curr. Biol. 12: 1484-95.

Pate, J.S., Peoples, M.B., van Bel, A.J.E., Kuo, J. and Atkins, C.A. (1985) **Diurnal water balance of the cowpea fruit.** Plant Physiol. 77: 148-156.

Pate, J.S., Peoples, M.B. and Atkins, C.A. (1984) **Spontaneous phloem bleeding from cryopunctured fruits of a ureide-producing legume.** Plant Physiol. 74: 499–505.

Pate, J.S., Atkins, C.A., Hamel, K., McNeil, D.L. and Layzell, D.B. (1979) **Transport of organic solutes in phloem and xylem of a nodulated legume.** Plant Physiol. 63: 1082–1088.

Pate, J.S., Kuo, J. and Hocking, P.J. (1978) **Functioning of conducting elements of phloem and xylem in the stalk of the developing fruit of *Lupinus albus* L.** Aust. J. Plant Physiol. 5: 321-336.

Pate, J.S., Sharkey, P.J. and Lewis, O.A.M. (1974) **Phloem bleeding from legume fruits—a technique for study of fruit nutrition.** Planta 120: 229–243.

Pate, J.S. (1965) **Roots as organs of assimilation of sulfate**. Science 149: 547-548.

Peel, A.J. (1975) **Investigations with aphid stylets into the physiology of the sieve tube.** In: Zimmermann, M.H. and Milburn, J.A. (Eds.), Encylopedia of Plant Physiology, vol 1: Transport in Plants. I. Phloem Transport. Springer, Berlin, pp. 171–195.

Peragine, A., Yoshikawa, M., Wu, G., Albrecht, H.L. and Poethig, R.S. (2004) ***SGS3*** **and *SGS2/SDE1/RDR6* are required for juvenile development and the production of trans-acting siRNAs in *Arabidopsis*.** Genes Dev. 18: 2368–2379.

Peterson, G. L. (1983) **Determination of total protein.** Methods Enzymol. 91: 95-119.

Plaxton, W.C. (1996). **The organization and regulation of plant glycolysis.** Annu. Rev. Plant Physiol. Plant Mol. Biol. 47: 185–214.

Pommerrenig, B., Barth, I., Niedermeier, M., Kopp, S., Schmid, J., Dwyer, R.A., McNair, R.J., Klebl, F. and Sauer, N. (2006) **Common plantain. A collection of expressed sequence tags from vascular tissue and simple and efficient transformation method.** Plant Physiol. 142: 1427–1441.

Rabilloud, T. and Charmont, S. (2000) **Detection of proteins on two-dimensional electrophoresis gels.** In: Rabilloud, T. (Ed.), Proteome Research: two-dimensional gel electrophoresis and identification methods. Springer-Verlag, Germany, pp. 107-126.

Raven, J.A. (1991) **Long-term functioning of enucleate sieve elements: possible mechanisms of damage avoidance and damage repair.** Plant Cell Environ. 14: 139-146.

Read, S.M. and Northcote, D.H. (1983) **Chemical and immunological similarities between the phloem proteins of three genera of the Cucurbitaceae.** Planta. 158: 119-127.

Regalado, A.P. and Ricardo, C.P.P. (1996) **Study of the intercellular fluid of healthy *Lupinus albus* organs. Presence of a chitinase and a thaumatin-like Protein**. Plant Physiol. 110: 227-232.

Reinhart, B.J., Weinstein, E.G., Rhoades, M.W. Bartel, B. and Bartel, D.P. (2002) **MicroRNAs in plants.** Genes Dev. 16: 1616-1626.

Rhoades, M.W., Reinhart, B.J., Lim, L.P., Burge, C.B., Bartel B. and Bartel, D.P. (2002) **Prediction of plant microRNA targets.** Cell 110: 513-520.

Ruiz-Medrano, R., Moya, J.H., Xoconostle-Cázares, B. and Lucas, W.J. (2007) **Influence of cucumber mosaic virus infection on the mRNA population present in the phloem translocation stream of pumpkin plants.** Funct. Plant Biol. 34: 292–301.

Ruiz-Medrano, R., Xoconostle-Cazares, B. and Lucas, W.J. (2001). **The phloem as a conduit for inter-organ communication.** Curr. Opin. Plant Biol. 4: 202-209.

Ruiz-Medrano, R., Xoconostle-Cázares, B. and Lucas, W.J. (1999) **Phloem long-distance transport of *CmNACP* mRNA: implications for supracellular regulation in plants.** Development 126: 4405-4419.

Sasaki, T., Chino, M., Hayashi, H. and Fujiwara, T. (1998) **Detection of several mRNA species in rice phloem sap.** Plant Cell Physiol. 39: 895-897.

Schobert, C., Gottschalk, M., Kovar, D.R., Staiger, C.J., Yoo, B.C. and Lucas, W.J. (2000) **Characterization of *Ricinus communis* phloem profilin, RcPRO1**. Plant Mol. Biol. 42: 719-730.

Schobert, C., Baker, L., Szederkényi, J., Großmann, P., Komor, E., Hayashi, H., Chino, M. and Lucas, W.J. (1998) **Identification of immunologically related proteins in sieve-tube exudate collected from monocotyledonous and dicotyledonous plants**. Planta 206: 245-252.

Schobert, C., Großmann, P., Gottschalk, M., Komor, E., Pecsvaradi, A. and Nieden, U.Z. (1995) **Sieve-tube exudate from *Ricinus communis* L. seedlings contains ubiquitin and chaperones.** Planta 196: 205-210.

Sjölund, R.D. (1997) **The phloem sieve element: a river runs through It.** Plant Cell 9: 1137-1146.

Spurr, A.R. (1969) **A low-viscosity epoxy resin embedding medium for electron microscopy.** J. Ultrastruct. Res. 26: 31-43.

Staiger, C.J., Gibbon, B.C., Kovar, D.R. and Zonia, L.E. (1997) **Profilin and actin-depolymerizing factor: modulators of actin organization in plants.** Trends Plant Sci. 2: 275-281.

Standing, K.G. (2003) **Peptide and protein *de novo* sequencing by mass spectrometry.** Curr. Opin. Struct. Biol. 13: 595-601.

Streitner, C., Danisman, S., Wehrle, L., Schöning, J.C., Alfano, J.R. and Staiger, D. (2008) **The small glycine-rich RNA binding protein *At*GRP7 promotes floral transition in *Arabidopsis thaliana*.** Plant J. 56: 239-250.

Sunkar, R. and Zhu, J.K. (2004) **Novel and stress-regulated microRNAs and other small RNAs from Arabidopsis.** Plant Cell 16: 2001-2019.

Sweetingham, M.W., Jones, R.A.C. and Brown, A.G.P. (1998) **Disease and pests.** In: Gladstones, J.S., Atkins, C. and Hamblin, J. (Eds.), Lupins as crop plants: biology, production and utilization. CABI Cambridge, UK, pp. 263-290.

Tamaki, S., Matsuo, S., Wong, H.L., Yokoi, S. and Shimamoto, K. (2007) **Hd3a protein is a mobile flowering signal in rice.** Science 316: 1033-1036.

Taoka, K., Ham, B-K., Xoconostle-Cázares, B., Rojas, M.R. and Lucas, W.J. (2007) **Reciprocal phosphorylation and glycosylation recognition motifs control NCAPP1 interaction with pumpkin phloem proteins and their cell-to-cell movement.** Plant Cell 19: 1866–1884.

Turnbull, C.G., Booker, J.P. and Leyser, H.M. (2002) **Micrografting techniques for testing long-distance signalling in Arabidopsis.** Plant J. 32: 255-262.

Valdés, O.L., Arenas, C.H., Ramírez, M., Girard, L., Sánchez, F., Vance, C.P., Reyes, J.L. and Hernández, G. (2008) **Essential role of MYB transcription factor: PvPHR1 and microRNA: PvmiR399 in phosphorus-deficiency signalling in common bean roots.** Plant Cell Env. 31: 1834-1843.

van Bel, A.J.E. and Gaupels, F. (2004) **Pathogen-induced resistance and alarm signals in the phloem.** Mol. Plant Pathol. 5: 495–504.

van Bel, A.J.E. (2003) **The phloem, a miracle of ingenuity.** Plant Cell Environ. 26: 125-149.

van Bel, A.J.E., Ehlers, K. and Knoblauch, M. (2002) **Sieve elements caught in the act.** Trends Plant Sci. 7: 126–132.

van Bel, A.J.E. and Knoblauch, M. (2000) **Sieve element and companion cell: the story of the comatose patient and the hyperactive nurse.** Aust. J. Plant Physiol. 27: 477–487.

van Bel, A.J.E. and van Rijen, H.V.M. (1994) **Microelectrode-recorded development of the symplasmic autonomy of the sieve element/companion cell complex in the stem phloem of *Lupinus luteus* L.** Planta 192: 165-175.

Varkonyi-Gasic, E., Wu, R., Wood, M., Walton, E.F. and Hellens, R.P. (2007) **Protocol: a highly sensitive RT-PCR method for detection and quantification of microRNAs.** Plant Methods. DOI:10.1186/1746-4811-3-12.

Vaucheret, H., Vazquez, F., Crété, P. and Bartel, D.P. (2004) **The action of ARGONAUTE1 in the miRNA pathway and its regulation by the miRNA pathway are crucial for plant development.** Genes Dev. 18: 1187-1197.

Vazquez, F., Gasciolli V., Crété, P. and Vaucheret, H. (2004) **The nuclear dsRNA binding protein HYL1 is required for microRNA accumulation and plant development, but not posttranscriptional transgene silencing**. Curr. Biol. 14: 346-351.

Vilaine, F., Palauqui, J.-C., Amselem, J., Kusiak, C., Lemoine, R. and Dinant, S. (2003) **Towards deciphering phloem: a transcriptome analysis of the phloem of *Apium graveolens*.** Plant J. 36: 67–81.

Walz, C., Juenger, M., Schad, M. and Kehr, J. (2002) **Evidence for the presence and activity of a complete antioxidant defence system in mature sieve tubes.** Plant J. 31: 189–97.

Walz, C., Giavalisco, P., Schad, M., Juenger, M., Klose, J. and Kehr, J. (2004) **Proteomics of curcurbit phloem exudate reveals a network of defence proteins**. Phytochemistry 65: 1795–1804.

Will, T. and van Bel, A.J.E. (2006) **Physical and chemical interactions between aphids and plants.** J. Exp. Bot. 57: 729–737.

Xoconostle-Cázares, B., Xiang, Y., Ruiz-Medrano, R., Wang, H.L., Monzer, J., Yoo, B.C., McFarland, K.C., Franceschi, V.R. and Lucas, W.J. (1999) **Plant paralog to viral movement protein that potentiates transport of mRNA into the phloem**. Science 283: 94-98.

Yamasaki, H., Abdel-Ghany, S.E., Cohu, C.M., Kobayashi, Y., Shikanai, T. and Pilon, M. (2007) **Regulation of copper homeostasis by microRNA in *Arabidopsis*.** J. Biol.Chem. 282: 16369-16378.

Yoo, B.C., Kragler, F., Varkonyi-Gasic, E., Haywood, V., Archer-Evans, S., Lee, Y.M., Lough, T.J. and Lucas, W.J. (2004) **A systemic small RNA signaling system in plants.** Plant Cell. 16: 1979-2000.

Yu, B., Bi, L., Zheng, B., Ji, L., Chevalier, D., Agarwal, M., Ramachandran, V., Li, W., Lagrange, T., Walker, J.C. and Chen, X. (2008) **The FHA domain proteins DAWDLE in *Arabidopsis* and SNIP1 in humans act in small RNA biogenesis.** Proc. Natl. Acad. Sci. USA 105: 10073–10078.

Yu, B., Yang, Z., Li, J., Minakhina, S., Yang, M., Padgett, R.W., Steward, R. and Chen, X. (2005) **Methylation as a crucial step in plant microRNA biogenesis.** Science 307: 932-935.

Zchut, S., Weiss, M. and Pick, U. (2003) **Temperature-regulated expression of a glycine-rich RNA-binding protein in the halotolerant alga *Dunaliella salina.*** J. Plant Physiol. 160: 1375-1384.

Zhang, C., Barthelson, R.A., Lambert, G.M. and Galbraith, D.W. (2008) **Global characterization of cell-specific gene expression through fluorescence-activated sorting of nuclei.** Plant Physiol. 147: 30–40.

Ziegler, H. (1975) **Nature of transported substances**. In: Pirson, A. and Zimmerman, M.H. (Eds.), Encyclopedia of Plant Physiology, New Series, vol 1. Springer-Verlag Berlin, Heidelberg and New York, pp. 59-100.

Zilberman, D., Cao, X. and Jacobsen, S.E. (2003) **ARGONAUTE4 control of locus-specific siRNA accumulation and DNA and histone methylation.** Science 299: 716–719.

Zimmermann, M.H. and Ziegler, H. (1975) **List of sugars and sugar alcohols in sieve-tube exudates.** In Zimmermann, M.H. Milburn, J.A. eds, Encyclopedia of Plant Physiology, vol.1: Transport in Plants. I. Phloem Transport. Springer Verlag, Berlin, pp. 480–503.

Appendix 1

Unidentified peptides in *L. albus* phloem exudate

Spot No.	Observed Protein Mw (kDa)	Partial aminoacid sequences
6	15	HVDYCNCTGDGVR Q/KNL/IL/IPCVL/IPRR YNVM/FL/IWNR
8	11	L/IQ/KGHEEGAL/IVL/IGEA L/ITL/IGDAL/IHVGM/FM/FR L/ITL/IGQ/KHCL/IVAL/IHCVTASR LQ/KGVVM/FPSTR EDEQ/KHWL/ICL/IDL/IR
9	11	L/IQ/KGVVM/FPSTR L/IGDAL/IHVTHL/IR EYGGEAHEGEL/IG L/IQ/KGHEEGVL/IAL/IGEA
10	10.5	L/IQ/KGHEEGQ/KL/IHRHL/IR L/IPTNVL/ICSTR L/IGDAL/IHVTHL/IR YEGEGHAGL/IM/FGDSR
11	10.5	AHWTPTGHQ/KL/IQ/KM/F L/IGL/IGEQ/KTNDR
13	15.5	Q/KRQ/KADYMSQ/KPL/IR NCMVL/IYPL/IR Q/KAWMM/FVYTDER RHCHM/FGCDER NVWTVPPAQ/KNNL/IVR
16	24	Unfavourable spectra
17	4.5	EL/IRL/INDWTL/IR
18	4	Unfavourable spectra
19	4.5	Unfavourable spectra
23	8	SGEEQ/KNEDNPR
25	8	Unfavourable spectra
30	14	TYVSSGPYM/FESM/FL/INRAR SESSACPSEL/IL/IEDL/IAR Q/KTGDL/IVM/FCTGGR

Unidentified peptides in *L. albus* phloem exudate

Spot No.	Observed Protein Mw (kDa)	Partial aminoacid sequences
49	10	L/IAL/IGGWAL/IHNL/IL/IR NMESNNNDL/ITHAVYM/FQ/KM/FQ/KR NANNEGANHNL/IL/IR ANMHL/ICAL/ISCR
50	9.5	YDRPDM/FER L/IQ/KL/IPSSHQ/KM/FNCM/FQ/KHR Q/KYDGENPM/FRTGSTTR
52	10.5	THDQ/KGGYATGGSSM/FL/INRAR MCSGGESVHAL/IGWYGR
54	7	NSSNSSDYYEQ/KVPEYNNR CAVVSSAEEEL/IERVAR DQ/KCGEEEL/IERVAR CAVCNEEQ/KTAARVAR
58	23	ACAL/IM/FSHVVQ/KL/IL/IYL/IAR GNYNL/IGEVGL/ISQ/K LVLNPKGFALNCSYMTR
67	14.5	L/IHHTAVSVNRVVSGM/FL/IRM/FR
69	16.5	VQ/KSL/IYSQ/KECSSQ/KL/I L/IQ/KNNVPTQ/KNSVGR CNSSQ/KPL/IHL/IRM/FGR
78	24.5	Unfavourable spectra
79	25	Unfavourable spectra
87	18	ESSPQ/KGCQ/KGCAR NHGNAGCGRWL/IRPNTRL/IGR NHGL/IAYSGAHQ/KR
88	18.5	HAPL/IGL/IGL/IL/ISL/IL/IAHR ESVSMNQ/KHSGAGNPEVAR
89	42	ACAM/FNVNM/FDQ/KM/FDR ECCGEGVEDGNR WQ/KEYMAEVYR
90	4.4	M/FNEVVL/INDR DQ/KCCTCVGMDEGGCGR
91	15.5	Q/KGM/FEDAM/FVYR L/ICEAVVSPEL/IGTR L/IYAAGGAAYDQ/KL/IETSGR Q/KGTVNHGHSGSGR

Unidentified peptides in *L. albus* phloem exudate

Spot No.	Observed Protein Mw (kDa)	Partial aminoacid sequences
92	15.5	WHL/IM/FEGESAR GYGMTGDQ/KL/IE L/IYL/IAL/IVSPEL/IGTR
93	15.5	EMDGCL/IL/IAHD MMGL/INASNANNVM/FNR Q/KSMHSNNVTQ/KHHMDM/FDR
98	9.5	M/FQ/KAEM/FPL/IHPR MM/FTCSNYVHNGR
99	23	HM/FMGDTWGYCR L/IMVVM/FDGTL/IQ/KRR
104	7.3	VRQ/KPNL/INSDGVT RESDYASNAASTANL/IAGR VL/IL/IVHSGDCVGL/I RDNNYCVVGL/IR
105	9.5	AHRHVEM/FSSGTM/FVQ/KR L/IDVPQ/KDSM/FVDHVR
110	4.5	Q/KL/IGEM/FTAYTR
111	16.7	Unfavourable spectra
113	16.7	Unfavourable spectra
116	12	CCYM/FASDL/IM/FVER HRGL/INCEEL/INYVR
118	6.5	HGSGSPMYSCATSR SSNGSGEEEEL/IEL/IGRR YQ/KL/IEERNTL/IGRR
119	6.3	HGMVPYNNGAHSR THNYAEHGHTL/IL/IRASSCNR
125	15.3	Unfavourable spectra
130	15.5	HL/ITL/IM/FSL/IL/IGR

Appendix 2

L. albus phloem exudate cDNA library clones with unknown function

Accession number	Similarity	Score (bits)	E-value
CAO44871.1	unnamed protein product [Vitis vinifera]	533	1.00E-150
CAO18187.1	unnamed protein product [Vitis vinifera]	528	1.00E-148
CAO66720.1	unnamed protein product [Vitis vinifera]	514	1.00E-144
CAO65935.1	unnamed protein product [Vitis vinifera]	503	1.00E-141
CAA10289.1	hypothetical protein [Cicer arietinum]	491	1.00E-137
CAO39286.1	unnamed protein product [Vitis vinifera]	471	1.00E-131
CAO44803.1	unnamed protein product [Vitis vinifera]	469	1.00E-130
CAO65211.1	unnamed protein product [Vitis vinifera]	458	1.00E-127
BAA88228.1	thiamin biosynthetic enzyme [Glycine max]	457	1.00E-127
CAO49304.1	unnamed protein product [Vitis vinifera]	451	1.00E-125
CAN63254.1	hypothetical protein [Vitis vinifera]	451	1.00E-125
CAO70618.1	unnamed protein product [Vitis vinifera]	425	1.00E-123
CAO21857.1	unnamed protein product [Vitis vinifera]	438	1.00E-121
CAO43786.1	unnamed protein product [Vitis vinifera]	437	1.00E-121
CAO40038.1	unnamed protein product [Vitis vinifera]	422	1.00E-116
CAO15636.1	unnamed protein product [Vitis vinifera]	409	1.00E-113
CAO43989.1	unnamed protein product [Vitis vinifera]	393	1.00E-108
CAO60892.1	unnamed protein product [Vitis vinifera]	387	1.00E-106
ABK96599.1	unknown [Populus trichocarpa x Populus deltoides]	386	1.00E-105
CAO65376.1	unnamed protein product [Vitis vinifera]	382	1.00E-104
CAN64994.1	hypothetical protein [Vitis vinifera]	381	1.00E-104
CAO15192.1	unnamed protein product [Vitis vinifera]	376	1.00E-103
CAO48194.1	unnamed protein product [Vitis vinifera]	373	1.00E-102
CAO61388.1	unnamed protein product [Vitis vinifera]	370	1.00E-101
ABD32814.1	hypothetical protein [Medicago truncatula]	366	1.00E-100
CAO23556.1	unnamed protein product [Vitis vinifera]	369	1.00E-100
ABK95228.1	unknown [Populus trichocarpa]	365	1.00E-99
CAO15903.1	unnamed protein product [Vitis vinifera]	355	2.00E-96
CAO45373.1	unnamed protein product [Vitis vinifera]	353	5.00E-96
CAO43035.1	unnamed protein product [Vitis vinifera]	351	3.00E-95
CAO71749.1	unnamed protein product [Vitis vinifera]	350	7.00E-95
CAO61488.1	unnamed protein product [Vitis vinifera]	298	9.00E-95
ABK96295.1	unknown [Populus trichocarpa x Populus deltoides]	343	8.00E-93
CAO71287.1	unnamed protein product [Vitis vinifera]	343	8.00E-93
CAO14950.1	unnamed protein product [Vitis vinifera]	342	1.00E-92
ABK93552.1	unknown [Populus trichocarpa]	339	1.00E-91
CAO66650.1	unnamed protein product [Vitis vinifera]	336	1.00E-90
CAO42343.1	unnamed protein product [Vitis vinifera]	334	4.00E-90
CAO41275.1	unnamed protein product [Vitis vinifera]	334	5.00E-90
ABK96203.1	unknown [Populus trichocarpa]	331	3.00E-89
CAO66272.1	unnamed protein product [Vitis vinifera]	329	1.00E-88
CAO64218.1	unnamed protein product [Vitis vinifera]	256	2.00E-88
CAO48327.1	unnamed protein product [Vitis vinifera]	326	1.00E-87
ABK96305.1	unknown [Populus trichocarpa x Populus deltoides]	324	3.00E-87

Accession number	Similarity	Score (bits)	E-value
ABK95775.1	unknown [Populus trichocarpa]	324	4.00E-87
CAN60740.1	hypothetical protein [Vitis vinifera]	323	6.00E-87
CAO18297.1	unnamed protein product [Vitis vinifera]	323	6.00E-87
CAO44273.1	unnamed protein product [Vitis vinifera]	321	4.00E-86
CAN80762.1	hypothetical protein [Vitis vinifera]	319	1.00E-85
CAO24389.1	unnamed protein product [Vitis vinifera]	318	2.00E-85
CAN75443.1	hypothetical protein [Vitis vinifera]	317	5.00E-85
CAO42285.1	unnamed protein product [Vitis vinifera]	315	3.00E-84
CAO22996.1	unnamed protein product [Vitis vinifera]	308	3.00E-82
BAF01964.1	hypothetical protein [Arabidopsis thaliana]	274	4.00E-82
CAO21314.1	unnamed protein product [Vitis vinifera]	305	2.00E-81
CAO40176.1	unnamed protein product [Vitis vinifera]	298	3.00E-79
CAO39385.1	unnamed protein product [Vitis vinifera]	297	4.00E-79
CAO67339.1	unnamed protein product [Vitis vinifera]	297	5.00E-79
CAO44301.1	unnamed protein product [Vitis vinifera]	297	5.00E-79
BAF75825.1	hypothetical protein [Malus x domestica]	297	5.00E-79
CAN64894.1	hypothetical protein [Vitis vinifera]	296	1.00E-78
CAO24542.1	unnamed protein product [Vitis vinifera]	294	4.00E-78
CAO66868.1	unnamed protein product [Vitis vinifera]	293	8.00E-78
CAO22937.1	unnamed protein product [Vitis vinifera]	292	2.00E-77
ABK94929.1	unknown [Populus trichocarpa]	288	2.00E-76
ABK92884.1	unknown [Populus trichocarpa]	288	2.00E-76
CAO40339.1	unnamed protein product [Vitis vinifera]	288	3.00E-76
CAO47376.1	unnamed protein product [Vitis vinifera]	287	4.00E-76
CAN72172.1	hypothetical protein [Vitis vinifera]	287	7.00E-76
CAO61102.1	unnamed protein product [Vitis vinifera]	286	8.00E-76
CAO62087.1	unnamed protein product [Vitis vinifera]	285	2.00E-75
CAO65647.1	unnamed protein product [Vitis vinifera]	285	2.00E-75
CAN64937.1	hypothetical protein [Vitis vinifera]	283	7.00E-75
CAO68379.1	unnamed protein product [Vitis vinifera]	280	9.00E-74
CAB51659.1	putative protein [Arabidopsis thaliana]	277	4.00E-73
ABK94241.1	unknown [Populus trichocarpa]	276	8.00E-73
CAO18146.1	unnamed protein product [Vitis vinifera]	275	1.00E-72
CAO16914.1	unnamed protein product [Vitis vinifera]	274	4.00E-72
CAO39662.1	unnamed protein product [Vitis vinifera]	274	5.00E-72
ABN05794.1	hypothetical protein [Medicago truncatula]	274	6.00E-72
CAO68979.1	unnamed protein product [Vitis vinifera]	273	8.00E-72
CAO21699.1	unnamed protein product [Vitis vinifera]	273	1.00E-71
ABK93406.1	unknown [Populus trichocarpa]	270	6.00E-71
AAM63369.1	unknown [Arabidopsis thaliana]	270	6.00E-71
CAN79693.1	hypothetical protein [Vitis vinifera]	268	2.00E-70
CAO66747.1	unnamed protein product [Vitis vinifera]	267	4.00E-70
CAO44335.1	unnamed protein product [Vitis vinifera]	257	5.00E-67
CAO16621.1	unnamed protein product [Vitis vinifera]	257	7.00E-67
CAO23276.1	unnamed protein product [Vitis vinifera]	256	9.00E-67
CAO63407.1	unnamed protein product [Vitis vinifera]	256	1.00E-66
CAO23149.1	unnamed protein product [Vitis vinifera]	256	1.00E-66
CAO40354.1	unnamed protein product [Vitis vinifera]	255	2.00E-66
CAO63610.1	unnamed protein product [Vitis vinifera]	256	2.00E-66
CAN80823.1	hypothetical protein [Vitis vinifera]	249	8.00E-65
CAO69187.1	unnamed protein product [Vitis vinifera]	247	6.00E-64
ABK95200.1	unknown [Populus trichocarpa]	247	7.00E-64

Accession number	Similarity	Score (bits)	E-value
CAO14701.1	unnamed protein product [Vitis vinifera]	242	2.00E-62
CAO41446.1	unnamed protein product [Vitis vinifera]	242	2.00E-62
CAO22537.1	unnamed protein product [Vitis vinifera]	239	1.00E-61
CAO44173.1	unnamed protein product [Vitis vinifera]	239	2.00E-61
CAB95830.1	hypothetical protein [Cicer arietinum]	238	3.00E-61
ABK95057.1	unknown [Populus trichocarpa]	235	3.00E-60
ABK94930.1	unknown [Populus trichocarpa]	233	5.00E-60
ABK95546.1	unknown [Populus trichocarpa]	233	9.00E-60
CAO66902.1	unnamed protein product [Vitis vinifera]	233	1.00E-59
CAO65442.1	unnamed protein product [Vitis vinifera]	231	2.00E-59
CAO14711.1	unnamed protein product [Vitis vinifera]	229	1.00E-58
CAA18194.1	putative protein [Arabidopsis thaliana]	228	4.00E-58
ABK92614.1	unknown [Populus trichocarpa]	226	7.00E-58
CAO43759.1	unnamed protein product [Vitis vinifera]	225	2.00E-57
CAO71132.1	unnamed protein product [Vitis vinifera]	222	1.00E-56
CAO40896.1	unnamed protein product [Vitis vinifera]	221	3.00E-56
ABK93477.1	unknown [Populus trichocarpa]	220	5.00E-56
CAB37492.1	putative protein [Arabidopsis thaliana]	218	4.00E-55
CAO17698.1	unnamed protein product [Vitis vinifera]	217	6.00E-55
ABK94675.1	unknown [Populus trichocarpa]	216	1.00E-54
NP_190603.1	unknown protein [Arabidopsis thaliana]	215	2.00E-54
CAN62024.1	hypothetical protein [Vitis vinifera]	214	6.00E-54
CAO15843.1	unnamed protein product [Vitis vinifera]	212	2.00E-53
CAO49409.1	unnamed protein product [Vitis vinifera]	210	7.00E-53
CAN81044.1	hypothetical protein [Vitis vinifera]	209	7.00E-53
CAN65779.1	hypothetical protein [Vitis vinifera]	207	3.00E-52
CAN61153.1	hypothetical protein [Vitis vinifera]	208	3.00E-52
CAO64505.1	unnamed protein product [Vitis vinifera]	207	6.00E-52
CAO21400.1	unnamed protein product [Vitis vinifera]	207	6.00E-52
CAO68222.1	unnamed protein product [Vitis vinifera]	204	2.00E-51
CAI84658.1	hypothetical protein [Nicotiana tabacum]	205	2.00E-51
CAO45214.1	unnamed protein product [Vitis vinifera]	204	4.00E-51
CAO39210.1	unnamed protein product [Vitis vinifera]	203	1.00E-50
CAO16473.1	unnamed protein product [Vitis vinifera]	201	1.00E-50
CAN67814.1	hypothetical protein [Vitis vinifera]	202	2.00E-50
CAO70908.1	unnamed protein product [Vitis vinifera]	201	4.00E-50
CAN77019.1	hypothetical protein [Vitis vinifera]	158	5.00E-50
CAO61780.1	unnamed protein product [Vitis vinifera]	200	6.00E-50
ABK94537.1	unknown [Populus trichocarpa]	198	3.00E-49
ABK95430.1	unknown [Populus trichocarpa]	196	6.00E-49
ABK95743.1	unknown [Populus trichocarpa]	197	6.00E-49
CAO15686.1	unnamed protein product [Vitis vinifera]	196	8.00E-49
CAO70074.1	unnamed protein product [Vitis vinifera]	196	1.00E-48
CAN64895.1	hypothetical protein [Vitis vinifera]	194	3.00E-48
CAO61631.1	unnamed protein product [Vitis vinifera]	193	4.00E-48
CAO47802.1	unnamed protein product [Vitis vinifera]	194	4.00E-48
ABK94218.1	unknown [Populus trichocarpa]	187	6.00E-46
CAN65949.1	hypothetical protein [Vitis vinifera]	187	1.00E-45
CAO61623.1	unnamed protein product [Vitis vinifera]	184	3.00E-45
ABK93574.1	unknown [Populus trichocarpa]	185	4.00E-45
CAN71308.1	hypothetical protein [Vitis vinifera]	183	8.00E-45
ABK96152.1	unknown [Populus trichocarpa]	181	4.00E-44

Accession number	Similarity	Score (bits)	E-value
CAN63850.1	hypothetical protein [Vitis vinifera]	181	4.00E-44
CAO21917.1	unnamed protein product [Vitis vinifera]	181	5.00E-44
CAO67077.1	unnamed protein product [Vitis vinifera]	181	6.00E-44
CAN80873.1	hypothetical protein [Vitis vinifera]	179	1.00E-43
CAO44961.1	unnamed protein product [Vitis vinifera]	179	1.00E-43
ABK93457.1	unknown [Populus trichocarpa]	178	2.00E-43
CAO38954.1	unnamed protein product [Vitis vinifera]	176	9.00E-43
ABK94521.1	unknown [Populus trichocarpa]	175	2.00E-42
CAO45481.1	unnamed protein product [Vitis vinifera]	174	3.00E-42
ABK93219.1	unknown [Populus trichocarpa]	170	5.00E-41
CAN64864.1	hypothetical protein [Vitis vinifera]	123	3.00E-40
CAO16953.1	unnamed protein product [Vitis vinifera]	167	4.00E-40
CAO43985.1	unnamed protein product [Vitis vinifera]	166	5.00E-40
ABK93697.1	unknown [Populus trichocarpa]	167	6.00E-40
CAO45573.1	unnamed protein product [Vitis vinifera]	149	9.00E-39
ABK94884.1	unknown [Populus trichocarpa]	161	4.00E-38
ABK22743.1	unknown [Picea sitchensis]	160	1.00E-37
CAN66505.1	hypothetical protein [Vitis vinifera]	159	1.00E-37
ABK94836.1	unknown [Populus trichocarpa]	158	3.00E-37
YP_588403.1	hypothetical protein [Zea mays subsp. mays]	151	3.00E-37
CAO41469.1	unnamed protein product [Vitis vinifera]	157	4.00E-37
ABD28368.1	hypothetical protein [Medicago truncatula]	156	7.00E-37
CAO71550.1	unnamed protein product [Vitis vinifera]	156	1.00E-36
CAO45477.1	unnamed protein product [Vitis vinifera]	154	2.00E-36
CAO44286.1	unnamed protein product [Vitis vinifera]	155	2.00E-36
CAO15629.1	unnamed protein product [Vitis vinifera]	99.4	2.00E-36
CAO48579.1	unnamed protein product [Vitis vinifera]	152	1.00E-35
CAB96688.1	putative protein [Arabidopsis thaliana]	152	2.00E-35
CAO15090.1	unnamed protein product [Vitis vinifera]	152	2.00E-35
CAO42363.1	unnamed protein product [Vitis vinifera]	152	2.00E-35
ABK93674.1	unknown [Populus trichocarpa]	151	3.00E-35
ABK94193.1	unknown [Populus trichocarpa]	151	3.00E-35
CAN61119.1	hypothetical protein [Vitis vinifera]	130	3.00E-35
CAO68283.1	unnamed protein product [Vitis vinifera]	151	4.00E-35
CAN74819.1	hypothetical protein [Vitis vinifera]	151	5.00E-35
CAO15842.1	unnamed protein product [Vitis vinifera]	145	2.00E-33
CAN62217.1	hypothetical protein [Vitis vinifera]	144	2.00E-33
ABK96304.1	unknown [Populus trichocarpa x Populus deltoides]	138	1.00E-31
CAO23602.1	unnamed protein product [Vitis vinifera]	138	4.00E-31
ABK94210.1	unknown [Populus trichocarpa]	135	2.00E-30
CAO16712.1	unnamed protein product [Vitis vinifera]	135	3.00E-30
CAO42932.1	unnamed protein product [Vitis vinifera]	134	4.00E-30
CAO69966.1	unnamed protein product [Vitis vinifera]	134	5.00E-30
CAO64960.1	unnamed protein product [Vitis vinifera]	132	6.00E-30
ABK92973.1	unknown [Populus trichocarpa]	131	2.00E-29
CAN79760.1	hypothetical protein [Vitis vinifera]	131	6.00E-29
CAO17337.1	unnamed protein product [Vitis vinifera]	130	1.00E-28
CAO67112.1	unnamed protein product [Vitis vinifera]	128	3.00E-28
ABK93131.1	unknown [Populus trichocarpa]	127	4.00E-28
CAN62511.1	hypothetical protein [Vitis vinifera]	124	7.00E-27

Accession number	Similarity	Score (bits)	E-value
CAO50031.1	unnamed protein product [Vitis vinifera]	124	8.00E-27
CAO66422.1	unnamed protein product [Vitis vinifera]	121	2.00E-26
CAO70557.1	unnamed protein product [Vitis vinifera]	120	8.00E-26
ABK92578.1	unknown [Populus trichocarpa]	118	1.00E-25
ABK94311.1	unknown [Populus trichocarpa]	117	2.00E-25
CAA10123.1	hypothetical protein [Cicer arietinum]	118	4.00E-25
ABK96690.1	unknown [Populus trichocarpa x Populus deltoides]	115	2.00E-24
CAO43566.1	unnamed protein product [Vitis vinifera]	115	4.00E-24
CAO24691.1	unnamed protein product [Vitis vinifera]	112	1.00E-23
CAO14801.1	unnamed protein product [Vitis vinifera]	107	2.00E-23
ABK96142.1	unknown [Populus trichocarpa]	112	2.00E-23
ABK93587.1	unknown [Populus trichocarpa]	110	4.00E-23
CAO70312.1	unnamed protein product [Vitis vinifera]	110	4.00E-23
CAB77598.1	putative protein [Arabidopsis thaliana]	108	2.00E-22
CAO67231.1	unnamed protein product [Vitis vinifera]	102	8.00E-21
CAO45301.1	unnamed protein product [Vitis vinifera]	102	9.00E-21
CAO68988.1	unnamed protein product [Vitis vinifera]	103	1.00E-20
CAO71442.1	unnamed protein product [Vitis vinifera]	102	3.00E-20
CAO43782.1	unnamed protein product [Vitis vinifera]	101	4.00E-20
NP_191358.1	unknown protein [Arabidopsis thaliana]	99.4	2.00E-19
ABK93164.1	unknown [Populus trichocarpa]	98.2	2.00E-19
CAN77855.1	hypothetical protein [Vitis vinifera]	98.6	4.00E-19
CAN82375.1	hypothetical protein [Vitis vinifera]	98.2	4.00E-19
CAN82126.1	hypothetical protein [Vitis vinifera]	95.1	1.00E-18
CAN70790.1	hypothetical protein [Vitis vinifera]	97.1	1.00E-18
AAM61659.1	unknown [Arabidopsis thaliana]	92	1.00E-17
CAO16187.1	unnamed protein product [Vitis vinifera]	90.9	2.00E-17
CAO42580.1	unnamed protein product [Vitis vinifera]	90.9	8.00E-17
ABK95674.1	unknown [Populus trichocarpa]	88.2	2.00E-16
CAO71849.1	unnamed protein product [Vitis vinifera]	89.7	2.00E-16
ABK93149.1	unknown [Populus trichocarpa]	88.2	3.00E-16
CAO14772.1	unnamed protein product [Vitis vinifera]	88.6	4.00E-16
CAO40090.1	unnamed protein product [Vitis vinifera]	88.2	6.00E-16
ZP_00874766.1	hypothetical protein [Streptococcus suis 89/1591]	67.8	3.00E-15
CAO38914.1	unnamed protein product [Vitis vinifera]	82	1.00E-14
CAO65372.1	unnamed protein product [Vitis vinifera]	80.9	3.00E-14
CAO47252.1	unnamed protein product [Vitis vinifera]	79.3	9.00E-14
CAO67977.1	unnamed protein product [Vitis vinifera]	78.2	3.00E-13
ABK23797.1	unknown [Picea sitchensis]	74.3	4.00E-12
CAO40846.1	unnamed protein product [Vitis vinifera]	59.7	8.00E-12
ABK93285.1	unknown [Populus trichocarpa]	72	1.00E-11
CAO45180.1	unnamed protein product [Vitis vinifera]	72.4	2.00E-11
CAO39276.1	unnamed protein product [Vitis vinifera]	70.1	4.00E-11
CAO48073.1	unnamed protein product [Vitis vinifera]	70.9	6.00E-11
XP_001067213.1	PREDICTED: hypothetical protein [Rattus norvegicus]	68.9	4.00E-10
CAO68098.1	unnamed protein product [Vitis vinifera]	497	1.00E-139
CAO21841.1	unnamed protein product [Vitis vinifera]	479	1.00E-134
CAO23214.1	unnamed protein product [Vitis vinifera]	429	1.00E-118
ABK93489.1	unknown [Populus trichocarpa]	407	1.00E-112
CAO63600.1	unnamed protein product [Vitis vinifera]	397	1.00E-109
ABK93226.1	unknown [Populus trichocarpa]	378	1.00E-103

Accession number	Similarity	Score (bits)	E-value
CAO63606.1	unnamed protein product [Vitis vinifera]	377	1.00E-103
CAO16101.1	unnamed protein product [Vitis vinifera]	372	1.00E-101
CAO69484.1	unnamed protein product [Vitis vinifera]	342	2.00E-92
NP_171983.2	unknown protein [Arabidopsis thaliana]	336	1.00E-90
ABK96759.1	unknown [Populus trichocarpa x Populus deltoides]	322	2.00E-86
CAN81221.1	hypothetical protein [Vitis vinifera]	316	1.00E-84
ABA46755.1	unknown [Solanum tuberosum]	292	2.00E-77
NP_568958.1	unknown protein [Arabidopsis thaliana]	159	5.00E-76
ABK93056.1	unknown [Populus trichocarpa]	219	1.00E-55
ABK96157.1	unknown [Populus trichocarpa]	202	6.00E-51
CAO42313.1	unnamed protein product [Vitis vinifera]	199	1.00E-49
ABK96772.1	unknown [Populus trichocarpa x Populus deltoides]	197	5.00E-49
CAO24297.1	unnamed protein product [Vitis vinifera]	151	3.00E-35
CAO14817.1	unnamed protein product [Vitis vinifera]	151	5.00E-35
CAO16964.1	unnamed protein product [Vitis vinifera]	150	8.00E-35
XP_001269594.1	hypothetical protein [Aspergillus clavatus NRRL 1]	73.6	1.00E-22
CAO41541.1	unnamed protein product [Vitis vinifera]	108	2.00E-22
NP_565728.1	unknown protein [Arabidopsis thaliana]	106	1.00E-21
EDP38581.1	hypothetical protein Bm1_05555 [Brugia malayi]	92	4.00E-17
ABK94233.1	unknown [Populus trichocarpa]	62	1.00E-08
ABN08062.1	Protein of unknown function [Medicago truncatula]	52.8	1.00E-05
CAO40971.1	unnamed protein product [Vitis vinifera]	129	2.00E-28
CAO22611.1	unnamed protein product [Vitis vinifera]	183	9.00E-45

Appendix 3

Absolute quantification of transcripts in *L. albus* phloem exudate and stem tissue

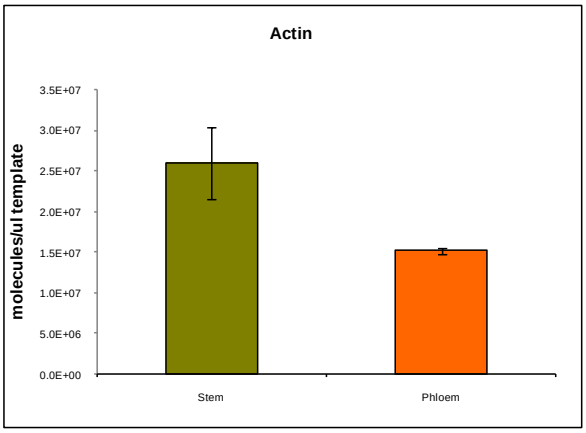

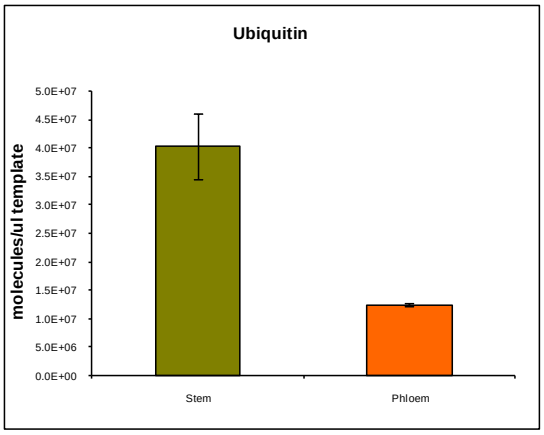

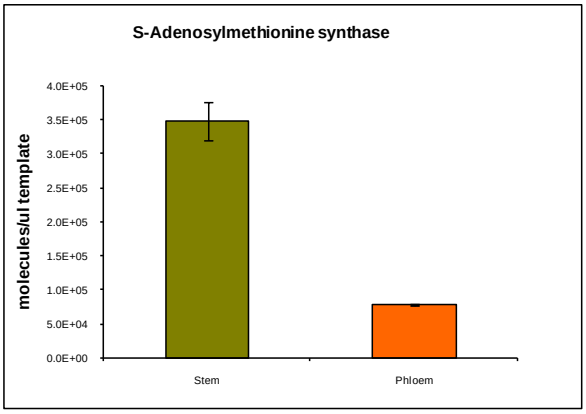

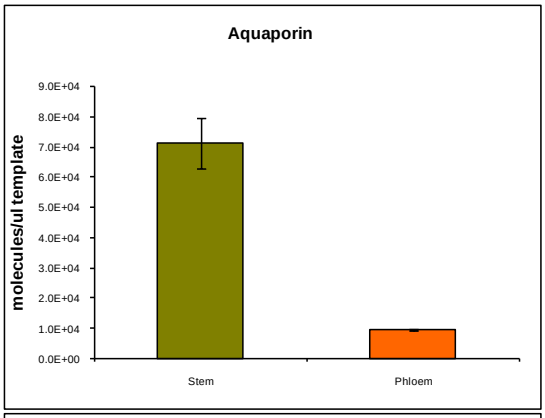

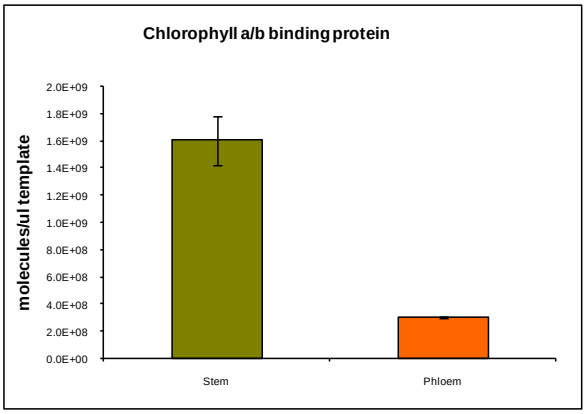

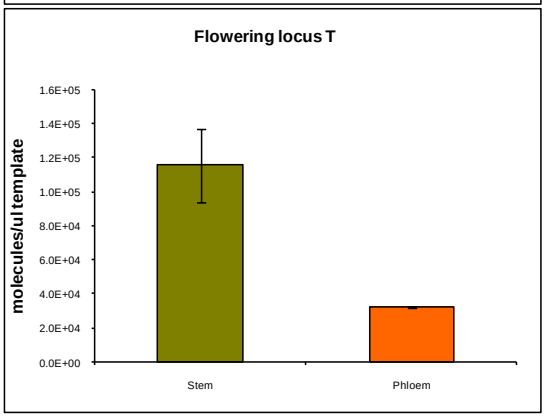

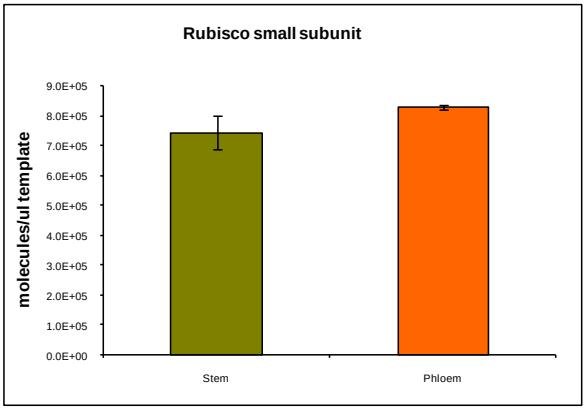

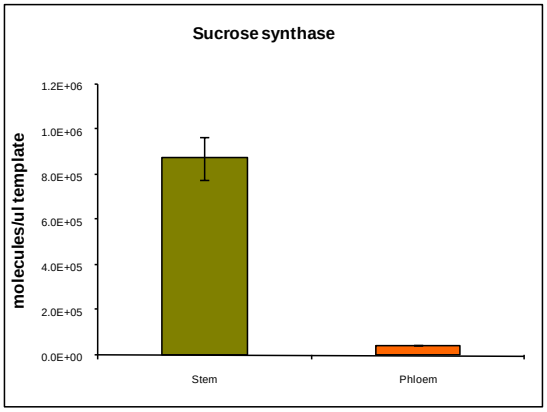

Absolute quantification of transcripts in *L. albus* phloem exudate and leaf tissue

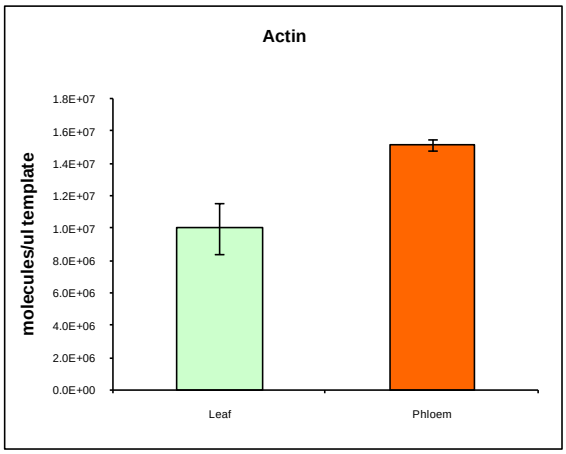

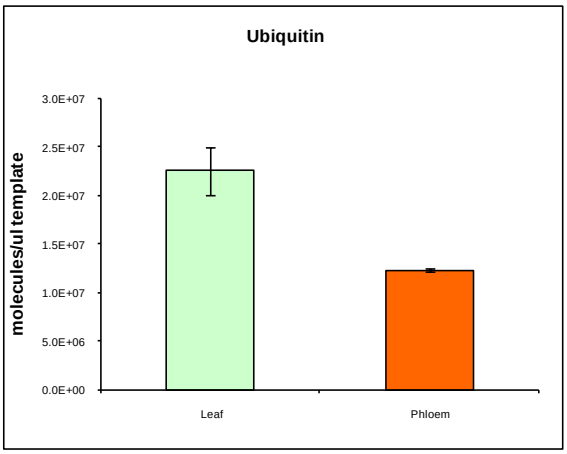

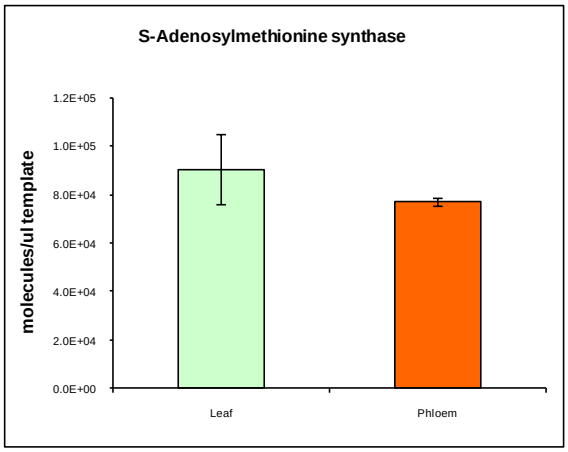

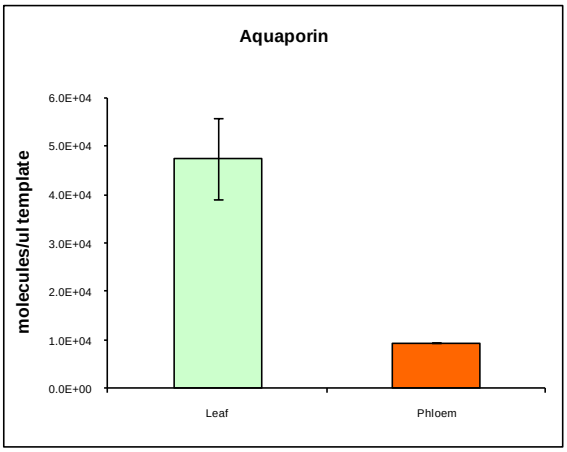

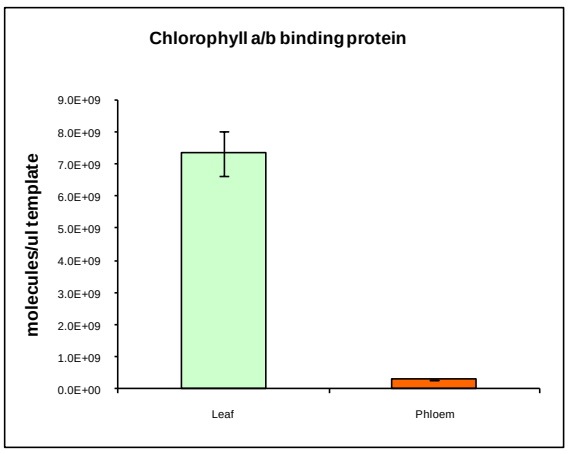

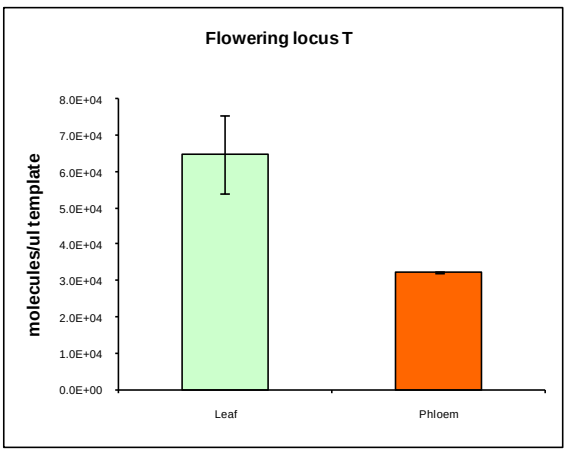

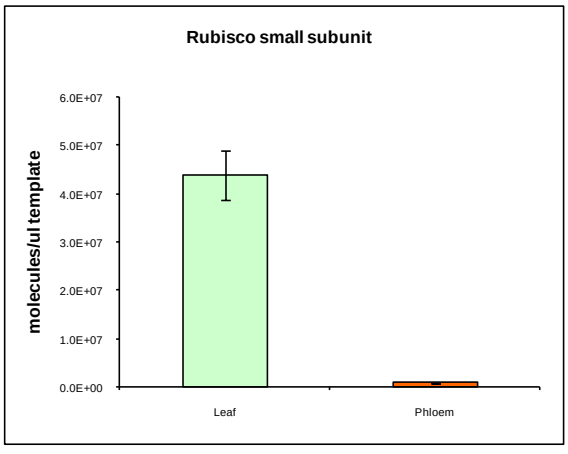

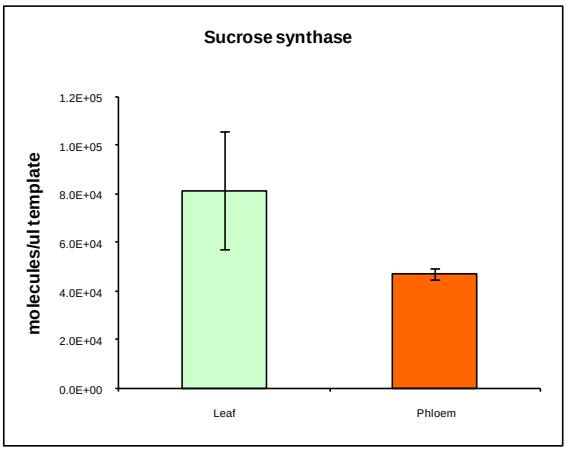

Absolute quantification of transcripts in *L. albus* phloem exudate and flower tissue

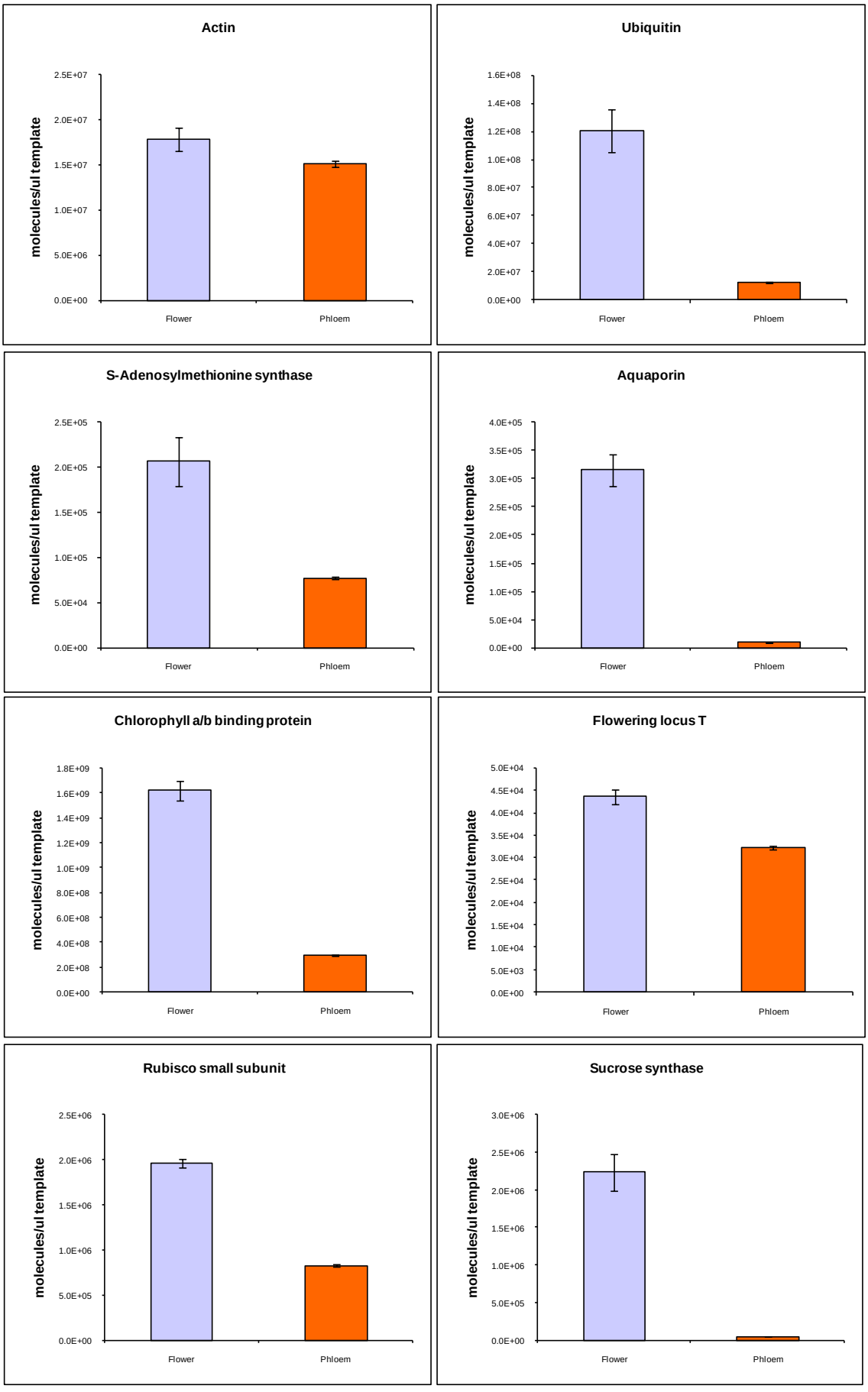

Appendix 4

Dissociation curves – Real-time RT-PCR

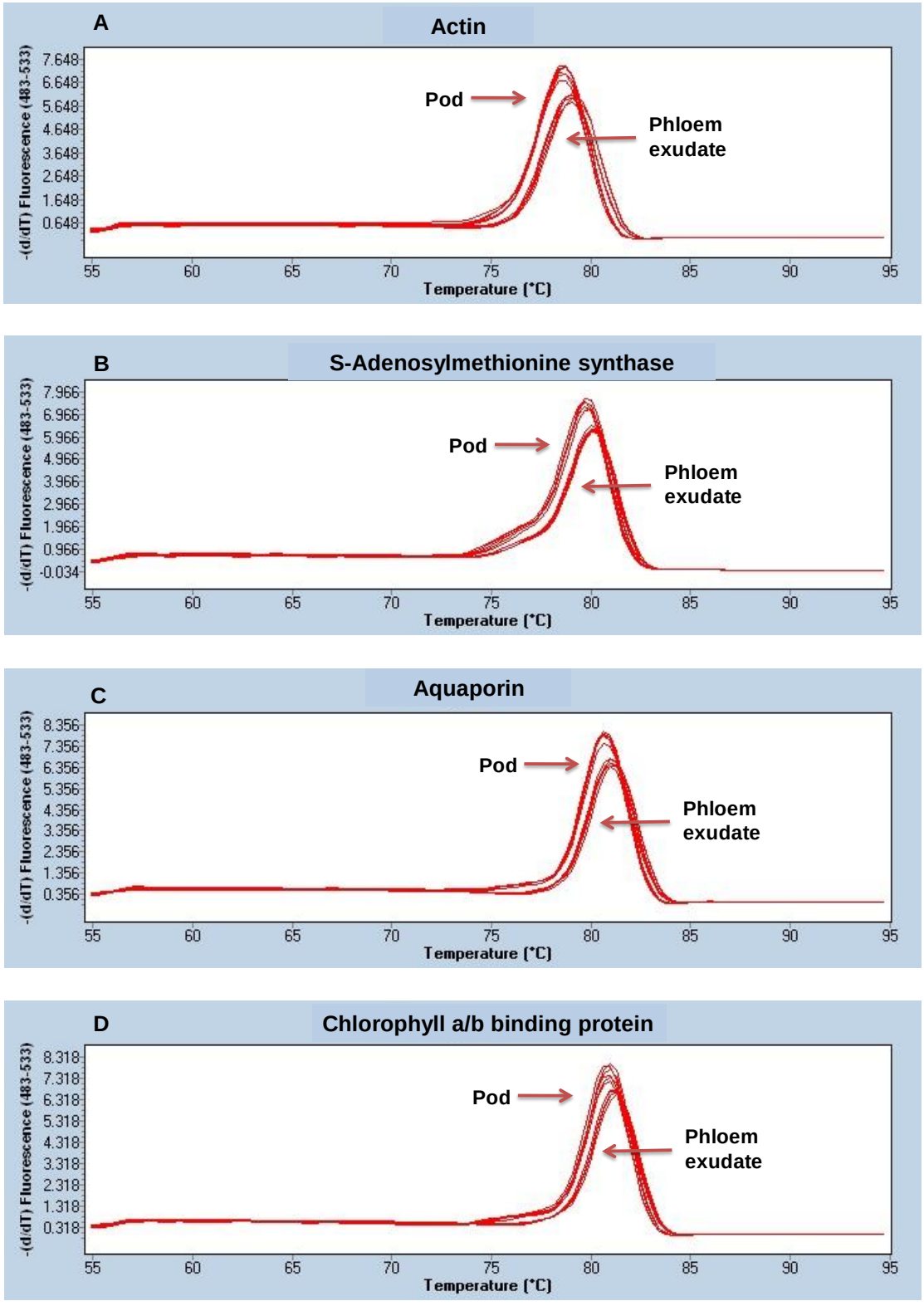

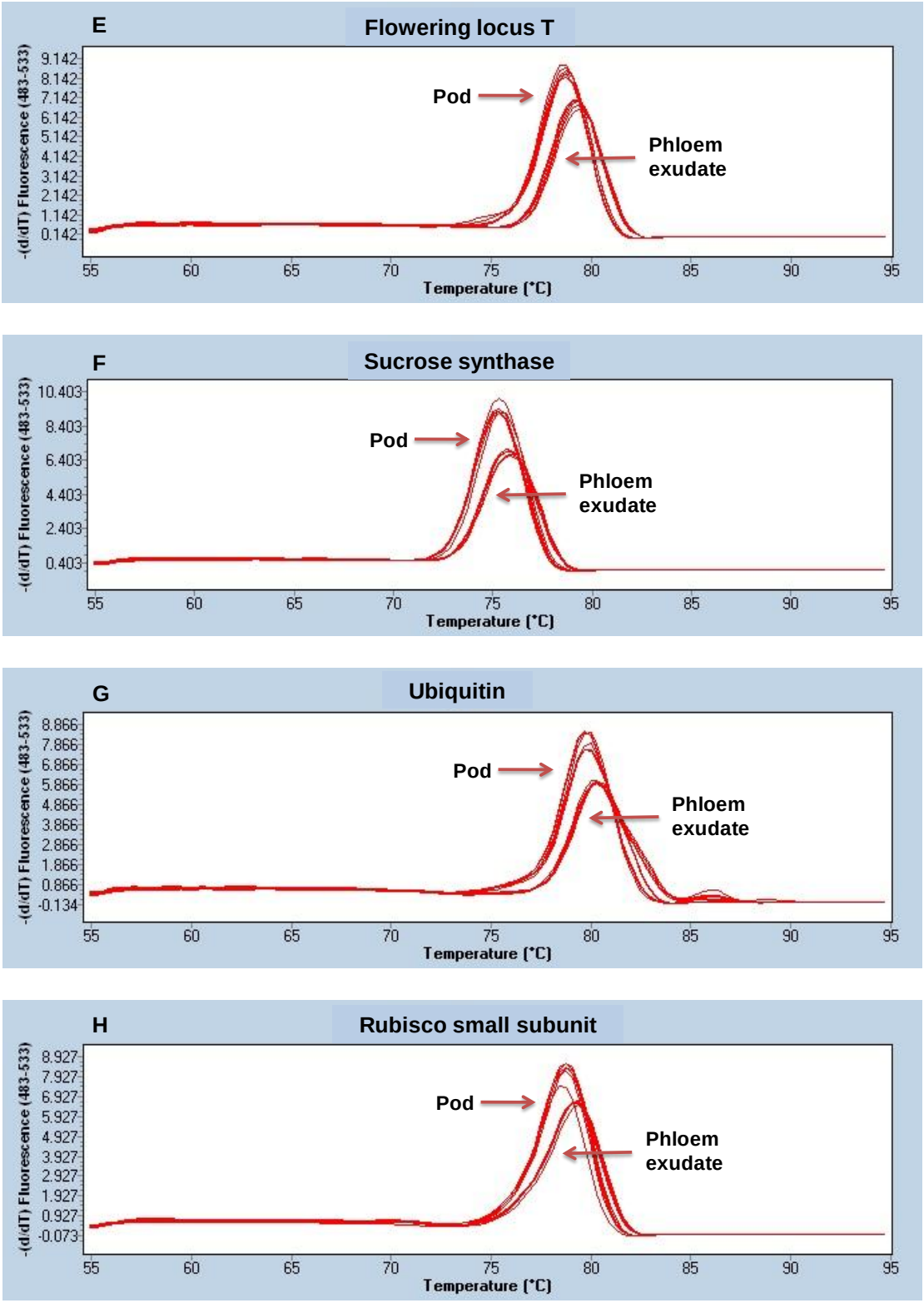

Appendix 4. Specificity of PCR amplification was confirmed by dissociation curves with single peaks for each gene (A-H). Melting curves were obtained with 3 biological replicates and 2 technical replicates per sample. PCR conditions were pre-incubation at 95°C for 10 min followed by 40 cycles of amplification at 95°C for 10 sec, 55°C for 10 sec and 72°C for 20 sec. For melting curve analysis, samples were heated at 95°C for 10 sec, cooled to 55°C for 30 sec. Fluorescence signal were collected continuously from 55ºC to 95ºC.

Appendix 5

Dissociation curves – Real-time RT-PCR

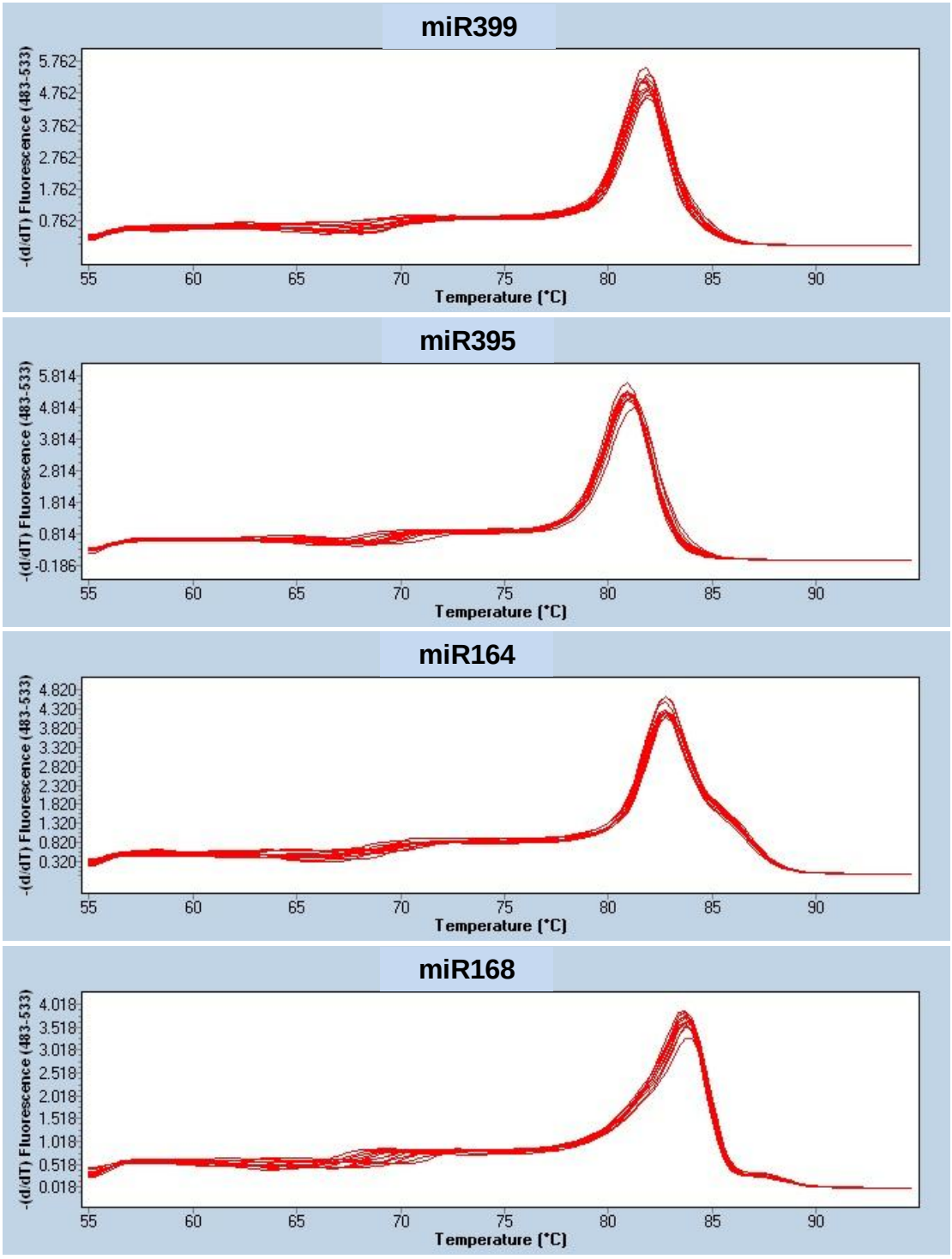

Appendix 5. Specificity of PCR amplification was confirmed by dissociation curves with single peaks for each miRNA used in translocation studies. Melting curves were obtained with 3 biological replicates and 2 technical replicates per sample. PCR conditions were pre-incubation at 95°C for 10 min followed by 40 cycles of amplification at 95°C for 10 sec, 55°C for 10 sec and 72°C for 20 sec. For melting curve analysis, samples were heated at 95°C for 10 sec, cooled to 55°C for 30 sec. Fluorescence signal were collected continuously from 55ºC to 95ºC

Appendix 6

Dissociation curves – Real-time RT-PCR

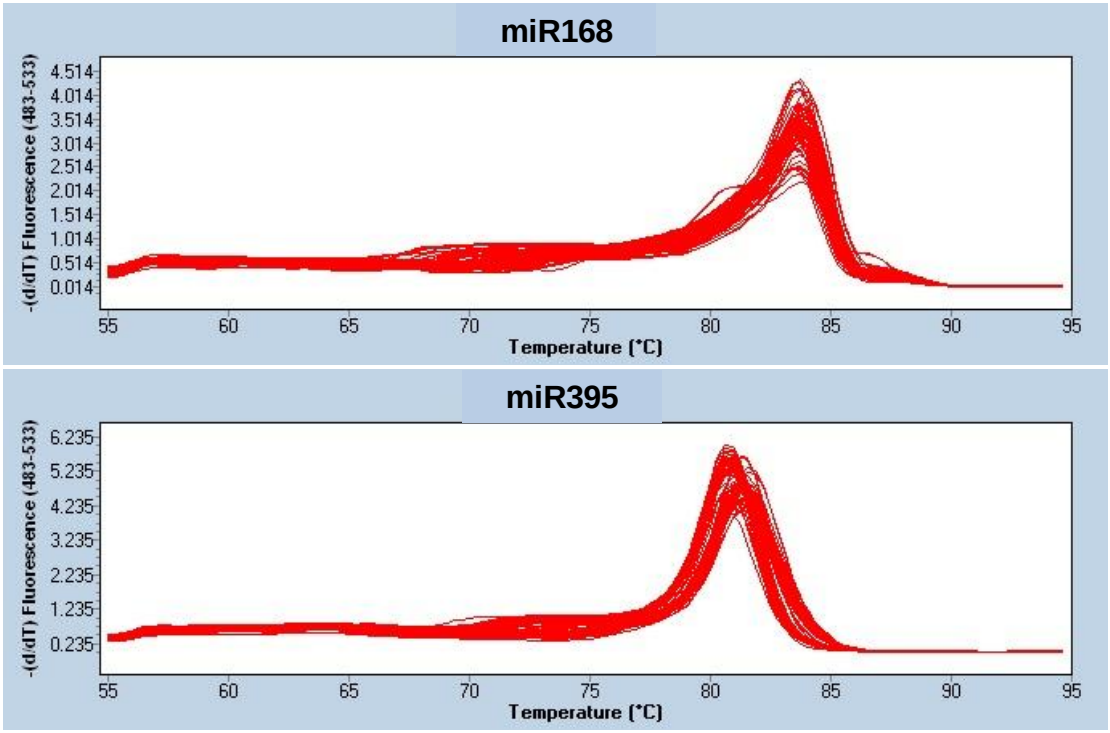

Appendix 6. Specificity of PCR amplification was confirmed by dissociation curves with single peaks for each miRNA used in the study of miRNA response to S-deficiency. Melting curves were obtained with 3 biological replicates and 2 technical replicates per sample. PCR conditions were pre-incubation at 95°C for 10 min followed by 40 cycles of amplification at 95°C for 10 sec, 55°C for 10 sec and 72°C for 20 sec. For melting curve analysis, samples were heated at 95°C for 10 sec, cooled to 55°C for 30 sec. Fluorescence signal were collected continuously from 55ºC to 95ºC